eman ta zabal zazu

Universidad del País Vasco
Euskal Herriko Unibertsitatea

Neuronetako eta mikrogliako proteinen sintesi lokalaren erregulazioa

DOKTOREGO TESIA

Maite Blanco Urrejola

2022

Zuzendariak:

Dra. Jimena Baleriola Gomez de Pablos

Dra. Elena Vecino Cordero

Por ti Marivi, ya puedes fardar de nieta

AURKIBIDEA

LABURDURAK

Euskaraz definitutako hitzekin bat ez datozen laburdurak (gehienak euskaraz idatzita egongo direlako) ingelesez letra etzanez definituko dira.

Aβ – β-amiloide peptidoa

Actb – β-aktinaren mRNA arratoietan

ACTB – β-aktinaren mRNA gizakietan

ANOVA – Bariantzaren analisia

ATP – Adenosina trifosfatoa

BSA –Behi-serum albumina

BrdU – 5-bromo-2`- deoxiuridina

DAPI – *4',6-diamidino-2-phenylindole*

DIV – *In vitro* egunak

DMEM – *Dulbecco's Modified Eagle's Medium*

DMSO – *Dimethyl sulfoxide*

DNA – Azido desoxirribonukleikoa

DNAsa –Desoxirribonukleasa, DNA digeritzen duen entzima

EA – Alzheimer gaixotasuna (Gaztelaniazko enfermedad del Alzheimer)

EGFP – Proteina berde fluoreszentea

EE – Erretikulu endoplasmatikoa

EEP – Erretikulu endoplasmatiko pikortsua

FBS – Behien fetu-seruma

FISH – *In situ* hibridazio fluoreszentea

GAPDH –Gliceraldehído 3-fosfato deshidrogenasa

GFAP – *Glial fibrillary acidic protein*

IBA1 – Kaltzio ionizatuari lotzeko molekula egokitzailea 1 (*Ionized calcium binding adaptor molecule 1)*

IMDM – *Iscove´s Modified Dubelcco´s Medium*

IZK – Inmunozitokimika

LPS – Lipopolisakaridoa

MCSF – Makrofagoen kolonien estimulazio-faktorea

mRNA – RNA mezularia

NS – Nerbio sistema

NSZ – Nerbio sistema zentrala

OPP – *O-propargil puromicyn*

Pard3 –Par-3 familiaren zelula-polaritatearen erregulatzailea

PBS – Fosfatoarekin tanpoitutako gatz-disoluzioa

PCR –Polimerasaren kate-erreakzioa

PDL – Poli-D-lisina

PFA – Paraformaldehidoa

Puro-PLA – *Puromicyn Proximity Ligation Assay*

RBP – RNA-rekiko lotura proteinak

RhoA –Ras homologoaren familiako A kidea

RNA –Azido ribonukleotidoa

RNAsa – Ribonukleasa, RNA digeritzen duen entzima

RNP – Ribonukleoproteina

LABURPENA

Konpartimentalizazioa funtsezkoa da zelula polarizatuetan, hala nola, neuronetan eta glia zeluletan, egiturazko eta funtzionalki definitutako zelulaz azpiko eremuak izan ditzaten. Zatikatze horrek zelula proteomaren banaketa asimetrikoa eskatzen du, non mRNAak garraiatzeak eta horiek eremu subzelularretan tokian-tokian itzulpenak, proteinen tokiko sintesia deritzona, garrantzia handia duten. Neuronetan proteinen %50a mRNAen tokiko itzulpenaren bidez sortzen dela kalkulatzen da. Horregatik, mekanismo hori desarautzea kaltegarria izan daiteke funtzio neuronaletarako, neuroendekapenezko zenbait gaixotasunetan ikusi den bezala.

Neurona-mikroglia elkarrekintzak funtsezkoak dira neuronen funtzionamendu egokirako, eta neuronen portaera zuzentzen duen proteoma modulatzen dute zenbait ingurune zelularretan. Proteoma subzelularra mRNA-aren tokiko itzulpenaren bidez erregulatu daitekeenez, gure helburuetako bat mikrogliak neuritetan ematen den proteinen tokiko sintesian eragina duen zehaztea izan da, bai baldintza fisiologikoetan, bai β amiloide peptidoak eragindako patologian. *De novo* sintetizatutako proteinak markatuz, ikusi dugu mikrogliak proteina neuritikoen ekoizpena erregulatzen duela, bai zelulaz kanpoko ingurunera jariatutako faktoreen bidez, bai neuritekin kontaktu zuzena izanez. Gainera, masa-espektrometriaren bidez identifikatutako profil proteomikoen azterketek berretsi egin dituzte behaketa horiek, eta, horri esker, mikrogliaren presentziak erregulatutako proteinak identifikatu ahal izan ditugu, bai oinarrizko kondizioetan, bai Aβ bidezko tratamenduaren ondoren. Azterketa horien arabera, garrantzi handia du mikroglia-neurona komunikazioak funtzio neuronalean eta NSZko patologietan duen inplikazioan.

Bestalde, tokiko proteinen sintesia neuronetara mugatuta ez dagoenez eta duela gutxi egindako azterketek mekanismo hau zelula glialetan deskribatu dutenez, gure beste helburuetako bat fenomeno hori prozesu periferiko mikroglialetan gertatzen den, eta funtzio mikrogliala mantentzeko garrantzia duen zehaztea izan da. Puromizilazio eta proteina-RNA ko-lokalizazioa saiakuntzen bidez, itzulpen lokala behatu dugu mikrogliaren prozesu periferikoetan, hala nola, lamelipodioetan eta filopodioetan, hanturari erantzuteko. Horrez gain, PuroPLA eta *in situ* hibridazio probek polaritate zelularrean parte hartzen duten *Actb* eta *Par3* mRNA-en presentzia eta itzulpen lokalizatua erakutsi dute, hantura- eta endekapen-estimuluen aurrean, mekanismo horrek testuinguru patologikoetan mikrogliak duen portaeran duen garrantzia iradokiz.

SARRERA

1. SARRERA

Ebolutiboki, ingurumen-erronken aurrean, zelula eukariotoak konplexuago bihurtu dira bi maila nagusitan: lehenik, organismo bereko zelulen arteko espezializazioa gertatu da, eta, bigarrenik, eta, horretan zentratuko garena, zelulak berak zatikatuta daude. Konpartimentalizazio horri esker, subzelular mailan eskualdeak bereiz daitezke, hala nola nukleoa, non DNAren erreplikazioa gertatzen den, edo erretikulu endoplasmatikoa (EE) eta Golgi aparatua, non proteinak sintetizatu eta heltzen diren, besteak beste. Zelulen erregionalizazioak zelula-proteomaren banaketa asimetrikoa dakar, eta, horri esker, konpartimentu subzelular bakoitzaren funtzioa mantendu daiteke. Dogmaren arabera, zelula eukariotoetan proteinak eskualde perinuklearrean sintetizatzen dira, mRNAak erribosoma zitosoliko askeekin (1Ai irudia) edo erretikulu endoplasmatiko pikortsuari (EEP) lotutako erribosomekin lotzen direnean (1Aii irudia). Sintetizatu berri diren proteinak prozesatu egiten dira, eta, heldu ondoren, mikrotubuluen bidez, dineina eta kinesinen bidez, edota miosinen bidezko aktina-filamentuen bidez, hainbat eremu periferikotara garraiatzen dira (1A irudia), eta bertan beraien funtzioa betetzen dute (Alberts *et al*, 2002). Proteinak domeinu subzelularretara banatzeko, normalean, lokalizazio-seinaleak erabiltzen dira, proteina-sekuentziaren barruan daudenak. Hala ere, zenbait zelula-konpartimentutara proteinak ekartzea, proteina garraiatzearen mende ez ezik, mRNA garraioaren mende ere egon daiteke; mRNA hori, berez, proteinak funtzioa bete behar duen domeinu subzelularrera garraiatzen da, bertan itzuliz. Prozesu horri proteinen sintesi lokala deritzo (1B irudia). Hain zuzen, zelula eukariotoetan RNAren lokalizazio-mekanismoak ugariak eta kontserbatuak direla frogatu da (Martin eta Ephrussi, 2009). Lokalizatzeko, mRNAak zelulaz azpiko konpartimentuetara garraiatzen dira RNA lotura-proteinekin (RBPak) elkartuta, eta konplexu erribonukleoproteikoak (RNPak) eratzen dituzte, itzulpen-errepresio egoeran (1B irudia). RBPak ugaztun zeluletako gene-adierazpenaren transkripzioaren osteko kontrolean inplikatuta daude (Castello *et al*, 2013). RNP konplexuak mintzik gabeko egitura supramolekularretan biltzen dira, hauei RNA pikorrak deitzen zaie, eta proteina motorrei lotzen zaizkie, hala nola kinesinari, horrela mRNAak zelularen periferiako azken helmugara garraiatzen dituzte. Hain zuzen, RNA/RBP elkarrekintza ugari dokumentatu dira, horietako asko mRNA-aren itzuli gabeko 3' eskualdeetara (3`UTR) zuzenduta daude, non transkribatutako lokalizazio-elementuak egoten diren (Cook *et al*, 2010). mRNA-ak bere xede-konpartimentura iristen direnean, RNPen konplexuetatik askatzen dira, eta, lokalki

itzultzen dira, proteinak sortuz, itzulpen-makinen bidez (1B irudia) (Jung *et al*, 2012). Beraz, proteina bat lokalki zehaztasunez sintetizatzeko, RBP-ekiko lotura, garraioa eta RNAren itzulpena fin-fin erregulatu behar dira. Itzulpen-makinen funtzionamendu ezegokiek edo desarautuek, mRNA-ren tokiko errepertorioko aldaketek, RBP-en eskuragarritasunak edo mRNA-ren garraioko akatsek tokiko proteoma aldatu dezakete. Asaldura horiek zelula-disfuntzio bat eragiten dute, eta, nerbio-sistemaren kasuan (NS), gaixotasun neurologiko eta neurodegeneratiboak eragiten dituzte (Lin *et al*, 2021; Baleriola *et al*, 2015).

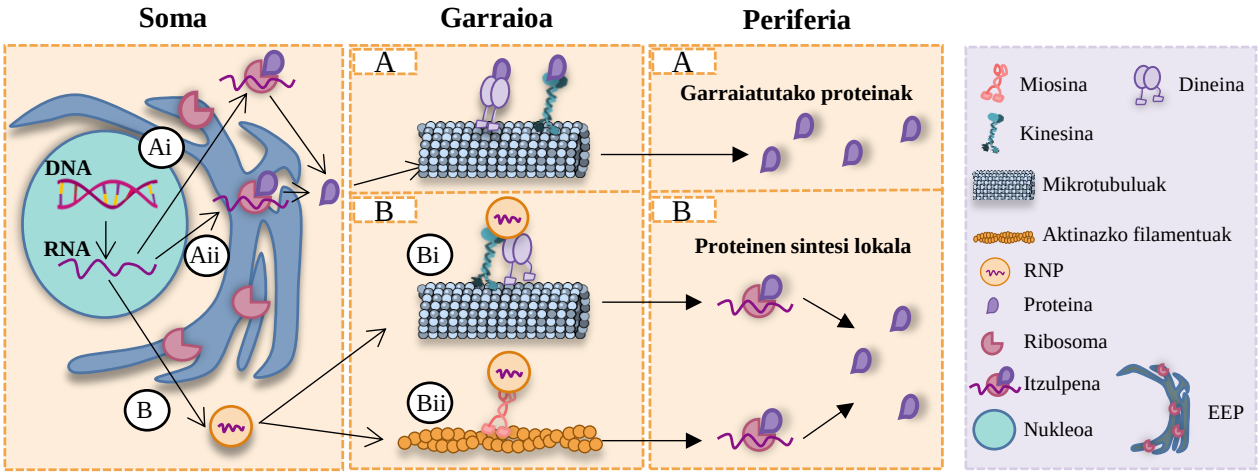

1. irudia. Zelula eukariotako mRNA eta proteinen trafikoaren diagrama. A) Proteinak, nagusiki, zitosolean erribosoma askeetan (Ai) edo erretikulu endoplasmatiko pikortsuari (EEP) atxikitako erribosometan (Aii) sintetizatzen dira, eta, ondoren, proteina motorren bidez (A) garraiatzen dira beren eginkizunerako. B) Zenbait mRNAk RNAren lotura-proteinekin (RBP) konbinatzen dira, konplexu erribonukleoproteikoak sortuz (RNP), eta mikrotubuluen bidez garraiatzen dira, kinesina eta dineina bidez (Bi) edo aktina-filamentuen bidez, miosina bidez (Bii). Beren helmugara iristean, mRNA askatu egiten dira eta lokalki itzultzen da proteinak sortuz, proteinen sintesi lokala deritzon prozesuaren bidez. Blanco-Urrejola *et al*, 2021 artikuluko diagrama eraldatua.

1.1.Proteinen sintesi lokala NS-n

1.1.1. Proteinen sintesi lokala neuronetan

Neuronak, morfologikoki, NS-ren zelula konplexuenak dira. Nukleoa zelula-gorputzean edo soman kokatzen da, eta bertatik hainbat neurita azaleratzen dira. Neuriten artean, dendritak (hamar milimetro inguru neur ditzakete) eta axoiak (ornodunetan metro bat luze izatera irits daitezke) bereiz daitezke (Bannister eta Larkman, 1995). Oso polarizatua den morfologia horri esker, neuronek zirkuitu neuronal egonkorrak sor ditzakete. Polaritate horri eusteko, konpartimentu neuronal bakoitzak era akutuan erreakzionatu behar du denboran eta espazioan, ingurunean gertatzen diren aldaketei azkar egokitzeko. Beraz, seinaleztapen-gertaera konpartimentatuak behar dira, eta, ondorioz, proteinak asimetrikoki banatu behar direla. Hori lortzeko, proteina helduak garraiatu behar dira, edo

mRNA-k garraiatu eta xede-konpartimentuetan lokalki itzuli behar dira (Rangaraju *et al*, 2017; Holt *et al*, 2019). Axoietako tokiko itzulpena 1899an postulatu zen, baina 1960ra arte ez zen frogatu azetilkolinesterasaren sintesia deskribatu zenean, nerbio periferikoetan (Koenig eta Koelle, 1960). Aurrerago erribosomen presentzia dendritetan deskribatu zen (Steward eta Lewy, 1982; Steward eta Fass, 1983) eta neuronen axoietan (Steward eta Fass, 1983). Orduz geroztik, proteinen sintesi lokala aztertu da neuronetan, batez ere baldintza fisiologikoetan. Adibidez, badakigu mekanismo hori axoien mantentzean, gidaritzan eta arborizazioan inplikatuta dagoela, eta sinapsiaren eraketa eta plastizitate sinapikoa sustatzen dituela (Zhang eta Poo, 2002; Martin, 2004; Yoon *et al*, 2012; Leal *et al*, 2014). Horrez gain, proteoma neuronalaren % 50a mRNA lokalizatuen itzulpenaren bidez sortzen dela kalkulatzen da (Zappulo *et al*, 2017); horregatik, mekanismo honen desarautzea kaltegarria izan daiteke funtzio neuronaletarako, gaixotasun neurodegeneratibo batzuetan gertatzen den bezala. Adibidez, Alzheimer gaixotasunean (EA, gaztelaniazko enfermedad del Alzheimer), neuronen axoietan 4 transkripzio-faktorearen (ATF4) mRNA areagotzen da, eta haren itzulpen lokalak heriotza neuronala eragiten du (Kobayashi *et al*, 2017; Baleriola *et al*, 2014). Bestalde Huntingtonen gaixotasunean, HTT deritzon RBPa desaraututa dago, eta, horren ondorioz, haren xede diren mRNA batzuen mailak, hala nola *Bdnf, Ip3r1* eta *Actb*, dendritetan eta axoietan asaldatuta daude (Savas *et al*, 2010). Bi adibide horiez gain, beste gaixotasun neurodegeneratibo batzuetako mRNAen banaketan izandako aldaketak dokumentatu dira, Gamarran *et al* (2021) artikuluan jasotzen den bezala. Ebidentzia horien arabera, proteinen sintesi lokala uste baino garrantzitsuagoa da. Testuinguru patologikoetako tokiko sintesia lesionatutako nerbio periferikoetan aztertuz zen lehenengo aldiz, non mRNAen errepertorio bat tokian bertan itzultzen den, proteina sintetizatu berri horiek birsorkuntza axonala eraginez. Era berean, nerbio ziatikoaren lesio baten ondoren, STAT3 eta PPARγ transkripzio-faktoreen sintesi axonala ematen da, eta horiek atzera garraiatzen dira nukleora. Han daudela, bai STAT3-k bai PPARγ-k nerbio-birsorkuntza bultzatzen duten transkripzio-programak sortzen dituzte (Ben-Yaakov *et al*, 2012). Bestalde, nerbio-sistema zentralean (NSZ), β amiloide peptidoaren (Aβ) metaketak Alzheimer gaixotasunarekin (EA) lotutako plaka neuritikoak eragiten ditu, eta heriotza neuronalean parte hartzen duten proteinen sintesi intra-axonala eragiten du (Baleriola *et al*, 2014; Walker *et al*, 2018). Aurkikuntza horiek zera erakusten dute, proteinen sintesi lokala lesionatutako nerbioen birsorkuntzan eta Aβ oligomeroen eragindako neuronen heriotzan inplikatuta dagoela (Gamarra *et al*, 2021). Beraz, gaixotasun

neurodegeneratiboetarako edo nerbioetako lesio traumatikoetarako tratamendu zehatzak garatzeko, ez dira ahaztu behar mRNA-ren garraioa eta neuritetako itzulpen lokalizatua.

1.1.2. Proteinen sintesi lokala glia zeluletan

Neuronetan egin dira RNAen lokalizazioari eta tokiko itzulpenari buruzko ikerkuntza gehienak. Hala ere, horiek ez dira NS-ren zelula polarizatu bakarrak. Glia prozesuak somatik urrun ere zabal daitezke, eta neurita batzuk baino gehiago neurtzera iritsiz (Blanco-Urrejola *et al*, 2021). Hori dela eta, ez da harritzekoa glia zelulen prozesu periferikoetan mRNAk aurkitzea eta haien itzulpen lokala ematea, glia zelulen funtzioa egokia mantentzeko.

Oligodendrozitoen prozesu distaletan mielinazko oinarrizko proteinaren (MBP) tokiko itzulpena izan zen aurkitu zen lehenetarikoa (Colman *et al*, 1982), nerbioaren eroankortasunaren eraginkortasun eta abiadurarako erabakigarria dena (Purves *et al*, 2001). *Mbp* oligodendrozitoetan ugarien den mRNA da, eta mielina-zorro trinkoak eratzeko garrantzitsua da. Hain zuzen, EA-n *Mbp*-ren tokiko sintesia aberrantea bihurtzen dela deskribatu da, mielinaren morfologian eta oligodendrozitoen garapenean aldaketa eraginez (Quintela-Lopez *et al*, 2019; Wu *et al*, 2017; Ferreira *et al*, 2020). Beste behin ere, proteinen sintesi lokalak testuinguru fisiologikoetan ez ezik, patologikoetan ere duen garrantzia iradokiz.

Astrozitoetan bi prozesu-mota deskribatu dira: 1) odol-hodiak ukitzen dituzten muturreko oinak, prozesu astrozitiko peribaskularrak (PvAPs) izenez ere ezagutzen direnak, funtzio baskularrak erregulatzen dituztenak dira, hala nola hesi hematoentzefalikoa (HHE), immunitatea (Álvarez *et al*, 2013) eta garuneko odol-fluxua mantentzen dute (Iadecola, 2017) eta 2) prozesu astrozitiko perisinaptikoak (PAPak); sinapsiekin nahiz dendritekin elkarreragiten dute, eta transmisio sinaptikoa erregulatzen dute (Ghézali *et al*, 2016). Bi prozesu periferiko motetan mRNAak eta itzulpen-makineriaren osagaiak hauteman dira, eta biek mRNAen errepertorio komuna duten arren, konpartimentu bakoitzean transkritu espezifikoak daudela ere ikusi da, polaritate funtzional astrozitikoa areagotuz (Mazaré *et al*, 2020). Beraz, PvAP-etan eta PAP-etan mRNAen lokalizazioaren desarautzeak, ziurrenik, garunaren fisiologia baskularrean eta transmisio sinaptikoan eragina izango du.

Duela gutxi, mikroglia-prozesuetan aberastutako mRNA-k deskribatu dira. Prozesu horiek defentsaren, mugikortasunaren eta fagozitosiaren parte dira (Vasek *et al*, 2021). Gainera, Iba1-erako positiboak diren mikroglia prozesuek RPL4 proteina erribosomikoa

kodetzen duten mRNAk dituzte. Horrek zera adierazten du tokiko itzulpenean parte hartzen duten erribosoma-proteinak ere lokalki itzul daitezkeela (Oudart *et al*, 2020). Nahiz eta ebidentziek mikroglien prozesu periferikoetan proteinak lokalki itzuli daitezkeela adierazten duten, ez dakigu fenomeno horrek baldintza patologikoetan duen inplikazioa.

1.2.Mikroglia

Mikroglia, garunean bizi den immunitate zelula, garuneko homeostasiari laguntzen dio, NSZ-aren funtzionamendurako funtsezkoak diren funtzioak betez; esaterako, sinapsien inausketa fagozitikoa garapenean zehar (Schafer *et al*, 2012) eta gaixotasunean (Hong *et al*, 2016; Vasek *et al*, 2016), zelula apoptotikoen ezabatzea (Marín-Teva *et al*, 2004), zaintza immunitarioa, patogenoen aurkako babesa eta faktore trofikoen iturria (Butovsky *et al*, 2006). Funtzio horiek baldintza patologikoetan aldatzen dira, eta eragina dute neuronen funtzio sinaptikoan, konektibitate neuronalean, neurogenesian, oligodendrozitoen mielinizazioan edo hesi hematoentzefalikoaren (HHE) iragazkortasunean (2. irudia; Sierra *et al*, 2019). Horregatik, mikrogliak funtzio horiek nola betetzen dituen ulertzea funtsezkoa da NSZ-aren funtzionamendu egokia ulertzeko.

Luzaroan "ez-aktibotzat" jo zen baldintza fisiologiko nahasezinetan, baina orain badakigu mikrogliak etengabe aztertzen duela parenkima, baita "egonean" ere. Mikrogliak modu aktibo eta etengabean hautematen ditu molekula-seinaleak bere ingurune lokalean, prozesu oso mugikorren bidez (prozesu periferiko mikroglialak) eta ingurunearen laginketa ahalbidetzen duen morfologia adarkatuaren bidez (Bolasco *et al*, 2018; Davalos *et al*, 2005; Nimmerjahn *et al*, 2005). Bai hilzorian dagoen zelula baten zelulaz kanpoko seinale espezifiko bat askatzeagatik, bai jarduera sinaptiko handiko eskualdeetatik datozen seinaleengatik, lehenengo bi urrats kritiko eman behar dira mikrogliak aldaketa fenotipiko bat izan dezan, eta, hala, “atsedeneko” egoera batetik bideratutako polarizazio eta migrazioko egoera batera igaro dadin. Mikrogliak (1) seinale molekularra detektatu behar du hasiera batean, eta (2) hartzaileak aktibatutako seinalea zelularen erantzun batean edo aldaketa morfologiko batean bilakatu behar da (Bernier *et al*, 2019).

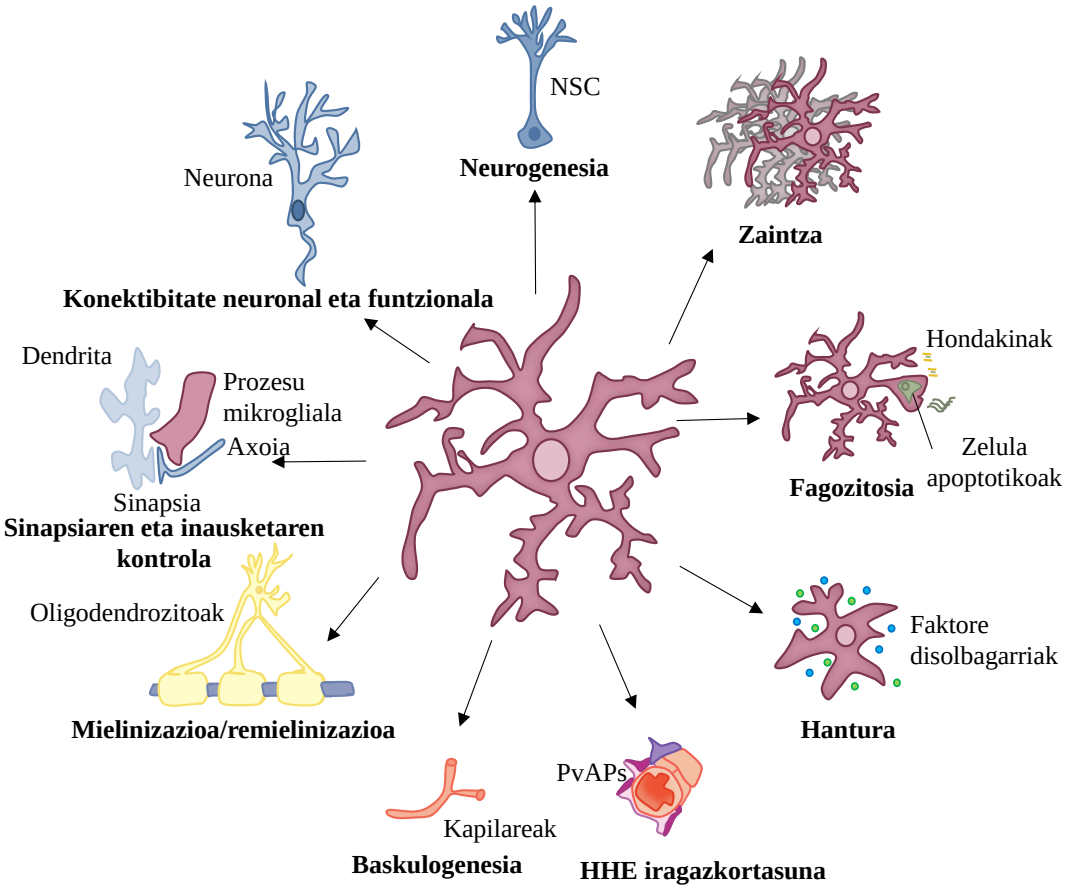

2. irudia: Funtzio mikroglialen diagrama. Sierra *et al*, 2019 artikulutik ateratako diagrama eraldatua.

1.2.1 Mikrogliaren bidezko funtzio neuronalaren erregulazioa

Biologia glialaren eta neuronekiko interakzioei buruzko interesa nabarmen handitu da azken urteotan, garun normalak nola funtzionatzen duen eta garuneko gaixotasunetan bere makineria disfuntzional zergatik bihurtzen den ulermen falta dela eta. Neurona-mikroglia elkarreraginak funtsezkoak dira garunaren funtzionamendu normalerako garapenean eta helduaroan. Gero eta gehiago aztertzen da mikrogliak neuronekin duen bi noranzkoko komunikazioaren garrantzia, garuna hainbat patologiatara egokitzeko gaitasuna, jarduera neuronalaren modulazioa eta aldaketa fenotipikoak, lesio neuronalen aurrean (Benarroch, 2005; von Bernhardi *et al*, 2016). Adibidez, jaio ondoko garapenean, axoien edo hazkunde-konoen eta zelula mikroglialen arteko elkarreragina funtsezkoa da bizirauteko eta neuronak berrantolatzeko (Fujita *et al*, 2020; Kitayama *et al*, 2011). Garun helduan, mikroglia prozesuek birpolarizatu egiten dute neurona hiperaktiboen axoien mintza, eta endekapenezko axoi horiek ezabatzen dituzte, birsorkuntza eta remielinizazioa sustatuz (Kato *et al*, 2016; Bechmann *et al*, 2001; Lloyd *et al*, 2019).

Mikroglia zelulen eta neuronen arteko komunikazioa hainbat mailatan gertatzen da: zeharkako mezulari disolbagarrien elkarrekintzetatik hasi eta mintzen arteko kontaktu zuzeneneraino doana (Cserép *et al*, 2020).

NSZ-eko zelulen arteko komunikazio bideetako bat zelulaz kanpoko besikulek osatzen dute. Zelulaz kanpoko besikulak (VE-ak) mintzezko besikulen familia bat dira, 100 nm eta 1 µm arteko tamainakoak, eta zelulen arteko komunikazioan inplikatuta daude. Zelula mota guztiak VEak askatzeko gai badira ere, zelula jariatzailearen arabera zelula hartzaile espezifikoetara bideratzen direla iradoki da. Bi zelulen arteko komunikazioaren berezitasuna, neurri batean, VEetan dauden mintz-proteinen, proteina zitosolikoen eta azido nukleikoen (DNA zatiak, mikroRNA-k eta mRNA-k) araberakoa da (Abels eta Breakefield, 2016). Saiakuntza proteomikoek mikrogliatik eratorritako VE-en edukia erakutsi dute, eta entzimak, txaperonak, tetraspaninak eta mintz-hartzaileak behatu dira (Paolicelli *et al*, 2019). Besikula horiek mRNA zein mikroRNA garraiatzen dutela frogatu denez, adierazpen genikoa urruneko posizioetan dauden zeluletan ere modulatzen dutela interpretatzen da, eta zelula hartzaileetan duten eragina komunikazio endokrinoaren bidez gauzatzen da (3. irudia). Mekanismo horrek xede zeluletako proteinen sintesi lokalaren erregulazioan parte har dezake. Izan ere, hantura-baldintzetan, mikrogliak askatzen dituen VEek proteina sinaptikoen maila erregulatzen dute, eta horrek sinapsi kitzikatzaileak galtzen laguntzen du (3. irudia; Prada *et al*, 2018). Zenbait ikerketak mikrogliatik eratorritako VEen funtzio onuragarriak deskribatu dituzten arren, hala nola proteina toxikoak ezabatzea, beste batzuek kalte neuronal eta sinaptikoarekin duten lotura nabarmendu dute. Frogatu da arratoietako mikroglia primarioen ereinketetatik isolatutako VEek Aβ forma disolbagarriak dituztela, eta forma horiek neurotoxikoak direla hazitako hipokanpoko neuronentzat (Joshi *et al*, 2014).

Zelulen arteko beste komunikazio bide bat faktore disolbagarrien bidezkoa da. Faktore horiek, VEek bezala, askotan beraien efektuak iturritik urrun eragiten dituzte. Zelula populazio handiagoak modulatzeko aukera ematen dute, baina VE-ek eta zuzeneko zelula-zelula elkarrekintzek baino modu ez espezifikoago batean. Mikrogliak jariatutako faktoreak, hala nola burmuinetik eratorritako faktore neurotrofikoak (BDNF) (Parkhurst *et al*, 2013), interleuzina (IL)-10 (Lim *et al*, 2013), IL-1b (Huang *et al*, 2011) edo alfa tumore-nekrosiaren faktoreak (TNF-α) (Olmos eta Llado, 2014) aktibitate neuronala eraldatzen dute (3. Irudia). Bestalde, ikusi da faktore disolbagarriak, hala nola ATP edo lipopolisakaridoak (LPS), VE mikroglialen askapenean inplikatuta daudela, eta garunean

hanturazko erantzunaren erregulazioa sustatzen dutela (Bianco *et al*, 2009; Takenouchi *et al*, 2015; Kumar *et al*, 2017). Neuronek ere seinaleak igortzen dituzte mikrogliara, metabolito purinergikoak (Davalos *et al*, 2005) edo glutamatoa (Eyo *et al*, 2014) bezalako bitartekari disolbagarriak erabiliz. Berriki frogatu da, jatorri neuronaleko ATP-ak adenosina mikrogliala sortzen duela neuronen erantzunak erregulatzeko (Badimon *et al*, 2020). Gainera, mikroglia zelulak ugaritzen dituen makrofago-kolonien faktore estimulatzaileak (M-CSF, ingelesezko siglengatik) neuronek jariatzen dute, eta horrek eragina izan dezake neuronen funtzioan (3. irudia; Dobbertin *et al*, 1997).

Azkenik, zelulen arteko mintzen zuzeneko elkarrekintzek komunikazio forma lokalizatuak ahalbidetzen dituzte zenbait prozesu biologiko kontrolatzeko (Giaume *et al*, 2010; Hamada eta Kole, 2015). Mikrogliak etengabe monitorizatzen du garun-parenkima bere prozesu mugikorrekin, baldintza fisiologikoetan (Nimmerjahn, 2005), eta deskribatu da jarduera neuronala prozesu horien mugikortasunaren bultzatzailea dela (Umpierre *et al*, 2020), bai eta jariatutako zenbait faktore ere, hala nola, lipopolisakaridoak (LPS) edo ATPa (Khurana *et al*, 2002). Garun osasuntsuan mikrogliaren gorputz zelularrak translokatzea mikroglia prozesuen mugimendua baino prozesu motelagoa denez (Eyo *et al*, 2018; Sipe *et al*, 2016), mikrogliaren eta neuronen arteko mintz-mintz kontaktu dinamikoak prozesu periferikoek ezartzen dituzte, batez ere. Interakzio mota horren adibiderik ezagunena mikroglia prozesuen eta sinapsien artekoa da (Weinhard *et al*, 2018). Izan ere, sinapsi glutamatergikoen %9a eta sinapsi g-aminobutirikoen %11 (GABA) prozesu mikroglialekin loturan daude (Cserép *et al*, 2020). Harreman horri esker, mikrogliak modulatu egiten ditu transmisioa eta plastikotasun sinaptikoa eta haren inausketa (3. irudia; Stevens *et al*, 2007; Lehrman *et al*, 2018; Shatz, 2009). Aurrekari horiek kontuan hartuta, ez litzateke harritzekoa izango prozesu mikroglialen eta neuritikoen arteko harreman zuzena funtsezkoa izatea neuronetako proteinen sintesi lokalaren modulazioarako, plastikotasun sinaptikoa eta inausketa sinaptikoa erregulatuz, beste funtzio biologiko batzuen artean.

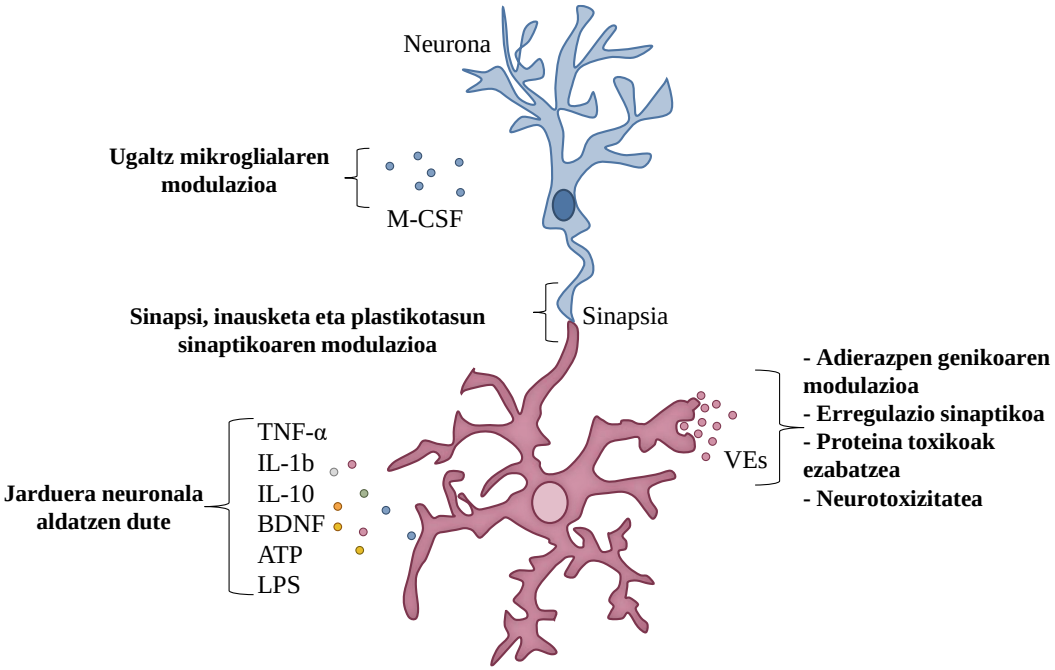

3. irudia: Mikrogliaren eta neuronen arteko interakzioek araututako funtzioen diagrama. VES, jariatutako faktoreak eta kontaktu bidezko komunikazioa.

1.2.2. Hantura estimuluen aurrean mikrogliaren erantzuna

Hantura da asaldura neurologiko askoren ezaugarri amankomuna, hala nola garuneko lesio traumatikoena eta gaixotasun neurodegeneratiboena, zeinak garun-zeluletan, zelula glialak barne, aldaketa estruktural eta funtzional handiak eragiten dituzten (Skaper *et al*, 2018). Hala, nahiz eta historikoki hantura gaixotasun neurodegeneratiboekin zerikusia ez zuela pentsatu, gaur egun badakigu hantura gaixotasun neuroendekapen kronikoetan guztiz inplikatuta dagoela, hala nola Alzheimer gaixotasunean (Streit *et al*, 2004). Hantura akutua edo kronikoa izan daiteke. Hantura akutuak agente kaltegarri bati berehala eta goiz erantzutea dakar, eta, funtsean, defentsa-erantzun bat da, kaltetutako eremua konpontzeko bidea errazten duena. Aldiz, etengabeko estimuluek eragiten dute hantura kronikoa (Streit *et al*, 2004). NSZ-erako hantura-prozesu onuragarriak deskribatu dira, garuneko homeostasia berreskuratzeko aukera ematen baitute, baina hantura iraunkorra ere kaltegarria izan daiteke.

Garun-ehunean patogenoek eragindako aldaketa edo lesio oro, mikrogliaren prozesu periferikoek hautematen dute lehenik, eta, prozesu horiek, hain zuzen, zenbait estekatzailerentzako hartzaileak adierazten dituzte (Jha *et al*, 2019). Hantura testuinguru batean jariatutako faktoreak askatuz gero, mikroglia zelulen migrazioa eta ugaritzea eragiten da. Zelula horiek garuneko gune kaltetuetan pilatzen dira eta agente patogenoari eraso egiten diote (Honda *et al*, 2001). Horretarako, mikrogliak forma ameboideoa duen

fenotipoa hartzen du. Hantura prozesua konpontzen ez bada eta garuneko homeostasia berreskuratzen ez bada, hantura kronikoko egoerara irits daiteke. Egoera horretako mikroglia kaltegarria da; izan ere, faktore proinflamatorioen etengabeko jarioek neuronen, astrozitoen eta oligodendrozitoen funtzioari eragiten diote (Benarroch, 2013), eta gaixotasun neurodegeneratibo kronikoak garatzen laguntzen dute (Polazzi eta Contegone, 2002; Streit, 2004).

LPS-aren administrazioa neuro-hantura eredu gisa erabili ohi da (Ho *et al,* 2015; Zakaria *et al*, 2017). LPS-ak Toll 4 (TLR4) motako hartzailearen mendeko bide batetik aktibatzen ditu mikroglia zelulak, eta horrekin batera, hanturazko zitokinak ekoizten eta askatzen dira, hala nola, IL-1β (Dinarello, 1996), IL-6 (Akira eta Kishimoto, 1993) eta TNF-α (Tracey eta Cerami, 1994). Fagozitosiarekin eta superoxidoarekin lotutako entzimen ekoizpena ere aktibatzen du (Suzumura *et al*, 1991), eta aldaketa morfologiko dramatikoak eragiten ditu. LPS-aren aurrean, mikroglia zelula handia, laua eta biribila bihurtzen da (Abs-El-Basset eta Fedoroff, 1995). Zelularen morfologian eta jardueran gertatzen diren aldaketekin batera zitoeskeletoaren zenbait proteinaren antolaketa eta adierazpena aldatu egiten direla ezarri da (Abs-El-Basset eta Fedoroff, 1995), eta LPSak funtzio mikroglialak aldatzen dituela iradokitzen da. Gauza bera gertatzen da lesio edo neuroendekapen batean, non ATP-ak askatzeak mikrogliaren mugikortasuna handitzen duen, eta hori funtsezkoa da mikrogliak bere babes-funtzioa bete dezan (Honda *et al*, 2001). Ikusi da, halaber, β-amiloide patologian, zeina EAko ohiko neurodegenerazioaren eragilea den, mikroglia zelulak hanturaren aldeko zitokinak ere jariatzen dituela, hala nola IL-1β, IL-6 edo TNF-α. Hauek funtsezkoak dira Aβ peptidoaren agregatuetara bideratutako mugikortasuna eragiteko eta horiek fagozitosiaren bidez ezabatzen laguntzeko (Eikelenboom eta van Gool, 2004).

1.3. Lanaren hipotesia

Aurrekari horiekin, argi dago proteinen tokiko sintesia prozesu garrantzitsua dela zelula polarizatuetan, adibidez, neurona eta glia zeluletan, proteoma subzelularra erregulatzeko. Tokiko itzulpenari buruzko azterketa gehienek testuinguru fisiologian duten zereginean jarri dute ardatza, nahiz eta berriki datuek frogatu fenomeno horrek testuinguru patologikoetan duen garrantzia, hala nola β amiloide peptidoaren metaketan edo nerbio periferikoei eragindako lesio traumatikoetan. Garunean neuronak glia zelulez inguratuta daudenez, eta bi zelula-motak etengabe komunikatzen direnez, mikrogliak neuritetako

proteinen sintesi lokalean zeregin garrantzitsua duela proposatzen dugu, bai baldintza fisiologikoetan, bai β amiloide peptidoak eragindako patologian.

Bestalde, proteinen sintesi lokala ez dago neuronara mugatuta. Berriki egindako ikerketek zelula glialetan deskribatu dute fenomeno hori, hala nola oligodendrozitoetan eta astrozitoetan. Mikroglian fenomeno horretaz ezer gutxi dakigunez, proposatzen dugu proteinen sintesi lokalak ere garrantzi handia duela mikroglia-funtzioa oinarrizko baldintzetan erregulatzeko eta hantura- eta neuroendekapen-estimuluei erantzuteko.

HELBURUAK

2. HELBURUAK

Doktorego-tesi honen helburu orokorra mikrogliak neuronetako proteinen sintesi lokalean nola eragiten dion aztertzea da, bai baldintza fisiologikoetan bai β amiloide peptidoaren erantzunean, eta, era berean, mekanismo hori mikroglia zeluletan nola ematen den ulertzea.

Hauek dira gure helburu espezifikoak:

1. helburua: mikrogliak NSZko neuronetan tokiko proteomari ekarpena egiten dion zehaztea, bai baldintza basaletan, bai peptido amiloideak eragindakoetan.

1.1. Kondizio fisiologiko eta patologikoetan mikroglia dagoenean edo ez dagoenean, neuriten proteina-ekoizpena aztertzea.

1.2. Mikrogliak neuriten tokiko proteoman duen eragina aztertzea.

1.3. Baldintza fisiologiko eta patologikoetan mikrogliaren aurrean neuritaren itzulpen-fokuak aztertzea.

2. helburua: mikrogliaren prozesu periferikoetan proteinen sintesi lokala zehaztea.

2.1. Hanturaren erantzunean, mikrogliaren prozesu periferikoetan proteinen sintesi lokala aztertzea.

2.1.1. Mikroglia prozesu periferikoetan proteina-sintesirik gertatzen den zehaztea eta hanturaren testuinguruan ea sintesia asaldatuta dagoen zehaztea.

2.1.2. Hanturara testuinguruan, mikrogliaren prozesu periferikoetan zein transkritu lokalizatzen diren aztertzea.

2.1.3. Mikrogliako prozesu periferikoetan tokiz itzulitako transkritu horien inplikazio funtzionala aztertzea.

2.2. Mikrogliaren prozesu periferikoetan proteinen sintesi lokala aztertzea, β-amiloide patologiaren testuinguruan.

2.2.1. Mikroglia prozesu periferikoetan proteinen sintesi lokala aldatu den zehaztea, β amiloide peptidoaren testuinguruan.

2.2.2. β amiloide peptidoari erantzunez, mikrogliaren prozesu periferikoetan zein transkritu lokalizatuta dauden aztertzea.

MATERIALAK ETA METODOAK

3. MATERIALAK ETA METODOAK

3.1. Animaliak

Animalien protokolo guztiek Europako 2010/63/EU zuzentarauari jarraitzen diote, eta UPV/EHUko etika-batzordeak onartu ditu. Sprague-Dawley arratoiak hazi ziren UPV/EHUren instalazioetan, eta CO_2 bidez hildako arratoien enbrioi-garunak eta jaiotza-ondokoak lortu ziren.

3.2. Hazkuntza zelularra

3.2.1. Mikroglia kulturak

0-2 (P0-2) eguneko jaiotza osteko arratoietako glia labore mistoetatik abiatuta mikroglia isolatu egin zen. Lortutako burmuinen kortexa eta hipokanpoa 4mL-tan disekzionatu ziren, Hanken gatz-soluzio orekatuarekin (HBSS, Gibco, Massachusetts, Estatu Batuak). Entzima-disoziazioa egin zen, %0,25 tripsina (Sigma Aldrich, Merck, Darmstadt, Alemania) eta %0,004 DNAsa (Sigma Aldrich) erabilita, 15 minutuz 37ºC-tan. Ondoren, antibiotikoak (penizilina eta estreptomizina) eta antimikotikoak (G anfoterizina) dituen IMDM medioan disolbatutako FBS-arekin (Hyclone serumaren % 10; Gibcorena dena) erreakzioa blokeatu zen. Ondoriozko zelulen esekidura 1200 b/min-ra zentrifugatu zen 6 minutuz giro-tenperaturan. Jalkina lehen aipatutako medioarekin berreseki zen, eta tamaina desberdinetako orratzetatik (21 G eta 23 G) pasatuz disoziatu zen. Zelulak berriro zentrifugatu ziren 1200 b/min-ra 6 minutuz, berriz IMDM medioarekin berreseki zirelarik eta aldez aurretik poli-D-lisinarekin tratatutako 75 cm^2-ko azalerako hazkuntza-flasko aireztatuetan erein ziren. Zelulak 37 ° C-tan mantendu ziren % 5eko CO_2-ko atmosferarekin hezetutako inkubagailuan. 24 ordura medioa aldatu zitzaien, %10eko FBS (Fisher Scientific, Massachusetts, Estatu Batuak), 2mM glutamina (Gibco) eta 50 u/mL antibiotikoak (penizilina eta estreptomizina; Gibco) dituen DMEM (Gibco) medioa gehituz. Medioa hiru egunetik behin berritzen joan zen.

10 DIV-ren (egun *in vitro*) ondoren, hazkuntza-flaskoak 180 b/min-ra astindu ziren 4 orduz eta 37ºC-tara, astrozito-geruzaren gainean hazten den mikroglia askatzeko. Astrozitoak hazkuntza-ontziari itsatsita geratzen dira. Mikroglian aberastutako gainjalkina zentrifugatu, zelulen esekidura berreseki eta mikroglia dentsitate desberdinetan erein zen (3.500-42.000 zelula/cm^2) aldez aurretik poli-D-lisinarekin tratatutako plaken gainean, esperimentu bakoitzaren beharren arabera: neuronekin

egindako ko-kultiboen kasuan 1:3 proportzioa erabili zen (mikroglia bat hiru neuronako) eta mikroglia-kultura primarioen kasuan, zelulak 15.500-21.000 zelula/cm^2-ko dentsitatean erein ziren (dentsitate txikiko kulturak) edo 31.000-42.000 zelula/cm^2-ko dentsitatean (dentsitate handiko kulturak). Kasu guztietan, mikroglia hiru egunez mantendu zen kultiboan (3 DIV) serumik gabeko neurobasaleko medioan, B27 eta glutamina 2 mM (guztiak Gibcorenak) gehiturik zituela. Medio hau bi arrazoirengatik erabili zen. Lehenik eta behin, neuronekin egindako ko-kultiboetan erabilitako medioa zelako (ikus 3.2.3 atala), neuronen bideragarritasuna errazteko. Bigarrenik, transfekzioek ez dute onartzen seruma duen mediorik, horrela, ko-kultiboetan erabilitako formulazioa egokia zela mikrogliaren hazkuntzarako egiaztatu ondoren, medio hori glia kultibo guztietan erabiltzea erabaki zen, esperimentuen arteko sendotasunari eusteko. Handik 3 egunera, zelulak honako hauekin tratatu ziren: LPS (150ng/mL, Sigma Aldrich), ATP (300µM, Tocris, Bristol, Ingalaterra), β-Amiloide (Aβ; 3µM, prestaketa materialen eta metodoen 3.3 atalean) edo M-CSF (25ng/mL, Preprotech, Nueva Jersey, Estatu Batuak) eta dagozkien garraiatzaileak, emaitzen atalean zehaztutako denboran.

3.2.2. Giza mikrogliako lerro zelularren kulturak

SV40 (RZ525016) linea zelularreko poteak desizoztu ziren eta zelulak DMEM-en (Gibco) berreseki ziren, % 10eko FBS (Fisher Scientific), 2mM glutamina (Gibco) eta 50 u/mL antibiotikoekin (penizilina eta estreptomizina, Gibco). Ondoren, 1200 b/min-ra zentrifugatu ziren 5 minutuz, hauspeakina berreseki zen eta mikroglia 75 cm^2-ko gainazaleko flaskoetan erein zen, aldez aurretik % 0,01eko kolagenoarekin tratatuak.

Zelulak % 80-100eko betegunera iristean, TrypLE™ Express-ean (Gibco) disoziatu ziren 10 minutuz 37ºC-tan. TrypLE ekintza %10-ko seruma duen DMEM medioarekin blokeatu zen. Zelulak 1500 b/min-ra zentrifugatu ziren 6 minutuz, giro-tenperaturan eta poli-D-lisinaz tratatutako 6 putzutako plaketan erein ziren, 42.000-62.000 zelula/cm^2 -ko dentsitatean.

3.2.3. Neurona kulturak eta mikrogliarekin ko-kulturak

18 enbrioi-eguneko (E18) arratoi-garunetatik abiatuta hipokanpoko neuronak prestatu ziren, Banker eta Goslin, 1998an deskribatu bezala. Labur-labur, enbrioi-garunetako hipokanpoak disekzionatu ziren eta TrypLE Express-en (Gibco) bitartez disoziatu ziren 10 min-tan, 37ºC-tara. Zelulak bi aldiz garbitu ziren HBSS (Gibco) bidez, eta % 10 behien fetu-seruma, 2 mM L-glutamina eta 50 u/mL penizilina-estreptomizina (guztiak

Gibcorenak) zuen Neurobasal medioan berreseki ziren. Zelulak pipeta batekin homogeneizatu ziren eta 5 minutuz 800 b/min zentrifugatu ziren giro-tenperaturan. Zentrifugazioaren ondoren, zelulak aurrez deskribatutako medioan berreseki ziren. Hipokanpoko neuronak poli-D-lisinaz estalitako objektuetan hazi ziren, dentsitate baxuko 24 putzuko plaketan (18.500 zelula/cm^2). Kulturak 37ºC-tan mantendu ziren % 5eko CO_2-ko atmosferarekin hezetutako inkubagailu batean. 24 ordura, medioa hazkunde-medioarekin ordezkatu zen (1X B27, 2 mM glutamina eta 50 u/mL penizilina eta estreptomizina Neurobasalean). 24 ordura glia ez hazteko, 20mM 5´ fluorodesoxiuridina eta uridina (FDU+U, Sigma Aldrich) gehitu ziren, eta 3 egunetik behin medioaren erdia medio freskoarekin ordezkatu zen, zeinak 5´fluorodesoxiuridina eta 20 mM uridina zituen. 7 DIV-etara neurona batzuk mikrogliarekin batera kultibatu ziren (mikroglia lortzea materialen eta metodoen 3.2.1 atalean azalduta dago), 1/3 proportzioari eutsiz (mikroglia/neurona). 9 DIV-etara egin ziren tratamenduak eta 10 DIV-etara zelulak finkatu egin ziren %4 paraformaldehidoa eta %4 sakarosa zuen PBS-rekin (4. irudia).

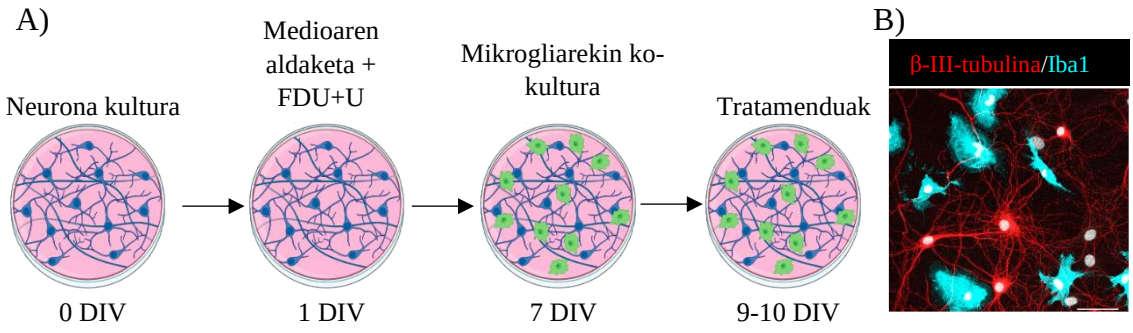

4. Irudia: A) Neuronen (urdina) eta mikrogliaren (berdea) arteko ko-kulturen denbora-lerroaren irudikapen grafikoa. B) Neurona (gorria) eta mikrogliaren (urdina) arte ko-kulturaren irudi adierazgarria. Anti-β-III tubulina (gorria) eta Iba 1 (urdina) antigorputzekin egindako kontrako tindaketa erakusten da. Eskala barra, 50µm.

3.2.3. Neurona kulturak eta mikrogliarekin ko-kulturak eraldatutako Boyden ganberetan (edo *transwells)*

Eraldatutako Boyden ganberak poliestireno gardeneko karkasak dira, 1 µm-ko diametroko poroak dituen polietilenozko tereftalatozko mintza dutenak. Neuronak mintzaren gainean hazten direnean, mintzak neuritei pasatzen uzten die, baina ez gorputz neuronalei (5. irudia). Horrek konpartimentu neuritikoaren tratamendua eta neuritetan aberastutako materialaren isolamendua errazten ditu.

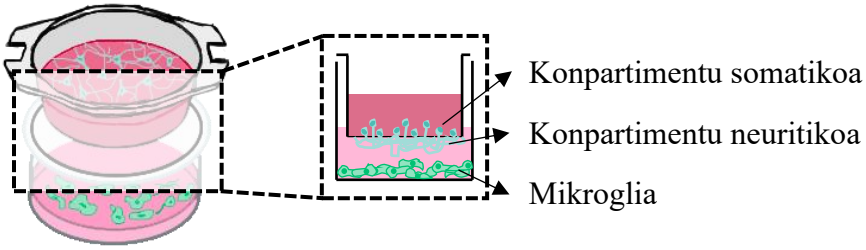

5. Irudia: Eraldatutako Boyden ganberen irudikapen grafikoa (*transwells*). Neuronak urdinez eta mikroglia berdez.

Hala, hipokanpoko neuronak lortzeko zehaztutako metodologia berari jarraituz (3.2.3 atala), kortexetik eta hipokanpotik isolatutako neuronak hazi ziren, eta Boyden ganberetan 1.000.000-1.300.000 zelula/cm^2 dentsitatean erein ziren. 7 DIV-ren ondoren, mikroglia gehitu zitzaien Boyden kameradun plakei, 1:3 proportzioan (mikroglia: neurona). 9 DIV-etan, zelulak Aβ edo DMSO-rekin tratatu ziren 24 orduz, eta itzulpen- edo proteomika-azterlanetarako laginak prozesatu ziren (materialen eta metodoen 3.6 atalean azalduta).

3.3. Aβ-ren oligomeroak prestatzea

Aβ oligomeriko disolbagarria ($A\beta_{1-42}$) prestatu zen, Steinek *et al* (2003) deskribatzen duten bezala. Labur-labur, $A\beta_{1-42}$ sintetikoa (Bachem, Budendorf, Suitza) hexafluoroisopropanolez (HFIP, Sigma Aldrich) disolbatu zen 1 mM-ko kontzentrazioraino; alikuotetan banatu eta lehortu egin zen. Oligomeroak eratzeko, peptidoak dimetilsulfoxido anhidroan berreseki ziren (DMSO; 5 mM, Sigma Aldrich), eta Hams F-12 gehitu zitzaion (PromoCell Labclinics, Bartzelona, Espainia) azken kontzentrazioa 100 mM-ra doitzeko. Peptidoak 4 °C-an inkubatu ziren gau osoan zehar. Aβ oligomerizatua gehitu zitzaien 9 DIV-eko neuronei eta 3 DIV-eko mikrogliari 3 μM-ko kontzentrazioan eta 24 orduz inkubatu zen. Kontrol gisa DMSO erabili zen.

3.4. *De novo* sintetizatutako proteinen markaketa

3.4.1. Puromizilazio-entseguak proteinen sintesia aztertzeko

Puromizina tirosinaren aminoazil-tRNAren antzeko antibiotikoa da eta erribosomek katalizatutako erreakzio batean sortzen den kate polipeptidikoan sartzen da. Anti-puromizina antigorputz espezifikoak proteinen sintesia *in situ* hautematea ahalbidetzen du. 10 DIV-etan, neuronak 2 µM puromizinarekin (Sigma Aldrich) tratatu ziren 10-30 minutuz. Mikrogliaren kasuan, puromizilazio-esperimentuak 3 DIV-etan egin ziren. Kontrol-zelulek hazkuntza freskoko bitarteko bakarra jaso zuten (ibilgailua). Puromizinak sintetizatu berri diren proteinak markatzen dituela egiaztatzeko, antibiotikoarekin tratatutako zelulak sintesi proteikoa inhibitzen duen anisomizinarekin (Sigma Aldrich) koinkubatu ziren 40 µM-tara. Zelulak 3 µg/ml digitoninarekin garbitu ziren PBS hotzean (Sigma Aldrich) neuronen kasuan, eta PBS-arekin mikrogliaren kasuan, %4 paraformaldehidoarekin (PFA) eta %4 sakarosarekin finkatu zirelarik. Ondoren, puromizina immunozitokimikaren bidez detektatu zen (materialak eta metodoak 3.7 atala) (6A irudia).

3.4.2. *Puromicyn Proximity Ligation Assay* (PuroPLA)

Sintetizatu berri diren proteina espezifikoak hurbiltasunaren bidezko lotura-erreakzioen edo *Proximity Ligation Assay*-en (PLA) bidez hauteman ziren, antigorputz anti-puromizina bat eta intereseko proteinen kontrako antigorputz espezifikoak konbinatuz. PLA seinalea Duolink erreaktiboekin (Sigma Aldrich) detektatu zen. Fluoreszentziaz markatutako zundak lotzeko eta anplifikatzeko plus zundak untxiaren aurkako antigorputz sekundarioei konjugaturik eta minus zundak arratoiaren aurkako antigorputz sekundarioei konjugaturik, “Duolink Red” (Sigma Aldrich) detekzio-erreaktiboekin konbinatuta erabili ziren. Labur esanda, emaitzak atalean zehaztutako estimuluak gehitu ondoren, puromizina gehitu zen 10 minutuz, eta %4ko PFA eta %4ko sakarosa duen PBS-arekin zelulak finkatu ziren. Kontrol negatibo gisa, sintesi proteikoa inhibitzen duen anisomizinarekin (40 µM) tratatutako mikroglia-zelulak erabili ziren, puromizinarekin edo puromizinarekin tratatu gabeko zelulekin konbinatuta. Finkatu ondoren, zelulek BGTrekin (PBS, %3ko BSArekin, 100 mM-ko glizinarekin eta %0,25 Triton X-100-arekin) iragazkortu eta blokeatu ziren 30 minutuz, eta anti-Par3 antigorputz primarioekin (1:1000, 07-330 Sigma Aldsigrich) edo anti-β-aktina antigorputz primarioarekin inkubatu ziren BGT soluzioan gau osoan zehar 4ºC-tara. Zelulak A garbiketa-tanpoian garbitu

ziren (Tris 0,01 M, NaCl 0,15 M, Tween20 %0,05) eta PLA zundekin inkubatu ziren fabrikatzailearen gomendioei jarraituz, 1 h 37 °C-tan. Garbiketa bakoitza 2 aldiz egin zen, 5 minutu bakoitza, A garbiketa-tanpoiarekin, eta 30 minutuz inkubatu ziren zelulak oligomeroak eta T4 ligasa duen lotura-erreaktiboekin, fabrikatzailearen gomendioen arabera prestatua (Duolink Red detekzio-erreaktiboak, Sigma Aldrich), 37 °C-tan. A garbiketa-tanpoiarekin 2 aldiz 5 minutuz garbitu ondoren, anplifikazioa egin zen ordu bat eta 40 minutuz, Phi29 polimerasak eta Texas Red hautemate-oligomeroak duten erreakzio-nahasketa batekin, fabrikatzailearen gomendioen arabera prestatua (Duolink Red detekzio-erreaktiboak, Sigma Aldrich) 37 °C-tan. Anplifikazioa B garbiketa-tanpoiarekin (Tris 0,2 M, NaCl 0,1 M) egindako hiru garbiketen bidez gelditu zen, ondoren PBS-arekin 5 minutuko hiru garbiketa egin zen. Azkenik, zelulak faloidinarekin inkubatu ziren Alexa-488 (10125092; Fisher Scientific) edo iFluor-647 (AB176759; Abcam, Cambridge, Erresuma Batuak) konjugaturik, F-aktina ikusteko. Faloidina-soberakina PBS-rekin garbitu ondoren, zelulak DAPI zuen Antifade ProLong Gold erreaktiboarekin (P-36930; Invrogen, Masssachusetts, Estatu Batuak) muntatu ziren (6B irudia).

3.4.3. *Click chemistry* edo klik kimikoa

Proteinen sintesi lokala hondo-seinaleen ratio altuagoarekin detektatzeko, klik kimika egin zen, hau da, aziden eta alkinoen lotura kobalentearen erreakzioa. Klik egiteko kimikan erabiltzen diren talde funtzionalak ugaztun-zeluletan berez ez daudenez, antigorputz anti-puromizinoaren eta markatu gabeko proteina endogenoen arteko lotura ez-espezifikoa saihets daiteke (Nagelreiter et al., 2018). Horretarako, O-propargil-puromizina (OPP, Jena Bioscience, Thüringen, Alemania) erabili zen, klik kimikarako egokia den puromizinaren antzeko alkino bat, non sintesian kate polipeptidikoen C-terminalean sartzen den, itzulpena geldiaraziz. C-terminal muturrean alkinoarekin markatutako proteinak geroago hautematen dira klik kimikaren bidez (aziden eta alkinoen Huisgen zikloadizioa), Cu-arekin (I) katalizaturik, biotina-talde bat sartuz azidarekin duen konjugazioari esker.

Kasu honetan, neuronak 1.000.000-1.300.000 zelula/cm^2ko dentsitatean hazi ziren Boyden ganberetan. 7 DIV-tara zenbait *transwells* mikrogliarekin batera kultibatu ziren (1:3 proportzioa, mikroglia: neurona), eta 9 DIV-tara 3 μM Aβ gehitu zitzaien edo haren ibilgailua, DMSO. 24 orduko tratamenduaren ondoren, zelulak OPP-arekin (25μM, Jena Bioscience) inkubatu ziren ordubetez. Kontrol negatibo gisa %0,1 DMSO-arekin

tratatutako zelulak erabili ziren. Isipu batekin konpartimentu somatikoa kendu ondoren, neuritak bi aldiz garbitu ziren PBS-rekin, eta proteina neuritikoak jaso ziren 20 mM Hepes, 100mM NaAc, 5mM MgAc, pH=7,5 zituen tanpoiarekin. Adierazten denean, zati somatikoa kendu zen OPP gehitu aurretik, eta laginak neurona desomatizatutzat hartu ziren. Ondoren, klik kimika egin zen, OPP-a azida-PEG_3-biotinarekin konjugatuz, Cu-ak (I) katalizatutako erreakzio batean. Biotina bidez markatutako proteinak hauspeatzeko azetona gehitu zen eta laginak -20ºC-tan inkubatu ziren 2 orduz. 15.000 x g-ra zentrifugatu ziren 5 minutuz eta hauspeakina metanolarekin garbitu zen. Proteinak 5 segundoz disolbatu ziren sonikazio bidez. Ondoren, berriro zentrifugatu ziren 15.000 x g-ra 2 minutuz, eta aurreko prozesua bi aldiz errepikatu zen. Azkenik, hauspeakina lagin-tanpoian berpiztu zen *western blotting* bidez proteina biotinilatuak detektatzeko (6C irudia; ikus 3.8 atala). Tanpoiak litio-dodezilsulfatoa (LDS), pH 8,5ean, SERVA Blue G250, fenol gorria (Invitrogen), eta 1,4-ditiotreitol (DTT, Thermo Scientific, Masssachusetts, Estatu Batuak) du.

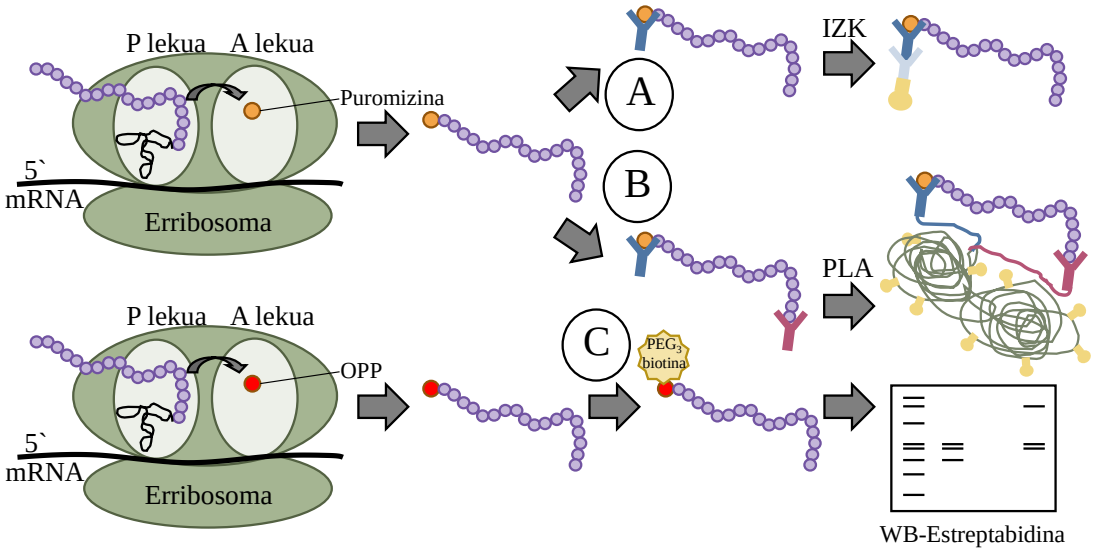

6. Irudia: **Proteina sintetizatu berriak markatzeko adierazpen eskematikoa.** A) Puromizilazio-entseguaren ondoren immunozitokimika (IZK), sintetizatu berri diren proteinak detektatzeko fluoreszentziaz markatutako antigorputz sekundario batekin. B) Puromizilazio-entsegua ondoren hurbiltasunaren bidezko lotura-erreakzioa (Puro–PLA) eginda. Puromizina sintetizatzen ari diren proteinei gehitzen zaie. Proteina konkretu bat N-terminalaren sekuentzia jakin bat ezagutzen duen antigorputz espezifiko bat erabilita eta anti-puromizina antigorputza erabilita hauteman daiteke. Bi antigorputzak behar bezain hurbil badaude, oligomero fluoreszente konkretu batekin lotu egiten da. Batista *et al*, 2017 irudi eraldatua. C) O-propargil-puromizina (OPP) gehitzea, eta, ondoren, klik kimika, non OPP-a modu kobalentean PEG_3-biotinarekin konbinatutako azida bateri lotzen den. OPP-PEG_3-biotina detektatzeko, Wester Blot (WB) erabiltzen da estreptavidina erabiliz.

3.5. Profil proteomikoen azterketa

Proteomika ikerketetarako, Boyden ganberetan hazitako neuronetatik ateratako estraktu neuritiko eta somatikoak erabili ziren goian deskribatu bezala. Proteinak erauzteko nahi ez zen konpartimentua isipu batekin kendu zen eta proteina neuritiko edo somatikoak 7M urea, 2M tiourea, %4 CHAPs eta 5mM DTT H_2O-n zituen buffer batekin bildu ziren. CICbioguneko proteomika zerbitzuak (Derio, Espainia) prozesatu ditu laginak. Labur esanda, proteinak FASP metodoaren bidez digeritu ziren (ingelesezko *Filter Aided Sample Preparation*; Wivniewski *et al*, 2009). Ondoren, laginaren proteinarekiko 1:20ko ratioa erabiliz proteinak tripsinizatu ziren, gau osoan zehar, 37 ºC-tara. Digestioaren ondoriozko peptidoak RVC2 25 kontzentragailuan (Christ) lehortu ziren, %0,1 azido formikoan berreseki ziren eta Cl8 puntak erabiliz gatzgabetu ziren (Millipore, Massachusetts, Estatu Batuak). Azkenik, peptidoak berriro ere %0,1 azido formikoan berreseki ziren.

Ondoriozko proteinak kromatografia likidoaren bidez aztertu ziren, masa-espektrometriari tandemean akoplatuta (LC-MS/MS), PASEFekin egindako timsTOF Pro espektrometro batean (Bruker Daltonics, Massachusetts, Estatu Batuak), Evosep ONE (Evosep) kromatografoari konektatuta. Lagin bakoitzetik 200 ng kargatu ziren eta 30 spd metodoaren bidez aztertu ziren, non 44 minutu inguruko gradienteak erabiltzen diren.

Proteinak MaxQuant softwarea erabiliz identifikatu eta kuantifikatu ziren (Tyanova *et al*, 2016). Bilaketa egiteko, Uniprot erreferentziako proteoma hartu zen, *Rattus norvegicus*-en sekuentziez osatua. 20 ppm eta 0.05 Da aitzindarien eta zatien tolerantzia gisa hartu ziren, hurrenez hurren. Ondorengo analisietan, proteinak identifikatzeko eta kuantifikatzeko, gutxienez %1<FD duten bi peptido dituztenak soilik hartu ziren kontuan. R ProBatch-en paketea erabili zen prozesatzeari eta lagin-taldeak lortzeari lotutako aldakortasun esperimentala zuzentzeko. Normalizatutako eta zuzendutako ugaritasunak Perseus programan (Tyanova *et al*, 2016) kargatu ziren adierazpen diferentziala Student-en t testaren bidez aztertzeko.

Proteinen ontologia genetikoaren (GO) analisia egin zen, osagai zelularra, funtzio biologikoa eta KEGG (Kiotoko Geneen eta Genomen Entziklopedia) seinaleztapen-bideak zehazteko.

3.6. Immunozitokimika (IZK)

Kulturen ondoren, neuronak eta mikroglia zelulak 4ºCtan finkatu ziren 20 minutuz, %4ko PFAn, %4ko sakarosarekin. Zelulak hiru aldiz garbitu ziren PBS erabiliz 5 minutuz, eta 30 minutuz iragazkortu eta blokeatu ziren BGT-an. Ondoren, laginak 4 ºC-tan inkubatu ziren gau osoan, intereseko proteinen kontrako antigorputz primarioekin (I. taula). Bost minutuko hiru garbiketa PBS-arekin egin ondoren, zelulak ordubetez inkubatu ziren giro-tenperaturan fluoroforoekin konbinaturik zuten antigorputz sekundarioekin: anti-sagua Alexa Fluor 594 (1:200, A-11005, Invitrogen), anti-arratoia Fluor 488 (1:200; A-11006), anti-akuria DyLight 350 (1:200, SA5-10093, Thermo Fisher Scientific) anti-untxia Alexa Fluor 488 (1:200, A-21206, Invitrogen) edo DyLight 405 (1:200, 611-146-002, Rockland Immunochemicals, Massachusetts, Estatu Batuak), anti-oilaskoa DyLight 350 (1:200, SA5-10069, Invitrogen). Inkubazioaren ondoren, hiru aldiz garbitu ziren laginak PBS-arekin, eta Antifade ProLong Gold (P-36930, Invitrogen) muntaiarekin DAPI-rekin edo gabe muntatu ziren.

Mikrogliarako, zelulak muntatu aurretik, Alexa Fluor-ekin 488 (10125092, Fisher Scientific) edo iFluor 647 (AB176759, Abcam) konjugaturik zuten faloidinarekin inkubatu ziren 20 minutuz, F-aktina markatzeko eta mikrogliaren prozesu periferikoak bistaratzeko.

I. Taula: Immunozitokimikan erabilitako antigorputz primarioak.

Antigorputz primarioak	**Espeziea**	**Erreferentzia**	**Diluzioa**
β-III tubulina	Untxiaren poliklonala	ab18207 (Abcam)	1/500
β-III tubulina	Oilaskoaren poliklonala	ab107216 (Abcam)	1/500
Anti-puromizina	Saguaren monoklonala	MABE343 (Merck)	1/500
Anti-kalretikulina	Untxiaren monoklonala	ab92516 (Abcam)	1/500
Actb	Untxiaren monoklonala	SAB5500001(Sigma Aldrich)	1/200
Par3	Untxiaren poliklonala	07-330 (Sigma Aldrich)	1/1000
Iba1	Untxiaren poliklonala	019-19741(Wako)	1:300
Iba1	Akuriaren poliklonala	234004 (Synaptic System)	1:500

Brdu	Arratoiaren monoklonala	ab8152 (Abcam)	1:1000

3.7. RNA markatzea

3.7.1. 5`Fluoruridinarekin (5`FU) markatzea

5`FU antimitotikoa RNAn sartzen da, sintesian zehar eta anti-BrdU (5-bromo-2-desoxiuridina) antigorputzen bidez bistaratzen da. Immunozitokimikaren bidez, beraz, zelularen RNA ikus daiteke.

Mikroglia lehenago deskribatu bezala kultibatu zen. 3 DIV-ren ondoren, zelulak 5`FU (200mM)-rekin inkubatu ziren 3 orduz. Zelulak 1X PBS-arekin garbitu ondoren, %4ko PFA eta %4ko sakarosa zuen PBS-arekin finkatu ziren. 5´FU markatzearen espezifikotasuna zehazteko, zelula batzuk 50 mg / ml DNAasa edo RNAsa-rekin (Sigma) inkubatu ziren 10 minutuz giro-tenperaturan.

3.7.2. RNA markatzea SYTO RNA Select bidez

SYTO RNA Select (Invitrogen) koloratzaile fluoreszente bat da, non RNAri selektiboki lotzen zaion. Immunozitokimikako prozedura estandarraren ondoren, zelulak 20 minutuz inkubatu ziren giro-tenperaturan, SYTO RNA Select erabiliz (500 nM, S-32703, Invitrogen) PBS-an. Laginak PBS-arekin garbitu eta Antifade ProLong Gold muntaketa-medioarekin muntatu ziren, DAPI-rekin edo gabe. SYTOren espezifikotasuna zehazteko, zelula batzuk 50 mg DNasa edo RNasa-rekin (Sigma Aldrich) inkubatu ziren 10 minutuz giro-tenperaturan.

3.8. *Western bloting* (proteinen immunodetekzioa)

Klik kimikaren ondoren (ikus 3.4.3 atala) biotinaz markatutako neuriten proteina-estraktuak %4-12ko gradiente jarraitua duten poliakrilamidazko geletan zatikatu ziren, eta nitrozelulosazko mintzetara transferitu ziren. Mintzak TBST (50 mM Tris, 150 mM NaCl eta% 0,1 Tween) zuen blokeo-tanpoiarekin eta % 5 behi-serum albuminarekin (BSA) blokeatu egin ziren giro-tenperaturan ordubetez. Ondoren, HRP peroxidasarekin (1:1000, Novex, Fisher Scientific) konbinatutako estreptavidinarekin inkubatu ziren blokeo-tanpoian 2 orduz, klik kimikaren bitartez *de novo* sintetizatutako proteinekin konjugatutako biotina detektatzeko (ikus 3.4.3 atala). TBST-arekin garbitu ondoren, mintzak ChemiDoc MP system (BioRad, Kalifornia, Estatu Batuak) gela-dokumentatzaile batean jaso ziren, kimioluminiszentearen bidez. Proteina biotinilatuen

kopurua atzemandako proteina-eduki guztiarekin normalizatu zen, Amidoblack bidez (Scharlau, Bartzelona, Espainia): mintzak minutu batez inkubatu ziren Amidoblack-ekin, %1 azido azetiko uretan diluituarekin garbitu ziren, lehortu eta ChemiDoc MP system (Biorad) gel-dokumentatzailean digitalizatu ziren. TBST-arekin garbitu ondoren, mintzak ChemiDoc MP system (BioRad, Kalifornia, Estatu Batuak) gel-dokumentatzaile batean errebelatu ziren, kimioluminiszentzia bidez.

Mikrogliako zelulen kasuan, proteinak RIPA tanpoiarekin erauzi ziren (5 mM Tris·HCl pH 7.6, 150 mM NaCl, %1 NP-40, %1 sodio desoxikolatoa, %0,1 Dodekaezilsulfato sodikoa; Pierce, Thermo Scientific) proteasa- eta fosfatasa-inhibitzaileen presentzian (Thermo Scientific). Proteina kopurua *BCA Protein Assay Kit* (Sigma 71285-M) deritzon kitarekin neurtu zen. Lagin bakoitzeko 6-20 μg proteina zatikatu ziren, %4-12 gradiente jarraituko poliakrilamidazko gel batean. Kasu honetan, transferentzia aurrez metanolarekin aktibatutako PVDF mintz batera egin zen (Cytiva Life Sciences™ Amersham™ Hybond™). Mintza blokeatu egin zen eta intereseko proteinen aurkako lehen mailako antigorputzekin inkubatu zen gau osoan, 4 ºC-tan: β-aktina (1:10000, SAB5500001 untxiaren poliklonala, Sigma), Zbp1 (1:500, PRS4401 untxiaren poliklonala, Sigma) edo GAPDH (1:10000, ab8245 saguaren monoklonala, Abcam). Inkubazioaren ondoren mintza 3 aldiz garbitu zen TBST-arekin eta peroxidasaz markatutako antigorputz egokiekin inkubatu zen (1:10000 Novex Fisher Scientific). Bigarren mailako antigorputza kendu ondoren, mintza hiru aldiz garbitu zen TBST-arekin, eta ChemiDoc MP system-ean (BioRad) errebelatu zen, kimioluminiszentzia bidez.

3.9. *In situ* hibridazioa

Ezagutu nahi ziren berariazko sekuentzien aurkako noranzkoko erribosonda espezifikoak transkribatu ziren, digoxigeninarekin (Roche, Basilea, Suitza) konjugatutako UTP zuten noranzkoko oligonukleotidoetatik abiatuta, *in vitro* MEGAshortscript (Ambion, Texas, Estatu Batuak) transkripzio-kitaren bidez. mRNA bakoitza detektatzeko, gainjarri gabeko bost erribosondako nahasketa bat erabili zen, antzeko GC edukiarekin. Erribosondak sortzeko erabilitako noranzkoko oligonukleotido guztiak T7 promotorearekin sintetizatu ziren (“GCCCTATAGTGTGTCGTATTAC-3’) 3' muturrean, aurretik mRNA bakoitzerako sekuentzia espezifiko hauek izanik:

RhoA.1: 5’-CCTGAAGAAGGCAGAGATATGGCAAACAGGATTGGCGCTTTTGG GTACAT-3'.

RhoA.2: 5’-CTCTGCAAGCTAGACGCGGGAAGAAAAAGTCGGGGTGCCTCATC TTGTGAGCCCTATAGTGAGTCGTATTAC-3'.

RhoA.3: 5’-CGGAGTCGTCGTCTTGAGCCTTGCATCTAAGAAGTCCCAGGTACT TTGTAGCCCTATAGTGAGTCGTATTAC-3'.

RhoA.4: 5’-CTCATAGTCTTCAGCAAGGACCAGTTCCCAGAGGTTTATGTGCCC ACGGT GCCCTATAGTGAGTCGTATTAC-3'.

RhoA.5: 5’-CTTCAGAGCTTTACTCCTTAACAGATTCCATTGGCAGAGCTCTGG GGTGG GCCCTATAGTGAGTCGTATTAC-3'.

Par3.1: 5’-GCCGTGCGGAGATGGCCGCATGAAAGTTTTCAGCCTTATCCAGC AGGCGG GCCCTATAGTGAGTCGTATTAC-3'.

Par3.2: 5’-TTCCACGAGAATGACTGCATTGTGAGGATTAACGATGGAGATCT TCGAAA GCCCTATAGTGAGTCGTATTAC-3'.

Par3.3: 5’-GGACGGTGGGATTCTAGACCTGGATGACATCCTCTGTGACGTTG CCGATG GCCCTATAGTGAGTCGTATTAC-3'.

Par3.4: 5’-TGCTTTTCGGCCTTATCAAACCACAAGTGAAATTGAGGTCACGCC TTCAG GCCCTATAGTGAGTCGTATTAC-3'.

Par3.5: 5’-TGCAGATTTGGGGATCTTCGTTAAGTCCATCATTAACGGGGGAG CTGCAT GCCCTATAGTGAGTCGTATTAC-3'.

Actb.1: 5´-AACCGTGAAAAGATGACCCAGATCATGTTTGAGACCTTCAACAC CCCAG CGCCCTATAGTGAGTCGTATTAC-3'.

Actb.2: 5´-ATGTGGATCAGCAAGCAGGAGTACGATGAGTCCGGCCCCTCCAT CGTGC AGCCCTATAGTGAGTCGTATTAC-3'.

Actb.3: 5´-AGACCTCTATGCCAACACAGTGCTGTCTGGTGGCACCACCATGT ACCCAG GCCCTATAGTGAGTCGTATTAC-3'.

Actb.4: 5´-GAGCGTGGCTACAGCTTCACCACCACAGCTGAGAGGGAAATCGT GCGT GAGCCCTATAGTGAGTCGTATTAC-3'.

Actb.5: 5´-TCCCTGGAGAAGAGCTATGAGCTGCCTGACGGTCAGGTCATCAC TATCGG GCCCTATAGTGAGTCGTATTAC-3'.

Kontrol negatibo gisa, arratoi-mikroglian berez aurkitzen ez den proteina berde fluoreszentea (Egfp) ezagutzen duten zundak erabili ziren. *Egfp*-ren aurkako zundak sekuentzia hauetatik sintetizatu ziren:

Egfp.1: 5'-GATGCCACCTACGGCAAGCTGACCCTGAAGTTCATCTGCACCAC CGGCAA GGCCCTATAGTGAGTCGTATTAC-3'.

Egfp.2: 5'-GACCACATGAAGCAGCACGACTTCTTCAAGTCCGCCATGCCCGA AGGCT AGGCCCTATAGTGAGTCGTATTAC-3'.

Egfp.3: 5'-ACTTCAAGGAGGACGGCAACATCCTGGGGCACAAGCTGGAGTAC AACTA CGGCCCTATAGTGAGTCGTATTAC-3'.

Egfp.4: 5'-AAGCAGAAGAACGGCATCAAGGTGAACTTCAAGATCCGCCACA ACATCG AGGCCCTATAGTGAGTCGTATTAC-3'.

Egfp.5: 5'-AGTTCGTGACCGCCGCCGGGATCACTCTCGGCATGGACGAGCTG TACAA GGGCCCTATAGTGAGTCGTATTAC-3'.

In situ hibridazio fluoreszentea Hengst *et al*, 2009an deskribatzen den moduan egin zen. Mikroglia zelulak objektu estalkian landu ondoren (dentsitatea: 15.500-21.000 zelula/cm^2), zelula horiek %4ko PFA- eta %4 sakarosa zuen PBS-arekin finkatu ziren 20 minutuz izotzetan. Ondoren, laginak etanoletan deshidratatu ziren, mRNAk hauspeatu eta gordetzeko. Hibridazioa egin aurretik, zelulak berhidratatu egin ziren, bi aldiz PBS-arekin garbituz, gero BGT-arekin iragazkortu ziren 30 minutuz giro-tenperaturan, eta azkenik, bi aldiz garbitu ziren PBS-arekin. Hala adierazten denean, 1µg Proteinasa K (Fisher Scientific) gehitu zitzaien 10 minutuz giro-tenperaturan, konplexu erribonukleoproteikoei lotutako proteinak digeritzeko. PBS erabiliz 5 minutuko garbiketak egin ziren hiru aldiz, zelulak PFA bidez finkatu ziren berriro, %4-ko sakarosarekin 10 minutuz, eta BGT-arekin garbitu ziren. Zelulak digoxigeninaz markatutako 50 ng erribosondarekin inkubatu ziren (5 erribosondetako bakoitzaren 10 ng), 15 µl hibridazio-tanpoiarekin (%50 formamida, 2X SSC, 0,2% de BSA, 1 mg ml^{-1} de E. coli tRNA, 1 mg ml^{-1} izokin-espermaren DNA) 3 ordu eta erdian, 37 °C-tan. Estalkiak behin garbitu ziren %50 formamidarekin, 2X SSC-an, eta %50 formamidarekin 1X SSC-an, biak 30 minutuz 37 °C-tan, eta hiru aldiz 1X SSC-rekin 15 minutuz, giro-

tenperaturan. Objektuak hiru aldiz garbitu ziren TBST-arekin, TBST-n blokeatu ziren %3 BSA-rekin, eta anti-digoxina antigorputzak (1: 500, DI-22, Sigma) eta anti-β aktina antigorputzak (1:200, SAB5500001, Sigma) inkubatu ziren blokeo-disoluzioan (TBST, %3 BSA-rekin) gau osoan zehar 4ºC-tara. Inkubazioaren ondoren, estalkiak hiru aldiz garbitu ziren TBST-arekin, eta saguaren aurkako bigarren mailako Alexa antigorputzak (488 edo 594) eta untxiaren aurkako antigorputzak (488 edo 594) erabili ziren, ordubetez giro-tenperaturan. Zelulak hiru aldiz garbitu ziren PBS-a erabiliz, 5 minutuz, giro-tenperaturan, garbiketa bakoitzean. Garbiketen ondoren, laginak DAPI zuen Antifade ProLong Gold (P-36930, Invitrogen) muntaketa medioarekin muntatu ziren.

3.10. Sindbis birusa bidezko transdukzioa

Infekzio biralaren bidez mikroglian intereseko proteinak gainadieraz zitezkeen zehazteko, Sindbis birusean oinarritutako bektore biralaren transdukzioa egin zen arratoi-mikroglia primarioetan. José Luis Zugazaren laborategiaren laguntzarekin, genetikoki eraldatutako Sindbis birusak (Invitrogen) lortu ziren EGFP sekuentzia sartzeko. pSInRep5 plasmidoa (7A irudia) oinarri gisa erabiliz, pEGFP/SR5 bektoretik digeritutako *Egfp*-ri dagokion sekuentzia subklonatu zen (7B irudia). Zelulak Sindbis birusarekin tratatu ziren hainbat diluziotan: 1/100, 1/150 eta 1/200, 48 orduz. Bestalde, 24 orduz Sindbisarekin tratatutako zelulen ingurune baldintzatua (1/100) erabili zen, birus-partikulen erreplikazioa errazteko eta, ondoren, 48 orduz beste mikroglia zelula batzuk berrinfektatzeko. Tratamenduen ondoren, zelulak %4ko PFA eta %4-ko sakarosarekin finkatu ziren, PBS-arekin garbitu ziren eta immunozitokimika bat egin zen, aurrez deskribatutako metodologiari jarraituz, oilasko poliklonalaren anti-GFP antigorputz batekin (1:1000, ab13970, Abcam).

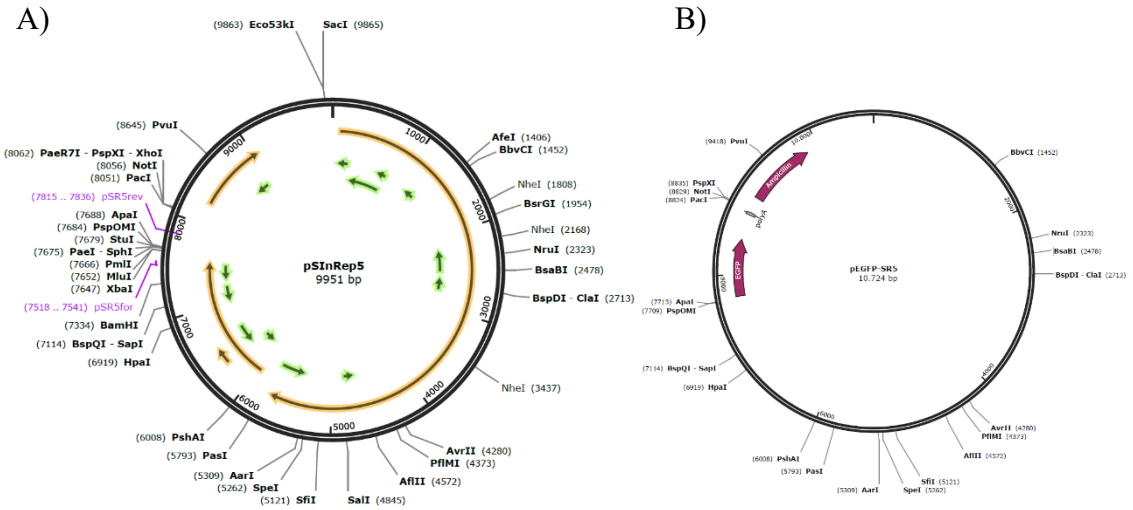

7. Irudia: pSInRep5 (A) plasmidoaren eta pEGFP -SR5 (B) bektorearen eskema grafikoa.

3.11. Transfekzioa RNA interferenteekin (siRNA)

RNA interferenteak erabili ziren *Actb* edo *Zbp1* geneak isilarazteko. Zbp1 DNA-RNA-rekin lotzen den proteina da, eta, β-aktinaren garraioarekin lotu da. Horretarako, RNA-n duplex interferenteak transferitu ziren lipofektamina erabiliz, fabrikatzailearen jarraibideei jarraituz (Invitrogen). Intereseko mRNA bakoitzeko bi siRNA mota diseinatu ziren: lehena, genearen eremu kodifikatzailearen kontra (*Actb* edo A; *Zbp1* edo Z), eta bigarrena, 3`UTR gunearen kontra (ingelesez *3´UnTranslated Region*), (3`*Actb* edo 3`A; *3`Zbp1* edo 3`Z).

siRNA-ek ezagutzen dituzten sekuentziak hauek dira:

- *Actb*-ren siRNA (9415, Ambion): 5`-GGAUUCCUAUGUGGGGACTT-3`
- 3`*Actb*-ren siRNA (s555268, Ambion): 5`-UUGACAAAACCUAACUUGCTT-3`
- *Zbp1*-ren siRNA (s139705, Ambion): 5`-GCAACGAGAUGAACCUCGATT-3`
- *3`Zbp1*-ren siRNA (555559, Ambion): 5`-CCACGUUAAGUGAAUGAAATT-3`

Transfekzioaren eraginkortasuna egiaztatu zen denbora errealeko RT-PCR eta *Western blot* bidez. Bestalde, siRNA-ek mikrogliaren prozesu periferikoetako intereseko mRNAen lokalizazioari eragiten zioten ere zehaztu zen, *in situ* hibridazioaren bidez.

3.12. Denbora errealeko RT-PCR

siRNA-ekin tratatutako mikroglia zelulak Trizol-arekin (Fisher Scientific) bildu ziren, eta RNA osoa fase-banaketaren bidez isolatu zen, fabrikatzailearen jarraibideei jarraituz. RNA 15 µl H_2O-tan berpiztu zen, eta NanoDrop™ (Thermo Fisher) espektrofotometroan neurtu zen haren kontzentrazioa. RNA-ren 300-500 ng tratatu ziren DNAsa-rekin, eta kontrako transkripzioa egin zitzaien Oligo $(dT)_{20}$ zebadoreari, SuperScript IV First-Strand Synthesis SuperMix (Fisher Scientific) kita erabiliz eta fabrikatzailearen jarraibideei jarraituz.

Zebadoreen eraginkortasuna zuzen patroiaren metodoaren bidez ebaluatu zen. Horretarako, esperimentu bateko lagin guztien RNA-k nahastu ziren, eta intereseko mRNA-k anplifikatu ziren guztizko mRNA kantitate desberdinetatik abiatuta: 100 ng, 10 ng, 1 ng, 100 pg eta 10 pg *Actb* eta *Gapdh* zebadoreen kasuan, eta 12 ng, 4.8 ng eta 2.4 ng *Zbp1*-aren kasuan (beste kopuru batzuk ez baitziren optimoak izan RNA anplifikaziorako). Kontzentrazioen logaritmoa (X ardatza) eta dagozkien zikloak (Y ardatza) erabiliz, zuzen patroi bat egin zen, R^2 determinazio-koefizientea eta dagokion ekuazioa lortuz (8. irudia). Zebadore bakoitzaren anplifikazio-eraginkortasunaren (Eamp) 2. oinarriko logaritmoa kalkulatu zen, baldintza bakoitzaren zikloaren atalaseak (Ct) zuzentzeko, ekuazio honen arabera:

$$\log_2 Eamp = \log_2 10^{1/-x}$$

Ondoren lortutako datu guztiak zuzen patroiaren bidez zuzendu ziren, nahiz eta *Zbp1*-en anplifikazio-eraginkortasuna balio onargarrietatik kanpo egon (%85-115 gure kasuan). Zbp1 gainerako anplifikadoreekin alderatzean bereziki nabarmenak diren zebadoreen arteko anplifikazio-diferentziak direla eta, Ct zuzentzea erabaki dugu. Anplifikaziorako Power SYBR Green PCR Master Mix (Fisher Scientific) kita erabili zen. Erreakzioek baldintza hauek bete zituzten: 95 ºC-ko 10 minutuzko, 95 ºC 15 segundozko, 60 ºC minutu batezko 40 ziklo. Hona hemen RNA interesgarri bakoitza anplifikatzeko erabili diren zebadoreen oligonukleotido sekuentziak:

- *Actb* (*Rattus norvegicus*): Fw: 5`-TACAACCTTCTTGCAGCTCC-3`; Rv*:* 5`-ATACCCACCA TCACACCCTG-3`.
- *Zbp1* (*Rattus norvegicus*): Fw: 5`-GTGCAAGTTCTGAAGCCACG-3`; Rv: 5`-GCCTGCACTT CATCC TCTCT-3`.

- *Gapdh* (*Rattus norvegicus*): Fw: 5`-TGCCAGCCTCGTCTCATAGA-3`; Rv: 5`-TGACTGTG CCGTTGAACTTG-3`.

Giza mikroglia zelula-lerroen kasuan, aurretik aipatutako protokolo bera egin zen, eta erabilitako zebadoreen oligonukleotido sekuentziak hauek dira:

- *ACTB* (*Homo sapiens*): Fw: 5`- CTGAAGTACCCCATCGAGCA-3`; Rv: 5`-GGTCTCAA ACATGATCTGGGT-3`.
- *GAPDH* (*Homo sapiens*): Fw: 5`-TGCCAGCCTCGTCTCATAGA-3`; Rv: 5`-TGACT GTGCCGTTGAACTTG-3`.

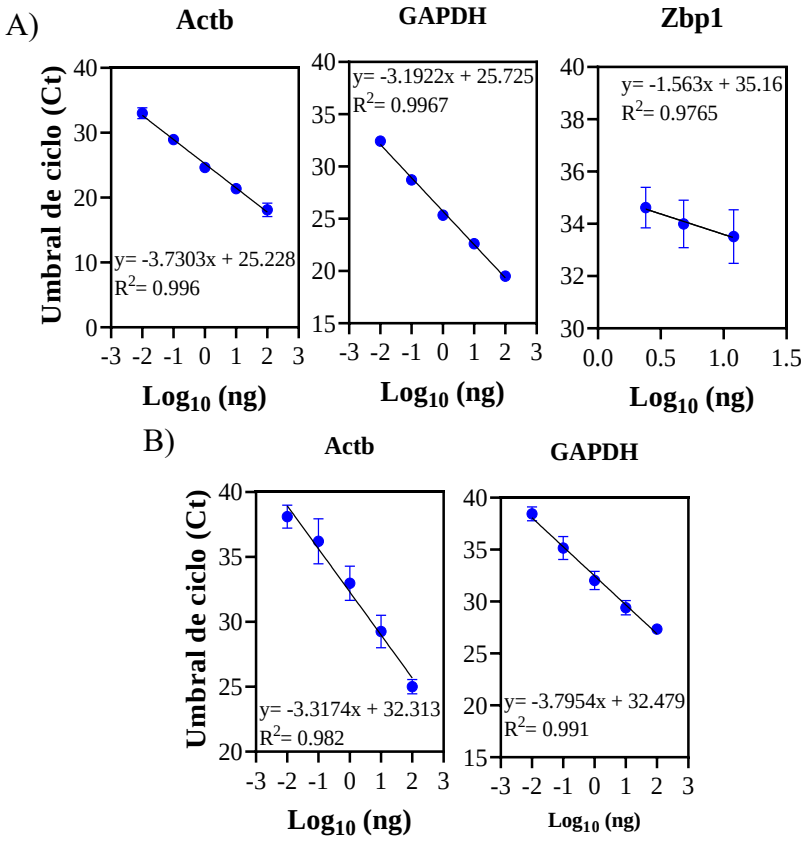

8. irudia: Zebadore bakoitzerako zuzen patroia. A) *Actb, Gapdh* eta *Zbp1* zebadoreen zuzen patroia arratoietatik lortutako mikrogiletarako. B) *ACTB* eta *GAPDH* zebadoreen zuzen patroia, giza mikroglia zelula-lerroetarako. Zuzen bakoitzari dagokion ekuazioa eta Pearson-en R-a.

3.13. Irudiak eskuratzea eta prozesatzea

Irudiak EC Plan-Neofluar 40 / 1,30 Oil DIC M27 objektiboa erabiliz eskuratu ziren, Axio-Observer Z1 mikroskopio batean, AxioCam MRm Rev.3 (Zeiss, Oberkochen, Alemania) eta Hamamatsu EM-CCD ImagEM (Hamamatsu Photonics, Hamamatsu, Japon). Irudiak hartzeko doikuntzak esperimentu bakoitzeko ibilgailuarekin tratatutako lagin baten ausazko eremu batean zehaztu ziren, pixel-intentsitateak maila linealaren barruan daudela

bermatuz eta seinalea asetzea saihestuz. Irudiak ZEN 2 softwarearen 2.0.0.0 bertsioarekin eskuratu ziren (Zeiss). Esperimentu jakin batean lagindutako zelula guztiek doikuntza berberak izan zituzten. Ahal izan zen guztietan, ausazko bost eremutako irudiak hartu ziren objektu-estalki bakoitzeko, eta bi estalki-objektu, baldintza esperimental bakoitzeko. Irudi gehienak AxioCam-ekin eskuratu ziren. Baina urrutiko espektro gorrikoak zituzten irudiak Hamamatsu kamera erabilita eskuratu ziren.

3.14. Intentsitateen analisia irudi ez-binarizatuetan

Proteina-ekoizpena neurtu zen puromizina bidezko markaketaren fluoreszentzia-intentsitatea kuantifikatuz, FIJI/ImageJ programaren bidez. Intentsitate horiek aztertu ziren atalak ausaz hautatu ziren, eta, ondoren, lerro-erremintaren bidez luzatu ziren ondorengoa eginez: FIJI/ImageJ > *File* > *Open (do not autoscale)* > *Segmented Line* > *Selection* > *Straighten* (Gamarra *et al*, 2020).

Luzatutako irudiaren gainean zirkulu zentrokideak sortu ziren, 10 µm-ko tarteetan, somaren ertzetik hasita, FIJI / ImageJ-rako makro batekin. Makro hori Jorge Valero doktoreak diseinatu zuen (*concentric_circles*). Luzatutako neuritetatik 150 µm betetzen zituzten 15 zirkulu sortu ziren. Mikrogliaren kasuan, zirkulu zentrokideen tartea 5 µm-koa izan zen, eta lamelipodioaren ertzetik ateratzen ziren, haren luzera osoa estali arte.

Tarte bakoitzeko fluoreszentziaren intentsitatea neurtu zen, eta horri hondoko pixelen intentsitatea kendu zitzaion.

3.15. Irudi binarizatuetako puntuen analisia

Hala adierazten denean, proteina-sintesia puromizina-tindaketaren foku diskretuen eta puromizina-fokuen eta SYTO RNA Select tindaketaren (proteina-RNA ko-lokalizazioa) fokuen arteko ko-lokalizazioaren arabera neurtu zen. Horretarako, Gamarran *et al* (2020) artikuluan argitaratutako protokoloa erabili zen. Hona hemen:

1) Irudiak FIJI/ImageJ > *File* > *Open* (*do not autoscale*) softwarean ireki ziren. Interesaren tindaketan (adibidez, puromizina)> *Process*> *Filter*> *Convolve* (ez prozesatu irudi guztiak).
2) Irudi hau konboluzionatu egin zen: *Image* > *Adjust* > *Brightness/Contrast* (esperimentu bereko lagin guztietan gutxieneko / gehieneko doikuntza bera)> *Image*> *Type*> *8 bit* > *Process* > *Binary*> *Make Binary (Method, MaxEntropy; Background, Default; Black background. Only convert current image).*

Irudiak binarizatu ondoren, neuritak edo mikrogliaren prozesu periferikoak aukeratu ziren, zatiketa lineala eginez. Luzatutako irudiaren gainean zirkulu zentrokideak sortu ziren 10 µm-ko tarteetan neuriten kasuan, eta 5 µm-koa lamelipodioen kasuan. Tamaina txikia zela eta, filopodioak tarterik sortu gabe aztertu ziren.

Mikroglian *de novo*-tik sintetizatutako proteinen eta RNAren arteko ko-lokalizazioa zehazteko, puromizina eta SYTO tindaketetatik datozen seinaleak binarizatu ziren. Bi irudietatik zetozen seinaleak irudi-kalkulagailuarekin> 1. irudia (Adibidez, Puromizina) *AND* 2. irudia (Adibidez, SYTO; egin klik leiho berria sortzean). Irudi hori Mask Entropy maskararekin leundu eta binarizatu egin zen, eta zirkulu zentrokideetan zatitu zen, 5 µm-ko tarteetan objektu-kopurua aztertzeko, arestian aipatu bezala.

Irudiak prestatzeko, tindatze interesgarria gris-eskala izatetik RGB izatera pasatu zen. Itzulpen-lekuen kuantifikazioan erabilitako irudi binarizatuak lortu ziren. Kasu guztietan, funtsa, kontrastea eta argitasuna doitu eta berdin ezarri ziren kontrol-baldintzetan eta baldintza esperimentaletan. Neuritak edo mikrogliak hautatzeko erabilitako markagailuak doitu egin ziren, irudiak ezin hobeto ikusteko.

3.16. Analisi estatistikoak

Laginaren tamaina irudien legendetan zehazten da. Analisi estatistikoak Prism 7-rekin (GraphPad Software) egin ziren ausaz egindako bloke-diseinu bati jarraituz, non esperimentu bereko laginak konbinatu baitziren esperimentuen arteko aldagarritasuna murrizteko. Aldagai bat kontuan hartuta, bi talde esperimentalen arteko konparazioa Student-en T testaren bidez egin zen. Alderaketa bi talde baino gehiagoren artean egin zenean, aldagai bat kontuan hartuta, bide bateko ANOVA (*one-way* ANOVA) erabili zen, eta, ondoren, Dunnet edo Holm-Sidak-en *post hoc* testa. Faktore bat baino gehiago izanez gero, bi bideko ANOVA (*Two-way* ANOVA) erabili zen, eta, ondoren, Tukey edo Dunnet-en *post hoc* testa, laginen eskakizunen arabera. Estatistikoki, $p<0,05$ adierazgarria da.

EMAITZAK

4. EMAITZAK

4.1. Mikrogliaren eragina neuriten tokiko itzulpenean, baldintza fisiologiko eta patologikoetan

4.1.1. Neuriten proteina-ekoizpena

Boyden edo *transwells* ganberetan kortex- eta hipokanpo-neuronak (E18) erein ziren. 7 DIV-ren ondoren, neuronak zituzten *transwell*-en erdiak mikrogliarekin batera erein ziren. Ko-ereinketa sistema horri esker, mikrogliak neuritetan duen eragina azter dezakegu, neuronak eta glia elkarrekin kontaktuan ez daudenean. Bi egun geroago, konpartimentu neuritikoak 3 µM DMSO-arekin edo Aβ oligomeroekin tratatu ziren, 24 orduz. Erauzketa baino lehen, konpartimentu neuritikoa OPP-arekin tratatu zen ordu batez, 37 ºC-tan, laginak digitoninarekin garbitu ziren eta proteina neuritikoak bildu ziren WB bidez aztertzeko. Bestalde, neuritak OPP-arekin tratatu aurretik, neuronak isipu batekin desomatizatu ziren. Lehenengo kasuan, Aβ-k neuritetan sintetizatu berri diren proteinen ekoizpena handitzen zuela ikusi zen kontrol negatiboarekiko, eta hori ez zen behatu DMSO-arekin tratatu ondoren (C vs Aβ; 9A irudia). Emaitza horiek bat datoz lehenago argitaratutako beste batzuekin, zeinak Aβ-ren oligomeroek axoietan proteinen sintesi lokala areagotzen dutela frogatzen duten (Baleriola *et al*, 2014). Hala ere, neuronak desomatizatu zirenean, ez zen Aβ-ren efektua ikusi, eta sintetizatu berri ziren proteina neuritikoen maila DMSO-arekin egindako tratamenduen ondoren aurkitutakoen antzekoa izan zen. Emaitza horiek Aβ-ak osagai somatikoa behar duela proteina neuritikoen ekoizpena handitzeko iradokitzen dute. (C vs Aβ; 9B irudia).

Bestalde, mikrogliaren presentziak kontrol negatiboarekin alderatuta somatizatutako neuritetan proteina gehiago ekoiztea eragiten du, bai baldintza basaletan (DMSO), bai Aβ bidezko tratamenduaren ondoren (M vs MAβ; 9A irudia). Efektu hori neurita desomatizatuetan ere kontserbatzen da (M vs MAβ; 9B irudia). Mikrogliaren presentziak proteina neuritikoen ekoizpenean duen eraginak ez duela osagai somatikoaren beharik iradokitzen da, eta ingurunera jariatutako faktoreek eragiten dutela, ez baitago neuronen eta mikrogliaren arteko harremanik hazkuntza-mota horretan.

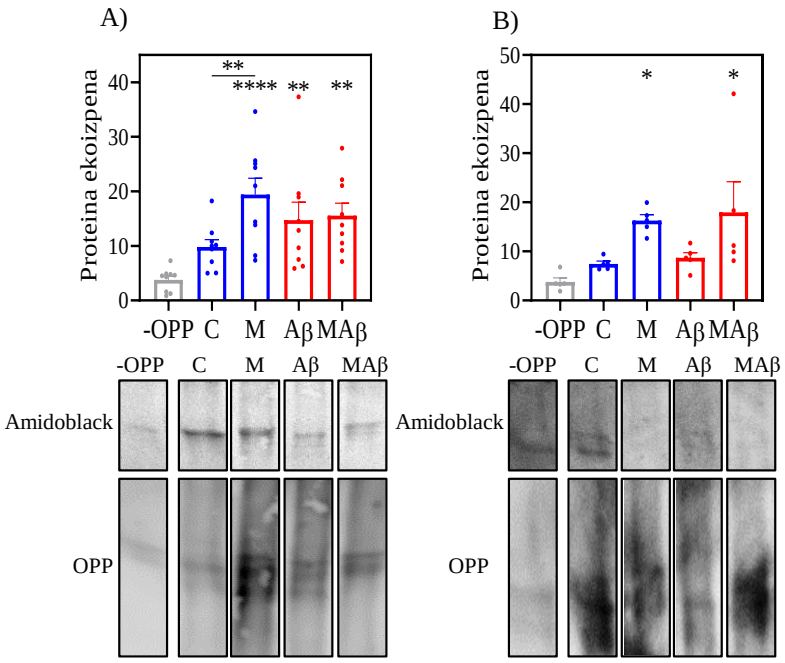

9. irudia: Proteina sintetizatu berrien ekoizpena neuritetan. OPP bidez egindako kimika bat erabiliz, sintetizatu berri diren proteinen ekoizpena Western transferentziaren analisiaren adierazpen grafikoa, soma (A) eta soma gabeko (B) neuritetan, Aβ-rik gabe edo Aβ-rekin tratatuak eta mikrogliarik (M) gabe edo batera hazita. Grafikoek 7 (A) eta 6 (B) esperimentu independenteen ± SEM batezbestekoa adierazten dute. Bide bateko ANOVAren analisia, eta, ondoren, Holm Sidak-en *post hoc* proba burutu da,* $p < 0.05$,** $p < 0.01$,**** $p < 0.0001$. Normalizatuak amidoblackari dagokionez. – OPP = OPP gehitu gabe; C = DMSO bidezko kontrola; Aβ = Aβ -rekin tratatzea; M = Mikrogliarekin ko-ereinketa; MAβ = mikrogliarekin ko-ereinketa eta Aβ tratamenduarekin.

4.1.2. Neuriten profil proteomikoaren azterketa mikrogliarekin edo gabe

Aldez aurreko datuek adierazten duten moduan, mikrogliaren presentziak proteina neuritikoen ekoizpena modulatzen du, bai baldintza basaletan, bai Aβ oligomeroen bidezko estimulazioaren ondoren. Mikrogliaren presentzian aldatutako proteinen identitatea zehazteko, neuriten profil proteomikoak aztertu ziren tandemeko masa-espektrometriara akoplatutako kromatografia likidoaren bidez (LC-MS/MS). Proteina neuritikoen aberastea ebaluatzeko kontrol diferentzial gisa, konpartimentu somatikoaren aterakin proteikoak erabili ziren. Doktorego-tesiaren proiektu honetan identifikatutako proteinak (set2), Maria Gamarra (set1) ikerketa-taldeko doktoratu aurreko ikertzaileak identifikatutakoekin batera aztertu ziren, astrozitoen presentziak neuritetan eragindako proteoma-aldaketetan interesa baitzuen. Bi datu-multzo horiek aldi berean aztertu ziren, bi talde esperimental berdin partekatzeagatik: DMSO-arekin edota Aβ oligomeroekin tratatutako kultibo neuronalak. Talde esperimental horiek kalitate-kontrolerako balio dute, analisien erreproduzigarritasuna egiaztatzeko aukera ematen baitute.

Neuritetako proteina bakoitzaren maila erlatiboak somako proteinekin alderatzean korrelazio positiboa (Pearson-en R 0.6556) somatzen da bi datu multzoen artean (set1 eta set2), baldintza esperimentalarekiko independentea delarik (10A irudia). Bi multzoetan 1828 proteina komun identifikatu ziren. Lehenengo taldean 988 (% 54) aurkitu ziren neuritetan eraldatuta somekiko; horietatik 565 (% 31) neuritetan aberastuta zeuden eta 423 (% 23) sometan (Set1; 10B irudia). Bigarren taldeari dagokionez, 1040 (% 57) proteina aldatuta aurkitu ziren neuritetan somari dagokionez, 622 (% 34) neuritetan aberastuta eta 418 (% 23) sometan (Set 2; 10B irudia). Nabarmen eraldatutako proteina guztietatik 619 proteina komunak izan ziren bi taldeetan (set1-aren % 63 eta set2-aren % 60; 2C irudia), baina guztiak ez zeuden zentzu berean aldatuta (10D irudia). Beraz, proteinak gene-ontologiaren (GO) analisiaren bidez zelula-kokapenaren arabera taldekatzeko, zelulaz azpiko konpartimentu berean aberastutakoak aukeratu ziren (10E irudian urdinez eta gorriz markatutakoak), bi datu-multzoetan. GO kategoriak zelula-osagaiaren arabera multzokatu ziren DAVID softwarea erabiliz (Huang *et al*, 2009a; Huang *et al*, 2009b). P balioan oinarrituta, 10 kategoria aberastuenak aztertu ziren. Konpartimentu somatikoan, proteina nuklearrak, erribosomalak, mRNA edo *splicing*-aren prozesamenduan inplikatutako proteinak, konplexu intrazelularraren osagaietako erribonukleoproteinak eta proteina nukleoarrak aberasten dira (10F irudia). Bestalde, neuritetan proteina zitosolikoak, atxikipen fokalean, hazkunde-konoan edota proiekzio neuronalean inplikatutako proteinak eta proteina zitoplasmatikoak aberasten dira (10G irudia). Emaitza horiek proteina neuritikoen isolamendua optimoa dela adierazten dute eta proteoma lokalaren eta proteoma somatikoaren (edo globalaren) analisi diferentziala ahalbidetzen dela.

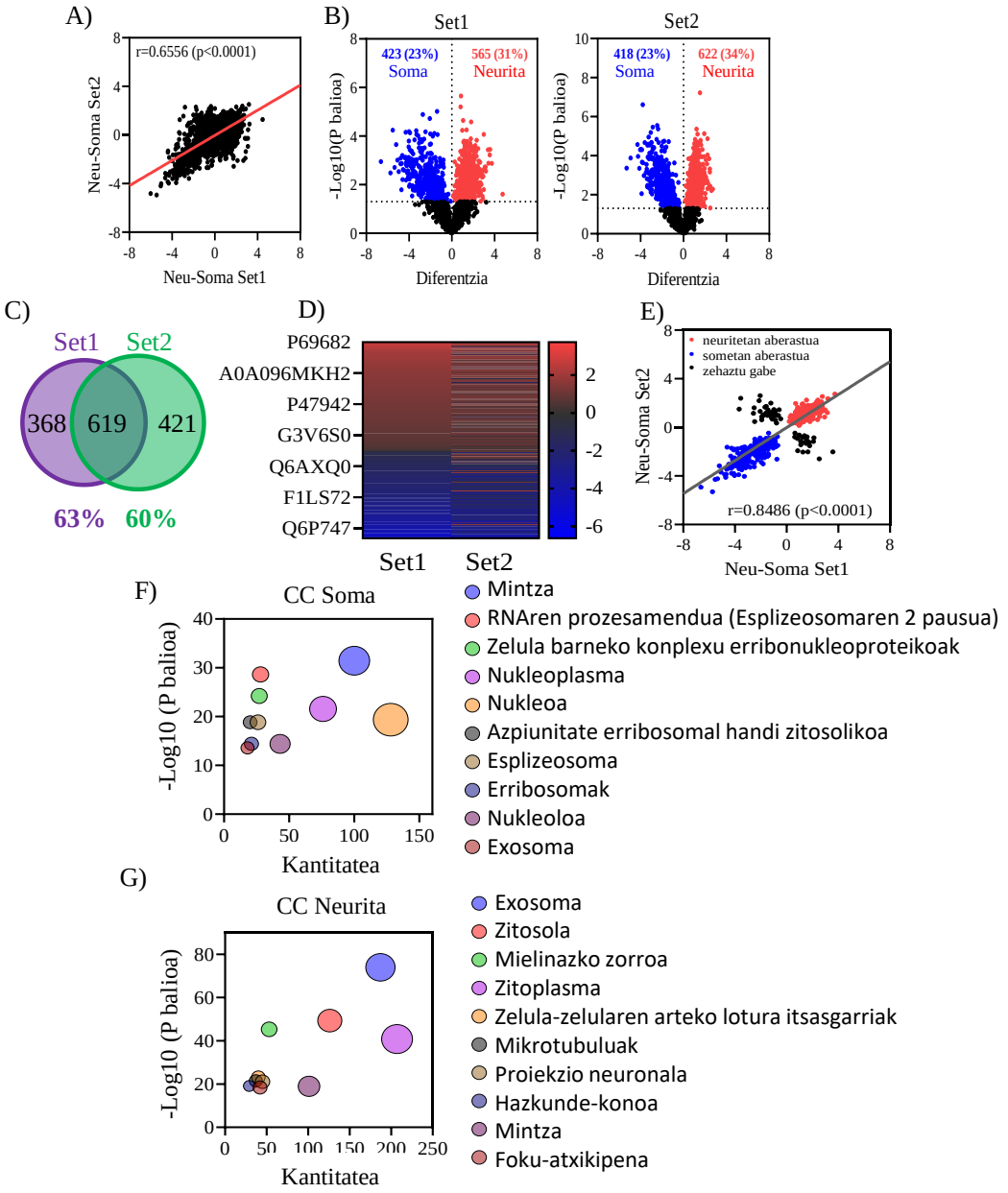

10. irudia. Neuriten profil proteomikoaren datuen normalizazioa, set 1 eta set 2 bidez lortuak. A) Proteina somatiko edo neuritiko guztien adierazpen erlatiboaren erdibitzailearen eta 2. setaren 1. setaren erdibitzaile totalaren (somatikoa eta neuritikoa) arteko korrelazioa, baldintza esperimentalarekiko independentea. B) "Volcano plot" grafikoa, bi esperimentu-setetako soma (urdina) edo neuritan (gorria) aberastutako proteinez osatua. Lerro bertikal gisa laginen arteko aldea zero dela eta esangura atalasea lerro horizontal gisa adierazten da (p = 0,05). C) Set1 eta Set2 identifikatutako proteinen arteko konparazioa. D) Bi esperimentu set-etan aldatutako proteina guztien bero-mapa. E) 1. eta 2. set-etan lortutako neuritan (gorria) edo soman (urdina) norabide berean aberastutako proteinen arteko korrelazioa. F) eta G) Frakzio somatikotik (F) eta frakzio neuritikotik (G) lortutako proteinen osagai zelularraren ontologia genetikoa (GO, ingelesez, "Gene ontology").

Proteina neuritikoak erauzteko gure metodoa balioztatu ondoren, tokiko proteoma aztertu genuen, esperimentu-baldintza desberdinen arabera: mikrogliaren presentzia edo gabezia baldintza basaletan edo Aβ oligomeroekin tratatu ondoren. Doktorego tesi honetan, mikrogliaren eragina aztertuko dugu (2. eta 3. laukiak; 11A irudia), astrozitoek neuritetan duten eragina aztertzen duten analisiak baztertuz (1. laukia; 11A irudia). Mikrogliaren presentziak 631 proteina neuritikoren adierazpena aldatzen duela ikusi zen. Proteina horietatik 341 proteina Aβ ez dagoenean edo presentzian erregulatzen dira (2. koadroa; 11A irudia). Bestalde, bai astrozitoak bai mikrogliak 127 proteina neuritiko aldatzen dituzte (3. laukia; 11A irudia).

Mikrogliak proteina neuritikoetan eragina duela ikusita, GO analisiaren bidez zein prozesu biologikotan eta seinaleztapen-bideetan parte hartzen duen aztertu nahi izan genuen. Neuronak mikrogliarekin batera haztean, zelula-atxikiduran, proteina-garraioan, endozitosian, *splicing*-ean eta neurotransmisoreen jariaketan parte hartzen zuten proteinak aberasten zirela ikusi genuen (11B irudia). Seinale-bideei dagokienez, besikula sinaptikoen zikloan, proteasoman, endozitosian, ardatz-gidan eta Huntingtonen gaixotasunean parte hartzen duten proteinak ugaritu egin ziren, besteak beste (11C irudia).

Bestalde, mikrogliak eta astrozitoak (127 proteina) aldatutako proteinak ere aztertu ziren. Kasu honetan, bi glia-mota hauek zelula-atxikiduran, proteina-garraioan, telomerasa bidezko telomeroaren mantentzearen erregulazio negatiboan, mikrotubuluen zeharreko besikula-garraioan eta proteina-tolesturan parte hartzen duten proteinen adierazpena aldatzen dela ikusi zen (11D irudia). Seinaleztapen-bideei dagokienez, kasu honetan ez genituen nabarmen aberastutako 5 termino baino gehiago ($p < 0,05$). Metabolismoarekin lotutako proteinen aldaketak hauteman ziren, hala nola antibiotikoen biosintesia, erretikulu endoplasmikoko prozesamendua, glikolisi/glukoneogenesia eta karbonoaren metabolismoa (11E irudia).

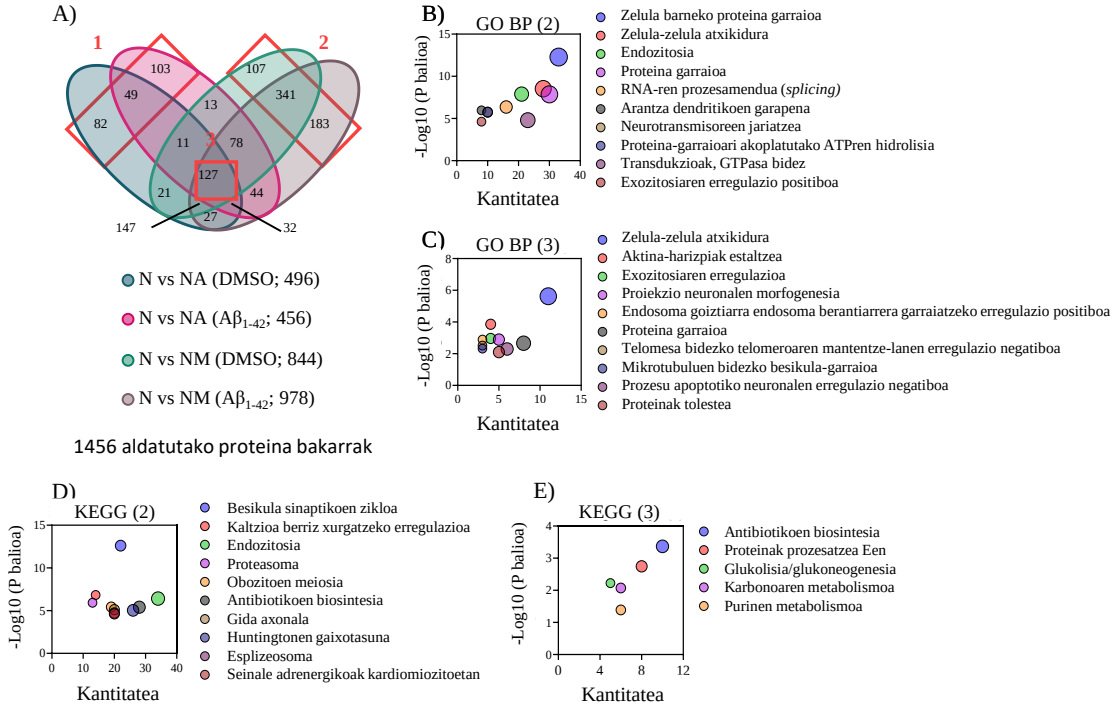

11. irudia: Mikrogliaren eraginez neuritetan aldatutako prozesu biologikoak eta seinaleztapen-bideak. A) Bi set-etako (Set1 eta Set2) neuritetan aldatutako proteinen guztien arteko konparazioa (1456 proteina), neuronen kulturan (N) astrozito-neurona ko-kulturekin (NA) alderatuta eta neuronen kulturan (N) mikroglia-neurona ko-kulturekin (NM) alderatuta, baldintza fisiologikoetan (DMSO) eta neurodegeneratiboetan (Aβ). B) Gene Ontologiaren (GO) analisia mikrogliak aldatutako 631 proteina neuritikoak biltzen dituzten prozesu biologikoak (BP). C) Kiotoko gene eta genomen entziklopediaren arabera (*Kyoto Encyclopedia of Genes and Genomes*, KEGG) mikrogliak aldatutako 631 proteina neuritikoek parte hartzen duten seinaleztapen-bideak. D) Gene Ontologiaren (GO) analisia mikrogliaren edo astrozitoen presentziak aldatutako 127 proteina neuritikoak taldekatzen dituzten prozesu biologikoak (BP). D) Kiotoko gene eta genomen entziklopediaren arabera (*Kyoto Encyclopedia of Genes and Genomes*, KEGG) mikrogliak edo astrozitoak aldatutako 127 proteina neuritikoek parte hartzen duten seinaleztapen-bideak.

Adibide zehatz batzuk jarrita, mikrogliaren presentziak funtzio desberdinetan parte hartzen duten proteinen beheranzko erregulazioa eragiten duela ikusi genuen, hala nola besikula sinaptikoen birziklapenean parte hartzen duten proteinetan (Snap25, Rab-3A, Cltc eta Atp6v1a); kaltzioaren birxurgapenean eta endozitosian parte hartzen duten proteinetan, hala nola Ap2b1, Ap2a2 eta Vta1; garapenean, birsorkuntzan eta gida axonalean parte hartzen dutenetan, hala nola Cdk5 eta Pak3; zelulen hazkundean eta heriotzan inplikatutako proteinetan (Cdc16); transkripzioan parte hartzen duten proteinetan, Prpf19 adibidez eta Aldoa bezalako proteinetan metabolismoan inplikatutakoak. Nabarmendu behar da proteina guzti horiek zentzu berean aldatzen direla, bai baldintza basaletan, bai Aβ oligomeroekin tratatu ondoren. Bestalde, mikrogliak zenbait proteinen beheranzko erregulazioa eragiten du baldintza basaletan, baina goranzko erregulazioa baldintza neurodegeneratiboetan, hala nola Magohb

(transkripzioan inplikatua) eta Casp3 (gaixotasun neurodegeneratiboen heriotza neuronalean inplikatua) bezalako proteinetan. Azkenik, gorantz erregulatutako proteina neuritikoak aurkitu genituen baldintza neurodegeneratiboetan, baina ez baldintza fisiologikoetan, hala nola Srsf7 (transkripzioan inplikatua), Eif4a3 (transkripzioan inplikatua) eta Aldh3a2 (metabolismoan inplikatua), besteak beste (12A irudia).

Bestalde, bai mikrogliak bai astrozitoak beherantza erregulatzen dituzte, bai DMSO-aren bai Aβ oligomeroen aurrean, LOC365985 (metabolismoan inplikatua), Stt3a (proteinen prozesamenduan inplikatua) eta Gpi (metabolismoan inplikatua) bezalako proteinak besteak beste (12B irudia).

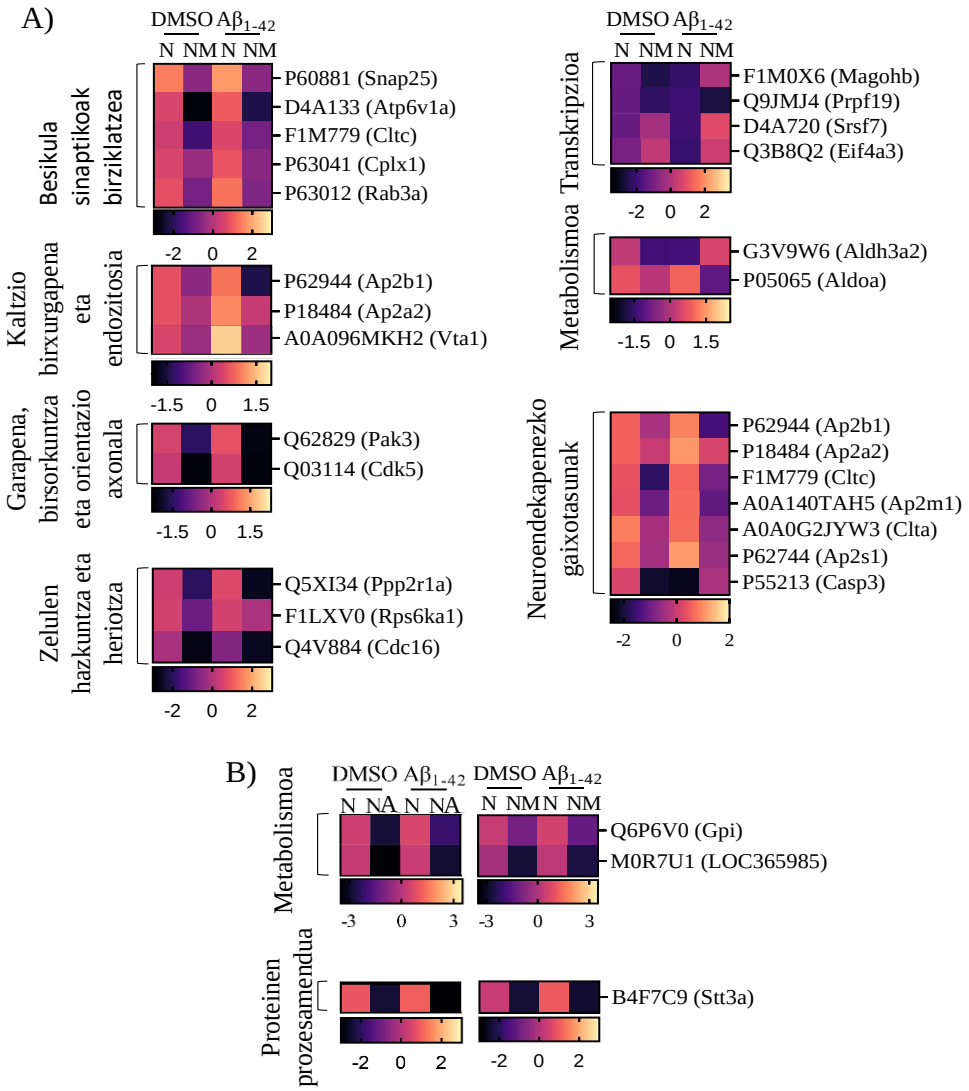

12. irudia. Kondizio fisiologiko eta patologikoetan (Aβ) mikrogliak erregulatutako proteina neuritikoen bero-mapak. A) Proteina neuritikoak mikrogliarik ezean (N) edo presentzian (NM) baldintza fisiologikoetan (DMSO) eta patologikoetan (Aβ), besikula sinaptikoen birziklapenean, kaltzioa birxurgatzean eta endozitosian, garapen, birsorkuntzan eta orientazio axonalean, zelulen hazkuntzan eta heriotzan, transkripzioan, metabolismoan eta neuroendekapenezko gaixotasunetan inplikatuak. B) Proteina neuritikoak mikrogliarik ezean (N) edo mikrogliaren presentzian (NM) edo astrozitoen presentzian (NA) egoera fisiologikoetan (DMSO) edo patologikoetan (Aβ), metabolismoan eta proteinen prozesamenduan inplikatuak.

Atal honetako emaitzen arabera, mikrogliak proteoma neuritikoa modulatzen du, eta hainbat prozesutan parte hartzen duten proteinak erregulatzen ditu; besteak beste, besikulen garraioa (birziklatzea, endozitosia), garapena eta metabolismoa.

4.1.3. Itzulpen-foku diskretuen detekzioa neuritetan

Mikrogliak proteina neuritikoen ekoizpena handitzen zuela ikustean, proteina zehatzetan aldaketak egiteaz gain, neuritetako itzulpen-gune diskretuen azterketa egin genuen mikroglia dagoenean edo ez dagoenean, oinarrizko baldintzetan eta Aβ oligomeroekin tratatu ondoren. Horretarako, hipokanpoko neuronak erein ziren poli-D-lisinaz estalitako objektuetan, eta 7 DIV-ren ondoren mikrogliarekin batera ko-erein ziren. *De novo* sintetizatutako proteinen foku diskretuak bistaratzeko, puromizilazio-saioak egin ziren. Literaturak islatzen duen bezala, leku neuritiko distaletako itzulpen-fokuek itzulpen lokalizatuko puntuak islatzen dituzte ziurrenik (Graber *et al*, 2013; Rangaraju *et al*, 2019). Proteinen sintesi lokala somari lotutako proteina-sintesia baino 20-30 aldiz txikiagoa izaten da, eta, beraz, erraza da fenomeno hori alde batera uztea (Gamarra *et al*, 2020). Puromizina-foku diskretuen kopurua neurita luzeenean zehar kuantifikatu zen, puromizinarako eta β-III tubulinarako positiboak ziren neuritetan, zoriaz lagindutako zeluletan eta 150 μm-ko distantziaraino aztertuz. Materialak eta Metodoak atalean aipatu dugun moduan, estrategia bat garatu dugu neuritetan puromizina detektatzeko, irudien prozesamenduan eta emaitzazko objektuen kuantifikazio lagunduan oinarrituta. Irudiak eskuratzea berdina izan zen baldintza guztietarako.

Lehenik eta behin, ikusi genuen Aβ-k handitu egiten zituela itzulpen-fokuak neuritetan, baina urrutitik baino ez (13. irudia). Honek Aβ-k eragina duela proteinen sintesi lokalean iradokitzen du, lehenago deskribatu den bezala (Baleriola *et al*, 2014).

Garuneko lesio traumatikoen ondorioz kaltetutako neuronek M-CSF adierazten dute. Faktore horrek mikroglia aktibatzen du, eta, horren ondorioz, ugaritzea eta lesioaren eremura migratzea eragiten du, kaltetutako neuronak desagerrarazteko (Takeuchi *et al*, 2001). Gainera, M-CSF-ak Aβ-ren jarduera fagozitikoa hobetzen du, neuronetan toxikotasuna prebenituz (Boissonneault *et al*, 2009). Horregatik, M-CSFa erabiltzen dugu mikroglia estimulatzeko eta neuriten itzulpenean duen eragina aztertzeko.. Kontrol gisa, M-CSF labore neuronalei aplikatzen diegu. Ikus dezakegunez, M-CSF-ak ez zuen eraginik Aβ-ren efektuan neuritetako proteinen sintesi lokalean (13. irudia).

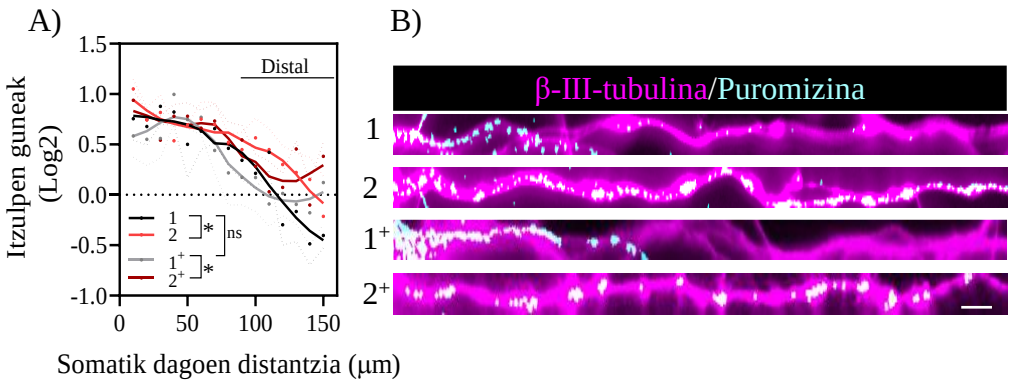

13. irudia. Itzulpen-fokuak neuritetan. A) DMSO (1), Aβ (2) eta/edo M-CSF (+)-rekin tratatutako neuronak. Grafikoak 5 esperimentu independenteren itzulpen-fokuak irudikatzen ditu, somatik neuritaren zati distaleraino. Bi bideko ANOVA analisia, neuriten alde distalean zentratuz, eta, ondoren, Tukey-ren *post hoc* proba, * $p<0.05$, ns ez esanguratsua. B) Itzulpen-guneen irudi adierazgarriak neuritan. Neurita luzeena marra segmentatu batekin aukeratu zen eta MaxEntropy (MaxEntropy) maskararekin zuzendu, leundu eta binarizatu egin zen. Anti-β-III Tubulina antigorputzarekin (magenta) eta itzulpen-puntuak anti-puromizina (cian) antigorputzekin egindako kontratindaketa erakusten da. Eskala-barra, 5µm. 1: Kontrola; 2: Aβ; 1^+: Kontrola+MCSF; 2^+: Aβ+M-CSF.

M-CSFren presentziak amiloideak neuritetan sortutako erantzunean eraginik ez zuela egiaztatu ondoren, M-CSF-aren gabezian eta presentzian mikrogliak proteina-sintesia aldatzen ote zuen aztertu genuen. Hala, mikrogliarekin eta mikrogliarik gabe hazi ziren neuronak, eta kultiboak DMSO-rekin edo Aβ oligomeroekin tratatu ziren 24 orduz. Lehenago esan bezala, neuritetan itzulpen-fokuak kuantifikatu ziren 150 µm-ko distantziara. Ko-ereinketetan, gliarekin kontaktuan zeuden eta ez zeuden neuritak aztertu ziren. Mikrogliaren presentziak itzulpen-foku distalak areagotzea eragiten zuela ikusi zen, baina soilik baldintza basaletan eta neuritak mikrogliarekin kontaktuan zeudenean (14A irudia). Hala ere, M-CSF bidezko mikrogliaren estimulazioak, mikrogliarekin kontaktuan zeuden neuritetan itzulpen-foku distalak areagotzea eragiteaz gain, gliarekin kontaktuan ez zeuden neuritetan itzulpen-foku distalak ugaritu zirela ere ikusi genuen (14B irudia).

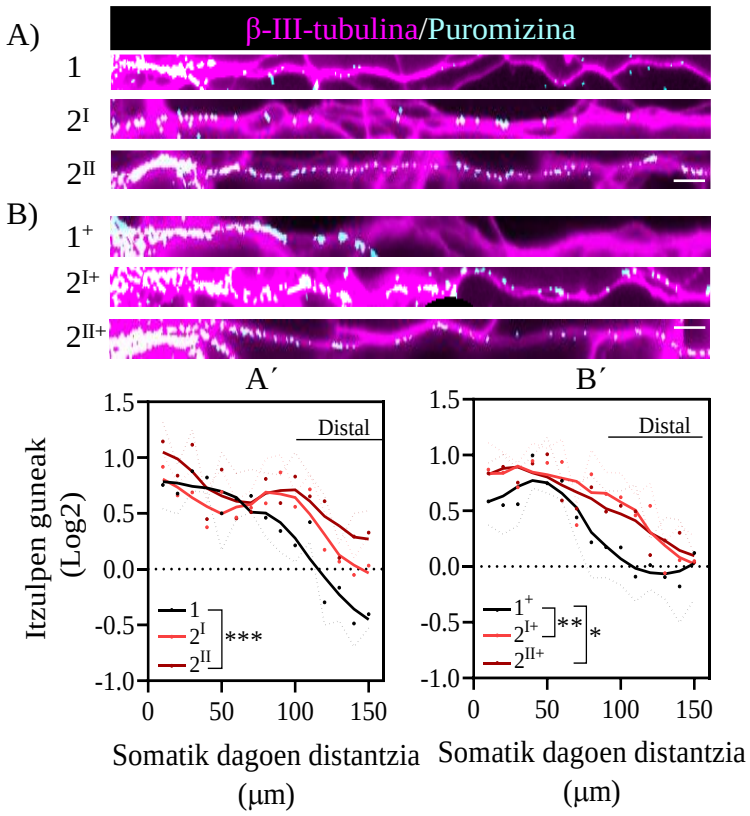

14. irudia: Itzulpen-fokuak neuritetan. Mikrogliarik gabeko neuronak (1) edo mikrogliaz batera ereindakoak (2), MCSF-arekin tratatu gabeak (A) edo MCSF-arekin tratatuak (B). Guztiak DMSO bidez tratatuak (kontrola). Grafikoek 5 esperimentu independenteko somatik neuritaren zati distalerainoko itzulpen-puntuak adierazten dituzte. Neuritetako alde distalean bi bideren ANOVA analisia, eta ondoren Dunneten *post hoc* proba,* $p < 0.05$,** $p < 0.01$,** $p < 0.001$. Neuriten itzulpen-puntuen irudi adierazgarriak. Neuritarik luzeena lerro segmentatu batekin hautatu zen eta MaxEntropy (MaxEntropy) maskararekin zuzendu, leundu eta binarizatu zen. Anti-β-III Tubulina antigorputzarekin (magenta) eta itzulpen-puntuak anti-puromizina (cian) antigorputzekin egindako kontratindaketa erakusten da. Eskala-barra, 5µm. Mikrogliarekin kontakturik ez duten neuritak (2^{I}) eta mikrogliarekin kontaktua duten neuritak (2^{II}).

Testuinguru neurodegeneratiboan, mikrogliaren presentziak ez zuen itzulpen-guneetan aldaketarik eragin, M-CSF (15A irudia) ez zegoenean. Aitzitik, M-CSF-arekin mikroglia estimulatzean, itzulpen-fokuak ugaritu ziren, baina soilik mikroglia ukitzen zuten neuritetan (15B irudia). Atal honetan deskribatutako emaitzek mikrogliaren presentziak neuronetako proteinen sintesi lokalean aldaketak eragiten dituela iradokitzen dute , batez ere baldintza basaletan, eta efektu hori indartu egiten da M-CSF bidezko mikroglia aktibatzean, bai baldintza basaletan, bai Aβ tratamenduaren ondoren.

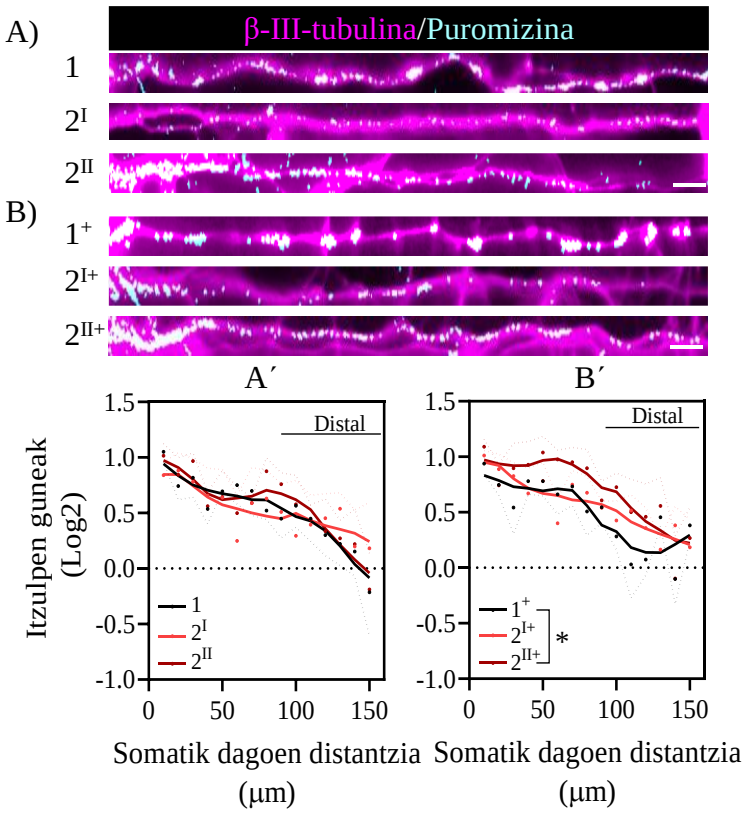

15. irudia: Itzulpen-fokuak neuritetan. Mikrogliarik gabeko neuronak (1) edo mikrogliaz batera ereindakoak (2), MCSF-arekin tratatu gabeak (A) edo MCSF-arekin tratatuak (B). Guztiak Aβ bidez tratatuak. Grafikoek 5 esperimentu independenteko somatik neuritaren zati distalerainoko itzulpen-puntuak adierazten dituzte. Neuritetako alde distalean bi bideren ANOVA analisia, eta ondoren Dunneten *post hoc* proba,* $p < 0.05$. Neuriten itzulpen-puntuen irudi adierazgarriak. Neuritarik luzeena lerro segmentatu batekin hautatu zen eta MaxEntropy (MaxEntropy) maskararekin zuzendu, leundu eta binarizatu zen. Anti-β-III Tubulina antigorputzarekin (magenta) eta itzulpen-puntuak anti-puromizina (cian) antigorputzekin egindako kontratindaketa erakusten da. Eskala-barra, 5µm. Mikrogliarekin kontakturik ez duten neuritak (2^{I}) eta mikrogliarekin kontaktua duten neuritak (2^{II}).

4.2. Proteinen sintesi lokala mikrogliaren prozesu periferikoetan

4.2.1. Mikrogliako zeluletan puromizilazio-saiakuntzak baliozkotzea

Lehenago esan bezala, puromizilazio-saiakuntzari esker, denbora-tarte jakin batean modu aktiboan sintetizatzen ari diren proteinak detekta ditzakegu. Gure laborategian metodo honen bidez neuronetako *de novo* sintesia atzeman dezakegula deskribatu genuenez (Gamarra et al., 2020) eta beraz, mikrogliako zeluletan ere baliagarria zela egiaztatu nahi izan genuen.

Mikrogliako zelulei puromizina gehitu zitzaien, eta immunozitokimikaren bidez, mikrogliaren prozesu periferikoetan (gure intereseko eskualdean) atzeman zen proteina-ekoizpena. Proteina-sintesia inhibitzen zuen anisomizina gehitzean, puromizinarekin batera, antigorputz anti-puromizinaren fluoreszentzia puromizinarik gabeko zelulen

mailara murriztu zen (16. irudia). Honek puromizilazio-saiakuntza baliagarria zela mikrogliaren prozesu periferikoetan proteinen sintesia detektatzeko adierazi zuen.

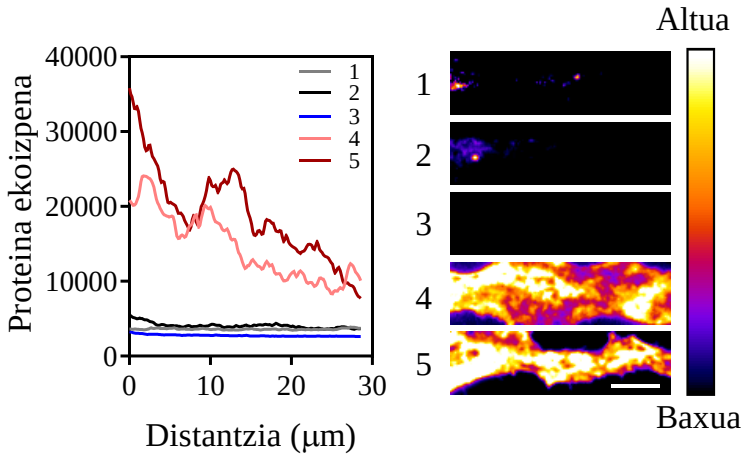

16. irudia. Mikrogliaren prozesu periferikoetako puromizina-intentsitatearen profila. Mikrogliaren prozesu periferikoen mikroskopia fluoreszentearen irudi adierazgarriak, anti-puromizinaz tindatuak. Mikroglia puromizinarekin tratatua, 10 minutuz eta anisomizinarekin, 30 minutuz (1); mikroglia puromizinarekin tratatua 30 minutuz eta anisomizinarekin, 30 minutuz (2); mikroglia puromizinarik gabe (3); mikroglia puromizinarekin tratatua 10 minutuz (4); mikroglia puromizinarekin tratatua 30 minutuz (5). Eskala-barra, 5µm**.**

Gure hurrengo galdera ea puromizina-seinalea erretikulu endoplasmatikotik (EE) zetorren izan zen. Zelula eukariotoetako proteinen sintesiaren zatirik handiena erretikulu endoplasmatikoari lotutako erribosometan edo zitosoleko erribosoma askeetan gertatzen da. EE, bereziki zimurtsua, polipeptido jaioberrien tolesturan parte hartzen duten proteinetan aberastua dago, eta Kalnexina / Kalretikulina sistema da proteina-konplexu ezagunenetako bat (Rutkevich eta Williams, 2011). Gure laborategiak distalki neuritetak ez dela kalretikulinarik hautematen frogatu du, , erretikulu endoplasmatikoaren markatzailea, baina bai sintetizatu berri diren proteinak, honek neuritetako proteinen tokiko sintesia ez dagoela erretikulu endoplasmatikoari lotuta adierazten duelarik (Gamarra *et al*, 2020). Era berean, mikroglia-zelulak prozesatu genituen kalretikulina immunotindatuz (Calr). Kontrol negatibo gisa, mikroglia-zelula batzuk immunozitokimika-prozeduraren mende jarri ziren, baina ez ziren inkubatu anti-Calr antigorputzarekin (antigorputz primariorik gabeko kontrola). Mikrogliaren prozesu periferikoetan kalretikulinarik dagoen zehazteko, antigorputz primariodun zelulen seinale fluoreszentea antigorputz primariorik gabeko zelulekin konparatu zen. Emaitzek erakutsi zuten kalretikulina-seinalea ezin dela detektatu mikrogliaren prozesu periferikoetan antigorputz primariorik gabeko kontrolari dagokionez, prozesu periferikoetan

puromizinaz markatutako proteinak zitosolean libre dauden erribosometatik datozela adieraziz (17. irudia).

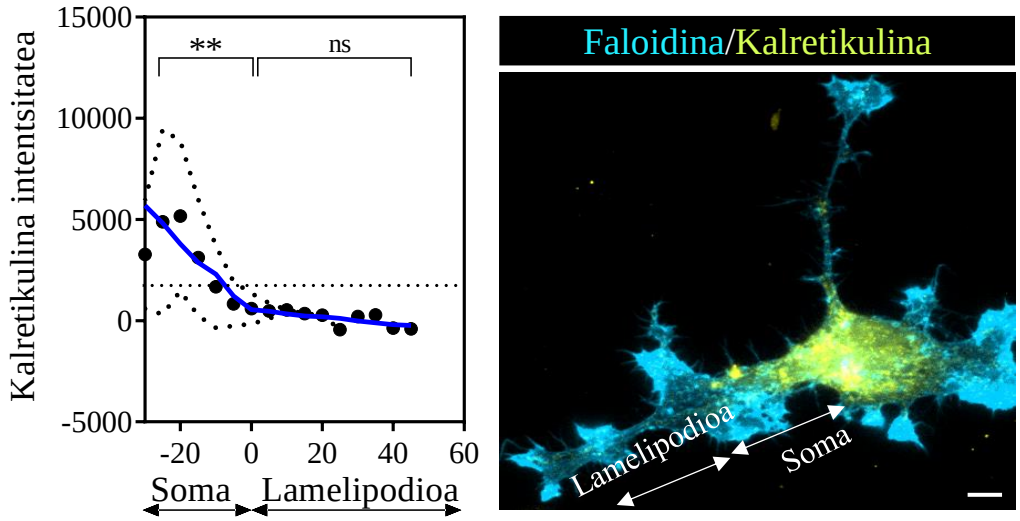

17. irudia. Kalretikulinaren intentsitate-profila mikroglian. Kalretikulinaz (horia) eta faloidinaz (ziana) tindatutako mikroglia-zelula baten mikroskopia fluoreszentearen irudi adierazgarria. Student T test parekatuaren analisia, ** $p<0.01$. Eskala-barra, 5µm.

4.2.2. Proteinen sintesi lokala mikrogliaren prozesu periferikoetan, hanturaren testuinguruan

Gure intereseko eskualdea mikrogliaren prozesu periferikoak dira, lamelipodioak eta filopodioak hain zuzen. Eskualde horietako proteinen tokiko sintesia deskribatzea izan dugu helburu, baita *RhoA*, *Par3* eta *Actb* bezalako transkritu zehatzak aztertzea ere. Transkritu horiek hazkunde-konoetan lokalki itzultzen dira (Wu *et al*, 2005; Hengst *et al*, 2009; Leung *et al*, 2006), eta, mikroglia-prozesuen antzera, lamelipodioak eta filopodioak dituzte. Mikrogliaren mugikortasuna prozesu mikroglialak hedatu, uzkurtu eta mugitzeagatik gertatzen da. Horri esker, mikrogliak bere ingurunea azter dezake, zelula-hondakinak ken ditzake, neuronekin eta beste glia-osagai batzuekin elkarreragin dezake eta zelulaz kanpoko matrizea birmoldatu dezake (Garden eta Möller, 2006). Hantura-testuinguru batean, mikroglia "aktibatu" egiten da, eta migrazio zelularra eragiten da (De Simone *et al*, 2010). Migrazio horretan, lamelipodioek eta filopodioek parte hartzen dute. Hantura-testuinguru horretan, baliteke prozesu periferikoetako proteinen sintesi lokala aldatzea. Hantura eragiteko LPS (150ng/mL) 30 minutuz eta 24 orduz, eta ATP (300µM) 30 minutuz erabili ditugu.

4.2.2.1. Proteinen-ekoizpena eta itzulpen-guneak mikrogliaren prozesu periferikoetan, LPSak eragindako hanturaren testuinguruan

Lehenik eta behin, LPSak proteina-sintesian duen eragina aztertu zen mikrogliaren prozesu periferikoetan, puromizilazio-saiakuntzen bidez. Mikroglia LPSarekin 30 minutuz estimulatzean, ez zen aldaketarik ikusi mikrogliaren prozesu periferikoetan, ez proteina ekoizpenean ez itzulpen gunetan (18. irudia). Hala ere, estimulua 24 orduz luzatzean, proteina ekoizpenak gora egin zuela ikusi genuen, bai lamelipodio eta filopodioetan (19A irudia), bai periferia osoan (19B irudia). Era berean, 24 orduko LPSak mikrogliako filopodioetako itzulpen-fokuak handitzea eragiten zuen (19A irudia). Beraz, 24 orduz LPS endotoxinak eragindako hanturak proteina-sintesia handitzea eragiten du, mikrogliaren prozesu periferikoetan neur daitekeena.

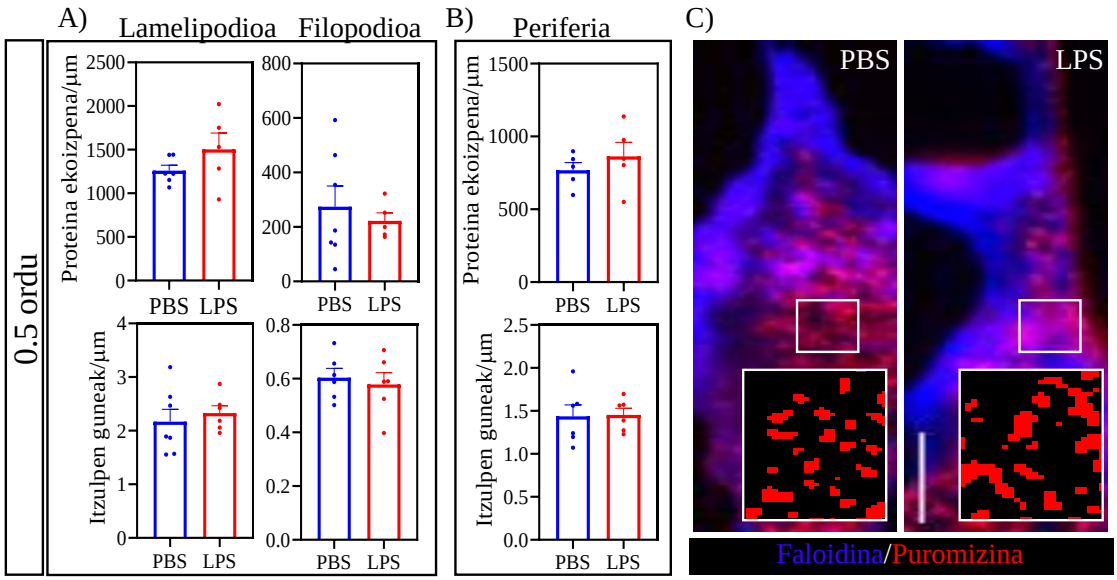

18. irudia: Proteinen ekoizpena eta itzulpen guneak mikrogliaren prozesu periferikoetan 30 minutuko LPSaren estimulazioa eta gero. A) Proteina-ekoizpenaren analisiaren irudikapen grafikoa (fluoreszentzia-intentsitate gisa neurtuta) eta itzulpen gune diskretuak mikrogliaren lamelipodietan eta filopodioetan, 30 minutuz ibilgailuz (PBS) edo LPS bidez trataturiko zeluletan. B) Proteina-ekoizpenaren eta itzulpen guneen analisiaren irudikapen grafikoa, mikrogliaren prozesu periferiko guztian zehar, 30 minutuz ibilgailuz edo LPS bidez trataturiko zeluletan. C) Itzulpen-puntuen (puromizina-puntuak) eta proteinen ekoizpenaren (puromizinaren intentsitatea) irudi adierazgarriak mikrogliaren periferian. Lamelipodioa lerro segmentatu batekin hautatu zen eta MaxEntropy (MaxEntropy) maskararekin zuzendu, leundu eta binarizatu zen. Faloidinarekin (urdina) eta puromizinarekin (gorria) egindako kontratindaketa erakusten da. Eskala-barra, 5µm. Grafikoek 7 esperimentu independenteren ± SEM batezbestekoa adierazten dute. Student-en T Test analisia.

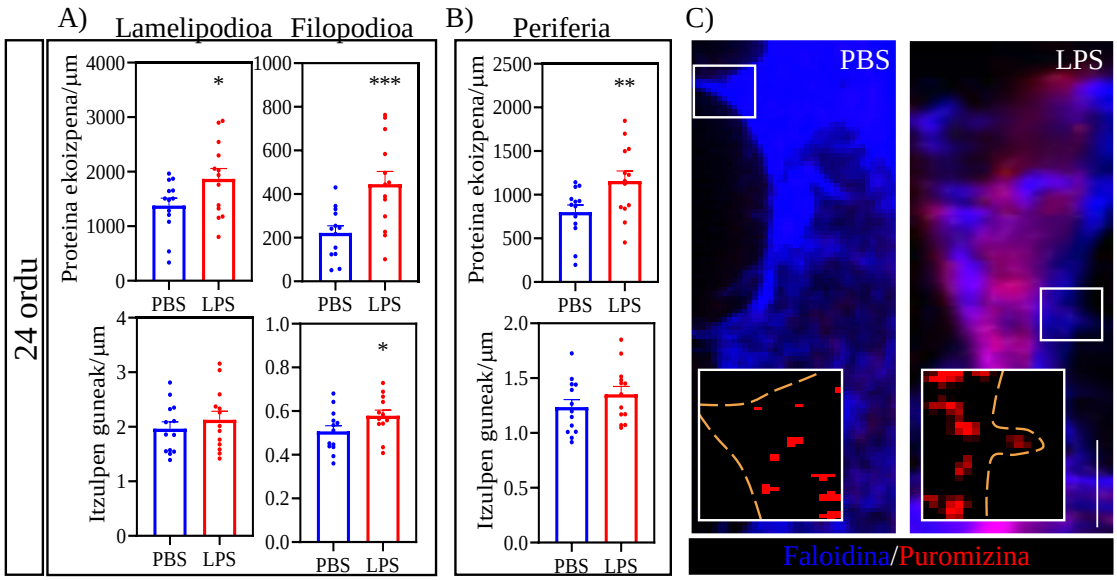

19. irudia: Proteinen ekoizpena eta itzulpen guneak mikrogliaren prozesu periferikoetan 24 orduko LPSaren estimulazioa eta gero. A) Proteina-ekoizpenaren analisiaren irudikapen grafikoa (fluoreszentzia-intentsitate gisa neurtuta) eta itzulpen gune diskretuak mikrogliaren lamelipodioetan eta filopodioetan, 24 orduz ibilgailuz (PBS) edo LPS bidez trataturiko zeluletan. B) Proteina-ekoizpenaren eta itzulpen guneen analisiaren irudikapen grafikoa, mikrogliaren prozesu periferiko guztian zehar, 24 orduz ibilgailuz edo LPS bidez trataturiko zeluletan. C) Itzulpen-puntuen (puromizina-puntuak) eta proteinen ekoizpenaren (puromizinaren intentsitatea) irudi adierazgarriak mikrogliaren periferian. Lamelipodioa lerro segmentatu batekin hautatu zen eta MaxEntropy (MaxEntropy) maskararekin zuzendu, leundu eta binarizatu zen. Faloidinarekin (urdina) eta puromizinarekin (gorria) egindako kontratindaketa erakusten da. Eskala-barra, 5µm. Grafikoek 13 esperimentu independenteren ± SEM batezbestekoa adierazten dute. Student-en T Test analisia, * p<0.05, **p<0.01, ***p<0.001.

4.2.2.2. RNA pikorrak eta RNA eta proteinaren ko-kokapenak mikrogliaren prozesu periferikoetan, LPSk eragindako hantura-testuinguruan

Aurreko atalean LPSari erantzunez hautemandako puromizina handitzea proteinen tokiko sintesiaren areagotzearen ondorioa ote zen zehazteko, periferian RNAren presentzia detektatu nahi izan genuen, mRNAak lokalki egotea ezinbesteko baldintza baita bere itzulpen lokalerako. Horretarako, transkripzioan RNA endogenoa markatzeko RNA kateetan sartzen den 5'fluoruridina (5`FU) erabili genuen. Marka hori puromizinarekin konbinatu genuen, RNAren eta itzulpen-guneen arteko kokagunea aztertzeko. Bi molekulak immunozitokimika bidez eta fluoreszentzia mikroskopio batean aztertu ziren.

Lehenik eta behin, 5´FU tratamendua puromizina tratamenduarekin konbina zitekeela ikusi genuen; izan ere, lehenengoa mRNA sintesian sartzeak eragina izan lezake haren itzulpenean, eta, beraz, puromizina eranstean. Ikusi genuenez, 5`FU-k ez zuen eraginik

puromizina sartzean, maila berean detekta genezakeelako puromizinaz markatutako zeluletan eta 5`FU eta puromizina markatutakoetan (20A irudia). Hala ere, 5`FUtik datorren seinalea aztertzean ez dela RNA detektatzeko markatzaile ona ikusi genuen; izan ere, RNAsa gehitzean ez dugu inolako jaitsierarik ikusten fluoreszentzia-mailetan, ez lamelipodioetan (20B irudia), ez zitoplasmaren multzoan (20C irudia), ezta nukleoan ere (20D irudia). Horregatik, baztertu egin genuen 5`FU erabiltzea RNA detektatzeko eta puromizinarekin batera ko-lokalizazio saiakuntzak egiteko.

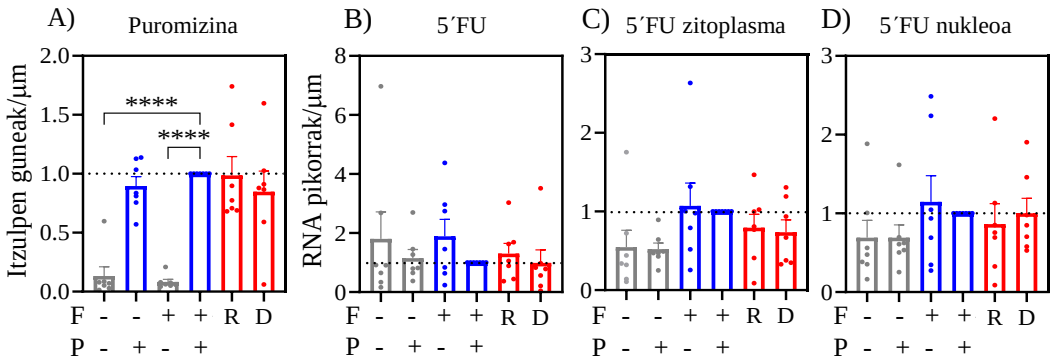

20. irudia: 5`FU eta puromizinaren konbinazioa, ko-lokalizazio saiakuntzetarako.** Itzulpen guneen (A) eta RNAren pikorren irudikapen grafikoa µm-ren arabera, mikrogliaren lamelipodioetan (B), zitoplasman (C) eta nukleoan (D), 5`FU (F) gabe edo 5`FU-rekin (F), puromizina gabe edo puromizinarekin (P) eta RNAsa-rekin (R), DNAsa-rekin (D) edo gabe tratatuak. Datu guztiak normalizatuta daude positibo bikoitzarekin (puromizina eta 5`FU bidezko tratamendua). Grafikoek 7 esperimentu independenteren ± SEM batezbestekoa adierazten dute. Bide bakarreko ANOVA eta ondoren Dunnet-en *post hoc* proba,* $p < 0.0001$.

Alternatiba gisa SYTO RNA Select erabili genuen RNA markatzeko. 5`FU ez bezala, SYTO RNA Select koloratzaile fluoreszente bat da, eta ez zaie kultiboei gehitzen, immunozitokimikako protokoloaren amaieran baizik. SYTO-k RNA endogenoa selektiboki markatzen duela egiaztatzeko, seinale fluoreszentea aztertu zen tratatu gabeko eta DNAsa edo RNAsa bidez tratatutako mikrogliaren prozesu periferikoetan. Mikrogliaren prozesu periferikoetan seinalea jaisten zela ikusi genuen, RNAsa-rekin tratatzean, baina ez DNAsa-rekin (21. irudia), SYTOk aukera ematen duela RNA endogenoa detektatzeko mikrogliaren prozesu periferikoetan adieraziz.

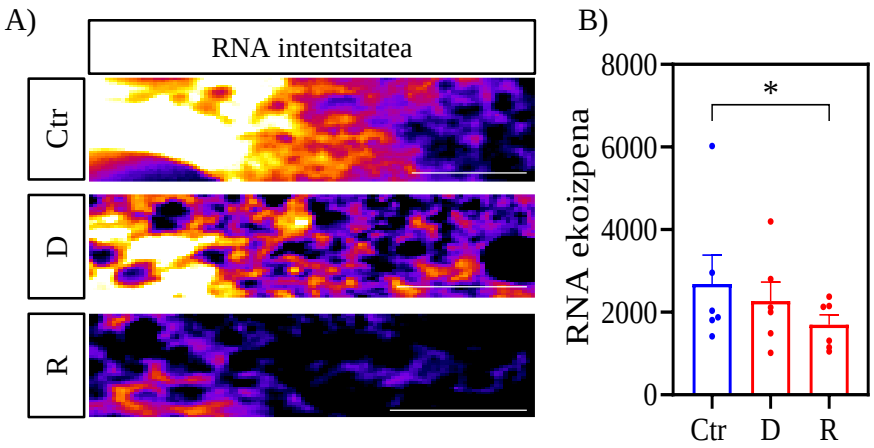

21. irudia: RNA markatzea SYTO RNA Select erabiliz. A) Nukleasarik gabe (Ctr), DNAsa-rekin (D) edo RNAsa-rekin (R) tratatutako zelulen mikrogliaren prozesu periferikoetan RNA dagoela adierazten duten irudi adierazgarriak. Eskala-barra, 5µm. B) RNA ekoizpena irudikatzen duen grafikoa, SYTO RNA Select bidez markatutako mikroglien prozesu periferikoetan, nukleasarik (Ctr) gabe eta DNAsa (D) edo RNAsa-rekin (R) tratatuak. Grafikoek 6 esperimentu independenteren ± SEM batezbestekoa adierazten dute. Kontrolarekiko ratioen Student T test parekatua, * $p<0.05$.

Jarraian, LPSari erantzunez SYTOren bidez markatutako RNA mailak aztertu genituen, baita RNAren eta puromizinaz markatutako itzulpen guneen arteko ko-lokalizazioa ere. Horretarako, bi markaketetatik datozen seinale fluoreszenteak aztertuko ditugu irudi binarizatuetan. 24 orduz LPS bidezko tratamenduak mikrogliaren lamelipodioetan (22A irudia) RNA granuluak ugaritzea eragiten du, periferia osoan bezala (22B irudia). Era berean, LPSak (24 ordu) RNA eta proteinaren ko-lokalizazioa areagotzen du mikrogliaren prozesu periferikoetan (22B irudia). Datu horiek LPSk eragindako hanturak mikrogliaren prozesu periferikoetako proteinen sintesi lokala areagotu egiten duela baieztatzen dute.

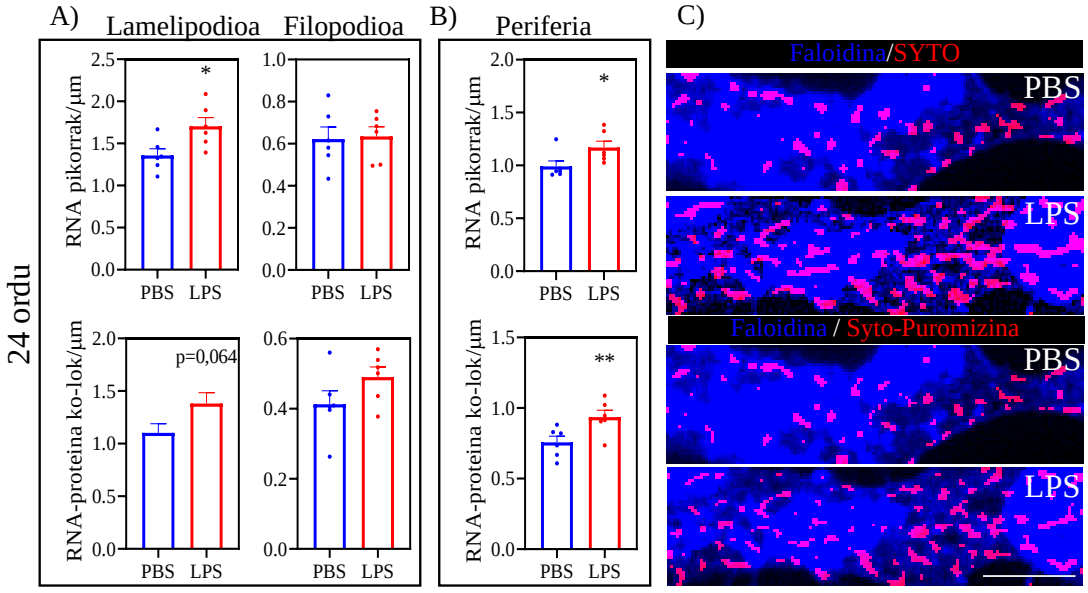

22. irudia: RNA pikorrak eta RNA eta proteina ko-lokalizazioa mikrogliaren prozesu periferikoetan, 24 orduz LPS bidezko estimulatu ondoren. A) RNA granuluen analisiaren eta RNA eta proteinaren elkar-kokapenaren irudikapen grafikoa, ibilgailuz (PBS) edo LPS bidez tratatutako mikrogliaren lamelipodio eta filopodioetan, 24 orduz. B) RNA granuluen eta RNA eta proteina ko-lokalizazioaren irudikapen grafikoa mikrogliaren prozesu periferikoetan. C) RNA (SYTO) granuluen eta RNA eta proteina (puromizina eta SYTO) ko-lokalizazioen irudi adierazgarriak mikrogliaren periferian. Lamelipodioa lerro segmentatu batekin hautatu zen eta MaxEntropy (MaxEntropy) maskararekin zuzendu, leundu eta binarizatu zen. Faloidina antigorputzaren (urdina) eta RNA pikorren edo RNA-proteinako-lokalizazioaren (gorria) ko-tindaketa erakusten da. Eskala barra, 5µm. Grafikoek 7 esperimentu independenteren ± SEM batezbestekoa adierazten dute. Student T test parekatuaren analisia,* $p < 0.05$.

4.2.2.3. LPSaren eragina Par3, Actb eta RhoAren sintesi lokalean mikrogliaren prozesu periferikoetan

Neuronetan, ardatz-hazkuntzako konoak morfologia dinamikoa du ingurunea zundatzeko, mintzaren protuberantziak hedatuz eta uzkurtuz, lamelipodio eta filopodio deiturikoak (Dent eta Gertler, 2003; Lowery eta Van Vactor, 2009). Deskribatu denez, badira zenbait proteina, bai filopodioetan bai lamelipodioetan sintetizatzen direnak; besteak beste, β-aktina (Leung *et al*, 2006), Par3 (Hengst *et al*, 2009) eta RhoA (Wu *et al*, 2005). Ondoren, *Actb* eta *Par3* mRNAk aztertu ziren mikrogliaren prozesu periferikoetan hantura-testuinguru batean, izan ere, mikrogliaren periferiak hazkunde-konoaren antzeko morfologia har dezake, lamelipodioekin eta filopodioekin zabaldu eta uzkurtu egiten delarik ingurunea aztertzeko. Horretarako, hurbileko lotailu-saiakuntzak egin genituen puromizina erabiliz, Par3 eta Actb-ren aurkako antigorputz espezifikoekin konbinatuta (PuroPLA). Metodo honekin Par3 eta Actb proteinen uneko sintesia detektatzea posible genuen, beti ere mikrogliaren prozesu periferikoetan zentratuz. LPSa, 30 minutuz, Par3 eta Actb-ren sintesia handitzeko gai da mikrogliaren prozesu periferikoetan; izan ere, anisomizina bidez itzulpena blokeatzean, proteina horiek jaitsi egiten dira, eta hori ez da gertatzen ibilgailuarekin tratatu ondoren (PBS; 23. irudia). LPSrekin denbora luzeagoan (24h) mikroglia estimulatzean, Par3ren sintesia ere handitu egiten da, eta anisomizinaren aurrean behera egiten du berriro ere (24A irudia). Kasu horretan ez zen aldaketarik hauteman β-aktinaren sintesian (24B irudia).

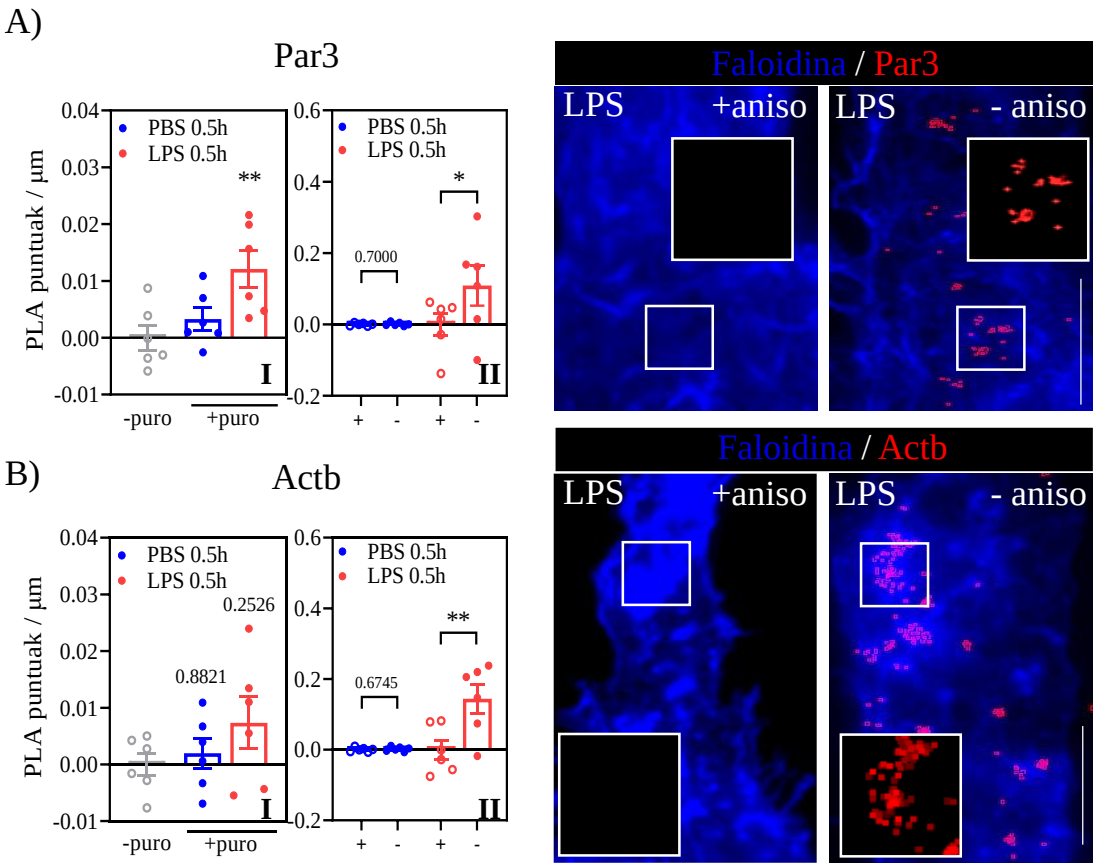

23. irudia: *Par3* eta *Actb*-en itzulpena mikrogliaren prozesu periferikoetan, 30 minutuz hantura eragin ondoren. *Pard3* (A) eta *Actb* (B) itzulpenaren irudikapen grafikoa mikrogliaren prozesu periferikoetan, 10 minutuko puromizina pultsuaren ondoren. Kontrol negatibo gisa, puromizinarekin tratatu gabeko zelulak erabili ziren (AI eta BI). Bide bakarreko ANOVA analisia, eta ondoren Dunnet-en *post hoc* proba;** $p < 0,01$, puromizina ezarekin (-puro) alderatuta. A II eta B II-n zelulak puromizina (-) edo puromizina eta anisomizina (+) pean jarri ziren proteina-sintesia blokeatzeko. Student T test parekatuaren analisia;* $p < 0,05$,** $p < 0,01$, anisomizina bidezko tratamenduekin alderatuta. C) 30 minutuz LPSarekin, anisomizinarekin edo anisomizinarik gabe tratatutako mikroglien Puro-PLAko puntu diskretuen irudi adierazgarriak. Faloidina (urdina) eta Puro-PLAko puntu diskretuak (gorria) erakusten dira. 5 µm-ko eskala-barra.

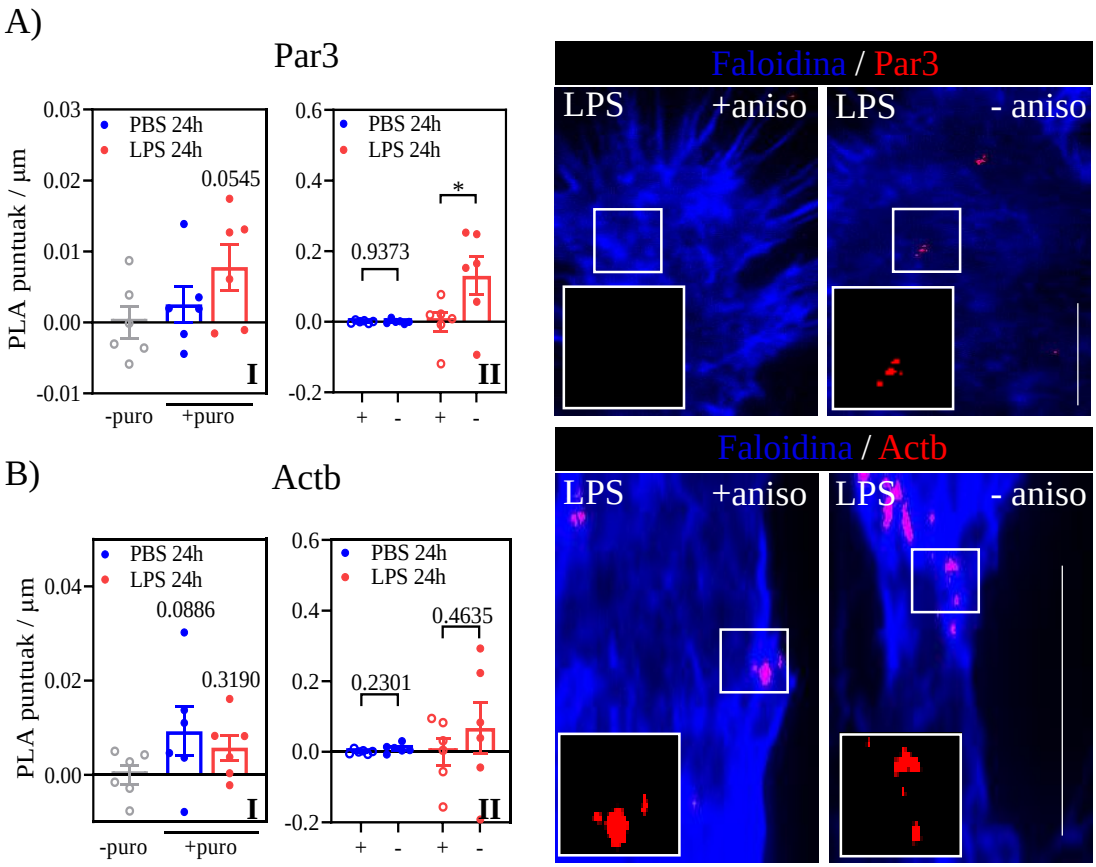

24. irudia: *Par3* eta *Actb*-en itzulpena mikrogliaren prozesu periferikoetan, 24 orduko hantura eragin ondoren. *Pard3* (A) eta *Actb* (B) itzulpenaren irudikapen grafikoa mikrogliaren prozesu periferikoetan, 10 minutuko puromizina pultsuaren ondoren. Kontrol negatibo gisa, puromizinarekin tratatu gabeko zelulak erabili ziren (AI eta BI). Bide bakarreko ANOVA analisia, eta ondoren Dunnet-en *post hoc* proba;** $p < 0,01$, puromizina ezarekin (-puro) alderatuta. A II eta B II-n zelulak puromizina (-) edo puromizina eta anisomizina (+) pean jarri ziren proteina-sintesia blokeatzeko. Student T test parekatuaren analisia;* $p < 0,05$,** $p < 0,01$, anisomizina bidezko tratamenduekin alderatuta. C) 24 orduz LPSarekin, anisomizinarekin edo anisomizinarik gabe tratatutako mikroglien Puro-PLAko puntu diskretuen irudi adierazgarriak. Faloidina (urdina) eta Puro-PLAko puntu diskretuak (gorria) erakusten dira. 5 µm-ko eskala-barra.

Periferian Par3 eta β-aktinaren sintesia haien transkribatuen tokiko itzulpenaren ondorioz handitu dela egiaztatzeko, *in situ* hibridazio fluoreszentea (FISH) egin genuen, *Actb* eta *Par3*-ren mRNAk detektatzeko.

Lehenik eta behin, RNA pikorrak desmaskaratzeko erabiltzen den K proteinasarik gabeko FISH protokolo bat erabili genuen, honek lagundu egiten baitu RNAen eta proteinen ko-tindaketa egiteko. Mikroglia zelulak ibilgailuarekin (PBS) edo LPSarekin tratatu genituen 30 minutu eta 24 orduz. Zelulak finkatu ondoren, FISHrako prozesatu genituen. Ez ginen gai izan *Par3* edo *Actb* presentzia detektatzeko zunda negatiboetatik gorako mailetan, ez lamelipodioetan, ez mikrogliaren filopodioetan (25A irudia). Hori dela eta, laginak K proteinasarekin digeritu genituen, intereseko mRNAek izan ditzaketen erribonukleoproteina-konplexuen proteinak degradatzeko. Hala, *Par3* LPSarekin

tratatutako mikrogliako lamelipodioetan zunda negatiboetatik gorako mailetara detekta zitekeela ikusi genuen, baina ez PBSrekin tratatutakoetan (25B, C irudiak). Halaber, *Actb* maila handitu egiten zen zunda negatiboekin alderatuta, eta *Actb* kontrol-mailarekin alderatuta mikrogliaren lamelipodioetan, LPS bidezko 30 minutuko estimulazioari erantzunez (26B, C irudiak). Emaitza horiek hantura akutuak *Par3* eta *Actb* mikrogliaren periferiara garraiatzea edo transkribatu lokalizatuak egonkortzea eragiten duela iradokitzen dute. mRNAtako bat ere ez zen detektatu edo aldatu LPSrekin 24 orduko tratamendua egin ondoren (25 eta 26 irudiak).

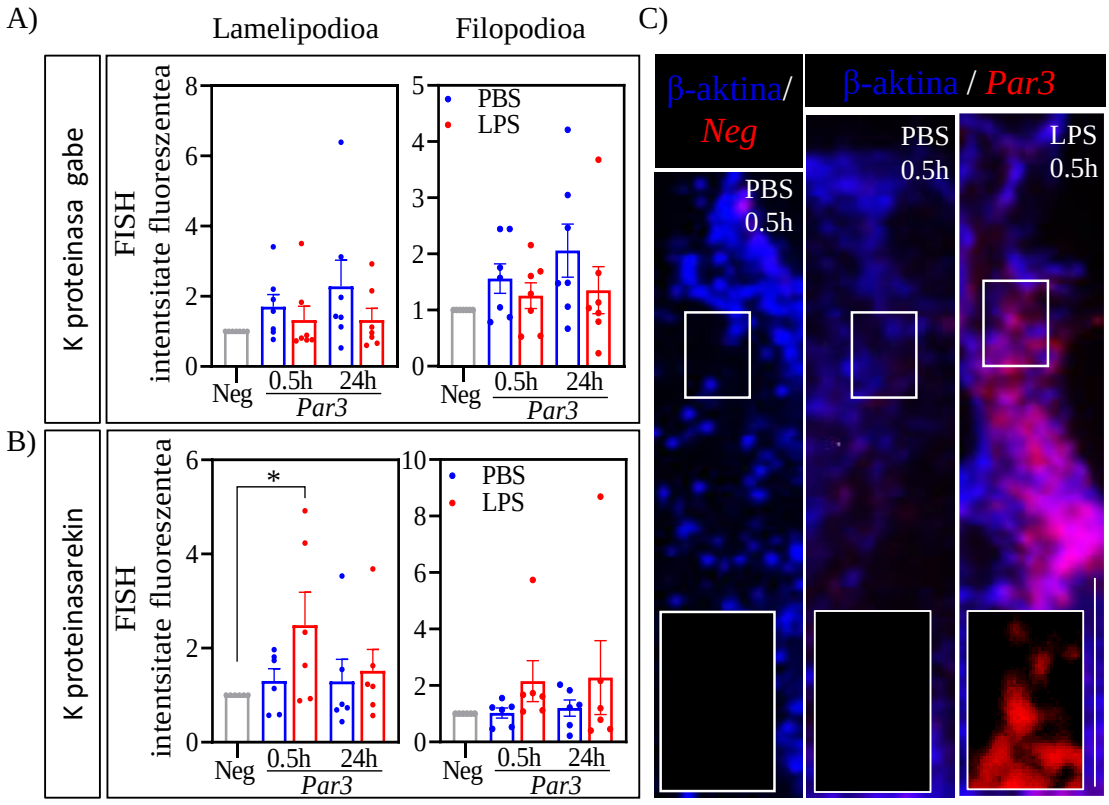

25. irudia: *Par3*ren mRNA, mikrogliaren prozesu periferikoetan, hantura-testuinguruan. *Par3* mRNAen irudikapen grafikoa PBS (urdina) edo LPS (gorria) bidez tratatutako mikrogliaren lamelipodioetan eta filopodioetan, 30 minutuz (0,5 h) eta 24 orduz, (A) gabe edo (B) K proteinasarekin (1µg/mL). Datuak zunda negatiboekin normalizatuta daude (Neg). C) Zunda negatiboen eta *Par3* (gorria) detektatzen dutenen irudiak, 30 minutuz PBS edo LPS bidez tratatutako zeluletan eta K proteinasarekin (1µg/mL). Eskala-barra, 5µm. Grafikoek 7 (K proteasarik gabe) eta 6 (K proteasarekin) esperimentu independenteen ±SEM batezbestekoa adierazten dute. Bide bateko ANOVA analisia, eta, ondoren, Holm-Sidak-en *post hoc* proba, * $p<0.05$.

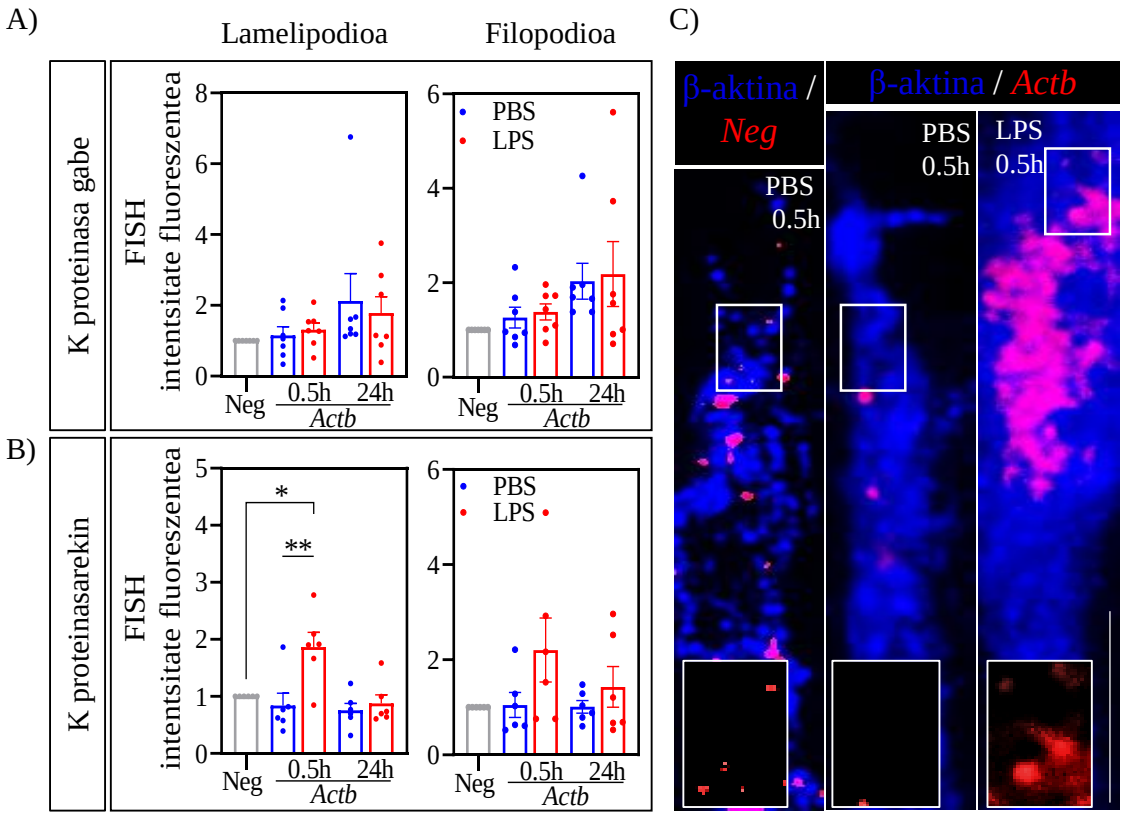

26. irudia: *Actb*ren mRNA, mikrogliaren prozesu periferikoetan, hantura-testuinguruan. *Actb* mRNAen irudikapen grafikoa PBS (urdina) edo LPS (gorria) bidez tratatutako mikrogliaren lamelipodioetan eta filopodioetan, 30 minutuz (0,5 h) eta 24 orduz, (A) gabe edo (B) K proteinasarekin (1µg/mL). Datuak zunda negatiboekin normalizatuta daude (Neg). C) Zunda negatiboen eta *Actb* (gorria) detektatzen dutenen irudi adierazgarriak, 30 minutuz PBS edo LPS bidez tratatutako zeluletan eta K proteinasarekin (1µg/mL). Eskala-barra, 5µm. Grafikoek 7 (K proteasarik gabe) eta 6 (K proteasarekin) esperimentu independenteen ±SEM batezbestekoa adierazten dute. Bide bateko ANOVA analisia, eta, ondoren, Holm-Sidak-en *post hoc* proba, * $p<0.05$, ** $p<0.01$.

Mikrogliaren prozesu periferikoetan LPSaren 30 minutuak *Par3* eta *Actb* mailak aldatzen zituela ikusita, eskualde perinuklearrean bi mRNA hauen presentzia aztertu genuen. Kasu honetan ez dugu aldaketarik ikusten ez *Par3* ez *Actb* mailetan. Antzeko emaitzak lortu genituen LPSrekin 24 orduz tratatu ondoren (27. irudia). Emaitza horiek iradokitzen dutenez, LPSrekin egindako hantura akutuak *Par3* eta *Actb*-en mRNAen mailak aldatzen ditu soilik mikrogliaren prozesu periferikoetan.

Orain arte atal honetan deskribatutako emaitzen arabera, LPS endotoxinak 30 minutuz eragindako hantura akutuak Par3 eta Actb proteinen sintesi lokala handitzen du mikrogliaren prozesu periferikoetan. Bestalde, LPS (24 h) estimulu luzeagoak bi proteinen sintesia areagotzen du prozesu periferikoetan. Hala ere, mRNA bi horietako bat ere ez da hautematen zelulen periferian. Horren arrazoia sintetizatu berri diren proteinen periferian behatutako handipena ez dela mRNAn tokiko itzulpen baten ondorio izan

daiteke, baizik eta proteinaren garraioaren areagotzearen ondorio, edo *Par3* eta *Actb*en itzulpena handitzean periferiako mRNA mailak jaisten direla eta, beraz, ezin direla detektatu.

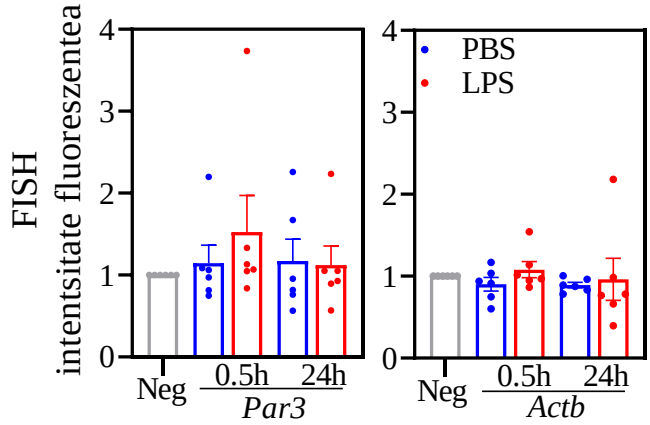

27. irudia: *Par3* eta *Actb*-en mRNAak mikrogliaren eskualde perinuklearrean. *Par3* eta *Actb* mRNAen irudikapen grafikoa PBS (urdina) edo LPS (gorria) bidez tratatutako mikrogliaren eskualde perinuklearrean, 30 minutuz (0.5h) eta 24 orduz, eta K proteinasarekin tratatuak (1µg/mL). Datuak zunda negatiboekin normalizatuta daude (Neg). Grafikoek 6 esperimentu independenteren ± SEM batezbestekoa adierazten dute. Bide bateko ANOVA analisia, eta ondoren, Holm-Sidak-en *post hoc* proba.

Azkenik, eta aurretiaz, LPSk RhoAren kokapenean duen eragina ere aztertu zen. RhoA/ROCKeko seinaleek funtzio neuronal ugari dituzte, besteak beste, zitoeskeletoaren dinamikan, neuriten hazkundearen erregulazioan eta zelularen mugikortasunean (Roloff *et al*, 2015). Gainera, LPSk eragindako hantura-testuinguruan, fagozitosi mikrogliala RhoA/ROCK bidez erregulatzen da (Scheiblich eta Bicker, 2017). Proteinasa k gabeko laginen tratamenduaren protokoloak ez zigun ahalbidetu mikrogliaren periferian mRNAk detektatzea (28. Irudia), eta, beraz, etorkizunean proteinasa k bidez esperimentuak egitea aurreikusten da, LPS bidez eragindako hanturak mikrogliaren prozesu periferikoetan RhoA mailak aldatzen dituen zehazteko.

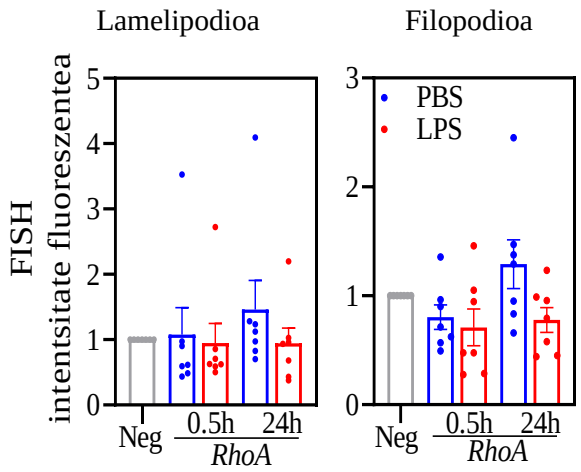

28. irudia: *RhoA*-ren mRNA mikrogliaren prozesu periferikoetan, hantura testuinguruan. *RhoA*ren mRNA-aren irudikapen grafikoa, PBS (urdina) edo LPS (gorria) bidez tratatutako mikroglien, lamelipodioetan eta filopodioetan, 30 minutuz edo 24 orduz. Datuak zunda negatiboekin normalizatuta daude (Neg). Grafikoek 7 esperimentu independenteren ±SEM batezbestekoa adierazten dute. Bide bateko ANOVA analisia, eta ondoren Holm-Sidak-en *post hoc* proba.

4.2.2.4. ATPak Par3, Actb eta RhoAren sintesi lokalean duen eragina mikrogliaren prozesu periferikoetan

Proteinen sintesi lokalaren gehikuntza LPS bidezko tratamenduena bakarrik ote zen zehazteko, zelulak ATP bidez tratatu genituen, hantura-prozesuetan zelulaz kanpoko espaziora askatzen den estimulu kimiotaktikoarekin hain zuzen (Honda *et al*, 2001). Zelulak ATParekin 30 minutuz tratatu ondoren, puromizilazio-saiakuntzak egin genituen proteina sintesia neurtzeko. ATPak ez du aldaketarik eragiten *de novo* sintetizatutako proteina mailan, itzulpen guneetan, mikrogliaren lamelipodioetan, ezta filopodoetan (29. irudia). Puromizina detekzioan aldaketarik ez egoteak ez du esan nahi transkritu zehatzek ATP bidezko tratamenduaren eragina jasango ez dutenik. Beraz, *RhoA*, *Par3* eta *Actb* mailak neurtu ziren FISH bidez mikrogliaren periferian. Zelulak 30 minutuz ATPrekin tratatu ondoren, ez dugu ez *RhoA* ez *Par3* detektatzen mikrogliaren prozesu periferikoetan. Hala ere, ATPrekin tratatutako zelulen filopodioetan zunda negatiboei dagokienez *Actb*-ren maila detektagarriak direla ikusten da, eta hau ez da ibilgailuarekin tratatutakoen zeluletan ikusten, eta horrek ATPk mikrogliaren periferian *Actb*-ren kokapena handitzen duela iradokitzen du (30. irudia). ATPri erantzunez *Actb*-a filopodioetan lokalki itzultzen den zehazteko, Puro-PLA saiakuntzak egingo dira etorkizunean.

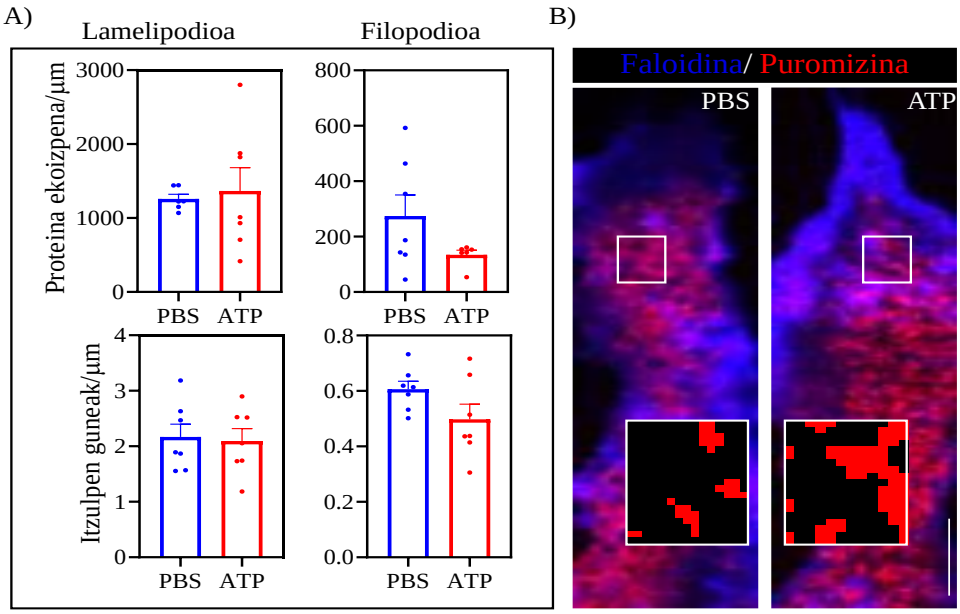

29. irudia. Proteina ekoizpena eta itzulpen guneak ATPrekin estimulatutako mikrogliaren prozesu periferikoetan. A) Proteina produkzioaren eta itzulpen guneen analisiaren irudikapen grafikoa, ibilgailuarekin (PBS) edo ATPrekin tratatutako mikrogliaren lamelipodioetan eta filopodioetan. B) Itzulpen guneen (puromizina-puntuak) eta proteina ekoizpenaren (puromizina-intentsitatea) irudi adierazgarriak mikrogliaren periferian. Lamelipodioa marra segmentatu batekin aukeratu zen eta MaxEntropy (MaxEntropy) maskararekin zuzendu, leundu eta binarizatu egin zen. Faloidinarekin (urdina) eta puromizinarekin (gorria) egindako kontratindaketa erakusten da. Eskala-barra, 5µm. Grafikoek 7 esperimentu independenteren ± SEM batezbestekoa adierazten dute. Student-en T Test-aren analisia.

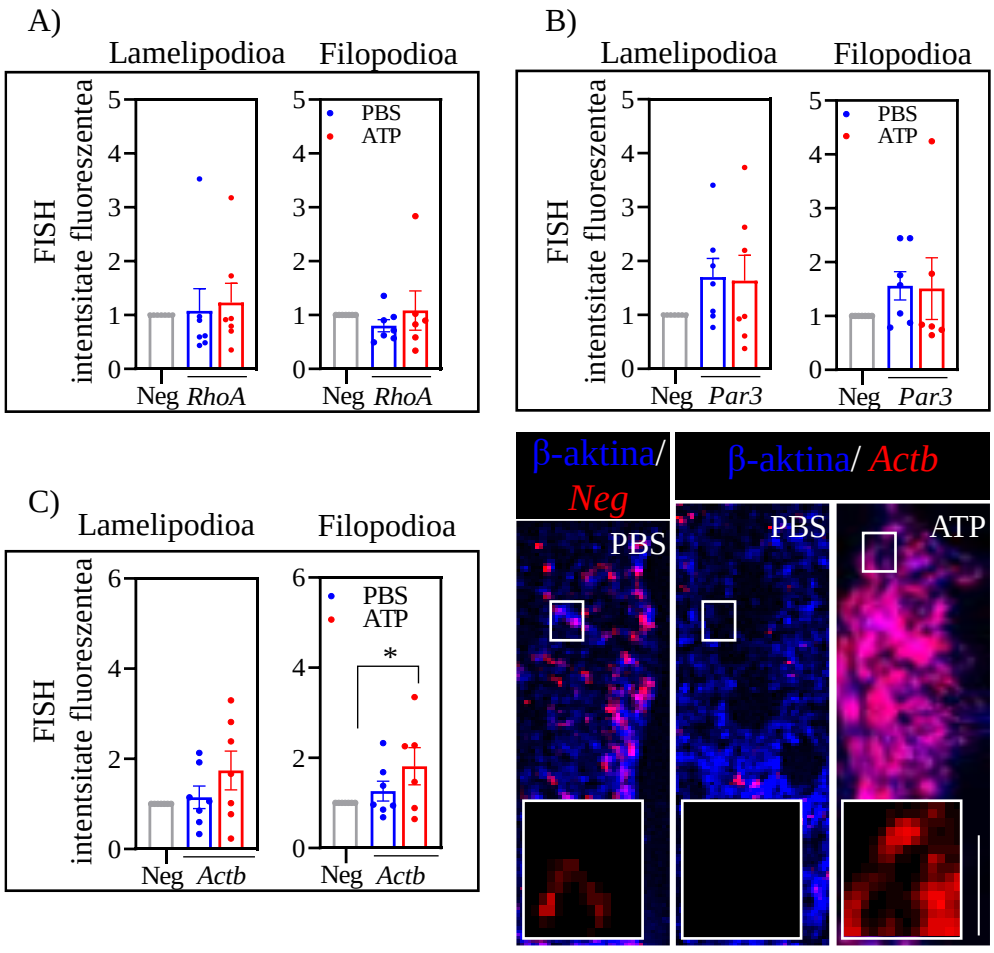

30. irudia: *RhoA, Par3* eta *Actb*-ren mRNAk mikrogliaren prozesu periferikoetan, ATPk eragindako hantura testuinguru batean. *RhoA* (A), *Par3* (B) eta *Actb* (C) mRNAen irudikapen grafikoa, PBS (urdina) edo ATP (gorria) 30 minutuz tratatutako mikrogliaren lamelipodioetan eta filopodioetan. Datu guztiak normalizatuta daude zunda negatiboei dagokienez (Neg). Zunda negatiboen eta *Actb*-ren irudi adierazgarriak (gorria) 30 minutuz PBS edo ATP bidez tratatutako zelulen periferian. Eskala-barra, 5µm. Grafikoek 7 esperimentu independenteen ±SEM batezbestekoa adierazten dute. Bide bateko ANOVA analisia, eta, ondoren, Holm-Sidak-en *post hoc* proba, * $p<0.05$.

4.2.2.5. Mikroglian *Actb* mailaren eta banaketaren manipulazioa

Mikroglia-zeluletan orain arte lortutako emaitzen arabera, hanturak *Actb*-ren adierazpena eta itzulpena erregulatzen du maila lokalean, eta honek zitoeskeletoa birmoldatzen lagun dezake hantura-estimuluei erantzunez. Horregatik, mikrogliaren periferiako *Actb* mailak aldatzea eta prozesu periferikoen morfologian eta polarizazio zelularrean duten eragina aztertzea erabaki genuen.

Aukeratutako lehen abordatze gisa GFP-β-aktina fusio proteinaren gainadierazpena aukeratu zen. Proteina horren mRNAk itzuli gabeko 3´ eskualdearen sekuentzia aurkezten du (3´UTR), eta zelulen periferiara heltzea ahalbidetzen du. Kontzeptu-froga gisa, GFP erreportaje-genea 3´UTR batekin (poliadenilazio-sekuentzia besterik ez du) gainadierazten saiatu ginen. Sindbis birusean oinarritutako adierazpen-sistema erabili genuen (Ni vitchanyong *et al*, 2009). Esperimentuak bai giza mikrogliako lerro zelularretan (emaitzak ez dira erakusten) bai arratoi jaioberrien kortexetik ateratako mikroglia primarioetan egin genituen. 3 DIV-tan ereindako mikroglia zelulak serum gabeko ingurune batean infektatu genituen, partikula biralen diluzio desberdinekin: 1/100, 1/150, 1/200. 48 ordu infekzioaren ondoren, GFP mailak aztertu ziren infektatu gabeko zelulekiko (kontrol negatiboa) immunozitokimikaren bidez, anti-GFP antigorputz bat erabiliz. Ez da kontrol negatiboa baino nabarmen handiagoa den seinale fluoreszenterik ikusi(31A irudia). Infekzioaren eraginkortasuna handitzeko, zelula mikroglialak 48 orduz aurrez infektatutako mikrogliaren gainjalkinarekin tratatu genituen. Kasu honetan ere ez da ikusi GFP fluoreszentziaren igoera kontrol negatiboarekiko (31B irudia). Horregatik, metodo hori baztertu genuen gure interes-genea gainadierazteko.

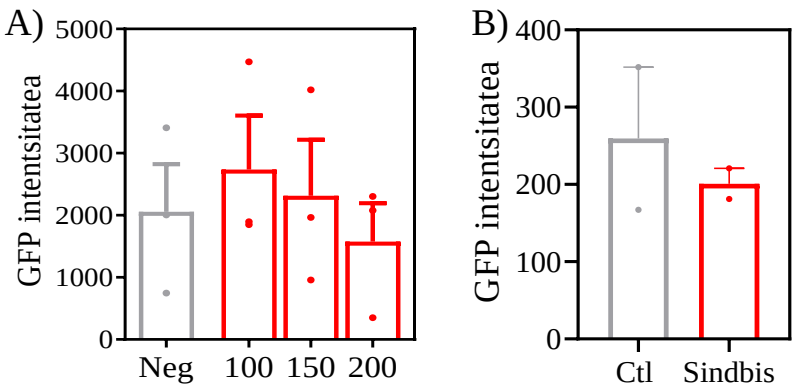

31. irudia: GFPren intentsitate mailak Sindbis birusarekin infektatutako mikroglia zeluletan. A) Diluzio desberdinekin (1/100, 1/150 eta 1/200) Sindbis birusarekin tratatutako mikroglia-zeluletako GFP intentsitatearen grafiko adierazgarriak. Grafikoek 3 esperimentu independenteren ±SEM batezbestekoa adierazten dute. Student-en T Test parekatuaren analisia. B) Sindbis birusekin (1/100 diluzioa) tratatutako mikroglien ingurune baldintzatuarekin tratatutako mikroglia-zelulen GFParen intentsitatearen grafiko adierazgarriak. Grafikoek 2 esperimentu independenteren ±SEM batezbestekoa adierazten dute. Student-en T Test parekatuaren analisia.

Bigarren aukera gisa, intereseko mRNAak isiltzea erabaki genuen, tamaina txikiko RNA interferenteak (siRNAak) erabiliz. Kontzeptu-froga gisa, berriz ere, *Actb*-ren aurkako siRNAk diseinatu genituen, bat eskualde kodetzaileari zuzendua (*Actb* edo A) eta bestea 3`UTR eskualdeari zuzendua (*3`Actb* edo 3'). Kontrol gisa, ausazko sekuentziako siRNA bat erabili genuen, inongo mRNA endogenoren osagarri ez dena. Kasu honetan ere arratoiaren mikroglia primarioak eta giza mikrogliaren lerro zelularrak erabili ziren. Transfekzioa serumik gabe hazitako zeluletan egin zen 24 eta 48 orduz. Isilarazpenaren eraginkortasuna ebaluatzeko, lehenik eta behin *Actb* mailak aztertu genituen RT-qPCR bidez. Ikusi genuenez, 3`*Actb* siRNA-ak 24 ordutan murrizten zituen *Actb*-en mailak mikroglia primarioan (32A irudia). Hori bera ikusten da giza mikrogliako zelula-lerroetan, non efektua iraunkorragoa izan zen; izan ere, *Actb* mailak ere jaitsi egin ziren, 3`Actb siRNA 48 ordutako transfekzioaren ondoren (32B irudia).

Ikusita *Actb*-ren 3`UTR sistemara zuzendutako siRNAk nabarmen murrizten dituela mRNA mailak, proteina mailetan duen eragina ere aztertu genuen. Horretarako, zelulak siRNA-ekin transfektatu ziren, eta 24 eta 48 ordutan neurtu ziren β-aktina mailak, *western blot* bidez. Kasu honetan, siRNA-ek ez zuten eraginik izan proteina mailetan, ez mikroglia primarioan (32C irudia), ezta giza mikrogliako lerro zelularretan ere (32D irudia).

Emaitza horiek *Actb*-ren 3`UTR sistemaren aurka diseinatutako siRNAek aukera ematen dutela mRNA mailak aldatzeko, baina ez direla optimoak proteina mailak murrizteko eta transkribu horren itzulpena aztertzeko iradokitzen dute.

Mikroglia zeluletan siRNA-ekin egindako isilarazteko abordatzea erabilgarria dela mRNA mailak murrizteko ikusita, *Zbp1*-era zuzendutako siRNAk diseinatu genituen *Actb*-ren isilarazpenaren alternatiba gisa. Zelula eukariotoen periferian lokalki itzultzen diren mRNAk RNA-ren lotura-proteinekin edo RBP-ekin (ingelesetik *RNA Binding Proteins*) garraiatzen dira periferiara. RBP-ek adierazpen genetikoa kontrolatzen dute itzulpenaren eraginkortasuna, mRNAren kokapen subzelularra edo degradazioa modulatuz (Vindry *et al*, 2014). Zbp1, *Actb* mRNA-ko 3 `UTR eskualdeari lotzen den proteinetako bat da, eta haren kokalekua zuzentzen du (Tiruchinapalli *et al*, 2003). Neuronetan, Zbp1 eskuragarritasuna murriztearen ondorioz, haren xede diren mRNA-en mailak murriztu egiten dira, *Actb*-arena barne (Donnelly *et al*, 2011).

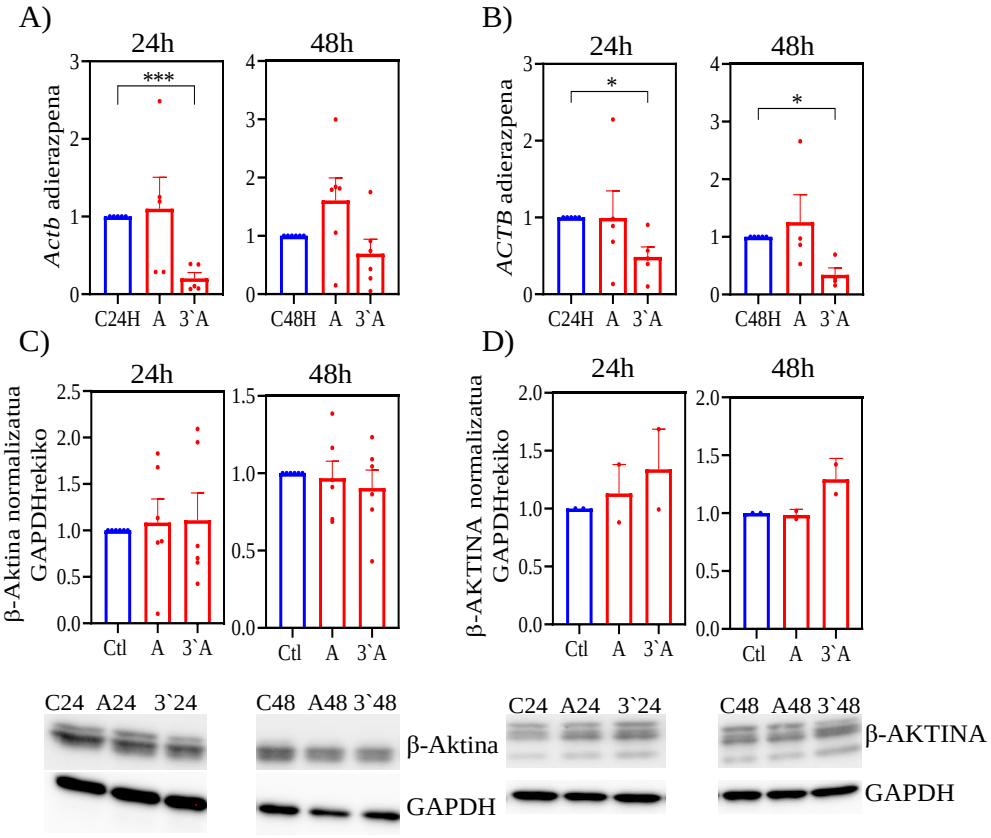

32. irudia: *Actb* genearen transfekzioa siRNAekin, kate kodifikatzailera (A) eta 3`UTR (3`A) katera zuzenduta, 24 orduz eta 48 orduz. A) *Actb*-ren mRNAren adierazpen grafikoak arratoi-mikroglietan (A) eta giza mikrogliako lerroetan (B), 24 orduz eta 48 orduz siRNA kontrolarekin edo *Actb* genearen kate kodifikatzaileari (A) edo 3`UTR (3`A) kateari zuzendutako siRNA bidez tratatuak. β-aktina mailak *Western blot* bidezko analisien irudikapen grafikoa arratoiaren mikroglia primarioetan (C) eta giza mikrogliako lerroetan (D), 24 orduz eta 48 orduz siRNA kontrolarekin edo *Actb* genearen kate kodifikatzaileari (A) edo 3`UTR (3`A) kateari zuzendutako siRNA bidez tratatuak. Grafikoek 2 (D), 5 (B) eta 6 (A eta C) esperimentu independenteen ± SEM batezbestekoa adierazten dute. Student T test parekatuaren analisia,* $p < 0.05$,** $p < 0.001$.

Zbp1 isilarazteko, bi siRNA diseinatu genituen: bata, eskualde kodifikatzailerantz zuzendua (*Zbp1* edo Z) eta bestea, 3`UTR-ri zuzendutakoa (3`*Zbp1* edo 3`Z). Kontrol negatibo gisa, berriz ere ausazko sekuentziako siRNA bat erabili genuen. Mikroglia primarioko kultiboak transfektatu genituen eta 24 eta 48 orduz siRNAen eraginkortasuna ebaluatu genuen RT-qPCR eta *western blot* bidez. Mikroglian *Zbp1*-eko mRNAren mailak murriztu egin zirela ikusi zen diseinatutako bi siRNA espezifikoekin, siRNA kontrolari dagokionez (33A irudia). Gainera, transfekzioaren ondoren, eragina 24 ordukoa eta 48 ordukoa izan zen. Bestalde, Josune Imaz, laborategiko doktoratu aurreko ikertzaileak egindako ikerketen arabera, 3`*Zbp1* siRNA-k Zbp1 proteina mailak murrizten dituela ikusi zen 24 orduko transfekzioaren ondoren (33B irudia). Beraz, *Zbp1*-ren 3`UTR aldera zuzendutako siRNA erabil daiteke 24 orduz, transkribatua isilarazteko.

Paraleloan, FISH bidez mikroglia zeluletan *Actb* mRNA-ren banaketa aztertu genuen bi siRNAek duten eragina aztertuz. 3`*Zbp1* siRNA bidez transfektatutako zeluletan, mikrogliaren periferian *Actb* mailak handitu egiten direla ikusi genuen, baina soilik ibilgailuz tratatutako zeluletan, ez LPS bidez tratatutakoetan, isilarazpenak *Actb*-ren banaketa aldatzen duela adieraziz, baldintza basaletan behintzat. (33C irudia). Etorkizunean Actb mRNA-ren tokiko itzulpena aldatuta dagoen ebaluatuko da, Puro-PLA bidez.

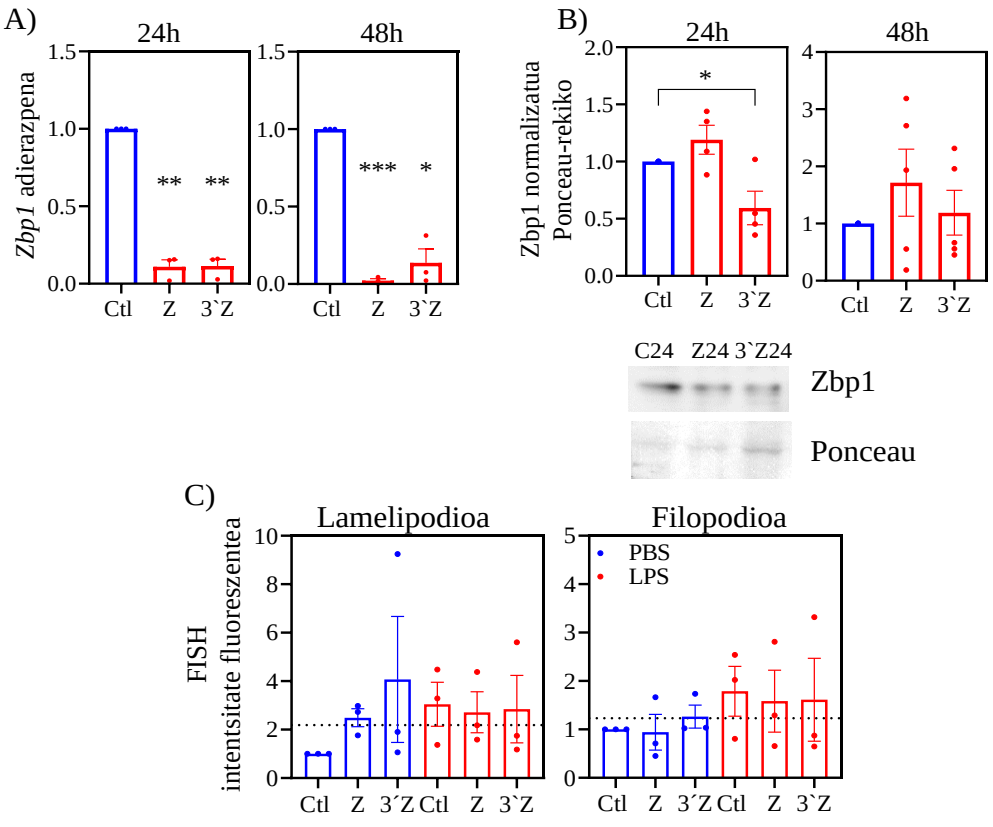

33. irudia: *Zbp1* mRNA-ko kate kodifikatzailera (Z) eta 3`UTR (3`Z) katera zuzenduta siRNA-kin egindako transfekzioa mikroglia zeluletan, 24 orduz eta 48 orduz. A) Mikroglia zeluletan *Zbp1* adierazpenaren grafikoak, siRNA kontrolarekin edo *Zbp1*aren aurka tratatutako siRNA-ekin, 24 orduz eta 48 orduz. B) Zbp1 proteinaren *western blot* bidezko analisiaren irudikapen grafikoa, siRNA kontrolarekin edo *Zbp1*en aurkako siRNAekin, 24 orduz eta 48 orduz tratatutako mikroglian. C) *Actb* transkritoaren banaketa mikrogliaren lamelopodio eta filopodioetan, *in situ* hibridazioaren bidez. Aurrez aipatutako siRNAekin eta 30 minutuz LPSrekin tratatutako zelulak. Grafikoek 3 (A, C) eta 4 (B) esperimentu independenteen ± SEM batezbestekoa adierazten dute. Student T test pareatuaren (A), ez parekatuaren(B) eta bide bakarreko ANOVAren analisia, eta ondoren Holm Sidak *Post hoc* proba (C),* $p < 0.05$,** $p < 0.01$,*** $p < 0.001$.

Azkenik, *Zbp1* edo 3`*Zbp1* siRNAek 24 orduz mikrogliaren morfologiari eragiten zioten egiaztatu zen. Horretarako, lamelipodioaren luzera, zabalera eta azalera aztertu ziren, µm-ko filopodio kopuruaz gain. Ez genuen aldaketarik ikusi ez luzeran, ez zabaleran, ez lamelipodioaren azaleran, inolako siRNArekin oinarrizko baldintzetan, ezta 30 minutuz LPS-arekin egindako tratamenduetan (34A, B, C irudia). Hala ere, ikusten dugu filopodio kopurua handitu egiten dela siRNA transfekzioaren ondoren, bereziki 24 orduz 3`*Zbp1* siRNA-ren tratamenduaren ondoren, LPSk 30 minutuz eragindako hantura testuinguruan (34D irudia). Bestalde, 3`*Zbp1* siRNA delakoak filopodioen banaketa aldatzen du mikroglian, filopodio gutxiago aurkituz lamelipodioen periferian eta gehiago eskualde perinuklearrean, LPS-arekin tratatutako zeluletan siRNA kontrolarekin alderatuta (34E, F, G irudia). Horrek mikroglia 3`*Zbp1* siRNArekin transfektatu ondoren filopodioen banaketa aldatu genuela adierazten digu.

30 minutuz LPS-arekin egindako esperimentuek hantura akutuak ez dituela mikroglian filopodio-kopuruak aldatzen adierazten dute. Hala ere, LPS estimulua 24 ordura luzatu ondoren, filopodioak ugaritu egin dira, eta, horietan, puromizinarekin markatutako *de novo* sintetizatutako proteinak metatzen dira (34H irudia). Horregatik, 24 orduz LPS-arekin tratatu ondoren, *Zbp1* eta 3`*Zbp1* siRNA-en eragina aztertuko da etorkizunean.

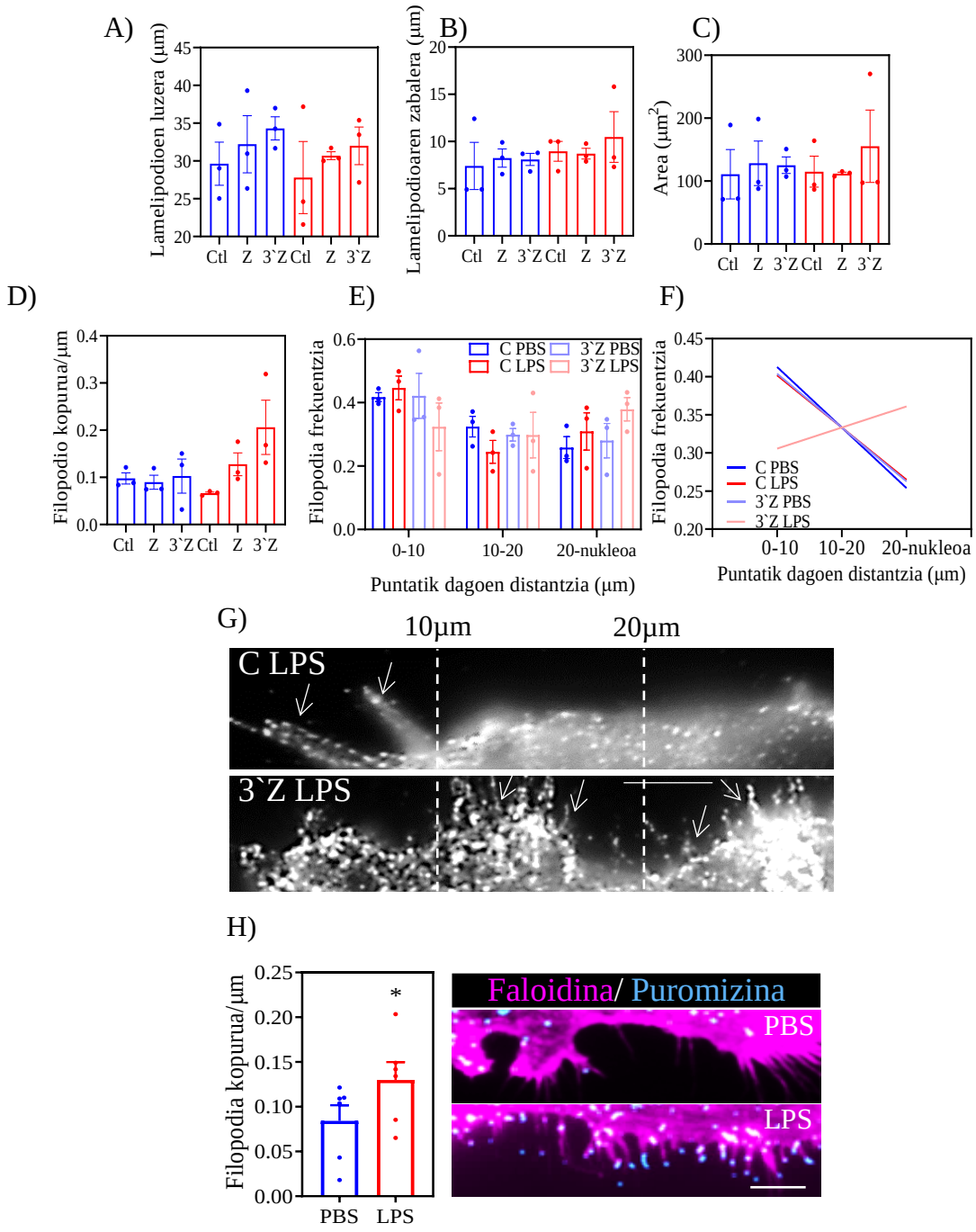

34. irudia: Mikrogliaren morfologia, LPS (30min) eta *Zbp1*-en kate kodifikatzailera (Z) edo 3`UTR (3`Z) zuzendutako siRNAekin tratatu ondoren, 24 orduz eta 48 orduz. Mikrogliaren lamelipodioen luzeraren (A), zabaleraren (B), azaleraren (C) eta filopodio-kopuruaren (D) grafiko adierazgarriak, 24 orduz eta 48 orduz siRNA kontrolarekin, *Zbp1*-en kate kodifikatzailera (Z) edo 3`UTR (3`Z) zuzendutako siRNAekin. Zelulak PBS edo LPS bidez tratatu ziren 30 minutuz E) Filopodioen maiztasuna 10µm bakoitzeko, lamelipodioen puntatik gune perinuklearreraino. F) Filopodioen maiztasunaren erregresio lineala, 10µm-ero, lamelipodioen puntatik gune perinuklearreraino. G) Mikrogliako filopodioen maiztasunaren argazki adierazgarriak, anti-β-aktina antigorputzarekin markatutako zeluletan. H) 24 orduz PBS edo LPS bidezko tratamenduaren ondorengo lamelipodioetako filopodio kopuruaren grafiko adierazgarriak,. Grafikoek 3 (A, B, C, D, E F, G) eta 6 (H) esperimentu independenteen ± SEM bataz bestekoa adierazten dute. Bide bakarreko ANOVA analisia, eta, ondoren, Holm Sidak *post hoc* proba (A, B, C, D), Student T test parekatuaren analisia (E),* $p < 0.05$ eta bi bideko ANOVA analisia, eta, ondoren, Holm Sidak *post hoc* proba (E).

4.2.3. Proteinen sintesi lokala mikroglia zeluletan β amiloide peptidoak eragindako patologiaren testuinguruan

4.2.3.1. Proteinen ekoizpena eta itzulpen guneak mikrogliaren prozesu periferikoetan, Aβ-ren oligomeroei erantzunez

Neuronetan eta oligodendrozitoetan Aβ extraneuronala izateak kultiboetan proteinen sintesi lokala handitzea dakar (Baleriola *et al*, 2014; Quintela-Lopez *et al*, 2019). Gainera, azterketa askok erakusten duten moduan neuroinflamazioaren parte-hartzea funtsezkoa da EAn ikusten diren aldaketa neuropatologikoen garapenean (Kinney *et al*, 2018). Aurrekari horiek eta hanturazko estimuluek proteinen sintesi lokalean duten eragina aztertuta, fenomeno horrek mikroglia-zeluletan duen eragina aztertu genuen.

Serumik gabeko testuinguruan 3 DIV-tara mikroglia zelulak 24 orduz 3 µM-ko Aβ oligomeroekin tratatu genituen. Proteina-sintesia neurtzeko, puromizilazio-saiakuntzak egin genituen. Ikus dezakegu Aβ-k ez duela aldaketarik eragiten ez proteina ekoizpenean, ez itzulpen guneetan mikrogliaren periferian (35. irudia).

Aβ-ren aurrean kontrolari dagokionez puromizina sartzean aldaketarik hauteman ez arren, RNAren presentzia aldatuta ote zegoen zehaztu nahi izan genuen. Horretarako, SYTO RNA Select erabili genuen mikrogliaren prozesu periferikoetako RNA endogenoa bistaratzeko. Halaber, RNA-proteina ko-lokalizazioa aztertu genuen. Ikus dezakegun bezala Aβ-k ez du aldaketarik eragiten ez RNAren mailan, ez RNA eta puromizinarekin markatutako proteinen ko-lokalizazioan, mikrogliaren prozesu periferikoetan (36. irudia). Emaitza horiek gorabehera, Aβ-k mRNA espezifikoen itzulpena alda zezakeen, baina hori ez zen islatzen puromizina gehikuntzan hauteman zitezkeen aldaketetan. Horregatik, amiloideak *Par3, Actb* eta *RhoA*-ren mikrogliaren periferian duten kokapenean eta haien itzulpen lokalean duen eragina aztertu genuen.

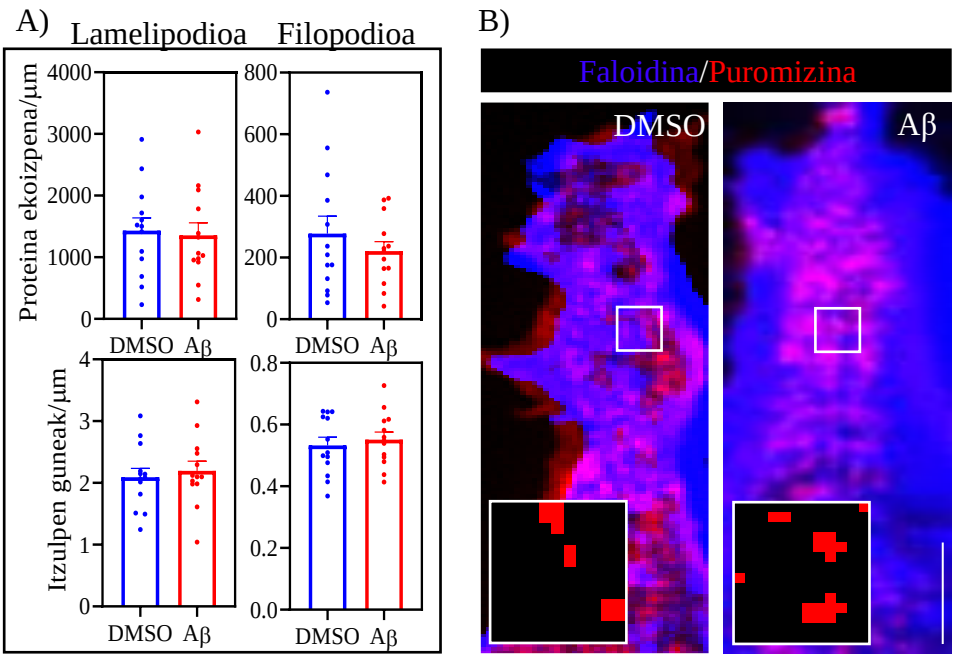

35. irudia. Proteinen ekoizpena eta itzulpen guneak mikrogliaren periferian. A) Proteinen ekoizpenaren eta itzulpen guneen analisiaren irudikapen grafikoa, ibilgailuz (DMSO) edo Aβ erabiliz tratatutako mikrogliaren lamelipodioetan eta filopodioetan. B) Mikrogliaren periferiako itzulpen puntuen eta proteina-ekoizpenaren irudi adierazgarriak. Lamelipodioa marra segmentatu batekin aukeratu zen eta MaxEntropy (MaxEntropy) maskararekin zuzendu, leundu eta binarizatu egin zen. Antigorputz faloidinarekin (urdina) eta puromizinarekin (gorria) egindako kotindaketa erakusten da. Eskala-barra, 5µm. Grafikoek 13 esperimentu independenteren ± SEM batezbestekoa adierazten dute. Student-en T test parekatuaren analisia.

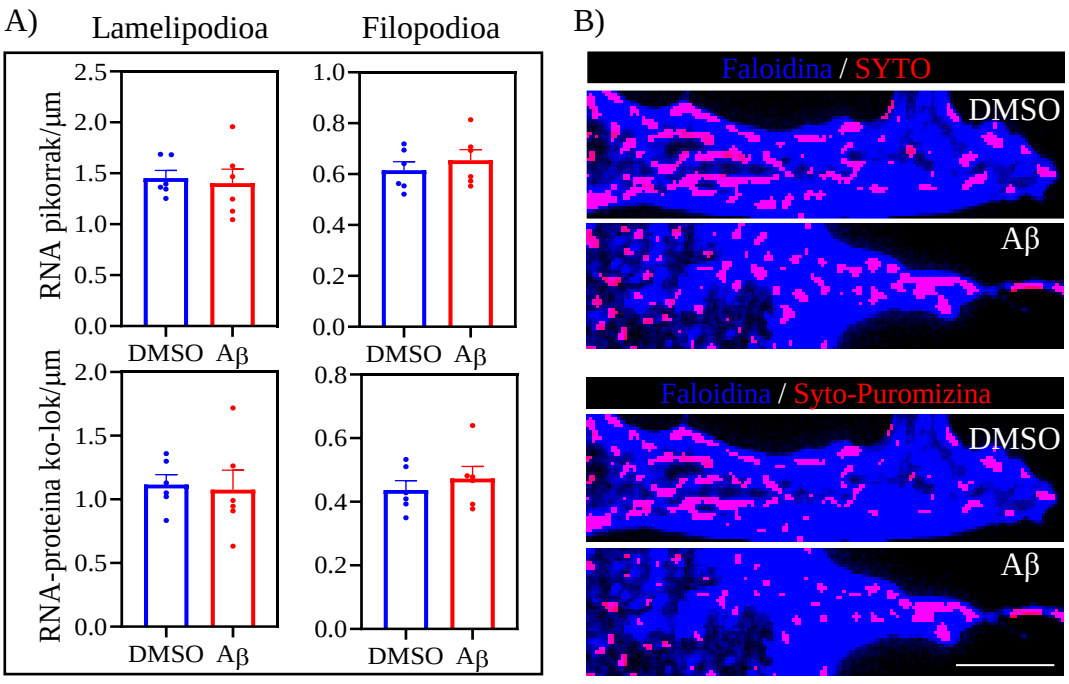

36. irudia. RNA pikorrak eta RNA eta proteinaren ko-lokalizazioa mikrogliaren periferian. A) RNA pikorren eta RNA eta proteinen ko-lokalizazioaren analisiaren irudikapen grafikoa, 24 orduz, ibilgailuz (DMSO) edo Aβ bidez tratatutako mikrogliaren lamelipodioetan eta filopodioetan. B) Mikroglia periferiaren RNA pikorren eta RNA-proteina ko-lokalizazioaren irudi adierazgarriak. Lamelipodioa marra segmentatu batekin aukeratu zen eta MaxEntropy (MaxEntropy) maskararekin zuzendu, leundu eta binarizatu zen. Faloidinaren antigorputzarekin (urdina) eta SYTO edo SYTO-puromizinarekin (gorria) egindako kotindaketa erakusten da. Eskala-barra, 5µm. Grafikoek 13 esperimentu independenteren ± SEM batezbestekoa adierazten dute. Student-en T test parekatuaren analisia.

4.2.2.2. Aβ-ren eragina Par3, Actb eta RhoA-ren sintesi lokalean mikrogliaren prozesu periferikoetan.

Lehenik eta behin, hantura estimuluekin egin genuen bezala, *Par3* eta *Actb*-en itzulpena neurtzeko saiakuntzak egin genituen Puro-PLA bidez. 24 orduz DMSO edo Aβ duen serumik gabeko 3 DIV mikroglia-zelulak tratatu ondoren, ikusi genuen Aβ oligomeroek igoera bat eragiten zutela bai Par3ren sintesian, bai β-aktinaren sintesian, Puro-PLA seinalea nabarmen murrizten baita anisomisina duten zeluletan, baina ez DMSO-rekin tratatutako zeluletan (37. irudia).

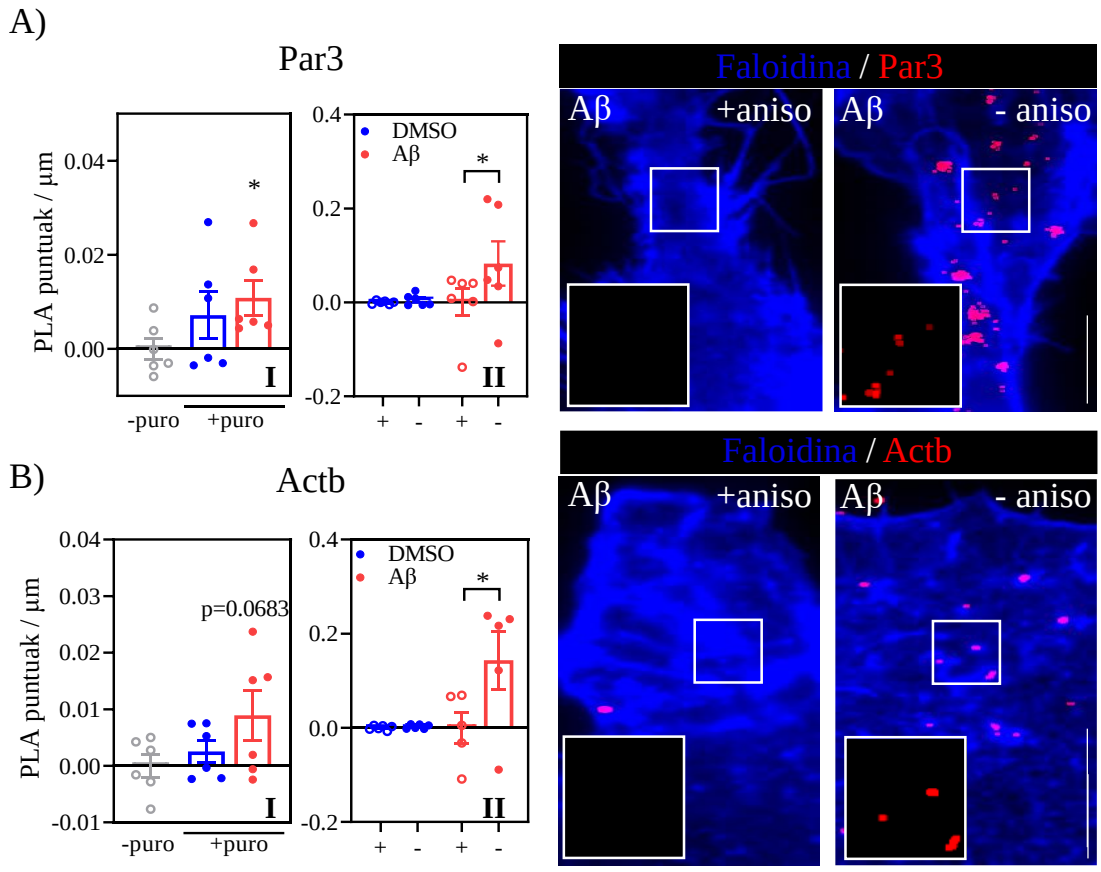

37. irudia. *Pard3* eta *Actb* itzulpenak mikrogliaren prozesu periferikoetan. Mikrogliaren prozesu periferikoetako *Pard3* (A) eta *Actb* (B) itzulpenaren adierazpen grafikoa, puromizina-pultsu baten ondoren (10 minutu), DMSOrekin edo Aβ-rekin tratatutako zeluletan. Kontrol negatibo gisa, puromizinarekin tratatu gabeko zelulak erabili ziren (A I eta B I). Bide bateko ANOVA, eta, ondoren Dunnet-en *post hoc* proba; * p<0,05, kontrol negatiborekin konparatuta. AII-n eta BII-n, berriz, puromizina-pultsu batez (-) edo puromizinaren eta anisomizinaren (+) pultsuez tratatutako zelulen Puro-PLA puntu diskretuak adierazten dira. Student-en T test parekatuaren analisia; * p<0.05, puromizinazko tratamenduak puromizinazko eta anisomizinazko tratamenduekin konparatzen dira baldintza esperimental bakoitzean. Puro-PLA puntu diskretuen irudi adierazgarriak Aβ anisomizinarekin edo gabe tratatutako zeluletan. Eskala-barra, 5µm.

Bestalde, *Par3* eta *Actb*-en mRNAek mikrogliaren prozesu periferikoetan duten presentzia aztertu genuen.

Alde batetik, *Par3* aztertu zen. K proteinasarik gabe egindako FISH protokoloaren kasuan, ez dugu aldaketarik ikusten mRNA-mailan, ez lamelipodioan, ez filopodioan (38A irudia). Hala ere, proteinak K proteinasarekin digeritzean, Aβ-k *Par3* maila handitu egin dela hauteman dugu mikrogliaren filopodioetan. Gainera, lamelipodioak handitzeko joera dago. (38B irudia). Honek Aβ-k mikrogliaren prozesu periferikoetako *Par3* mailak erregulatzen dituela adierazten du.

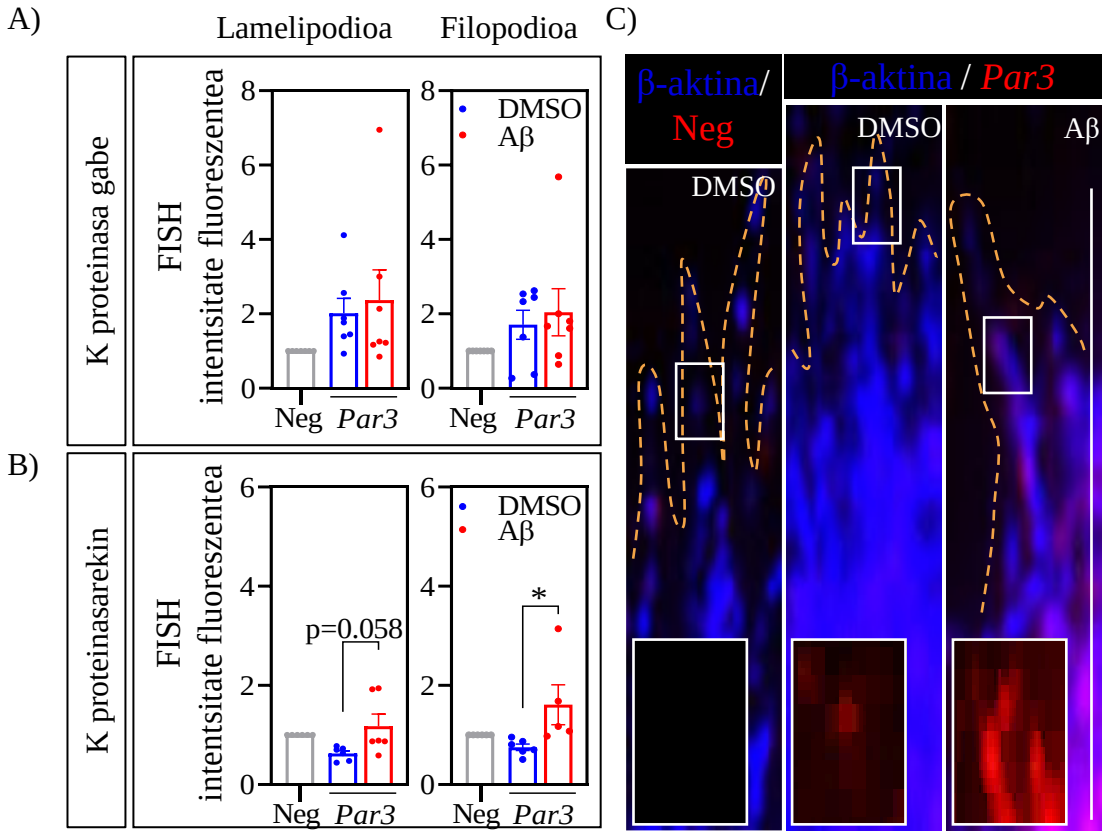

38. irudia: *Par3*ren mRNA mikrogliaren prozesu periferikoetan. *Par3* mRNAa 24 orduz DMSO-rekin (urdina) edo Aβ-rekin (gorria) tratatutako mikroglietako lamelipodioetan eta filopodioetan, K proteinasa gabe (1µg/mL) (A) edo K proteinasarekin (B). Zunda negatiboei dagozkien datuetara normalizatuta daude (Neg). C) Mikrogliaren filopodioen *Par3* genearen (gorria) irudi adierazgarriak, Aβ gabe/rekin eta K proteinasarekin (1µg/mL). Eskala-barra, 5µm. Grafikoek 7 (K proteinasarik gabe) eta 6 (K proteinasarekin) esperimentu independenteren ±SEM batezbestekoa adierazten dute. Bide bakarreko ANOVA analisia, eta, ondoren Holm-Sidak *post hoc* proba, * $p<0.05$.

Bestalde, *Actb* aztertu zen. Ikus dezakegunez, Aβ-k ez zuen aldaketarik eragiten *Actb* mailan, ez lamelipodioetan, ez mikrogliaren filopodioetan, K proteinasarekin tratatu gabeko zeluletan (39A irudia). Kasu honetan, *Actb* mailari dagokionez Aβ-k proteinen digestio eragiten duen K proteinasa duten zeluletan ere ez zuen eragin handirik izan mikrogliaren prozesu periferikoetarako (39B irudia). Horrek adierazten du Aβ-k ez dituela mikrogliaren prozesu periferikoetako *Actb*-mailak erregulatzen.

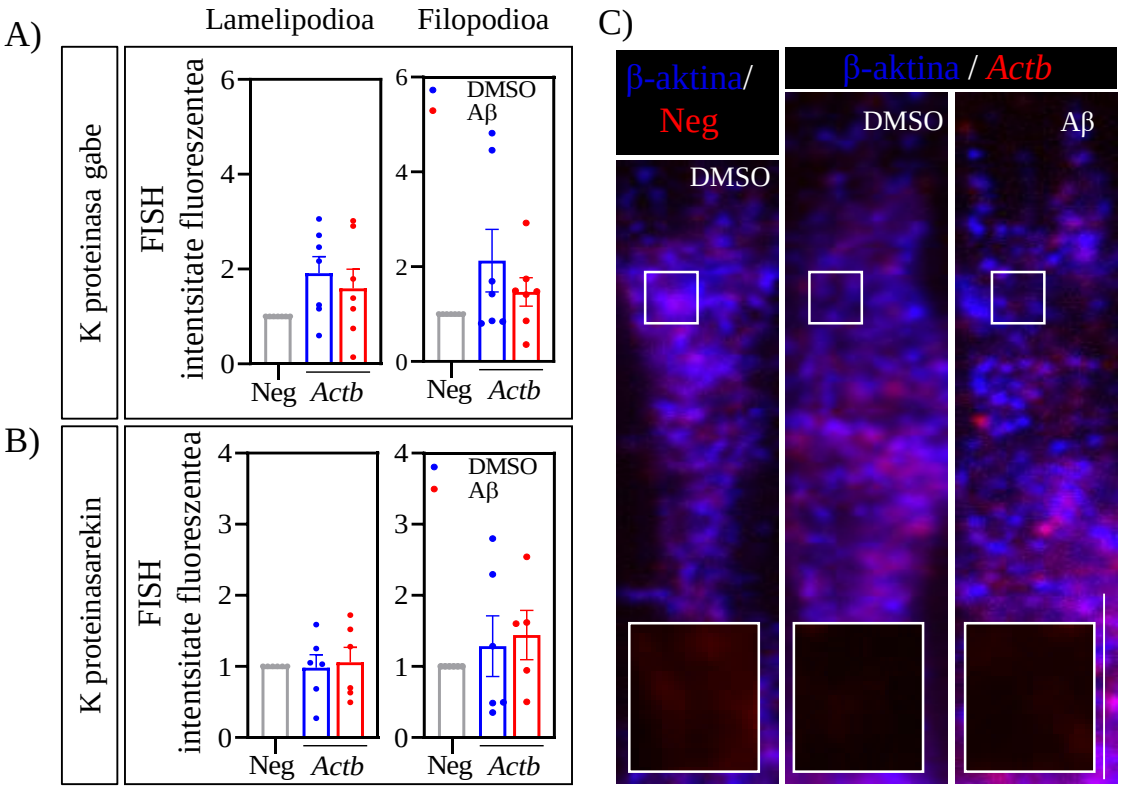

39. irudia: *Actb*-ren mRNA mikrogliaren prozesu periferikoetan. *Actb* mRNAa 24 orduz DMSO-rekin (urdina) edo Aβ-rekin (gorria) tratatutako mikrogliatako lamelipodioetan eta filopodioetan, K proteinasa gabe (1µg/mL) (A) edo K proteinasarekin (B). Zunda negatiboei dagozkien datuetara normalizatuta daude (Neg). C) Mikrogliaren lamelipodioen *Actb* genearen (gorria) irudi adierazgarriak, Aβ gabe/rekin eta K proteinasarekin (1µg/mL). Eskala-barra, 5µm. Grafikoek 7 (K proteinasarik gabe) eta 6 (K proteinasarekin) esperimentu independenteren ±SEM batezbestekoa adierazten dute. Bide bakarreko ANOVA analisia, eta, ondoren Holm-Sidak *post hoc* proba.

Azkenik, eskualde perinuklearrean *Par3* eta *Actb* mailak aztertu genituen, DMSO-arekin edo Aβ-rekin tratatutako zeluletan. Bi mRNA-tako bat ere ez zegoen eraldatuta (40. irudia).

Emaitza horiek eta Puro-PLA saiakuntzetatik lortutakoek mikrogliaren filopodioetan Aβ-k *Par3*-ren itzulpena erregulatzen duela iradokitzen dute.

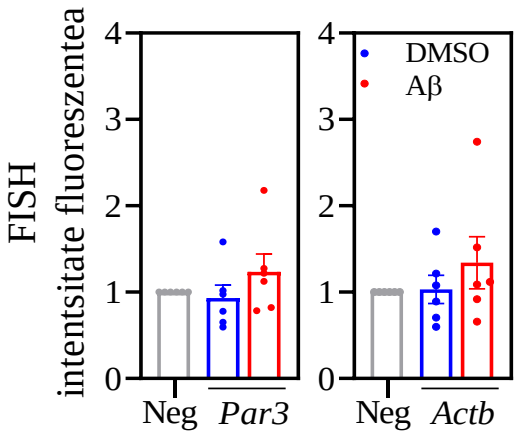

40. irudia*: Par3* eta *Actb*-en mRNAak mikrogliaren eskualde perinuklearrean. *Par3* eta *Actb* mRNA-n adierazpen grafikoa 24 orduz DMSOrekin (urdina) eta Aβ-rekin (gorria) tratatutako mikrogliaren eskualde perinuklearrean, eta K proteinasarekin (1µg/mL). Datuak zunda negatiboekiko normalizatuta daude (Neg). Grafikoek 6 esperimentu independenteren ±SEM batezbestekoa adierazten dute. Bide bakarreko ANOVA analisia, eta, ondoren Holm-Sidak *post hoc* proba.

Hanturaren testuinguruan egindako esperimentuen antzera, amiloideko tratamenduei erantzunez RhoA mailak aztertu genituen. Kasu honetan, ez dugu Aβ-k eragindako aldaketarik ikusi mikrogliaren lamelipodioetan eta filopodioetan (41. irudia), nahiz eta esperimentu horiek K proteinasarik gabe egin ziren, beraz, oraindik zehazteke dago proteinen digestioak aukera emango ote digun Aβ-k mRNA horren kokapenean izan dezakeen eragina argitzeko.

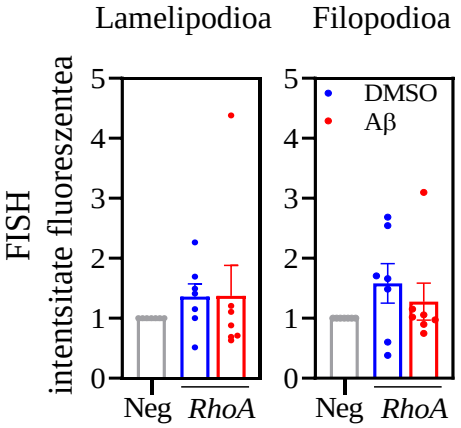

41. irudia: *RhoA*-ren mRNA mikrogliaren prozesu periferikoetan. *RhoA* mRNA-ren irudikapen grafikoa 24 orduz DMSO-rekin (urdina) eta Aβ-rekin (gorria) tratatutako mikrogliaren lamelipodioetan eta filopodioetan. Datuak zunda negatiboekiko normalizatuta daude (Neg). Grafikoek 6 esperimentu independenteren ±SEM batezbestekoa adierazten dute. Bide bakarreko ANOVA analisia, eta, ondoren Holm-Sidak *post hoc* proba.

EZTABAIDA

5. EZTABAIDA

Tesi hau bi hipotesi nagusitan oinarritzen da: lehena, mikrogliak eragina du neuriten tokiko proteoman, testuinguru fisiologikoan eta Aβ-ren oligomeroek eragindako patologian. Bigarrena, mikrogliaren prozesu periferikoetan proteinen sintesi lokala ematen da, eta aldatu egin daiteke hantura eta β-amiloide patologiaren testuinguruan.

Hipotesi horiek frogatzeko, aurrez aipatutako testuinguruetan neuritetan eta mikrogliaren prozesu periferikoetan proteinen sintesi lokala karakterizatu zen. Gure azken helburua NSZaren funtzionamendu egokirako oso ezaguna ez den baina beharrezkoa den mekanismo bat deskribatzea da.

5.1. Mikrogliaren eragina neuriten tokiko itzulpenean, baldintza fisiologiko eta patologikoetan

Ebidentziek zelula glialak ez direla nerbio-sistemaren osagai pasiboak erakusten dute, funtzio neuronala modulatzen duten eta homeostasia hainbat baldintzatan mantentzen duten funtsezko osagaiak baizik. Neurona-glia eta glia-glia elkarrekintzak funtsezkoak dira garunaren ohiko funtzionamendurako (Meyer eta Kaspar, 2017). Neurona-glia komunikazioaren ondorioz, neuronen funtzioak neuronek erregulatzen dituzte, baina baita gliak modu ez-autonomoan eta alderantziz ere. Horrek aukera ematen du mikrogliak neuronen portaera gidatzen duen proteoma modulatzeko hainbat zelula testuingurutan. Proteoma hori modu asimetrikoan banatzen da zelula polarizatuetan, eta, neurri batean, eremu subzelularretara egindako itzulpenen bidez arautu daiteke. Gure ustez, mikrogliak zeregin garrantzitsua du tokiko erregulazio horretan. Izan ere, gure emaitzek agerian uzten dute Boyden ganberetan egindako neuronen kultiboetan mikroglia egoteak neuronek proteina neuritikoak ekoizteko duten gaitasuna handitzea dakarrela oinarrizko baldintzetan (8. irudia). Aβ oligomeroekin egindako tratamenduek ere neuronen itzulpen gaitasuna handitu egiten dute, aurretik argitaratutako ikerketen ildotik (Baleriola et al, 2014), nahiz eta mikrogliaren aurrean ez den aldatzen (8. irudia). Hurrengo paragrafoetan adieraziko den moduan, mikrogliak amiloidea duten neuritetako *de novo* sintetizatutako proteinetan eraginik ez izateak ez du esan nahi proteina jakin batzuetan aldaketarik gertatzen ez denik.

Gure emaitzen arabera, mikrogliak tokiko proteina-ekoizpena modulatzen du neuritetan, gutxienez oinarrizko baldintzetan. Baieztapen hori berresteko, zelula desomatizatuetako proteinen puromizilazioa aztertu genuen, somatik datozen proteinen ekarpena kentzeko.

Hala, bada, *de novo s*intetizatutako proteina mailan gerta daitezkeen aldaketek transkritu lokalizatuen itzulpenean izandako aldaketak adieraziko lituzkete. Kasu horretan, Aβ-k eragindako proteina-sintesia ezin izan zen hauteman, zelula somatizatuetan ikusitakoan ez bezala. Izan ere, zelulak desomatizatzean, neuritetako mRNAen errepertorioan aldaketak eragiten ari gara, edo periferiara eskualde perinuklearrean sintetizatutako proteinen ekarpena eten egiten da. Hala ere, gliaren presentziak, bai oinarrizko kondizioetan, bai Aβ-ren aurrean, proteina neuritikoen ekoizpena handitzen jarraitzen du, nahiz eta somarik ez egon. Honek mikrogliaren presentziak proteina neuritikoen tokiko sintesiaren erregulazioa frogatzen du. Erregulazio hori neuritetako mRNAk itzultzea eragiten duten seinaleak askatzearen ondorioz, edo, gure ikuspuntutik erakargarriagoa dena, proteina erribosomalak gliatik neuronetara transferitzearen ondorioz gerta daiteke, baita mRNA mikroglialen ekarpenaren ondorioz. Hain zuzen ere, nerbio-sistema periferikoan (NSP), nerbioetan lesio bat izan ondoren, Schwan zelulek mRNAk eta erribosomak transferitzen dituzte besikulen bidez (Müller *et al*, 2018). Horregatik, ez da harritzekoa hori bera gertatzea NSZean.

Hain zuzen, nabarmentzekoa da Boyden ganberetako ereinketetan (5. irudia) faktore jariatuen bidezko zelulen arteko komunikazioa bultzatzen dela, neuronak eta mikroglia maila desberdinetan ereiten baitira. Honek aukera ematen du neuritetako proteinen sintesiaren erregulazioa VEen bidez edo zelulaz kanpoko ingurunera askatutako faktore batzuen bidez modulatzeko. Zelula hartzaileen gene-adierazpena erregulatzeko gai diren funtsezko edukiak dituzten VEak deskribatu dira, hala nola azido nukleikoak (DNA zatiak, microRNAak eta mRNAak), mintz-proteinak eta zitosolikoak (Abels eta Breakefield, 2016). Nerbio sistema zentral helduan zelula mota askok VEak askatzen dituzte, neuronak, astrozitoak, oligodendrozitoak eta mikroglia barne (Pascual *et al*, 2020; Paolicelli *et al*, 2019). Horregatik ez litzateke harritzekoa mikrogliatik eratorritako VEek neuritetako proteinen sintesia modulatzea. Baina, gainera, neuronek ere aska ditzakete VEak, mikroglia-neurona komunikazioaren ondorioz, proteoma neuritikoa modulatuz. Gure laborategiko azterketek bi aukera hauek aztertu dituzte, neurona-astrozito komunikazioaren testuinguruan, eta, emaitzek bai astrozitoetatik eratorritako VEek bai neuronetatik eratorritakoak, neuritetan proteinen sintesi lokala erregulatzen dutela iradokitzen dute, testuinguru esperimental desberdinetan.

Proteina neuritikoen masen espektrometria bidezko azterketek, glia dagoenean edo ez dagoenean, mikrogliaren presentziaren ondorioz neuriten tokiko proteomaren

modulazioa berretsi egin dute (42 Ai irudia). Adibidez, besikula sinaptikoak birziklatzen dituzten proteinak gutxitu egin dira, bai oinarrizko baldintzetan, bai baldintza patologikoetan; esaterako, Rab3A (12. irudia), besikula sinaptikoak heltzean, birziklatzean eta garraiatzean inplikatua (Star *et al*, 2005). Besikula sinaptikoek neurotransmisoreak biltegiratzen dituztenez eta kaltzioak eragindako exozitosiagatik askatzen direnez (Takamori, 2009), mikrogliak faktore jariakorren bidez funtzio sinaptikoari eragin diezaioke, besikula sinaptikoak birziklatzearekin lotutako proteinak gutxituz. Emaitza horiek bat datoz mikrogliak aurrez deskribatutako transmisio sinaptikoan duen parte-hartzearekin (Schafer *et al*, 2013).

Neuroendekapenezko testuinguru batean, proteomaren erregulazioa ere aldatu egin zen. Mikrogliak zeregin garrantzitsua du β-amiloide patologian. Tradizioz, mikrogliak Aβ agregatuak fagozitatzen zituela uste izan da, neurobabesa eraginez (Pan *et al*, 2011; Yin *et al*, 2017). Hala ere, Aβ peptidoaren agregazioak ere heda lezake, neurodegenerazio handiagoa eraginez (Venegas *et al*, 2017). Eif4a3 proteina aberastu egin dela ikusi dugu, Aβ-k eragindako baldintzetan eta mikrogliaren aurrean (12. irudia). Eif4a3-k itzulpenaren hasiera arautzen du eta zeregin garrantzitsua du indar sinaptikoari eusteko, plastikotasun sinaptikoari lagunduz (Giorgi *et al*, 2007). Proteina horren goranzko erregulazioa bateragarria da mikrogliaren funtzio neurobabesle batekin. Hala ere, kaspasa-3 (casp-3) proteinaren aberastea ere ikusi dugu (12. irudia), neuronen heriotzan inplikatuta dagoena (Song *et al*, 2009); beraz, gure ereinketetan mikrogliaren presentziak Aβk eragindako neurodegenerazioan parte har lezake. Mikrogliaren aurrean biziraupen edo heriotza neuronala ebaluatzeko esperimentuak egiteko asmoa dugu, baldintza patologikoetan proteoma lokalaren erregulazioa neurodegenerazio handiago batean edo neuronen babes batean gertatzen den zehazteko.

Neuronen eta mikrogliaren arteko interakzioa kontaktu zuzenaren bidez ere gerta daiteke, eta, horri esker, jariatutako faktoreek eragindakoa baino seinaleztapen lokalizatuagoa egin daiteke (Giaume *et al*, 2010; Hamada eta Kole, 2015). Interakzio mota horrek neuritetako proteinen tokiko sintesia ere erregulatzen duen zehazteko, neuronak eta mikroglia plano berean erein ziren (4. irudia, ko-ereinketa arruntak). Neuronen eta mikrogliaren arteko kontaktuak neuritetako itzulpen-guneak modulatzen dituela ikusi dugu, oinarrizko baldintzetan, itzulpena gertatzen den guneak handituz (14A irudia; 42 Aii irudia). Gainera, bi zelula motak elkar ukitzeko aukerak murriztu egiten du jariatutako faktoreen bidezko itzulpenaren erregulazioa; izan ere, mikrogliaren presentziak ez dio

eragiten gliatik urrun dauden neuritetako itzulpenari, ez oinarrizko kondizioetan, ez Aβ oligomeroen presentzian. Mikrogliaren M-CSF bidezko estimulazioak proteina neuritikoen sintesia handitzen ote zuen zehaztu nahi izan genuen. Horrela, oinarrizko baldintzetan, itzulpen-fokuak handitu egiten dira mikrogliarekin kontaktuan dauden neuritetan, baita gliatik urrun zeudenetan, mikrogliaren estimulazioak neuritetako tokiko itzulpenari mesede egiten diola iradokiz, bai kontaktu bidez, bai jariatutako faktoreen bidez (14B irudia). Aβ aurrean jariatutako faktoreek neuronetako itzulpen lokalean eragindako efektua ez da hain argia, izan ere, M-CSF bidezko estimulazioaren ondorioz, soilik mikroglia ukitzen zuten neuriten itzulpen-fokuetan eman zen igoera (15B irudia; 42 Aii irudia). Nolanahi ere, ezin da baztertu proteinen identitatea neurita distaletan mikrogliarekiko desberdina izatea, Boyden ganberetako ereinketen emaitzek adierazten duten bezala (12. irudia).

Laburbilduz, gure emaitzek mikrogliak neuritetako proteinen sintesi lokala modulatu egiten duela iradokitzen dute, eta gainera, proteoma neuritikoa aldatu egiten duela jariatutako faktoreen bidez, bai oinarrizko kondizioetan, bai Aβ-ren oligomeroen bidezko estimulazioaren ondoren (42 Ai irudia). Hori dela eta, neuronetako proteinen sintesi lokalaren erregulazio gliala aztertzera bideratutako etorkizuneko ikerketak baliagarriak izan litezke zelulen arteko komunikazioa eta NSZren patologietan duten inplikazioa hobeto ulertzeko.

5.2. Mikrogliaren prozesu periferikoetako proteinen sintesi lokala

Prozesu glialetako proteinen sintesi lokala ere funtzio gliala erregulatzeko beharrezko mekanismoa da. Astrozitoen prozesu periferikoetako mekanismo hori garuneko fisiologia baskularraren erregulazioan eta transmisio sinaptikoaren erregulazioan inplikatuta dago (Boulay *et al*, 2017; Sakers *et al*, 2017). Prozesu periferiko oligodendrozitikoetan, MBPren sintesi lokala mielinizazioan inplikatuta dago (Quintela-Lopez *et al*, 2019). Behaketa horien ondorioz, mRNAk mikrogliaren prozesu periferikoetan ere aurki daitezkeela eta tokian-tokian itzul daitezkeela hipotetizatu dugu.

Hanturak zenbait gaixotasun neurodegeneratiboren progresioan laguntzen du, eta, testuinguru horretan, mikrogliaren aktibazioa funtsezko osagaia da (Block *et al*, 2007). NSZ-ean bizi diren zelula immuneak direnez, mikrogliak etengabe monitorizatzen du bere mikroingurunea, eta gutxieneko aldaketa homeostatikoei erantzuteko gaitasuna du (Nimmerjahn *et al*, 2005). Mehatxu patologikoei erantzunez, mikrogliak aldaketa morfologiko dramatikoak jasaten ditu, eta zelula adarkatuak izatetik zelula ameboideak

izatera igarotzen da, zelulei egokitzapen zelular handiagoa eta material neuronal kaltetua edo apoptotikoa fagozitatzeko gaitasuna ematen dielarik (Kreutzberg 1996; Hanisch eta Kettenmann, 2007). Lan honetan, ameboide fenotipoan jarri dugu arreta, *in vitro*, estimulazio baten aurrean edo neuronen aurrean mikrogliak morfologia hori izateko joera baitu. Horrek ez du esan nahi mikroglia adarkatuan proteinen sintesi lokalik ez dagoenik. Zelula ameboideetan, bi egitura periferiko hartu ditugu kontuan: lamelipodioak eta filopodioak, mikrogliaren mugikortasunerako garrantzitsuak direnak (Sankar eta Bamburg, 2004). Bi egitura periferiko horiek bai mikroglia ameboidean bai adarkatuan ikus daitezke (Kreutzberg, 1996). Gure emaitzek konpartimentu periferiko horietan erretikulu endoplasmatikorik ez dagoela iradokitzen dute, eta, beraz, hautematen den proteina-sintesi oro zitosoleko erribosoma libreetatik dator (17. irudia).

LPS edo ATP bidezko estimulazio baten aurrean, seinaleztapen-bideak aktibatzen dira TLR4 edo P2Y hartzaileen bidez (Lehnardt *et al*, 2002; Jesudasan *et al*, 2021), hanturazko zitokinak askatuz, hala nola IL-1β, NO edo TNF-α (Mrak eta Griffin, 2005). Aβ-k, halaber, zitokina hauen askapena ere eragiten du, eta horiek Alzheimer gaixotasunaren ezaugarriak dira (Eikelenboom eta van Gool, 2004). Zitokina horiek, LPS, ATP eta Aβ bezala, mugikortasun zuzendua eragiten dute, "mugikortasun kimiotaktikoa" ere deitua (Khurana *et al*, 2002), mikroglia-prozesuen uzkurdura, hedapena eta mugimendua eraginez. Axoietako hazkuntza konoan bezala, non axoien mugimenduan inplikatutako mRNA-k lokalizatzen diren, mikroglia-prozesuak oso dinamikoak dira, eta, horregatik, ez da harritzekoa proteina-sintesi lokalak paper garrantzitsua jokatzea mikroglia-mugikortasunean. Hain zuzen, gure emaitzek mikrogliaren prozesu periferikoetan mRNAen tokiko itzulpena handitu egiten dela aditzera ematen dute, hanturari eta β-amiloide patologiari erantzuteko.

24 orduz LPS-arekin eragindako hanturak *de novo* sintetizatutako proteinen kopurua handitzea eragiten du mikrogliaren periferian, bai eta itzulpen-fokuen kopurua handitzea, proteina-sintesi lokala dagoela iradokiz (19. irudia). Tokiko itzulpena berresteko, ko-lokalizazio saiakuntzak egin genituen, mikrogliaren prozesu periferikoetan mRNA pikorren eta RNA-proteinen arteko ko-lokalizazioaren presentzia egiaztatuz (20. irudia).

Zelula polarizatuetan, hala nola mikroglian, mRNA-ren lokalizazioa egoteak zenbait abantaila ditu: 1) zenbait proteina molekula sintetiza daitezke mRNA molekula bakar batetik abiatuta, eta energia gutxiago behar da mRNA lokalizatzeko proteinen ordez; 2) garraioan zehar gerta daitekeen proteinen difusioak sortzen duen adierazpen ektopikoa,

zelularentzako kaltegarria dena, saihesten du (Derrigo *et al*, 2000). Hain zuzen, mRNAren lokalizazioak eta tokiko itzulpena polaritate zelularraren funtsezko determinatzaileak dira (Buxbaum *et al*, 2015). Gainera, hainbat zelula motatan mRNA ugari leku subzelularretara garraiatzen direla ikusi da, transkritu lokal gisa ezarriz, zelularen erantzun polarizatua erregulatzen dutelarik (Engel *et al*, 2020). Transkritu desberdinen itzulpen lokalak mikrogliaren polarizazioan duten inplikazioa ezezaguna da.

RhoA, Par3 eta *Actb* deritzen transkritoak lokalizatu egiten dira axoi neuronaletan, hazkunde-konoetan hain zuzen, eta axoien aurreratzea erregulatzen dute garapenean zehar gida axonalaren molekulei erantzuteko (Wu *et al*, 2005; Hengst *et al*, 2009; Basell *et al*, 1998). Aldez aurretik aipatutako zitokinek, LPS, ATP edo Aβ molekulak bezala, aldaketa morfologikoak eragiten dituzte mikroglian, eta, ondorioz, fenotipo ameboide bat hartzen du (Suzumura *et al*, 1991). Aldaketa morfologiko horiekin batera zelularen mugikortasuna, zitoeskeletoaren proteinen berrantolatzea, zelula-mintzaren modulazioa eta aktinaren goranzko erregulazioa ere ematen da (Abd-el-Basset eta Fedoroff, 1995; Abd-el-Basset *et al*, 2004). Beraz, hanturazko estimuluei erantzuteko *RhoA, Par3* eta *Actb* mikrogliaren prozesu periferikoetan itzultzen direla hipotetiza daiteke, polarizazioa eta mugikortasuna erregulatuz.

Par3-k zenbait prozesutan parte hartzen du, hala nola, polarizazio zelularrean, migrazioan eta bereizketan (Rodriguez-Boulan eta Macara, 2014). Gure emaitzek mikrogliaren periferiako Par3-ren erregulazio lokala iradokitzen dute, LPSk eragindako hantura akutuko testuinguru batean; izan ere, Par3-ren sintesia eta mRNAren presentzia handitu egiten dira prozesu periferikoetan 30 minutuko estimulazioaren ondoren (23A eta 25B irudiak). LPS bidezko estimulazio luzeagoak periferian ikusten den Par3-ren itzulpena handitzen badu ere, mRNA ez da hautematen ez lamelipodioetan ez filopodioetan. Eskualde perinuklearretik proteina-ekarpen bat egin delako gerta daiteke hori edo mRNAk gutxitu direlako, tokian tokira itzuli ahala. Eskualde perinuklearretik balizko ekarpen bat eginez gero, mikrogliaren prozesu periferikoetan LPSk modu desberdinean erregulatzen duela Par3-ren itzulpena iradokiko luke , eta lokala dela estimulu akutu baten aurrean.

Aktinak garrantzi handia du zelula egituraren eta mugikortasunaren mantentze lanetan (Abd-el-Basset eta Fedoroff, 1995; Abd-el-Basset et al, 2004); horrek, hanturari erantzuteko, aktinaren β isoforma mikrogliaren aldaketa morfologikoetan erabakigarria izan daitekeela iradokitzen du. Hain zuzen, Basset-ek *et al* (2004) LPSk, ATPk edo Aβk,

IL-1β eta TNF-α zitokinek bezala, β-aktinaren goranzko erregulazioa eragiten zutela frogatu zuten, mikroglia hantura-fokuetara migratzea sustatuz. Gure emaitzak bat datoz aurkikuntza horiekin; izan ere, mikrogliaren prozesu periferikoetan β-aktinaren sintesiaren goranzko erregulazioa ikusi dugu (23B irudia). Horrekin batera, *Actb*-ren mRNA handitu egiten da lamelipodioetan, hantura akutuko testuinguru batean (LPS 30 minutuz) (26B irudia). Era berean, ATP bidezko estimulazio akutuak ere *Actb* mRNA handitzea eragiten du mikrogliaren periferian, eta hori lokalki itzul daiteke (30C irudia).

Fibroblastoetan, β-aktina lamelipodioetan lokalizatzen da, funtsezkoa izanik mugikortasun zelularrarentzat (Lawrence eta Singer, 1986). β aktinak eta bere itzulpen lokalizatuak polarizazioan eta mikrogliaren mugikortasunean duen garrantzia ebaluatzeko, doktorego tesi honetan Actb-ren eta bere kokapena arautzen duen RBP proteinaren, Zbp1 proteinaren, gene-isiltzea egin zen. Kontzeptu froga gisa, *Actb*-ren transkripziorako siRNAak erabili genituen. SiRNA bat mRNA-aren eremu kodetzaileari zuzendua diseinatu genuen, eta beste bat 3`UTR eskualdeari zuzendua, haren egonkortasunaz eta lokalizazioaz arduratzen dena (Mignone *et al,* 2002), *Actb*-ren transkritoaren funtzionalitatea aztertu ahal izateko. *Actb*-ren 3`UTR eskualdeari zuzendutako siRNAren bidez transfektatutako zeluletan, 24h-z, *Actb* mRNAen jaitsiera orokorra ikusi genuen (32A irudia). Hala ere, ez genuen aldaketarik ikusi proteina mailan (32C irudia). Hau β aktinaren egonkortasunaren ondorio izan daiteke, izan ere, proteina horrek 10 eguneko batez besteko bizitza izan dezake (Marston eta Redwood, 2003). SiRNAek zeluletan modu endogenoan dauden miRNAk mimetizatzen dituzte, eta azken hauek, batez ere, itzultzen edo itzultzen ari diren mRNAekin lotzen dira, itzuli gabeko mRNAen ordez, siRNAek *Actb*-en itzulpenean eragina izan dezaketela iradokiz (Kobayashi eta Singer, 2022). Horregatik, *in situ* hibridazio-saiakuntzak eta PuroPLA egin beharko genituzke *Actb*-en 3`UTR-ari zuzendutako siRNAk mRNAren kokapena aldatzen duen zehazteko, bai eta transkrituaren eta haren itzulpenaren maila globalak ere (tokikoa ala ez), polarizazioan eta mikroglia mugikortasunean β-aktinak duen ekarpena ebaluatzeko, LPS-ari erantzunez. Nolanahi ere, gure emaitzen arabera, siRNA-k erabil daitezke zelula mikroglietan intereseko geneak isilarazteko.

RBP-ek mRNAen kokalekua eta itzulpena arautzen dute, eta mRNA-en 3`UTR eskualdea ezagutzen dute (Vindry *et al*, 2014). RBP horiek mRNAen prozesamenduan edo *splicing*-ean parte hartzen dute, baita poliadenilazioan, eskualde subzelular periferikoetarako garraioan eta lokalizazioan, itzulpenean eta degradazioan, hala, transkrituen

metabolismoa espazio-denborari dagokionez erregulatuz (Biswas *et al*, 2019). *Actb*-en RBP ezagunenetako bat Zbp1 da (Biswas *et al*, 2019). Gure emaitzek erakusten dutenez, gai gara Zbp1 isilarazteko, mRNA-aren 3`UTR-ra zuzendutako siRNA bat erabiliz, 24 orduz, murrizketa transkritu eta proteina mailan ikusiz. *In situ* hibridazioaren atariko emaitzek adierazten dute mikroglian Zbp1 isiltzeak *Actb*-en pikorren banaketa alda lezakeela, gutxienez oinarrizko baldintzetan (33. irudia). Alterazio hori ez dirudi LPS-arekin tratatutako zeluletan gertatzen denik; hala ere, PuroPLA saiakuntzak egin behar ditugu, izan ere, Zbp1-ek *Actb*-ren tokiko itzulpena ere kontrola dezake (Nicastro *et al*, 2017). Aldi berean, azterketa morfologikoak egin genituen, eta Zbp1-en 3´UTR-ri zuzendutako siRNArekin isiltzeak, 30 minutuz LPS-arekin tratatutako mikroglia zeluletan, filopodioen kopurua handitzeko duela ikusi genuen. Gainera, filopodioen banaketa aldatu egiten da, eta hanturazko baldintzetan, 3`Zbp1 siRNA bidez transfektatutako zelulen eskualde perinuklearrean filopodio gehiago aurkitzen dira (34E, F, G). Eskualde perinuklearretik hurbil gertatzen den filopodioen hazkunde horri polaritate aberrante deritzo, Costa *et al*-en (2020) deskribatzen den bezala, non Rab13 mRNA periferiako lokalizazioaren desarautzeak, HUVEC eta fibroblasto zeluletan, filopodioen banaketa aldatzen zuela ikusi zuten. Horrek *Actb*-en banaketa espaziala aldatzean polaritate mikrogliala asaldatzen dela iradokitzen du, eta horrek proteinen sintesi lokalak mikrogliaren prozesu periferikoetan duen garrantzia adierazten du, hantura-testuinguruan. Gure emaitzek, halaber, LPSrekin egindako 24 orduko tratamenduek handitu egiten dutela filopodioen sorrera adierazten dute; gainera, egitura horietan, *de novo* sintetizatutako proteinak metatzen dira (34H irudia). Interesgarria litzateke, beraz, Zbp1-en isiltzeak polarizazioan eta mikrogliaren morfologian duen eragina aztertzea LPS-arekin egindako estimulazio baten ondoren.

Gogoratu behar da 24 orduzko LPS estimulazioak mikroglia zeluletan handitu egiten duela *de novo* sintetizatutako proteina maila periferian; *Par3* eta *Actb*-ri buruzko azterketek, berriz, bi transkritu hauek LPS estimulu akutuaren ondoren lokalki itzultzen direla ondoriozta dezakegu. 24 orduko tratamenduaren ondoren lortutako emaitzak ez erabakigarriak izanik. Azkenik, gure azterketek, estimulu iraunkorrago bati erantzunez, Par3 edo Actb mikrogliaren periferian itzultzen ez direla adierazten badute ere, beste mRNA batzuk aztertzea merezi du. Bestalde, 30 minutuz LPSk ez du eraginik proteina puromizilatuen mailan, nahiz eta modu lokalizatuan erregulatzen dituen *Par3* eta *Actb* mRNAak. LPS-ak transkritu jakin batzuetan duen eragina ez da islatzen *de novo*

sintetizatutako proteinen maila orokorrean. Hau bera ikusi izan da β-amiloide oligomeroekin tratatutako mikroglia zeluletan.

Aβ-k, LPS-aren estimulu akutuak bezala, ez zuen aldaketarik eragin proteina sintesian edo itzulpen guneetan mikrogliaren prozesu periferikoetan (35. irudia), ez eta RNAren mailetan edo RNAren kokapen-kolokalizazioan (36. irudia). Hala ere, PuroPLA bidezko saiakuntzen bidez *Par3* eta *Actb*-ren itzulpena ematen zela ikusi genuen, Aβ erantzunean (37. irudia). *Par3*-ren mRNA bakarrik hauteman ahal izan zen mikrogliaren periferian, zehazki filopodioetan (38. irudia). Beraz, Aβ-ren oligomeroek Par3-ren sintesi lokala eragiten dutela ondoriozta dezakegu, zeinak filopodioen dinamikan eta zelula-polarizazioaren erregulazioan parte har dezakeen. Izan ere, Par3-ren alterazioak arantza dendritikoetan aldaketak eragiten dituela ikusi da, filopodioen egitura antzekoak direnak (Hakanen *et al*, 2019). Hala ere, funtzionaltasun saiakuntzak egin beharko lirateke hipotesi hori frogatzeko.

LPS-ak eragindako fagozitosi mikrogliala RhoA/ROCK bidez erregulatzen da (Scheiblich eta Bicker, 2017). Hori dela eta, LPS-ak mikrogliaren periferian *RhoA*-ren transkritua maila lokalean arautu zezakeela planteatu genuen, aldi berean mikrogliaren funtzio fagozitikoa arautuz. Gure emaitzek ez dute erregulazio hori iradokitzen, baina, beste esperimenturik ezean, ezin da baztertu aukera hori. Bestalde, mikrogliaren prozesu periferikoetan Par3ren sintesi lokala behatuta, ez legoke gaizki Par6 aztertzea, RhoA-ren jarduera inhibi dezakeela ikusi baita p190 RhoGAP aktibatuz (Hakanen *et al*, 2019).

Azken batean, gure emaitzen arabera, mikrogliaren lamelipodioetan eta filopodioetan tokiko itzulpena dago, eta fenomeno horrek garrantzia du β amiloideak eragindako patologiari eta hanturari erantzuteko (42B irudia). Beraz, ez dira ahaztu behar mRNA-ren garraioa eta transkrituen itzulpen lokalizatuak testuinguru desberdinetan, fenomeno horiek arrasto garrantzitsuak eman baititzakete mikrogliak testuinguru fisiologiko eta patologikoetan duen portaerari buruz.

A) Neuronak

Ai) Jariatutako faktoreak

Proteina	Kontrola	Aβ
Snap25	↓	↓
Rab3A	↓	↓
Ap2b1	↓	↓
Casp3	↓	↑
Pak3	↓	↓
Cdc16	↓	↓
Prpf19	↓	↓
Magohb	↓	↑
Srsf7	=	↑
Eif4a3	=	↑
AldoA	↓	↓
Aldh3a2	=	↑

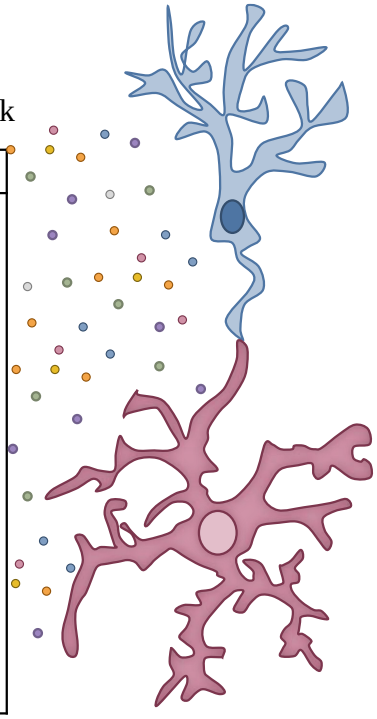

Aii) Kontaktua

Trat	Kontrola	Aβ
- M-CSF	↑	=
+ M-CSF	↑	↑

B) Mikroglia

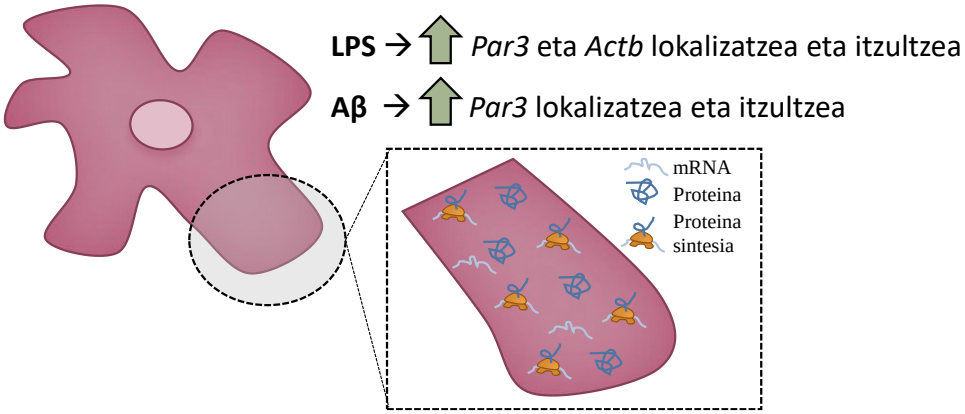

42. irudia. Ondorioen diagrama. A) Ai) Mikrogliak neuriten tokiko proteoma kondizio fisiologiko eta patologikoetan modulatzen du, jariatutako faktoreen bidez. Aii) Mikrogliak itzulpen-guneak modulatzen ditu neuritetan kontaktu bidez, baldintza fisiologiko eta patologikoetan. B) Mikrogliaren prozesu periferikoetan proteinen sintesi lokala ematen da, LPS eta Aβ bidez estimulatuta.

ONDORIOAK

6. ONDORIOAK

1. Mikrogliak, jariatutako faktoreen bidez, neuriten proteina-ekoizpena erregulatzen du, baldintza fisiologiko eta patologikoetan.
2. Neuriten tokiko proteoma aldatu egiten da mikrogliaren presentzian, baldintza fisiologiko eta patologikoetan.
3. Neurona eta mikrogliaren arteko harremanak ere neuritetan zehar ematen den itzulpen-eredua aldatzen du.
4. Prozesu periferiko mikroglialek proteinak sortzen dituzte lokalki hanturari erantzuteko.
5. *Par3* eta *Actb* mRNA-k prozesu periferiko mikroglialetan lokalizatu eta itzuli egiten dira hantura-estimulu akutu baten ondoren.
6. Mikrogliaren prozesu periferikoetako *Actb*-aren sintesi lokala polarizazio zelularrean nahasita egon daiteke.
7. *Par3* mikrogliaren prozesu periferikoetan lokalizatu eta itzuli egiten da β-amiloideari erantzunez, beraz, Alzheimerraren gaixotasunean nahasita egon daiteke.

BIBLIOGRAFIA

7. BIBLIOGRAFIA

abd-el-Basset, E., eta Fedoroff, S. (1995). Effect of bacterial wall lipopolysaccharide (LPS) on morphology, motility, and cytoskeletal organization of microglia in cultures. *Journal of neuroscience research*, *41*(2), 222–237. https://doi.org/10.1002/jnr.490410210.

Abd-El-Basset, E. M., Prashanth, J., eta Ananth Lakshmi, K. V. (2004). Up-regulation of cytoskeletal proteins in activated microglia. *Medical principles and practice : international journal of the Kuwait University, Health Science Centre*, *13*(6), 325–333. https://doi.org/10.1159/000080469.

Abels, E.R. eta Breakefield, X.O. (2016) Introduction to extracellular vesicles: biogenesis, RNA cargo selection, content, release, and uptake. *Cell Mol Neurobiol*, 36:301–312.

Akira, S., Taga, T., eta Kishimoto, T. (1993). Interleukin-6 in biology and medicine. *Advances in immunology*, *54*, 1–78. https://doi.org/10.1016/s0065-2776(08)60532-5.

Alberts, B., Lewis, J., Raff, M., Roberts, K. eta Walter, P. (2002). *Molecular Biology of the Cell*, 4th ed.; Garland Science: New York, NY, USA.

Álvarez, J. I., Katayama, T., eta Prat, A. (2013). Glial influence on the blood brain barrier. *Glia*, 61(12), 1939–1958. https://doi.org/10.1002/glia.22575.

Badimon, A., Strasburger, H.J., Ayata, P., Chen, X., Nair, A., Ikegami, A., Hwang, P., Chan, A.T., Graves, S.M., Uweru, J.O., *et al.* (2020). Negative feedback control of neuronal activity by microglia. *Nature*, 586, 417–423.

Baleriola, J., Walker, C.A., Jean, Y.Y., Crary, J.F., Troy, C.M., Nagy, P.L., *et al* (2014). Axonally synthesized ATF4 transmits a neurodegenerative signal across brain regions. *Cell* 158, 1159–1172. doi: 10.1016/j.cell.2014.07.001.

Baleriola, J. eta Hengst, U. (2015). Targeting axonal protein synthesis in neuroregeneration and degeneration. *Neurotherapeutics*. 12, 57–65.

Banker, G., eta Goslin, K. (1988). Developments in neuronal cell culture. Nature, 336(6195), 185–186. https://doi.org/10.1038/336185a0.

Bannister, N. J., eta Larkman, A. U. (1995). Dendritic morphology of CA1 pyramidal neurones from the rat hippocampus: I. Branching patterns. *The Journal of comparative neurology*, 360(1), 150–160. https://doi.org/10.1002/cne.903600111.

Bechmann, I., Peter, S., Beyer, M., Gimsa, U. eta Nitsch, R. (2001). Presence of B7–2 (CD86) and lack of B7–1 (CD(80) on myelin phagocytosing MHC-IIpositive rat microglia is associated with nondestructive immunity in vivo. *FASEB J.*, 15, 1086–1088.

Ben-Yaakov, K., Dagan, S. Y., Segal-Ruder, Y., Shalem, O., Vuppalanchi, D., Willis, D. E., Yudin, D., Rishal, I., Rother, F., Bader, M., Blesch, A., Pilpel, Y., Twiss, J. L., eta Fainzilber, M. (2012). Axonal transcription factors signal retrogradely in lesioned peripheral nerve. *The EMBO journal*, 31(6), 1350–1363. https://doi.org/10.1038/emboj.2011.494.

Benarroch, E. E. (2005). Neuron-astrocyte interactions: partnership for normal function and disease in the central nervous system. *Mayo Clin. Proc.*, 80, 1326–1338. doi: 10.4065/80.10.1326.

Benarroch, E. E. (2013). Microglia: multiple roles in surveillance, circuit shaping, and response to injury. *Neurology*, 81, 1079–1088. doi: 10.1212/WNL.0b013e3182a4a577.

Bernier, L. P., Bohlen, C. J., York, E. M., Choi, H. B., Kamyabi, A., Dissing-Olesen, L., Hefendehl, J. K., Collins, H. Y., Stevens, B., Barres, B. A., eta MacVicar, B. A. (2019). Nanoscale Surveillance of the Brain

by Microglia via cAMP-Regulated Filopodia. *Cell reports*, 27(10), 2895–2908.e4. https://doi.org/10.1016/j.celrep.2019.05.010.

Bianco, F., Perrotta, C., Novellino, L., Francolini, M., Riganti, L., Menna, E., *et al* (2009). Acid sphingomyelinase activity triggers microparticle release from glial cells. *EMBO J.*, 28, 1043–1054. doi: 10.1038/emboj.2009.45.

Biswas, J., Nunez, L., Das, S., Yoon, Y. J., Eliscovich, C., eta Singer, R. H. (2019). Zipcode Binding Protein 1 (ZBP1; IGF2BP1): A Model for Sequence-Specific RNA Regulation. *Cold Spring Harbor symposia on quantitative biology*, *84*, 1–10. https://doi.org/10.1101/sqb.2019.84.039396.

Blanco-Urrejola, M., Gaminde-Blasco, A., Gamarra, M., de la Cruz, A., Vecino, E., Alberdi, E., eta Baleriola, J. (2021). RNA Localization and Local Translation in Glia in Neurological and Neurodegenerative Diseases: Lessons from Neurons. *Cells*, *10*(3), 632. https://doi.org/10.3390/cells10030632.

Block, M. L., Zecca, L., eta Hong, J. S. (2007). Microglia-mediated neurotoxicity: uncovering the molecular mechanisms. *Nature reviews. Neuroscience*, *8*(1), 57–69. https://doi.org/10.1038/nrn2038.

Boissonneault, V., Filali, M., Lessard, M., Relton, J., Wong, G., eta Rivest, S. (2009). Powerful beneficial effects of macrophage colony-stimulating factor on beta-amyloid deposition and cognitive impairment in Alzheimer's disease. *Brain: a journal of neurology*, *132*(Pt 4), 1078–1092. https://doi.org/10.1093/brain/awn331.

Bolasco, G., Weinhard, L., Boissonnet, T., Neujahr, R., eta Gross, C. T. (2018). Three-Dimensional Nanostructure of an Intact Microglia Cell. *Frontiers in neuroanatomy*, 12, 105. https://doi.org/10.3389/fnana.2018.00105.

Boulay, A. C., Saubaméa, B., Adam, N., Chasseigneaux, S., Mazaré, N., Gilbert, A., Bahin, M., Bastianelli, L., Blugeon, C., Perrin, S., Pouch, J., Ducos, B., Le Crom, S., Genovesio, A., Chrétien, F., Declèves, X., Laplanche, J. L., eta Cohen-Salmon, M. (2017). Translation in astrocyte distal processes sets molecular heterogeneity at the gliovascular interface. *Cell discovery*, 3, 17005. https://doi.org/10.1038/celldisc.2017.5.

Butovsky, O., Ziv, Y., Schwartz, A., Landa, G., Talpalar, A. E., Pluchino, S., Martino, G., eta Schwartz, M. (2006). Microglia activated by IL-4 or IFN-gamma differentially induce neurogenesis and oligodendrogenesis from adult stem/progenitor cells. *Molecular and cellular neurosciences*, 31(1), 149–160. https://doi.org/10.1016/j.mcn.2005.10.006.

Buxbaum, A. R., Haimovich, G., eta Singer, R. H. (2015). In the right place at the right time: visualizing and understanding mRNA localization. *Nature reviews. Molecular cell biology*, *16*(2), 95–109. https://doi.org/10.1038/nrm3918.

Castello, A., Fischer, B., Hentze, M.W. eta Preiss, T. (2013). RNA-binding proteins in Mendelian disease. *Trends in Genetics.*29:318–27.

Chen, S. H., Oyarzabal, E. A., Sung, Y. F., Chu, C. H., Wang, Q., Chen, S. L., et al. (2015). Microglial regulation of immunological and neuroprotective functions of astroglia. *Glia*, 63, 118–131. doi: 10.1002/glia.22738.

Colman, D.R., Kreibich, G., Frey, A.B. eta Sabatini, D.D. (1982). Synthesis and incorporation of myelin polypeptides into CNS myelin. *J. Cell Biol.*, 95, 598–608.

Cook, K.B., Kazan, H., Zuberi, K., Morris, Q., Hughes, T.R. (2011). RBPDB: a database of RNA-binding specificities. *Nucleic Acids Research*. 39:D 301–308.

Costa, G., Bradbury, J. J., Tarannum, N., eta Herbert, S. P. (2020). RAB13 mRNA compartmentalisation spatially orients tissue morphogenesis. *The EMBO journal*, *39*(21), e106003. https://doi.org/10.15252/embj.2020106003.

Cox, L. J., Hengst, U., Gurskaya, N. G., Lukyanov, K. A., eta Jaffrey, S. R. (2008). Intra-axonal translation and retrograde trafficking of CREB promotes neuronal survival. *Nature cell biology*, 10(2), 149–159. https://doi.org/10.1038/ncb1677.

Cserép, C., Pósfai, B., eta Dénes, Á. (2021). Shaping Neuronal Fate: Functional Heterogeneity of Direct Microglia-Neuron Interactions. *Neuron*, 109(2), 222–240. https://doi.org/10.1016/j.neuron.2020.11.007.

Dalmau, I., Finsen, B., Zimmer, J., Gonza´ lez, B. eta Castellano, B. (1998). Development of microglia in the postnatal rat hippocampus. *Hippocampus*, 8, 458–474.

Davalos, D., Grutzendler, J., Yang, G., Kim, J. V., Zuo, Y., Jung, S., Littman, D. R., Dustin, M. L., eta Gan, W. B. (2005). ATP mediates rapid microglial response to local brain injury in vivo. *Nature neuroscience*, 8(6), 752–758. https://doi.org/10.1038/nn1472.

De Simone R., Niturad C.E., De Nuccio C., Ajmone-Cat M.A., Visentin S. eta Minghetti L. (2010). Tgf-β and lps modulate adp-induced migration of microglial cells through p2y1 and p2y12 receptor expression. *J. Neurochem*. 2010;115:450–459. doi: 10.1111/j.1471-4159.2010.06937.x.

Dent, E.W. eta Gertler, F.B. (2003). Cytoskeletal dynamics and transport in growth cone motility and axon guidance. *Neuron* 40: 209–227.

Derrigo, M., Cestelli, A., Savettieri, G., eta Di Liegro, I. (2000). RNA-protein interactions in the control of stability and localization of messenger RNA (review). *International journal of molecular medicine*, *5*(2), 111–123.

Dinarello C. A. (1996). Biologic basis for interleukin-1 in disease. *Blood*, *87*(6), 2095–2147.

Dobbertin, A., Schmid, P., Gelman, M., Glowinski, J., eta Mallat, M. (1997). Neurons promote macrophage proliferation by producing transforming growth factor-beta2. The *Journal of neuroscience: the official journal of the Society for Neuroscience*, 17(14), 5305–5315. https://doi.org/10.1523/JNEUROSCI.17-14-05305.1997.

Donnelly, C. J., Willis, D. E., Xu, M., Tep, C., Jiang, C., Yoo, S., *et al.* (2011). Limited availability of ZBP1 restricts axonal mRNA localization and nerve regeneration capacity. *EMBO J.* 30, 4665–4677. doi: 10.1038/emboj.2011.347.

Eikelenboom, P., eta van Gool, W. A. (2004). Neuroinflammatory perspectives on the two faces of Alzheimer's disease. *Journal of neural transmission (Vienna, Austria: 1996)*, *111*(3), 281–294. https://doi.org/10.1007/s00702-003-0055-1.

Engel, K. L., Arora, A., Goering, R., Lo, H. G., eta Taliaferro, J. M. (2020). Mechanisms and consequences of subcellular RNA localization across diverse cell types. *Traffic (Copenhagen, Denmark)*, *21*(6), 404–418. https://doi.org/10.1111/tra.12730.

Eyo, U.B., Peng, J., Swiatkowski, P., Mukherjee, A., Bispo, A. eta Wu, L.-J. (2014). Neuronal hyperactivity recruits microglial processes via neuronal NMDA receptors and microglial P2Y12 receptors after status epilepticus. *J. Neurosci.*, 34, 10528–10540.

Eyo, U.B., Mo, M., Yi, M.H., Murugan, M., Liu, J., Yarlagadda, R., Margolis, D.J., Xu, P. eta Wu, L.J. (2018). P2Y12R-Dependent translocation mechanisms gate the changing microglial landscape. *Cell Rep.*, 23, 959–966.

Ferreira, S., Pitman, K. A., Wang, S., Summers, B. S., Bye, N., Young, K. M., eta Cullen, C. L. (2020). Amyloidosis is associated with thicker myelin and increased oligodendrogenesis in the adult mouse brain. *Journal of neuroscience research*, *98*(10), 1905–1932. https://doi.org/10.1002/jnr.24672.

Fujita, Y., Nakanishi, T., Ueno, M., Itohara, S., and Yamashita, T. (2020). Netrin-G1 regulates microglial accumulation along axons and supports the survival of layer V neurons in the postnatal mouse brain. *Cell Rep*, 31, 107580.

Gamarra, M., Blanco-Urrejola, M., Batista, A., Imaz, J., eta Baleriola, J. (2020). Object-Based Analyses in FIJI/ImageJ to Measure Local RNA Translation Sites in Neurites in Response to Aβ1-42 Oligomers. *Frontiers in neuroscience*, 14, 547. https://doi.org/10.3389/fnins.2020.00547.

Gamarra, M., de la Cruz, A., Blanco-Urrejola, M., eta Baleriola, J. (2021). Local Translation in Nervous System Pathologies. *Frontiers in integrative neuroscience*, 15, 689208. https://doi.org/10.3389/fnint.2021.689208.

Garden., G.A. eta Möller., T. (2006). Microglia biology in health and disease. *J. Neuroimmune Pharmacol*; 1:127–137. doi: 10.1007/s11481-006-9015-5.

Garner, C. C., eta Matus, A. (1988). Different forms of microtubule-associated protein 2 are encoded by separate mRNA transcripts. *The Journal of cell biology*, 106(3), 779–783. https://doi.org/10.1083/jcb.106.3.779.

Ghézali, G., Dallérac, G., eta Rouach, N. (2016). Perisynaptic astroglial processes: dynamic processors of neuronal information. *Brain structure eta function*, 221(5), 2427–2442. https://doi.org/10.1007/s00429-015-1070-3

Giaume, C., Koulakoff, A., Roux, L., Holcman, D. eta Rouach, N. (2010). Astroglial networks: a step further in neuroglial and gliovascular interactions. *Nat.Rev. Neurosci*., 11, 87–99.

Giorgi, C., Yeo, G. W., Stone, M. E., Katz, D. B., Burge, C., Turrigiano, G., eta Moore, M. J. (2007). The EJC factor eIF4AIII modulates synaptic strength and neuronal protein expression. *Cell*, *130*(1), 179–191. https://doi.org/10.1016/j.cell.2007.05.028.

Graber, T.E., Hebert-Seropian, S., Khoutorsky, A., David, A., Yewdell, J.W., Lacaille, J.C., *et al*. (2013). Reactivation of stalled polyribosomes in synaptic plasticity. *Proc. Natl. Acad. Sci. U.S.A.* 110, 16205–16210. doi: 10.1073/pnas.1307747110.

Hakanen, J., Ruiz-Reig, N., eta Tissir, F. (2019). Linking Cell Polarity to Cortical Development and Malformations. *Frontiers in cellular neuroscience*, *13*, 244. https://doi.org/10.3389/fncel.2019.00244.

Hamada, M.S. eta Kole, M.H.P. (2015). Myelin loss and axonal ion channel adaptations associated with gray matter neuronal hyperexcitability. *J. Neurosci.*, 35, 7272–7286.

Hanisch, U. K., eta Kettenmann, H. (2007). Microglia: active sensor and versatile effector cells in the normal and pathologic brain. *Nature neuroscience*, *10*(11), 1387–1394. https://doi.org/10.1038/nn1997.

Hengst, U., Deglincerti, A., Kim, H. J., Jeon, N. L., eta Jaffrey, S. R. (2009). Axonal elongation triggered by stimulus-induced local translation of a polarity complex protein. *Nature cell biology*, 11(8), 1024–1030. https://doi.org/10.1038/ncb1916.

Ho, Y. H., Lin, Y. T., Wu, C. W., Chao, Y. M., Chang, A. Y., eta Chan, J. Y. (2015). Peripheral inflammation increases seizure susceptibility via the induction of neuroinflammation and oxidative stress in the hippocampus. *Journal of biomedical science*, *22*(1), 46. https://doi.org/10.1186/s12929-015-0157-8.

Holt, C.E., Martin, K.C. eta Schuman, E.M. (2019). Local translation in neurons: Visualization and function. *Nat. Struct. Mol. Biol.* 26, 557–566.

Honda, S., Sasaki, Y., Ohsawa, K., Imai, Y., Nakamura, Y., Inoue, K., eta Kohsaka, S. (2001). Extracellular ATP or ADP induce chemotaxis of cultured microglia through Gi/o-coupled P2Y receptors. *The Journal of neuroscience : the official journal of the Society for Neuroscience*, *21*(6), 1975–1982. https://doi.org/10.1523/JNEUROSCI.21-06-01975.2001.

Hong, S., Beja-Glasser, V. F., Nfonoyim, B. M., Frouin, A., Li, S., Ramakrishnan, S., Merry, K. M., Shi, Q., Rosenthal, A., Barres, B. A., Lemere, C. A., Selkoe, D. J., eta Stevens, B. (2016). Complement and microglia mediate early synapse loss in Alzheimer mouse models. *Science* (New York, N.Y.), 352(6286), 712–716. https://doi.org/10.1126/science.aad8373.

Huang, d., Sherman, B. T., eta Lempicki, R. A. (2009a). Bioinformatics enrichment tools: paths toward the comprehensive functional analysis of large gene lists. *Nucleic acids research*, *37*(1), 1–13. https://doi.org/10.1093/nar/gkn923.

Huang, d., Sherman, B. T., eta Lempicki, R. A. (2009b). Systematic and integrative analysis of large gene lists using DAVID bioinformatics resources. *Nature protocols*, *4*(1), 44–57. https://doi.org/10.1038/nprot.2008.211.

Huang, Y., Smith, D.E., Iba´ n˜ ez-Sandoval, O., Sims, J.E. eta Friedman, W.J. (2011). Neuron-specific effects of interleukin-1b are mediated by a novel isoform of the IL-1 receptor accessory protein. *J. Neurosci*., 31, 18048–18059.

Iadecola C. (2017). The Neurovascular Unit Coming of Age: A Journey through Neurovascular Coupling in Health and Disease. *Neuron*, 96(1), 17–42. https://doi.org/10.1016/j.neuron.2017.07.030.

Jesudasan, S., Gupta, S. J., Churchward, M. A., Todd, K. G., eta Winship, I. R. (2021). Inflammatory Cytokine Profile and Plasticity of Brain and Spinal Microglia in Response to ATP and Glutamate. *Frontiers in cellular neuroscience*, *15*, 634020. https://doi.org/10.3389/fncel.2021.634020.

Jha, M. K., Jo, M., Kim, J. H., eta Suk, K. (2019). Microglia-astrocyte crosstalk: an intimate molecular conversation. *Neuroscientist*, 25, 227–240. doi: 10.1177/1073858418783959.

Joshi, P., Turola, E., Ruiz, A., Bergami, A., Libera, D. D., Benussi, L., Giussani, P., Magnani, G., Comi, G., Legname, G., Ghidoni, R., Furlan, R., Matteoli, M., eta Verderio, C. (2014). Microglia convert aggregated amyloid-β into neurotoxic forms through the shedding of microvesicles. *Cell death and differentiation*, 21(4), 582–593. https://doi.org/10.1038/cdd.2013.180.

Jung, H., Yoon, B.C. eta Holt, C.E. (2012). Axonal mRNA localization and local protein synthesis in nervous system assembly, maintenance and repair. *Nat. Rev. Neurosci.* 13, 308–324.

Kato, G., Inada, H., Wake, H., Akiyoshi, R., Miyamoto, A., Eto, K., Ishikawa, T., Moorhouse, A.J., Strassman, A.M. eta Nabekura, J. (2016). Microglial Contact Prevents Excess Depolarization and Rescues Neurons from Excitotoxicity. *ENeuro*, 3, 761–770.

Khurana, B., Khurana, T., Khaire, N., eta Noegel, A. A. (2002). Functions of LIM proteins in cell polarity and chemotactic motility. *The EMBO journal*, *21*(20), 5331–5342. https://doi.org/10.1093/emboj/cdf550.

Kinney, J. W., Bemiller, S. M., Murtishaw, A. S., Leisgang, A. M., Salazar, A. M., eta Lamb, B. T. (2018). Inflammation as a central mechanism in Alzheimer's disease. *Alzheimer's eta dementia (New York, N. Y.)*, *4*, 575–590. https://doi.org/10.1016/j.trci.2018.06.014.

Kitayama, M., Ueno, M., Itakura, T. eta Yamashita, T. (2011). Activated microglia inhibit axonal growth through RGMa. *PLoS ONE*, 6, e25234.

Kobayashi, S., Tanaka, T., Soeda, Y., Almeida, O., eta Takashima, A. (2017). Local Somatodendritic Translation and Hyperphosphorylation of Tau Protein Triggered by AMPA and NMDA Receptor Stimulation. *EBioMedicine*, 20, 120–126. https://doi.org/10.1016/j.ebiom.2017.05.012.

Kobayashi, H., eta Singer, R. H. (2022). Single-molecule imaging of microRNA-mediated gene silencing in cells. *Nature communications*, *13*(1), 1435. https://doi.org/10.1038/s41467-022-29046-5.

Koenig, E., eta Koelle, G. B. (1960). Acetylcholinesterase regeneration in peripheral nerve after irreversible inactivation. *Science* (New York, N.Y.), 132(3435), 1249–1250. https://doi.org/10.1126/science.132.3435.1249.

Kreutzberg G. W. (1996). Microglia: a sensor for pathological events in the CNS. *Trends in neurosciences*, *19*(8), 312–318. https://doi.org/10.1016/0166-2236(96)10049-7.

Kumar, A., Stoica, B. A., Loane, D. J., Yang, M., Abulwerdi, G., Khan, N., Kumar, A., Thom, S. R., eta Faden, A. I. (2017). Microglial-derived microparticles mediate neuroinflammation after traumatic brain injury. *Journal of neuroinflammation*, 14(1), 47. https://doi.org/10.1186/s12974-017-0819-4.

Lawrence, J. B., eta Singer, R. H. (1986). Intracellular localization of messenger RNAs for cytoskeletal proteins. *Cell*, *45*(3), 407–415. https://doi.org/10.1016/0092-8674(86)90326-0.

Leal, G., Comprido, D., eta Duarte, C. B. (2014). BDNF-induced local protein synthesis and synaptic plasticity. *Neuropharmacology*, 76 Pt C, 639–656. https://doi.org/10.1016/j.neuropharm.2013.04.005.

Lehnardt, S., Lachance, C., Patrizi, S., Lefebvre, S., Follett, P. L., Jensen, F. E., Rosenberg, P. A., Volpe, J. J., eta Vartanian, T. (2002). The toll-like receptor TLR4 is necessary for lipopolysaccharide-induced oligodendrocyte injury in the CNS. *The Journal of neuroscience : the official journal of the Society for Neuroscience*, *22*(7), 2478–2486. https://doi.org/10.1523/JNEUROSCI.22-07-02478.2002.

Lehrman, E.K., Wilton, D.K., Litvina, E.Y., Welsh, C.A., Chang, S.T., Frouin, A., Walker, A.J., Heller, M.D., Umemori, H., Chen, C. eta Stevens, B. (2018). CD47 Protects Synapses from Excess Microglia-Mediated Pruning during Development. *Neuron*, 100, 120–134.e6.

Leung, K. M., van Horck, F. P., Lin, A. C., Allison, R., Standart, N., eta Holt, C. E. (2006). Asymmetrical beta-actin mRNA translation in growth cones mediates attractive turning to netrin-1. *Nature neuroscience*, 9(10), 1247–1256. https://doi.org/10.1038/nn1775.

Lim, S.-H., Park, E., You, B., Jung, Y., Park, A.-R., Park, S.G. eta Lee, J.-R. (2013). Neuronal synapse formation induced by microglia and interleukin 10. *PLoS ONE*, 8, e81218.

Lin, J. Q., van Tartwijk, F. W., eta Holt, C. E. (2021). Axonal mRNA translation in neurological disorders. *RNA biology*, 18(7), 936–961. https://doi.org/10.1080/15476286.2020.1822638.

Lloyd, A.F., Davies, C.L., Holloway, R.K., Labrak, Y., Ireland, G., Carradori, D., Dillenburg, A., Borger, E., Soong, D., Richardson, J.C., *et al.* (2019). Central nervous system regeneration is driven by microglia necroptosis and repopulation. *Nat. Neurosci*., 22, 1046–1052.

Lowery, L.A. eta Van Vactor, D. (2009). The trip of the tip: understanding the growth cone machinery. *Nat Rev Mol Cell Biol*, 10: 332 –343.

Marín-Teva, J. L., Dusart, I., Colin, C., Gervais, A., van Rooijen, N., eta Mallat, M. (2004). Microglia promote the death of developing Purkinje cells. *Neuron*, 41(4), 535–547. https://doi.org/10.1016/s0896-6273(04)00069-8.

Marston, S. B., eta Redwood, C. S. (2003). Modulation of thin filament activation by breakdown or isoform switching of thin filament proteins: physiological and pathological implications. *Circulation research*, *93*(12), 1170–1178. https://doi.org/10.1161/01.RES.0000105088.06696.17.

Martin K. C. (2004). Local protein synthesis during axon guidance and synaptic plasticity. *Current opinion in neurobiology*, 14(3), 305–310. https://doi.org/10.1016/j.conb.2004.05.009.

Martin, K.C. eta Ephrussi, A. (2009). mRNA localization: Gene expression in the spatial dimension. *Cell*. 136, 719–730.

Mazaré, N., Oudart, M., Moulard, J., Cheung, G., Tortuyaux, R., Mailly, P., Mazaud, D., Bemelmans, A.P., Boulay, A.C., Blugeon, C., *et al.* (2020). Local Translation in Perisynaptic Astrocytic Processes Is Specific and Changes after Fear Conditioning. *Cell Rep.*, 32, 108076.

Meyer, K. eta Kaspar, B. K. (2017). Glia-neuron interactions in neurological diseases: testing non-cell autonomy in a dish. *Brain Res.*, 1656, 27–39. doi: 10.1016/j.brainres.2015.12.051.

Mignone, F., Gissi, C., Liuni, S. eta Pesole G. (2002). Untranslated regions of mRNAs. *Genome Biol* 3, reviews0004.1. https://doi.org/10.1186/gb-2002-3-3-reviews0004.

Mrak, R. E., eta Griffin, W. S. (2005). Glia and their cytokines in progression of neurodegeneration. *Neurobiology of aging*, *26*(3), 349–354. https://doi.org/10.1016/j.neurobiolaging.2004.05.010.

Müller, K., Schnatz, A., Schillner, M., Woertge, S., Müller, C., von Graevenitz, I., Waisman, A., van Minnen, J., eta Vogelaar, C. F. (2018). A predominantly glial origin of axonal ribosomes after nerve injury. *Glia*, *66*(8), 1591–1610. https://doi.org/10.1002/glia.23327.

Nagelreiter, F., Coats, M. T., Klanert, G., Gludovacz, E., Borth, N., Grillari, J., eta Schosserer, M. (2018). OPP Labeling Enables Total Protein Synthesis Quantification in CHO Production Cell Lines at the Single-Cell Level. *Biotechnology journal*, *13*(4), e1700492. https://doi.org/10.1002/biot.201700492.

Nicastro, G., Candel, A. M., Uhl, M., Oregioni, A., Hollingworth, D., Backofen, R., Martin, S. R., eta Ramos, A. (2017). Mechanism of β-actin mRNA Recognition by ZBP1. *Cell reports*, *18*(5), 1187–1199. https://doi.org/10.1016/j.celrep.2016.12.091.

Nimmerjahn, A., Kirchhoff, F., eta Helmchen, F. (2005). Resting microglial cells are highly dynamic surveillants of brain parenchyma in vivo. *Science* (New York, N.Y.), 308(5726), 1314–1318. https://doi.org/10.1126/science.1110647.

Olmos, G. eta Llado, J. (2014). Tumor necrosis factor alpha: a link between neuroinflammation and excitotoxicity. *Mediators Inflamm.*, 861231.

Oudart, M., R. Tortuyaux, P. Mailly, N. Mazare, A.C. Boulay eta M. Cohen-Salmon. (2020). AstroDot - a new method for studying the spatial distribution of mRNA in astrocytes. *J Cell Sci*. 133.

Ohsawa, K., Imai, Y., Kanazawa, H., Sasaki, Y., eta Kohsaka, S. (2000). Involvement of Iba1 in membrane ruffling and phagocytosis of macrophages/microglia. *Journal of cell science*, *113 (Pt 17)*, 3073–3084.

Pan, X. D., Zhu, Y. G., Lin, N., Zhang, J., Ye, Q. Y., Huang, H. P., eta Chen, X. C. (2011). Microglial phagocytosis induced by fibrillar β-amyloid is attenuated by oligomeric β-amyloid: implications for Alzheimer's disease. *Molecular neurodegeneration*, *6*, 45. https://doi.org/10.1186/1750-1326-6-45.

Paolicelli, R. C., Bergamini, G., eta Rajendran, L. (2019). Cell-to-cell Communication by Extracellular Vesicles: Focus on Microglia. *Neuroscience*, 405, 148–157. https://doi.org/10.1016/j.neuroscience.2018.04.003.

Parkhurst, C. N., Yang, G., Ninan, I., Savas, J. N., Yates, J. R., 3rd, Lafaille, J. J., Hempstead, B. L., Littman, D. R., eta Gan, W. B. (2013). Microglia promote learning-dependent synapse formation through brain-derived neurotrophic factor. *Cell*, 155(7), 1596–1609. https://doi.org/10.1016/j.cell.2013.11.030.

Polazzi, E., eta Contestabile, A. (2002). Reciprocal interactions between microglia and neurons: from survival to neuropathology. Reviews in the neurosciences, 13(3), 221–242. https://doi.org/10.1515/revneuro.2002.13.3.221.

Prada, I., Gabrielli, M., Turola, E., Iorio, A., D'Arrigo, G., Parolisi, R., De Luca, M., Pacifici, M., Bastoni, M., Lombardi, M., Legname, G., Cojoc, D., Buffo, A., Furlan, R., Peruzzi, F., eta Verderio, C. (2018). Glia-to-neuron transfer of miRNAs via extracellular vesicles: a new mechanism underlying inflammation-

induced synaptic alterations. *Acta neuropathologica*, *135*(4), 529–550. https://doi.org/10.1007/s00401-017-1803-x.

Purves, D., Augustine, G.J., Fitzpatrick, D., *et al*. (2001). Increased Conduction Velocity as a Result of Myelination. *Neuroscience*. 2nd edition. Sunderland (MA): Sinauer Associates. https://www.ncbi.nlm.nih.gov/books/NBK10921/.

Querfurth, H. W., eta LaFerla, F. M. (2010). Alzheimer's disease. *The New England journal of medicine*, 362(4), 329–344. https://doi.org/10.1056/NEJMra0909142.

Quintela-Lopez, T., Ortiz-Sanz, C., Serrano-Regal, M.P., Gaminde-Blasco, A., Valero, J., Baleriola, J., Sanchez-Gomez, M.V., Matute, C. eta Alberdi, E. (2019). Abeta oligomers promote oligodendrocyte differentiation and maturation via integrin beta1 and Fyn kinase signaling. *Cell Death Dis.*, 10, 445.

Rangaraju, V., Tom Dieck, S., eta Schuman, E. M. (2017). Local translation in neuronal compartments: how local is local?. *EMBO reports*, 18(5), 693–711. https://doi.org/10.15252/embr.201744045.

Rangaraju, V., Lauterbach, M. eta Schuman, E.M. (2019). Spatially stable mitochondrial compartments fuel local translation during plasticity. *Cell* 7:e15. doi: 10.1016/j.cell.2018.12.013.

Rodriguez-Boulan, E., eta Macara, I. G. (2014). Organization and execution of the epithelial polarity programme. *Nature reviews. Molecular cell biology*, *15*(4), 225–242. https://doi.org/10.1038/nrm3775.

Roloff, F., Scheiblich, H., Dewitz, C., Dempewolf, S., Stern, M., eta Bicker, G. (2015). Enhanced neurite outgrowth of human model (NT2) neurons by small-molecule inhibitors of Rho/ROCK signaling. *PloS one*, *10*(2), e0118536. https://doi.org/10.1371/journal.pone.0118536.

Rutkevich, L.A. eta Williams, D.B. (2011). Participation of lectin chaperones and thiol oxidoreductases in protein folding within the endoplasmic reticulum. *Curr. Opin. Cell Biol.* 23, 157–166. doi: 10.1016/j.ceb.2010.10.011.

Sakers, K., Lake, A.M., Khazanchi, R.; Ouwenga, R.; Vasek, M.J., Dani, A. eta Dougherty, J.D. (2017). Astrocytes locally translate transcripts in their peripheral processes. *Proc. Natl. Acad. Sci.*, 114, E3830–E3838.

Maiti, S., eta Bamburg, J. R. (2004). Actin-Capping and -Severing Proteins. *Encyclopedia of Biological Chemistry*, 19–26. https://doi.org/10.1016/B0-12-443710-9/00003-X.

Savas, J. N., Ma, B., Deinhardt, K., Culver, B. P., Restituito, S., Wu, L., Belasco, J. G., Chao, M. V., eta Tanese, N. (2010). A role for huntington disease protein in dendritic RNA granules. *The Journal of biological chemistry*, *285*(17), 13142–13153. https://doi.org/10.1074/jbc.M110.114561.

Schafer, D. P., Lehrman, E. K., Kautzman, A. G., Koyama, R., Mardinly, A. R., Yamasaki, R., Ransohoff, R. M., Greenberg, M. E., Barres, B. A., eta Stevens, B. (2012). Microglia sculpt postnatal neural circuits in an activity and complement-dependent manner. *Neuron*, 74(4), 691–705. https://doi.org/10.1016/j.neuron.2012.03.026.

Schafer, D. P., Lehrman, E. K., eta Stevens, B. (2013). The "quad-partite" synapse: microglia-synapse interactions in the developing and mature CNS. *Glia*, *61*(1), 24–36. https://doi.org/10.1002/glia.22389.

Scheiblich, H., eta Bicker, G. (2017). Regulation of Microglial Phagocytosis by RhoA/ROCK-Inhibiting Drugs. *Cellular and molecular neurobiology*, *37*(3), 461–473. https://doi.org/10.1007/s10571-016-0379-7.

Shatz, C.J. (2009). MHC class I: an unexpected role in neuronal plasticity. *Neuron*, 64, 40–45.

Sierra, A., Paolicelli, R. C., eta Kettenmann, H. (2019). Cien Años de Microglía: Milestones in a Century of Microglial Research. *Trends in neurosciences*, *42*(11), 778–792. https://doi.org/10.1016/j.tins.2019.09.004.

Sipe, G.O., Lowery, R.L., Tremblay, M.E., Kelly, E.A., Lamantia, C.E. eta Majewska, A.K. (2016). Microglial P2Y12 is necessary for synaptic plasticity in mouse visual cortex. *Nat. Commun*., 7, 10905.

Skaper, S. D., Facci, L., Zusso, M. eta Giusti, P. (2018). An inflammation-centric view of neurological disease: beyond the neuron. *Front. Cell. Neurosci.*, 12:72. doi: 10.3389/fncel.2018.00072.

Stevens, B., Allen, N.J., Vazquez, L.E., Howell, G.R., Christopherson, K.S., Nouri, N., Micheva, K.D., Mehalow, A.K., Huberman, A.D., Stafford, B., *et al*. (2007). The classical complement cascade mediates CNS synapse elimination. *Cell*, 131, 1164–1178.

Song, Y., Liang, X., Hu, Y., Wang, Y., Yu, H., eta Yang, K. (2008). p,p'-DDE induces mitochondria-mediated apoptosis of cultured rat Sertoli cells. *Toxicology*, *253*(1-3), 53–61. https://doi.org/10.1016/j.tox.2008.08.013.

Star, E. N., Newton, A. J., eta Murthy, V. N. (2005). Real-time imaging of Rab3a and Rab5a reveals differential roles in presynaptic function. *The Journal of physiology*, *569*(Pt 1), 103–117. https://doi.org/10.1113/jphysiol.2005.092528.

Steward, O., eta Fass, B. (1983). Polyribosomes associated with dendritic spines in the denervated dentate gyrus: evidence for local regulation of protein synthesis during reinnervation. *Progress in brain research*, 58, 131–136. https://doi.org/10.1016/S0079-6123(08)60013-8.

Steward, O., eta Levy, W. B. (1982). Preferential localization of polyribosomes under the base of dendritic spines in granule cells of the dentate gyrus. *The Journal of neuroscience: the official journal of the Society for Neuroscience*, 2(3), 284–291. https://doi.org/10.1523/JNEUROSCI.02-03-00284.1982.

Stine, W. B., Jr, Dahlgren, K. N., Krafft, G. A., eta LaDu, M. J. (2003). In vitro characterization of conditions for amyloid-beta peptide oligomerization and fibrillogenesis. *The Journal of biological chemistry*, 278(13), 11612–11622. https://doi.org/10.1074/jbc.M210207200.

Streit, W. J., Mrak, R. E., eta Griffin, W. S. (2004). Microglia and neuroinflammation: a pathological perspective. *Journal of neuroinflammation*, *1*(1), 14. https://doi.org/10.1186/1742-2094-1-14.

Suzumura, A., Marunouchi, T., eta Yamamoto, H. (1991). Morphological transformation of microglia in vitro. *Brain research*, *545*(1-2), 301–306. https://doi.org/10.1016/0006-8993(91)91302-h.

Takamori, S. (2009). Synaptic vesicles. *Encyclopedia of Neuroscience* (pp.801-808). Academic Press. https://doi.org/10.1016/B978-008045046-9.01392-9.

Takeuchi, A., Miyaishi, O., Kiuchi, K., eta Isobe , K. (2001). Macrophage colony-stimulating factor is expressed in neuron and microglia after focal brain injury. *Journal of neuroscience research*, *65*(1), 38–44. https://doi.org/10.1002/jnr.1125.

Takenouchi, T., Tsukimoto, M., Iwamaru, Y., Sugama, S., Sekiyama, K., Sato, M., Kojima, S., Hashimoto, M., eta Kitani, H. (2015). Extracellular ATP induces unconventional release of glyceraldehyde-3-phosphate dehydrogenase from microglial cells. *Immunology letters*, 167(2), 116–124. https://doi.org/10.1016/j.imlet.2015.08.002.

Tiruchinapalli, D. M., Oleynikov, Y., Kelic, S., Shenoy, S. M., Hartley, A., Stanton, P. K., et al. (2003). Activity-dependent trafficking and dynamic localization of zipcode binding protein 1 and beta-actin mRNA in dendrites and spines of hippocampal neurons. *J. Neurosci.* 23, 3251–3261. doi: 10.1523/JNEUROSCI.23-08-03251.2003.

Tracey, K. J., eta Cerami, A. (1994). Tumor necrosis factor: a pleiotropic cytokine and therapeutic target. *Annual review of medicine*, *45*, 491–503. https://doi.org/10.1146/annurev.med.45.1.491.

Tremblay, M.E., Lowery, R.L. eta Majewska, A.K. (2010). Microglial interactions with synapses are modulated by visual experience. *PLoS Biol.*, 8, e1000527.

Turola, E., Furlan, R., Bianco, F., Matteoli, M., eta Verderio, C. (2012). Microglial microvesicle secretion and intercellular signaling. *Frontiers in physiology*, 3, 149. https://doi.org/10.3389/fphys.2012.00149.

Tyanova, S., Temu, T., eta Cox, J. (2016a). The MaxQuant computational platform for mass spectrometry-based shotgun proteomics. *Nature protocols*, 11(12), 2301–2319. https://doi.org/10.1038/nprot.2016.136.

Tyanova, S., Temu, T., Sinitcyn, P., Carlson, A., Hein, M. Y., Geiger, T., Mann, M., eta Cox, J. (2016b). The Perseus computational platform for comprehensive analysis of (prote)omics data. *Nature methods*, 13(9), 731–740. https://doi.org/10.1038/nmeth.3901.

Umpierre, A.D., Bystrom, L.L., Ying, Y., Liu, Y.U., Worrell, G. eta Wu, L.-J. (2020). Microglial calcium signaling is attuned to neuronal activity in awake mice. *eLife*, 9, e56502.

Vasek, M. J., Garber, C., Dorsey, D., Durrant, D. M., Bollman, B., Soung, A., Yu, J., Perez-Torres, C., Frouin, A., Wilton, D. K., Funk, K., DeMasters, B. K., Jiang, X., Bowen, J. R., Mennerick, S., Robinson, J. K., Garbow, J. R., Tyler, K. L., Suthar, M. S., Schmidt, R. E., … Klein, R. S. (2016). A complement-microglial axis drives synapse loss during virus-induced memory impairment. *Nature*, 534(7608), 538–543. https://doi.org/10.1038/nature18283.

Vasek M.J., Deajon-Jackson J.D., Liu Y., Crosby H.W., Yi J. eta Dougherty J.D. (2021). Microglia perform local protein synthesis at perisynaptic and phagocytic structures. *bioRxiv*. doi: 10.1101/2021.01.13.426577.

Venegas, C., Kumar, S., Franklin, B. S., Dierkes, T., Brinkschulte, R., Tejera, D., Vieira-Saecker, A., Schwartz, S., Santarelli, F., Kummer, M. P., Griep, A., Gelpi, E., Beilharz, M., Riedel, D., Golenbock, D. T., Geyer, M., Walter, J., Latz, E., eta Heneka, M. T. (2017). Microglia-derived ASC specks cross-seed amyloid-β in Alzheimer's disease. *Nature*, *552*(7685), 355–361. https://doi.org/10.1038/nature25158.

Vindry, C., Vo Ngoc, L., Kruys, V. eta Gueydan, C. (2014). RNA-binding protein-mediated post-transcriptional controls of gene expression: Integration of molecular mechanisms at the 3’ end of mRNAs?. *Biochemical Pharmacology*. http://dx.doi.org/10.1016/j.bcp.2014.04.003.

von Bernhardi, R., Eugenin-von Bernhardi, J., Flores, B. eta Eugenin Leon, J. (2016). Glial cells and integrity of the nervous system. *Adv. Exp. Med. Biol.*, 949, 1–24. doi: 10.1007/978-3-319-40764-7_1.

Walker, C. A., Randolph, L. K., Matute, C., Alberdi, E., Baleriola, J., eta Hengst, U. (2018). Aβ1-42 triggers the generation of a retrograde signaling complex from sentinel mRNAs in axons. *EMBO reports*, 19(7), e45435. https://doi.org/10.15252/embr.201745435.

Weinhard, L., di Bartolomei, G., Bolasco, G., Machado, P., Schieber, N.L., Neniskyte, U., Exiga, M., Vadisiute, A., Raggioli, A., Schertel, A., *et al.* (2018). Microglia remodel synapses by presynaptic trogocytosis and spine head filopodia induction. *Nat. Commun*., 9, 1228.

Wiśniewski, J. R., Zougman, A., y Mann, M. (2009). Combination of FASP and StageTip-based fractionation allows in-depth analysis of the hippocampal membrane proteome. Journal of proteome research, 8(12), 5674–5678. https://doi.org/10.1021/pr900748n.

Wu, K. Y., Hengst, U., Cox, L. J., Macosko, E. Z., Jeromin, A., Urquhart, E. R., eta Jaffrey, S. R. (2005). Local translation of RhoA regulates growth cone collapse. *Nature*, 436(7053), 1020–1024. https://doi.org/10.1038/nature03885.

Yoon, B. C., Jung, H., Dwivedy, A., O'Hare, C. M., Zivraj, K. H., eta Holt, C. E. (2012). Local translation of extranuclear lamin B promotes axon maintenance. *Cell*, 148(4), 752–764. https://doi.org/10.1016/j.cell.2011.11.064.

Zakaria, R., Wan Yaacob, W. M., Othman, Z., Long, I., Ahmad, A. H., eta Al-Rahbi, B. (2017). Lipopolysaccharide-induced memory impairment in rats: a model of Alzheimer's disease. *Physiological research*, *66*(4), 553–565. https://doi.org/10.33549/physiolres.933480.

Zappulo, A., van den Bruck, D., Ciolli Mattioli, C., Franke, V., Imami, K., McShane, E., Moreno-Estelles, M., Calviello, L., Filipchyk, A., Peguero-Sanchez, E., Müller, T., Woehler, A., Birchmeier, C., Merino, E., Rajewsky, N., Ohler, U., Mazzoni, E. O., Selbach, M., Akalin, A., eta Chekulaeva, M. (2017). RNA localization is a key determinant of neurite-enriched proteome. *Nature communications*, 8(1), 583. https://doi.org/10.1038/s41467-017-00690-6.

Zhang, X. H., eta Poo, M. M. (2002). Localized synaptic potentiation by BDNF requires local protein synthesis in the developing axon. *Neuron*, 36(4), 675–688. https://doi.org/10.1016/s0896-6273(02)01023-1.

ERANSKINAK

8. ERANSKINAK

Blanco-Urrejola, M., Gaminde-Blasco, A., Gamarra, M., de la Cruz, A., Vecino, E., Alberdi, E., & Baleriola, J. (2021). RNA Localization and Local Translation in Glia in Neurological and Neurodegenerative Diseases: Lessons from Neurons. *Cells*, *10*(3), 632. https://doi.org/10.3390/cells10030632.

Gamarra, M., Blanco-Urrejola, M., Batista, A., Imaz, J., & Baleriola, J. (2020). Object-Based Analyses in FIJI/ImageJ to Measure Local RNA Translation Sites in Neurites in Response to Aβ1-42 Oligomers. *Frontiers in neuroscience*, *14*, 547. https://doi.org/10.3389/fnins.2020.00547.

Gamarra, M., de la Cruz, A., Blanco-Urrejola, M., & Baleriola, J. (2021). Local Translation in Nervous System Pathologies. *Frontiers in integrative neuroscience*, *15*, 689208. https://doi.org/10.3389/fnint.2021.689208.

cells

MDPI

Review

RNA Localization and Local Translation in Glia in Neurological and Neurodegenerative Diseases: Lessons from Neurons

Maite Blanco-Urrejola [1,2,3,†], Adhara Gaminde-Blasco [1,2,4,†], María Gamarra [1,2], Aida de la Cruz [1,2], Elena Vecino [3], Elena Alberdi [1,2,4] and Jimena Baleriola [1,3,5,*]

1 Achucarro Basque Center for Neuroscience, 48940 Leioa, Spain; maite.blanco@achucarro.org (M.B.-U.); adhara.gaminde@achucarro.org (A.G.-B.); maria.gamarra@achucarro.org (M.G.); aida.delacruz@achucarro.org (A.d.l.C.); elena.alberdi@ehu.eus (E.A.)
2 Departamento de Neurociencias, Universidad del País Vasco (UPV/EHU), 48940 Leioa, Spain
3 Departamento de Biología Celular e Histología, Universidad del País Vasco (UPV/EHU), 48940 Leioa, Spain; elena.vecino@ehu.eus
4 Centro de Investigación en Red de Enfermedades Neurodegenerativas (CIBERNED), 48940 Leioa, Spain
5 IKERBASQUE, Basque Foundation for Science, 48009 Bilbao, Spain
* Correspondence: jimena.baleriola@achucarro.org
† These authors contributed equally to this work.

Abstract: Cell polarity is crucial for almost every cell in our body to establish distinct structural and functional domains. Polarized cells have an asymmetrical morphology and therefore their proteins need to be asymmetrically distributed to support their function. Subcellular protein distribution is typically achieved by localization peptides within the protein sequence. However, protein delivery to distinct cellular compartments can rely, not only on the transport of the protein itself but also on the transport of the mRNA that is then translated at target sites. This phenomenon is known as local protein synthesis. Local protein synthesis relies on the transport of mRNAs to subcellular domains and their translation to proteins at target sites by the also localized translation machinery. Neurons and glia specially depend upon the accurate subcellular distribution of their proteome to fulfil their polarized functions. In this sense, local protein synthesis has revealed itself as a crucial mechanism that regulates proper protein homeostasis in subcellular compartments. Thus, deregulation of mRNA transport and/or of localized translation can lead to neurological and neurodegenerative diseases. Local translation has been more extensively studied in neurons than in glia. In this review article, we will summarize the state-of-the art research on local protein synthesis in neuronal function and dysfunction, and we will discuss the possibility that local translation in glia and deregulation thereof contributes to neurological and neurodegenerative diseases.

Keywords: mRNA transport and localization; local protein synthesis; neurons; neurites; glia; processes; neurological and neurodegenerative diseases

Citation: Blanco-Urrejola, M.; Gaminde-Blasco, A.; Gamarra, M.; de la Cruz, A.; Vecino, E.; Alberdi, E.; Baleriola, J. RNA Localization and Local Translation in Glia in Neurological and Neurodegenerative Diseases: Lessons from Neurons. *Cells* **2021**, *10*, 632. https://doi.org/10.3390/cells10030632

Academic Editor: Nadia D'Ambrosi

Received: 27 January 2021
Accepted: 9 March 2021
Published: 12 March 2021

1. Introduction: What Is Local Protein Synthesis?

Protein synthesis is an essential process for cellular homeostasis. The classical view is that most RNAs in eukaryotic cells are translated within the soma, either in cytosolic free ribosomes or in rough endoplasmic reticulum (RER)-bound ribosomes. Once the proteins are generated and become mature, many of them are targeted to different subcellular compartments where they elicit their function [1]. An accurate targeting of the subcellular proteome is especially relevant in highly polarized, morphologically complex cells where proteins need to be asymmetrically sorted in order to establish distinct structural and functional domains. Subcellular protein distribution is typically achieved by localization signals within the protein sequence (Figure 1A,B). However, protein delivery to distinct cellular compartments can rely, not only on the transport of the protein itself but also on the transport of the mRNA that is then translated at target sites (Figure 1C). Although once

considered heretical, mechanisms of localizing RNAs have proven to be highly prevalent and conserved in eukaryotes [2]. Additionally, translation of localized mRNAs, also known as local protein synthesis, is increasingly being recognized as a crucial mechanism that contributes to the physiology of the nervous system (NS) [3].

Proteins need to fulfil three main criteria in order to be considered as locally synthesized in a particular subcellular domain: (1) the mRNAs that encode them and components of the translation machinery (ribosomes, regulatory elements) have to co-localize in the same compartment; (2) de novo protein synthesis should be detected at a subcellular level by techniques such as protein metabolic labeling, puromycilation of nascent peptides or translating ribosome affinity purification (TRAP) (Table 1); (3) protein levels after blocking protein synthesis need to decrease in subcellular domains [4].

mRNAs are delivered to subcellular compartments in association with RNA-binding proteins (RBPs) in a translationally repressed state. Ribonucleoprotein complexes (RNPs) are typically packaged into membraneless supramolecular structures, known as RNA granules, which bind to motor proteins that transport the mRNAs to their final destination at the periphery of the cell. Once the mRNAs reach their target compartment, they are released from the RNP complexes and translated locally into protein by the also localized translation machinery (Figure 1C^{i} and C^{ii}) [5]. Hence, to accurately synthesize a protein locally, both RNA transport and translation need to be finely regulated. Malfunctioning of RBPs, deregulation of the translation machinery, changes in the local mRNA repertoire or failure of molecular motors to accurately sort mRNAs to their target compartment can contribute to the disruption of protein homeostasis at a subcellular level. These alterations on the local proteome lead to cellular dysfunction, which in the case of the NS translate into neurological and neurodegenerative diseases [3,6].

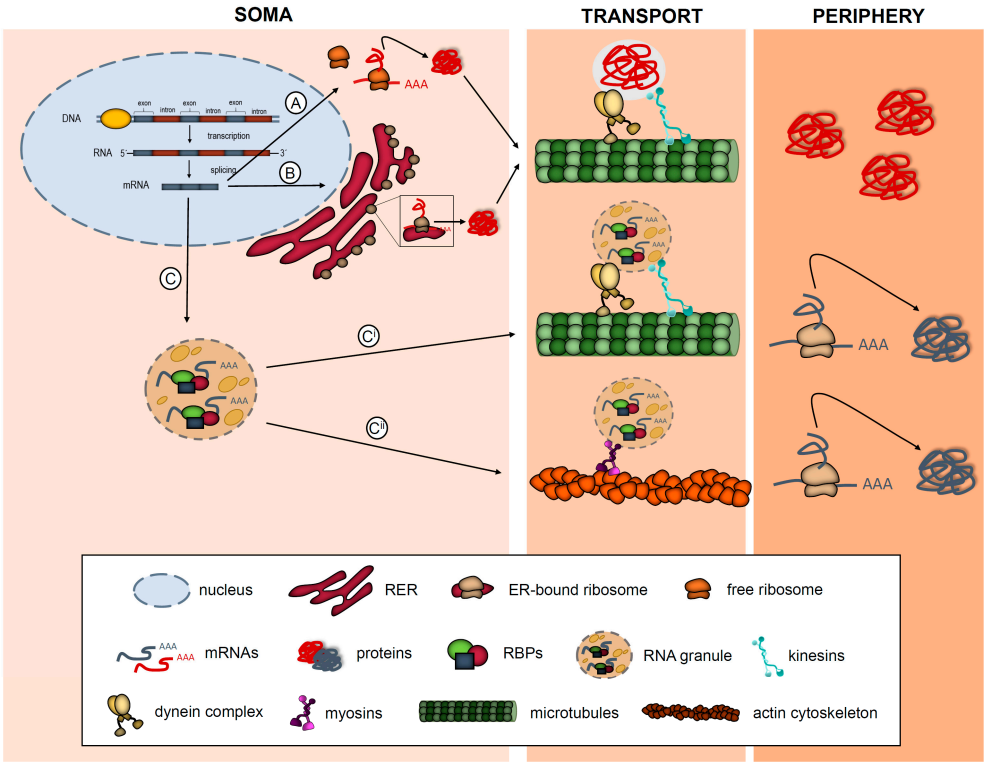

Figure 1. Simplified model of protein and mRNA trafficking in eukaryotic cells. Typically, proteins are thought to be synthesized in the soma by free ribosomes (**A**) or endoplasmic reticulum (ER)-bound ribosomes (**B**) and then transported to different destinations in the cells where they elicit their function. Some mRNAs associate to RNA-binding proteins (RBPs) and are transported in RNA granules (**C**) by microtubules using motor proteins kinesis and dynein (**C^{i}**) or by actin using myosin (**C^{ii}**). Once they reach the target compartment the mRNAs are translated into protein.

Local protein synthesis in the NS has been studied best in neurons, despite neurons not being the only morphologically and functionally complex cells therein. In neurons, local translation occurs both in dendrites and axons. Since the first studies that unambiguously demonstrated the existence of local translation in subneuronal compartments, most interest in the field has focused on the role of locally synthesized proteins in neuronal physiology. However, no evidence existed on the contribution of local protein synthesis to neuronal damage, until almost 20 years ago when activation of intra-axonal protein synthesis in response to nerve injury was reported [7]. Since then, local translation and its defects in neurons have also been linked to amyotrophic lateral sclerosis (ALS) [8–10], spinal muscular atrophy (SMA) [11–13] or Alzheimer's disease (AD) [14–17] to mention but a few NS disorders. Surprisingly, almost no work so far has explicitly reported on the impact of localized translation in glia in neurological or neurodegenerative diseases. In this article we will review the existing evidence of local protein synthesis in neuronal and glial subcellular domains in vertebrates.

First, we will summarize the current knowledge on local translation in neurons and we will refer to existing data that report mainly on the deregulation of RBPs and the localization or/and localized translation of certain mRNAs in neurological and neurodegenerative diseases. Evidence found in neurons will serve as a canvas to depict the possible contribution of glial localized translation to CNS dysfunction.

Table 1. Techniques utilized to measure de novo protein synthesis in neurites.

	Technique	Label	Detection	References
Protein metabolic labeling	BONCAT/ FUNCAT	Noncanonical aminoacids (azide or alkyne)	Covalent cycloaddition reaction with fluorescently tagged or biotinylated reactive group (alkyne or azide)	[18,19]
	SILAC/ pSILAC	Stable isotope	Mass spectrometry	[20,21]
Puromycilation of nascent peptides	SUnSET/ PUNCH-P	tRNA analogue puromycin; biotinylated puromycin	Puromycin immunodetection; biotin-streptavidin conjugation; mass spectrometry following purification of tagged peptides	[22–26]
Translatomic approach	TRAP/ Ribo-Seq	Epitope-tagged ribosome	Epitope immunoprecipitation followed by mRNA purification and detection by RNA-Seq	[27,28]

2. Neuronal RNA Localization, Local Translation and Nervous System Diseases

2.1. Brief Introduction to RNA Localization and Local Translation in Neuronal Processes

Neurons are considered the most morphologically complex cells in the NS. They consist of a cell body or soma from which several processes (dendrites and axons) emerge. Vertebrate neuronal processes can extend from a dozen millimeters (in the case of dendrites) to a meter (in the case of axons) away from the soma [29]. Upon a local signal sensed by neurites, canonical protein synthesis in the cell body followed by protein transport would result in a delayed response from dendrites and axons. Conversely, the presence of localized mRNAs in peripheral neuronal processes allows a rapid reaction of neurites to local stimuli without fully relying on the cell body [5,30]. Local translation in neurons is also involved in the maintenance of the local proteome homeostasis in basal conditions and thus supports basal dendritic and axonal functions [24,31].

Local protein synthesis in neurons was first attributed to dendrites, since for many years axons were thought to be devoid of RNAs and ribosomes [30]. Among the first mRNAs detected in dendrites were the ones encoding high molecular weight microtubule-

associated protein 2a/b (*Map2a/b*) [32], calcium/calmodulin-dependent protein kinase 2 alpha (*Camk2a*) and the calcium-binding protein neurogranin (*Ng/RC3*) [33,34], the inositol 1,4,5-trisphosphate receptor type 1 (*InsP3R1*) [35], some glutamate receptor and glycine receptor subunits [36,37], and the activity-regulated cytoskeleton-associated protein (*Arc*) [38,39]. mRNAs encoding BDNF, TrkB and ß-Actin are localized to dendrites and /or dendritic spines upon neuronal stimulation [40,41]. More importantly, intra-dendritic synthesis, including the one of β-Actin among other proteins mentioned above, is crucial for nervous system plasticity [42,43].

Actb (*ß-actin*) was also the first transcript identified in vertebrate axons in culture [44]. In *Xenopus* embryos, axonal translation of *Actb* contributes to growth cone turning in response to attractive cues and to arbor formation during development [45,46]. Other cytoskeleton- and membrane-associated proteins are locally synthesized upon axon stimulation in rodent neurons: RhoA, Par3, TC10, β catenin and SNAP25 are involved in growth cone behavior [47,48], membrane expansion [49] and synapse formation [50,51]. Local translation is not only required for axon dynamics in response to external cues but also for axon maintenance: axonally synthesized COXIV, LaminB2 and Bcl-W avoid degeneration by regulating mitochondrial function [31,52,53]. Additionally, transcription factors (TFs) can also be locally produced in axons. Two examples thereof include CREB1, which is involved in neuronal survival of dorsal root ganglion neurons [52] and Smad1/5/8, required for axon specification in trigeminal nuclei [53]. As it will be mentioned later, locally synthesized TFs can also be involved in regeneration of peripheral injured nerves [54] and Alzheimer's-related neurodegeneration [14].

Until recently, local translation in neuronal processes was studied by candidate-based approaches. The transcripts of interest were frequently identified in subneuronal compartments by in situ hybridization and/or quantitative RT-PCR analyses of axonal or neuritic (axonal and dendritic) extracts. Interference strategies and protein synthesis inhibitors were used to determine localized translation and the physiological role of concrete proteins found at subneuronal levels. These studies allowed the characterization of a limited amount of locally synthesized proteins in dendrites and axons. However, the development of massive RNA sequencing techniques has provided a much broader view on the local neuronal transcriptome in different experimental setups. More importantly, recent estimates indicate that ~50% of the local neuronal proteome is generated through translation of localized transcripts [28]. Thus, local protein synthesis in neurons is more extended than it was previously thought.

Most work on local translation in neurons has focused on the role of locally produced proteins in NS physiology. However, much less has been reported on the role of local protein synthesis in pathologies. In 2001, Zheng and colleagues showed the ability of injured peripheral axons to synthesize proteins when allowed to regrow in vitro. In addition, inhibiting local translation induced the collapse of new growth cones generated in culture [7]. These results strongly suggested that axons could synthesize proteins in peripheral neuropathies, including nerve injury, and that local translation could be involved in axon regeneration and maintenance of lesioned axons. From then on, other studies supported the knowledge that local protein synthesis was affected in damaged peripheral nervous system (PNS) neurons. Finally, as we will review, this knowledge was more recently extended to the CNS as well [6].

2.2. Neuronal Local Translation in NS Dysfunction

2.2.1. In Traumatic Nerve Injury

Upon nerve dissection, the proximal portion of the axon forms a growth cone-like structure known as the nerve bulb. Similar to developing axons, severed axons respond to cues in their environment and attempt to grow. mRNAs and components of the translation machinery are recruited to nerve bulbs [6]. Among the proteins which are axonally synthesized after sciatic nerve crush, the TFs STAT3 and PPARγ have been identified. They are then retrogradely transported to neuronal cell bodies where they trigger specific

transcriptional programs required for regeneration of injured nerves [54,55]. One of the complexes necessary for the retrograde transport of locally synthesized proteins is importin α/β and importin β is synthesized in lesioned axons too [56]. On the other hand, the master regulator of protein synthesis mTOR is also translated in axons after sciatic nerve injury. A reduction in local mTOR protein levels leads to an overall decrease in protein synthesis in axons. As a result, survival of lesioned neurons becomes compromised [25].

In the case of CNS, the redistribution of RBPs to different subneuronal compartments upon damage has been reported. The RNA-binding protein with multiple splicing (RBPMS), which in retinal ganglion cells is expressed exclusively in the soma, becomes sorted to dendrites and axons upon hypoxia and axotomy, respectively [57]. These results indicate that RNA localization to axons is required to adjust the local proteome to the demands of damaged axons also in the CNS.

Altogether these data suggest that increasing local translation in axons has an important implication in the regeneration of lesioned nerves.

2.2.2. In Motor Neuron Diseases

Whilst changes in the levels of newly synthesized proteins in axons in pathological conditions was first reported in lesioned peripheral nerves [7], recent studies suggest that local translation can also be altered in motor neuron diseases (MNDs). Amyotrophic lateral sclerosis (ALS), also called classical MND, is a disorder whose main feature is the progressive degeneration of upper and lower motor neurons. Among ALS-linked proteins, TDP-43 and FUS can be found in subneuronal compartments. TDP-43 is a RBP that appears aggregated in 97% of ALS patients as well as in many cases of frontotemporal dementia (FTD) [58]. TDP-43 plays a key role in pre-mRNA splicing, mRNA transport and translation in neurites. Studies performed both in *Drosophila* and human samples have identified *Futsch* mRNA (*Map1b* mRNA in mammals) as a TDP-43 target. Interestingly, TDP-43 overexpression leads to a significant reduction of *Futsch* at mRNA and protein levels in neuromuscular junctions while higher levels are observed in the soma of motor neurons. Similarly, MAP1B increases in motor neuron cell bodies in spinal cords from ALS patients. These observations suggest defects in TDP-43 impair *Futsch/Map1b* mRNA localization to axons and its translation [8]. Regarding FUS, it is detected in axons at translation sites and ALS-linked FUS mutations inhibit intra-axonal protein synthesis leading to a stress response with loss of synaptic activity [9]. Interestingly, both TDP-43 and FUS can be found as part of dendritic RNA granules, however the extent to which dendritic localization of both RBPs regulate intra-dendritic translation and contributes to ALS still requires characterization [59].

Spinal muscular atrophy (SMA) is a fatal disorder characterized by a progressive degeneration of spinal motor neurons and skeletal muscle atrophy caused by a reduction of survival motor neuron protein (SMN) due to mutations in the human *SMN1* gene. Lack of SMN has been related to mRNA mislocalization in SMN-deficient axons. SMN associates with the RBPs HuD and IMP1 and engages in the assembly of RNP complexes required for mRNA transport to axons. RNP complexes containing SMN recruit mRNAs such as *Actb*, *Nrn1* and *Gap43*, all involved in axon growth and presynaptic function. Thus, SMN loss impairs the formation of RNP complexes and alters axonal mRNA localization and translation, leading to the phenotypic features of SMA [13]. Other mRNAs whose localization is heavily affected by a ~50% loss of SMN are *Anxa2* and *Cox4i2* [11]. Reduced SMN levels also causes an increase in microRNA-183 which leads to reduced levels of axonally synthesized mTOR. As a consequence, mTOR-dependent translation in axons is affected [12]. Translation via mTOR is also regulated by muscle-secreted factors such as C1q/TNF-Related Protein 3 (CTRP3) whose levels are reduced by *SMN1* mutation [60].

2.2.3. In Alzheimer's Disease and Dementia

Alzheimer's disease (AD) is the leading cause of dementia and it is characterized by the gradual loss of cognitive functions. Despite efforts in developing therapies to stop

the progression of this disease, there is still no cure. AD spreads through the brain in a non-random manner indicating propagation along connecting fiber tracts [61], however the molecular mechanisms leading to this spread are poorly understood. What seems clear is that aggregates of extracellular amyloid β peptide (Aβ) and of hyperphosphorylated microtubule associated protein tau (MAPT or Tau) are post-mortem hallmarks of the disease. Thus, Aβ peptides and Tau are considered the main drivers of AD [62–64]. In 2014, it was reported that in vitro exposure of axons to Aβ peptides induced local protein synthesis and altered the axonal transcriptome [14]. The mRNAs of 9 out of the ~20 susceptibility genes (ca. 45%) reported in late onset AD were found to be recruited above defined threshold levels to Aβ-treated axons: *App*, *Clu*, *ApoE*, *Sorl1*, *Bin1*, *Picalm*, *Ptk2*, *Celf1* and *Fermt2* [14,60]. Interestingly, local *App* and *Clu* mRNAs were significantly increased upon challenging isolated axons with Aβ compared to vehicle-treated axons [14]. Additionally, the mRNA encoding activating transcription factor 4 (ATF4, previously known as CREB2) is locally translated in response to Aβ oligomers. Axonally synthesized ATF4 is retrogradely transported to the nucleus where it mediates neuronal death by regulating transcription both in vitro and in vivo. Interestingly, *Atf4* mRNA recruitment to axons is itself regulated by local translation of sentinel mRNAs including the intermediate filament protein vimentin (*Vim*) [14,15].

Mapt is (together with *Actb*) one the earliest examples of an axonally translated mRNA in hippocampal neurons in vitro. Although the presence of *Mapt* mRNA has been reported both in dendrites and axons [17], Tau protein is heavily localized to axons in healthy neurons partially through the localized translation of its transcript [65,66]. In the context of amyloid pathology, Tau is aberrantly translated in dendrites [17]. Increased dendritic translation leads to Tau hyperphosphorylation and the formation of neurofibrillary tangles [16]. Thus, local synthesis of Tau in the inappropriate subcellular compartment could lead to Tau pathology in AD and related disorders.

Besides changes in local mRNA translation, loss of heterogeneous nuclear ribonucleoproteins A/B (hnRNP A/B) has been reported in entorhinal cortices from AD brains. Interestingly, the authors propose that loss of hnRNP A7B might impact on RNA localization in the AD brain based on the observation that hnRNP A2 is part of RNP complexes that deliver mRNAs to the periphery of oligodendrocytes, as will be mentioned later on [67,68].

Frontotemporal dementia (FTD) is a group of brain disorders characterized by loss of neurons in the frontal and temporal lobes of the brain. As in AD, FTD patients manifest cognitive impairment but, in some cases, they also develop motor symptoms. Indeed 15% of ALS patients have FTD. Both ALS and FTD are characterized by the accumulation of TDP-43 and FUS aggregates. As stated before, both TDP-43 and FUS are involved in RNA localization and localized translation of dendritic and axonal mRNAs [8,9,65]. Thus, deregulation of protein synthesis caused by malfunctioning of both RBPs could contribute to the development of FTD. Interestingly, in 50% of FTD cases an accumulation of Tau fibrils has also been reported [69]. Since Tau is normally synthesized within axons of healthy neurons but its local translation becomes aberrant in AD, we cannot discard that deregulation of local Tau synthesis is involved in some pathological aspects of FTD as well.

All these results indicate that unlike peripheral nerve injury, localized translation in AD and related disorders leads to degeneration rather than neuronal maintenance, survival or axon growth. Additionally, evidence mentioned so far suggests that local protein synthesis is more involved in dementias than was previously acknowledged. Thus, in order to develop accurate treatments, mRNA transport and localized translation should not be disregarded.

2.2.4. In Movement Disorders

Huntington's disease (HD) or Huntington's chorea is a fatal monogenic neurodegenerative disease characterized by involuntary non-stereotypical movements, as well as behavioral and cognitive impairment. HD is caused by CAG repeat expansions in the Huntingtin (*HTT*) gene resulting in repeated polyQ tracts in the N-terminal region of HTT

protein. Mutated HTT is associated with selective toxicity in striatal neurons [70]. The exact role of HTT is not fully understood. Interestingly however, HTT, as well as APP is transported along axons and has been implicated in dendritic RNA delivery [71–75]. Indeed, dendritic HTT co-localizes with the RBPs Ago2 and Staufen, with P-body proteins as well as with the 3'UTR of *Ip3r1*, *Actb*, and *Bdnf* mRNAs. HTT knockout reduces the levels of dendritic *Actb* mRNA, Ago2 protein, and P-bodies. Additionally, HTT suppresses translation of a reporter construct in cortical dendrites. Thus, HTT regulates RNA transport and local translation [73–75]. The toxic effect of mutated HTT seems to be driven by its ability to sequester RBPs such as MBNL1 and SRSF6, and therefore mRNA localization is likely impaired in HD. Importantly, aberrant increased protein synthesis is observed in HD mouse models and human brain samples [76,77].

2.2.5. In Fragile X Syndrome, Autism Spectrum Disorders and Intellectual Disabilities

Fragile X syndrome (FXS) is probably the best example of a disease linked to defects in intra-dendritic mRNA translation as reviewed by Swanger and Bassell [59]. FXS is the most frequent monogenic autism spectrum disorder (ASD), accounting for 2% of all cases [78], and is caused by a mutation in the fragile X mental retardation 1 (*FMR1*) gene which causes loss of FMRP protein. FMRP is a RBP that negatively regulates protein synthesis as well as mRNA stability and transport. FMRP associates to dendritic mRNAs encoding well-known synaptic proteins, including *Arc*, *Camk2a*, *Dlg4* or *Map1b*. Therefore, defects in local protein synthesis have been suggested as a key feature underlying FXS, including defects in spine morphology [79]. Interestingly, *Fmrp* mRNA itself is also localized to and translated within dendrites [79]. Moreover, FMRP is expressed in developing and mature axons [80–83] where its loss alters synaptic connectivity in both *Drosophila* and mouse FXS models [3].

One interesting aspect of the loss of FMRP function is that it impacts mTOR activity, which is not only a key regulator of intra-axonal protein synthesis but also of intra-dendritic translation. Furthermore, mTOR-dependent dendritic translation is suspected to contribute to Rett syndrome, tuberous sclerosis and Down syndrome (DS) [84–86]. Interestingly, Down syndrome cell adhesion molecule (DSCAM) is locally produced in dendrites and its localized translation becomes impaired in DS mouse models. Additionally, dendritic BDNF and BDNF-mediated local translation are also increased in DS [59,86–88]. All in all, local protein synthesis deregulation has been observed in autistic disorders (including FXS) and intellectual disabilities.

To sum up, although early work on protein synthesis in subneuronal compartments was mainly performed in neurons under physiological conditions, an increasing body of evidence indicates that mRNA localization and local translation are altered in pathological contexts as summarized in Figure 2. More importantly, locally produced proteins can actively contribute to the pathophysiology of neurological and neurodegenerative diseases as discussed.

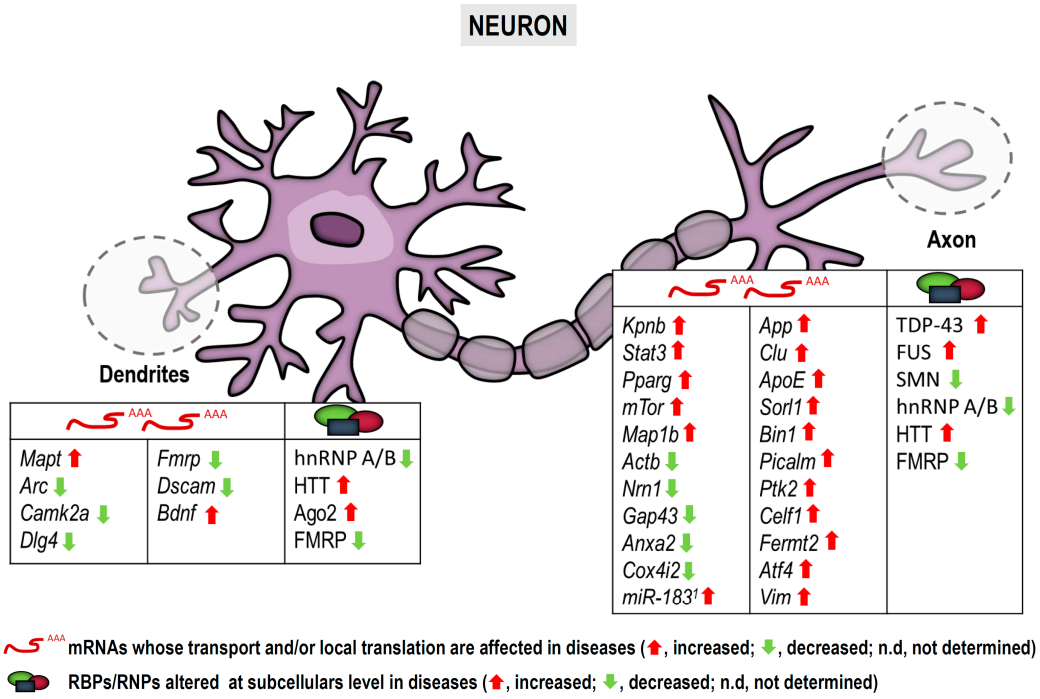

Figure 2. Neurite-localized transcripts and RBPs affected in pathological conditions. Note that some mRNAs and RBPs depicted differ between dendrites and axons. [1] Indicates miR-83 which is not an mRNA but a microRNA, yet it is localized to axons and regulates local protein synthesis [12]. Arrows indicate altered levels (red, increase; green, decrease) of mRNAs and/or proteins in diseases.

3. RNA Localization and Localized Translation in Glia

RNA localization and local translation have been studied far more in neurons than they have in glia. However, neurons are not the only morphologically complex cells in the NS. Glial processes can extend from dozens to some hundred microns from the cell body and can be extremely ramified. It is thus not surprising that in glia too, mRNAs are delivered to distal processes and locally translated into protein in order to maintain the local protein homeostasis and support glial functions. Evidence on local translation in glia was first reported in the early 1980s in oligodendrocytes, in particular in the myelin fraction [89].

In astrocytes and radial glia, RNA localization to peripheral process was first addressed over two decades later [90,91]. As in neurons, glial mRNA localization and localized translation have been reported primarily in the healthy CNS, and evidence on the contribution of local protein synthesis or its deregulation to CNS pathology is very sparse. We will, however, review the few existing studies on glial local translation in neurological and neurodegenerative diseases. We will also discuss the possibility that impaired localization of both RBPs and mRNAs to glial processes contribute to CNS dysfunction.

3.1. RNA Localization and Local Translation in Oligodendroglia

Oligodendrocytes enwrap the axons of the CNS with multiple layers of myelin membrane, which increase the nerve conduction efficiency and speed. In addition, these cells provide axons with trophic support, and therefore maintain axonal health and proper cognitive function. Oligodendrocytes are a very stable cell population with the turnover of only 1 in 300 annually. Nonetheless, the myelin is highly dynamic with one cell producing 10^5 myelin protein molecules per minute and making more than 100 myelin sheaths per cell. This huge biochemical flow is coordinated to ensure the tight temporal and spatial control of the different components of myelin [92,93].

In oligodendrocytes, many mRNAs have been reported as being translated under local regulation at the myelin sheath and in distal processes. The myelin basic protein

mRNA (*Mbp*) was the first transcript detected in peripheral oligodendroglial processes [89]. Some years later, the mRNAs encoding carbonic anhydrase II (CAII) [94], MAPT/Tau [95], myelin-associated oligodendrocytic basic protein (MOBP) [96] and amyloid precursor protein (APP) [97] were also detected in peripheral domains. Interestingly, *Mbp* and *Mobp* mRNAs are also heavily enriched in myelin, as well as transcripts encoding ferritin 1 (FTH1) and pleckstrin (PLEKHB1) [98]. Oligodendrocytes express an array of RBPs which likely regulate RNA localization and localized translation in order to meet protein requirements in each myelin sheath.

From all localized mRNAs in oligodendroglia, *Mbp* is the most studied due to its importance in proper formation of CNS myelin. *Mbp* mRNA is sorted to the periphery of oligodendrocytes within RNA granules in a translationally inactive state. The sorting mechanism involves the recognition of cis-acting A2 response element (A2RE) in the *Mbp* mRNA by the transacting factor hnRNP A2/B1 [67,68]. Other RBPs including hnRNP E1, hnRNP H/F, hnRNP K and QKI also take part in this process [99–101]. Interestingly, the mRNA encoding RBP QKI is one of the most abundant myelin transcripts [98]. Once packaged in RNA granules *Mbp* mRNA is transported along microtubules to peripheral processes and the myelin fraction [102].

Given that many myelin components are transported in specialized RNA granules where RBPs and the microtubule network play critical roles impaired RNA processing, transport failure and/or aggregation of RBPs could affect local translation and even lead to ectopic expression of myelin proteins. Although very little evidence has been published in this regard, we will list below possible links between impaired RNA localization and/or local translation in oligodendrocytes and neurological /neurodegenerative disorders.

3.1.1. In Motor Neuron Diseases

As stated before, 97% of all ALS cases are characterized by the aggregation of the RBP TDP-43 [58]. Interestingly, the vast majority of glial TDP-43 inclusions are found in oligodendrocytes, which are in fact severely affected in this disease [103]. Individuals suffering from ALS, also show a reduction of MBP in both the motor cortex and the ventral spinal cord [104]. Thus, ALS seems not to be a neurodegenerative disease exclusively affecting motor neurons. hnRNP A2/B1 is a known binding partner of TDP-43, and similar to TDP-43, hnRNP A2/B1 has intrinsically disordered aggregation-prone domains which makes it susceptible to fibrillation and incorrect folding. In oligodendrocytes, TDP-43 is physiologically localized in the nucleus, where it binds hnRNP A2/B1. At the same time, hnRNP A2/B1 binds *Mbp* and regulates its distribution towards oligodendroglial processes and the myelin compartments. Therefore, it is feasible that disrupted interaction between TDP-43 and hnRNP A2/B1, due to their pathological aggregation, impairs *Mbp* mRNA transport and its localized translation leading to defects in sheath formation [105,106]. In line with this possibility is the fact that oligodendrocyte-specific deletion of TDP-43 results in defective myelination in mice. While in these mice *Mbp* mRNA remains unchanged, protein levels are decreased, suggesting that MBP protein deficits are caused by deregulation of local translation [107].

About 25–40 % of all familial cases and 8 % of sporadic cases of ALS are caused by a hexanucleotide repeat in the chromosome 9 open reading frame 72 gene (*C9orf72*). C9orf72 protein is known to be involved in mRNA metabolism including mRNA translocation between the nucleus and the cytoplasm. Importantly, C9orf72 also binds hnRNP A2/B1 in oligodendrocytes. It is still unclear whether the toxic effects of mutated C9orf72 reported in *C9orf72*-mediated ALS are elicited by a loss of function of the wildtype protein or a gain of function of the mutant one. In any case, impaired mRNA metabolism and sequestering of RBPs have been suggested as pathological mechanisms leading to ALS [105,108].

It is worth noting that in ALS patients, as well as in ALS mouse models, myelin pathology precedes axonal degeneration, which suggests that oligodendroglial dysfunction should be targeted earlier than motor neuron pathology [103,104]. From this point of view, understanding the extent to which deregulation of local *Mbp* translation contributes

to functional alterations in oligodendrocytes could be crucial to understanding the early stages of ALS.

3.1.2. In Demyelination:

Similar to C9orf72, the RBP QKI also regulates the shuffle of *Mbp* mRNA from the nucleus to the cytoplasm and its localization to myelin [109,110]. A spontaneous mutation affecting the promoter region of the *QKI* gene in *quaking viable* mice (qk^v) heavily reduces the expression of QKI and decreases the levels of *Mbp* mRNA levels in myelin fractions [109]. Interestingly, these mice present demyelination in different regions on the CNS which has been partially attributed to defects in *Mbp* mRNA localization and the consequent defects in localized translation [111]. Moreover, recent work by Lavon and colleagues has reported that QKI is impaired in the brain of a mouse model of experimental autoimmune encephalomyelitis (EAE) as well as in the blood of patients with neuromyelitis-optica and multiple sclerosis (MS). These observations open the possibility that a dysregulation in the *Mbp* mRNA metabolism due QKI dysfunction could impair local MBP synthesis contributing to demyelinating diseases.

3.1.3. In Alzheimer's Disease and Dementias

AD has been traditionally considered as a gray matter disease, but during the last decade neuroimaging techniques have revealed micro- and macro-structural changes in white matter (WM), suggesting that, in addition to the neuronal loss, WM degeneration and demyelination are important pathophysiological features in AD, as reviewed by Nasrabady and colleagues in 2018 [112]. More recently, Aβ-induced *Mbp* mRNA local translation was reported in oligodendrocytic processes, establishing a direct link between accumulation of Aβ peptides and aberrant local protein synthesis in oligodendroglia. Local MBP production in distal processes is regulated by Fyn-mediated signaling pathways promoting oligodendrocyte differentiation [113]. Consistent with these observations, the AD APP/PS1 mouse model shows an upregulation of MBP in the hippocampus and increased myelin thickness [114,115]. Taken together, these results suggest that local translation of *Mbp* mRNA could be disrupted in AD, altering myelin morphology and oligodendrocyte development.

Globular glial tauopathy (GGT) is a rare 4R Tau pathology with abnormal accumulation of phospho-Tau in neurons as well as in astrocytes and oligodendrocytes. From a clinical viewpoint GGT shares features with frontotemporal lobal degeneration including FTD. However, motor manifestations have also been reported [116]. Because tauopathy is considered the main driver of the disease we decided to include GGT in this paragraph. Lately, it has been demonstrated that oligodendrocytes are principal targets and dysfunctional players in the pathogenesis of GGT. In GGT cases, a decreased expression of the myelin related proteins MBP, PLP1, CNP, MAG, MAL, MOG, and MOBP has been described indicating that Tau deposits have consequences in oligodendrocyte function and transport of myelin components leading to defective myelin synthesis [117]. Interestingly, the mRNAs encoding all the myelin proteins mentioned are enriched in myelin extracts compared to cerebellar extracts in adult mice suggesting their localized translation [98]. Tau plays a key role in myelination providing the track for the intracellular translocation of myelin products and controlling cell morphology. Loss of Tau in oligodendrocytes disturbs microtubule stability, impairing process outgrowth and intracellular transport [118]. Tau could thus contribute to mRNA localization in oligodendroglia. Interestingly, Tau hyperphosphorylation has been linked to aberrant local translation, at least in neurons [16,17]. Thus, this event could also lead to phospho-Tau accumulation in oligodendrocytes. It is therefore safe to speculate that deregulation of mRNA transport and localized translation in oligodendroglia is more widespread in GGT than was previously acknowledged.

Although defects in oligodendroglial local translation in FTD have not been suggested so far, as in GGT, Tau accumulation has been reported in 50% of FTD cases [69]. Additionally, the hexanucleotide repeat mutation in *C9orf72* is the most common genetic cause of

FTD and is also involved in the development of some AD, HD and PD cases [108]. Overall, these data strongly support the idea that local protein synthesis in oligodendrocytes plays a crucial role in the context of neurodegenerative diseases and thereby, should be studied more in detail.

3.1.4. In Fragile X Syndrome

As previously mentioned, FXS is the most common inheritable form of ASD caused by loss of FMRP [78]. The RBP FMRP selectively binds 4% of brain mRNAs, including *Mbp*, to regulate their transport, translation, and stability [119]. While WM abnormalities have been established in FXS, the effects of FMRP loss in oligodendrocytes and on myelin production are still partially unknown. The specific function of FMRP in mRNA regulation in oligodendroglia is contradictory. Some in vitro and in vivo studies have shown no effect of FMRP loss on *Mbp* translation or myelin components [120], whereas another study has suggested a inhibitory role for FMRP in *Mbp* translation in vitro [121]. Conversely, delayed myelination has been observed in a mouse model of FXS which is consistent with the reported role of FMRP in promoting myelin sheath growth through the local regulation of MBP synthesis in the CNS of *Xenopus* embryos [122,123]. The latter in vivo studies suggest that altered *Mbp* local translation could contribute to FXS. However, in view of current published work, further investigations are needed to clarify the role of FMRP in oligodendroglial local translation in this disease.

Altogether, the data (summarized in Figure 3) strongly suggest that deregulated local translation in oligodendrocytes plays an important role in neurological and neurodegenerative diseases. Areas of future research must seek to understand the molecular mechanisms underlying local translation in order to develop drugs that selectively control NS disorders involving oligodendroglia dysfunction.

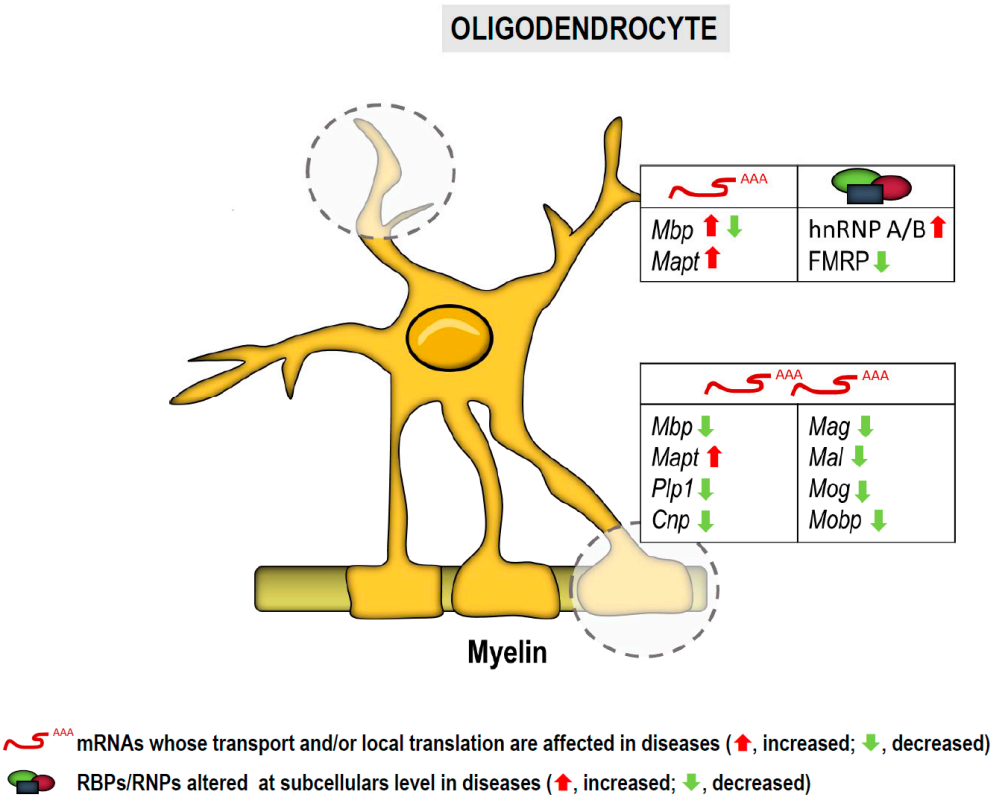

Figure 3. Transcripts and RBPs localized to subcellular compartments in oligodendroglia potentially involved in neurological and neurodegenerative diseases. Local translation occurs both in processes (upper table) and in the myelin sheath (lower table). Arrows indicate altered levels (red, increase; green, decrease) of mRNAs and/or proteins in diseases.

3.2. RNA Localization and Local Translation in Astroglia

Astrocytes are the most abundant type of glia in the mammalian brain. They provide neurons with metabolic, structural and trophic support, they participate in synapse and axon formation and function, and they regulate the cerebral flow by maintaining the blood–brain barrier [124,125]. As neurons, astrocytes are extremely polarized cells with ramifications extending ca. 50 microns away from the soma in rodents and up to 1 millimeter in humans. Astrocytic processes can be classified into branches, branchlets, leaflets and endfeet. Leaflets are thin long processes able to regulate synaptic function and are also known as perisynaptic astrocytic processes (PAPs), whereas endfeet contact the blood vessels, they control blood–brain barrier (BBB) integrity and are also known as perivascular astrocytic processes (PvAPs) [125,126]. Astrocytic processes can be as long as some neurites and it is thus not surprising that they contain RNAs and have the capacity to produce proteins locally. Indeed, early high-throughput analyses of astroglial protrusions revealed that primary mouse astrocytic processes contain ~2200 RNAs at relative levels similar to somatic RNAs or higher, suggesting their enrichment in the periphery of cells [127]. More recently, Sakers and colleagues measured de novo protein synthesis in cortical astrocytes and observed that 73% of translation occurs more than 9 microns away from the nucleus and does not decay in the periphery [111]. Interestingly, years before these studies were performed, mRNA isoforms encoding the glutamate transporter 1 (GLT1) were analyzed in the rat brain by in situ hybridization. *Glt1a* mRNA was detected in abundant levels in astrocytic processes while *Glt1b* mRNA was mainly restricted to the soma [90]. Similarly, *Gfap* isoform α is mainly detected in astroglial protrusions while *Gfapδ* shows mainly somatic localization [128]. Altogether, these results suggest that differential mRNA distribution and localized translation are relevant for functional asymmetry in astrocytes.

PAPs can contact up to 2 million synapses in humans and thus play a major role in synaptic function [129]. Consistent with this function, a variety of ribosome-bound mRNAs involved in glutamate and GABA metabolism (e.g., *Slc1a2*, *Slc1a3*, *Glul*) as well as in synaptogenesis and pruning (e.g., *Mertk*, *Sparc*, *Thbs4*) were identified in PAPs by Sakers and colleagues. Components of the cytoskeleton and proteins involved in fatty acid metabolism are also locally produced in PAPs according to this same study [111]. A more recent study additionally detected translating mRNAs that encode ribosomal proteins and translation regulators as being enriched in PAPs consistent with results obtained in subneuronal compartments. Interestingly, this study performed by Mazaré and colleagues also described how the repertoire of PAP-translated transcripts were regulated by fear conditioning [130].

Similarly, PvAPs or endfeet, which interact with blood vessels and control BBB integrity and cerebral blood flow, contain mRNAs and are competent for local translation. mRNAs which encode proteins involved in BBB immune quiescence (e.g., *Gja1*), BBB integrity (e.g., *Agt*) and perivascular homeostasis (e.g., *Aqp4*, *Kir4.1*, *Hepacam* and *Mlc1*) are enriched in endfeet [131]. Thus, mRNA localization to PvAPs likely contributes to the regulation of brain vascular physiology.

PAPs and PvAPs share the vast majority of their actively translating mRNAs according to work published in 2020 by Mazaré and colleagues [130]. However, some mRNAs are enriched in PAPs compared to PvAPs including *Ezr*, *Rplp1* and *Fth1* [130]. These results suggest that not only a distinct distribution of transcripts between cell bodies and astrocytic processes contributes to the functional polarity of astroglia, but that processes that support different functions in the brain differ in specific mRNA subsets.

Deregulation of the interaction between astrocytes and neurons and astrocytes and the vascular system leads to the development and progression of many neurological and neurodegenerative diseases as previously reviewed [132,133]. Additionally, the complex morphology of astrocytes is altered in brain disorders [126]. Given that astroglial polarity seemingly relies on mRNA localization and local translation as mentioned, it is expected

that locally translated transcripts and/or an aberrant local protein synthesis in astroglial processes are linked to CNS dysfunction as we will review below.

3.2.1. In Motor Neuron Diseases

TDP-43 is a binding protein for the glutamate transporter *Glt1* (*Eaat2*) mRNA and TDP-43 aggregates are associated with astroglial GLT1/EAAT2 loss in ALS mouse models and ALS patients [134,135]. Although TDP-43 aggregation occurs in most ALS cases, in those rare occasions in which its accumulation is absent, patients carry *SOD1* and/or *FUS* mutations. Interestingly, mouse models with ALS-associated *SOD-1* mutations also show reduced levels of GLT1/EAAT2 in astrocytes. Although there is no evidence that decreased astrocytic GLT1/EEAT2 levels are causative of ALS, it seems clear that GLT1 is impaired in this disease [124]. Whether different isoforms of *Glt1* mRNA are selectively affected in ALS suggesting impaired mRNA localization to astrocytic processes and localized translation still requires investigation.

Additionally, a great number of mRNAs localized to PAPs contain QKI response elements (QREs) [111]. As mentioned before, QKI dysregulation has been involved in demyelination but its role in other diseases such as ALS has not been discarded [136].

3.2.2. In Alzheimer's Disease and Dementia

Glial fibrillary acidic protein (GFAP) is the most abundant protein expressed in astrocytes. GFAP plays relevant roles in myelination, white matter vascularization and in keeping BBB integrity [137]. Interestingly, immunohistochemical analyses have shown increased expression of both GFAPα and GFAPδ in reactive astrocytes near amyloid plaques in postmortem AD brains, suggesting a role for both proteins in disease progression [138]. *Gfapα* and *δ* mRNAs are distinctly localized in rodent astrocytes: *Gfapα* is restricted to processes while *Gfapδ* is found in the soma. However, in the APPswe/PS1dE9 AD mouse model, the distribution pattern of both mRNAs varies [139]. Moreover, *Gfap* is regulated by the RBP QKI which is upregulated in sporadic AD cases [140]. Thus, *Gfap* mRNA transport and its localized translation are likely disrupted in AD.

Additionally, some of the ribosome-bound mRNAs known to be enriched in PAPs [111,130] are also localized to amyloid-treated axons [14]. Intriguingly, 24.59% of common transcripts (from a total of 130) categorized in significantly represented GO terms (biological process; false discovery rate (FDR) < 0.05) are involved in translation (Figure 4A). These observations strengthen the belief that components of the translation machinery and translation regulators are themselves locally produced. If we narrow down the analysis to those mRNAs significantly changed in amyloid- vs. non-amyloid-treated axons, 21 mRNAs can be found in both the axonal transcriptome and the PAP translatomes (Figure 4B), one of them being *Gfap* and 7 involved in aging (*Lrp1*, *Timp3*, *Aldoc*, *Clu*, *Eef2*, *Fads1* and *Vim*). *Gfap* mRNA is also bound to ribosomes in PvAPs [131]. Other transcripts identified in a PvAP translatome or "endfeetome" are also among the significantly changed transcripts in amyloid-treated axons (*Aqp4*, *Gpm6b*, *Gja1* and *Mlc1*) [14,131]. The coincidence between these datasets is highly suggestive of the presence of a subset of amyloid-responsive mRNAs in astrocytic processes that could contribute to AD.

PAPs are also enriched in memory-related mRNAs. It would thus not be surprising that their dysregulation could contribute to memory impairment and dementia. Although this point should be confirmed, *Fth1* and *Ftl1* are linked to superficial siderosis and brain iron accumulation, both leading to neurodegeneration and dementia [141], and are bound to PAP ribosomes. Interestingly, both transcripts are reduced upon fear conditioning in mice [130].

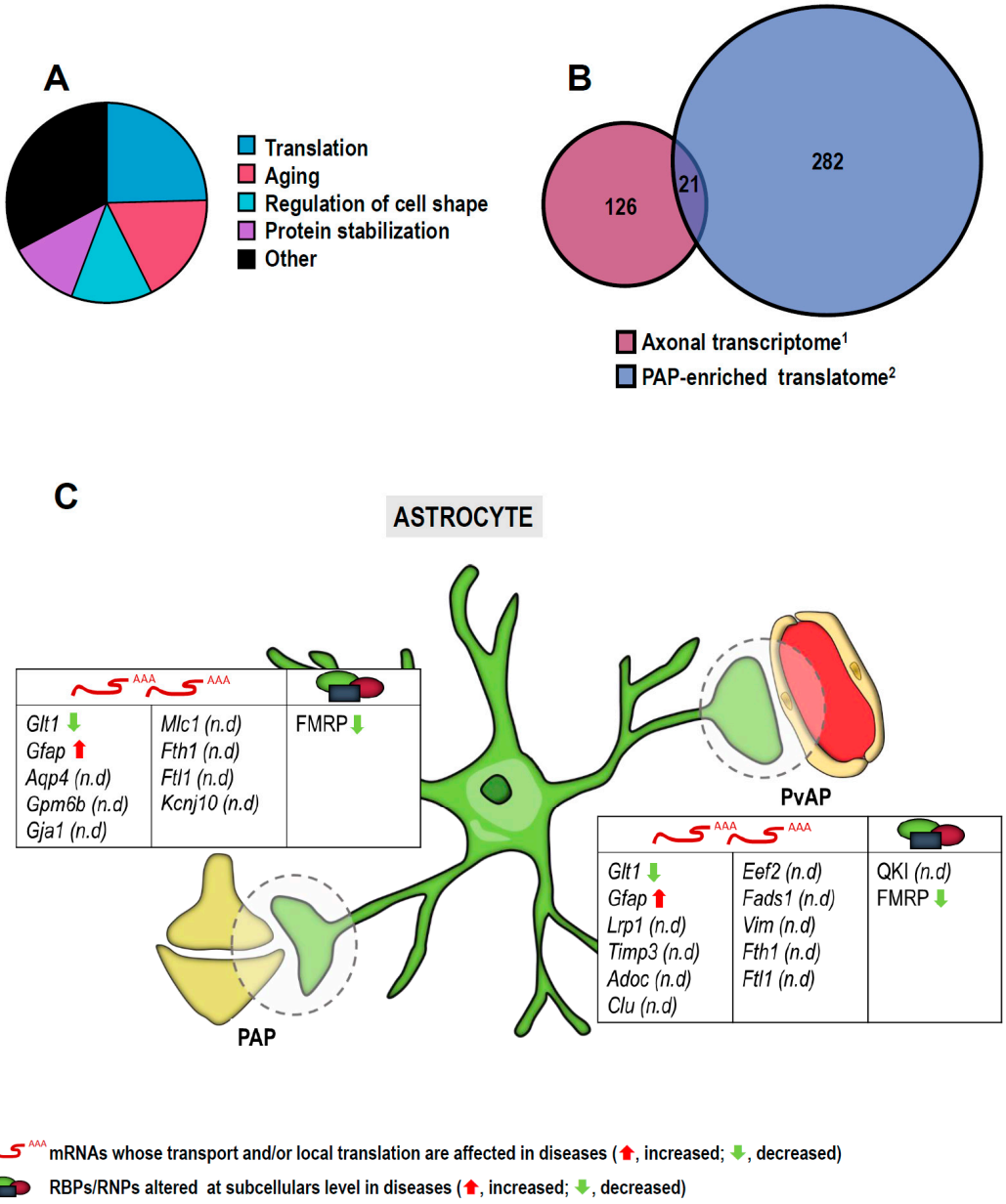

Figure 4. Taking advantage of the detailed analyses performed on the local translatome in astroglial peripheral processes [111,130] and on the axonal transcriptome of Aβ-treated axons [14], a GO term analysis of common localized transcripts found in astrocytes and neurons is shown (FDR < 0.05) (**A**). Focusing on significantly changed transcripts in Aβ-treated axons compared to controls ([1]), 21 one of them are also found in perisynaptic astrocytic process (PAP) translatome datasets ([2]) (**B**). Local translation occurs both in PAPs (upper table) and in perivascular astrocytic processes (PvAPs) (lower table). Arrows indicate altered levels (red, increase; green, decrease) of mRNAs and/or proteins in diseases (**C**). n.d, not described.

3.2.3. In Movement Disorders

HTT inclusions are found in striatal astrocytes in a mouse model of HD. Accumulation of HTT in astrocytes coincides with deficits in the inward-rectifying potassium channel Kir4.1 leading to extracellular potassium accumulation in the brain and enhanced neuronal excitability in striatal medium-sized spiny neurons (MSN). Interestingly, overexpression of Kir4.1 in astrocytes partially recovered the HD phenotype in these mice and rescued a number of MSN in the onset of neurodegeneration [142]. Whether *Kcnj10* mRNA (which encodes Kir4.1 protein) localization is altered in HD has not been addressed but given its presence in PvAPs [131], it would be interesting to determine if altered Kir4.1 synthesis in

astroglial processes contributes to the manifestation of HD symptoms and the progression of the disease.

3.2.4. In Fragile X Syndrome

Fmr1 knockout mice which model the loss of FMRP function in FXS show a significant protein synthesis-dependent reduction in the glutamate transporter GLT1/EEAT2 and in glutamate uptake. The involvement of astroglial GLT1 to this phenotype was reported by Higashimori and colleagues in 2016. Importantly, loss of astroglial FMRP contributes to GLT1 dysregulation, impaired glutamate uptake, cortical synaptic deficits and other FXS phenotypes [143,144]. These results point towards the possibility that *Glt1* mRNA localization and translation are altered in astrocytic processes, however addressing whether the loss of the process-specific *Glt1* mRNA isoform (*Glt1a*) [90] contributes to FXS would lead to more conclusive results.

3.2.5. In Other Neurological Disorders

Aqp4 and *Gja1* (which encodes the hemichannel protein Cx43) deregulation might not only be involved in AD as previously mentioned. Both transcripts are locally translated in PvAPs and these astroglial peripheral structures play relevant roles in BBB maintenance and immunoregulation. In some neurological conditions the BBB integrity becomes compromised and polarized expression of Aqp4 and Cx43 is lost suggesting that their localized translation in PvAPs might be affected [145]. For example, in the mouse model of middle cerebral artery occlusion (MCAO), Aqp4 is increased during edema and ischemia and its polarization is lost, whereas Cx43 increases in peri-infarct area several days after MCAO. Both proteins are thus potential therapeutic targets for stroke [146–148]. In MS BBB, dysfunction is also evident, and astrocytes are considered active participants in the progression of the disease rather than simple scarring cells [149]. Interestingly, Aqp4 is reduced in endfeet and Cx43 polarity is lost [145]. Finally, loss of perivascular Aqp4 and its mislocalization have been associated to epilepsy in the latent phase preceding seizures [150]. Altogether, these results suggest that mislocalization of mRNAs and defects in localized translation in PvAPs are associated with loss of BBB integrity in some neurological conditions and might contribute to disease progression.

The data reviewed in this paragraph (and summarized in Figure 4C and Table 2) add to a mounting body of evidence indicating the relevance of local protein synthesis in astrocytic processes in proper NS function.

3.3. RNA Localization and Local Translation in Radial Glia

Radial glia cells (RGCs) are the neural progenitors of the developing cortex. Their bipolar structure comprises a cell body located close to the ventricular surface (apical) of the neuroepithelium, a basal process and an endfoot that contacts the pial surface (basal) (Figure 5). In contrast to neuroepithelial cells, RGCs express astroglial markers but have both neurogenic and gliogenic potential [151–153]. RGCs receive numerous signals from cells located at the basal side of the epithelium including Cajal-Retzius cells, meningeal cells and excitatory upper layer neurons. It is believed that these signals released by the basal niche reach the endfeet which in turn "transfer" them to the cell bodies located near the ventricles and 150–450 μm away from the pial surface [154–156].

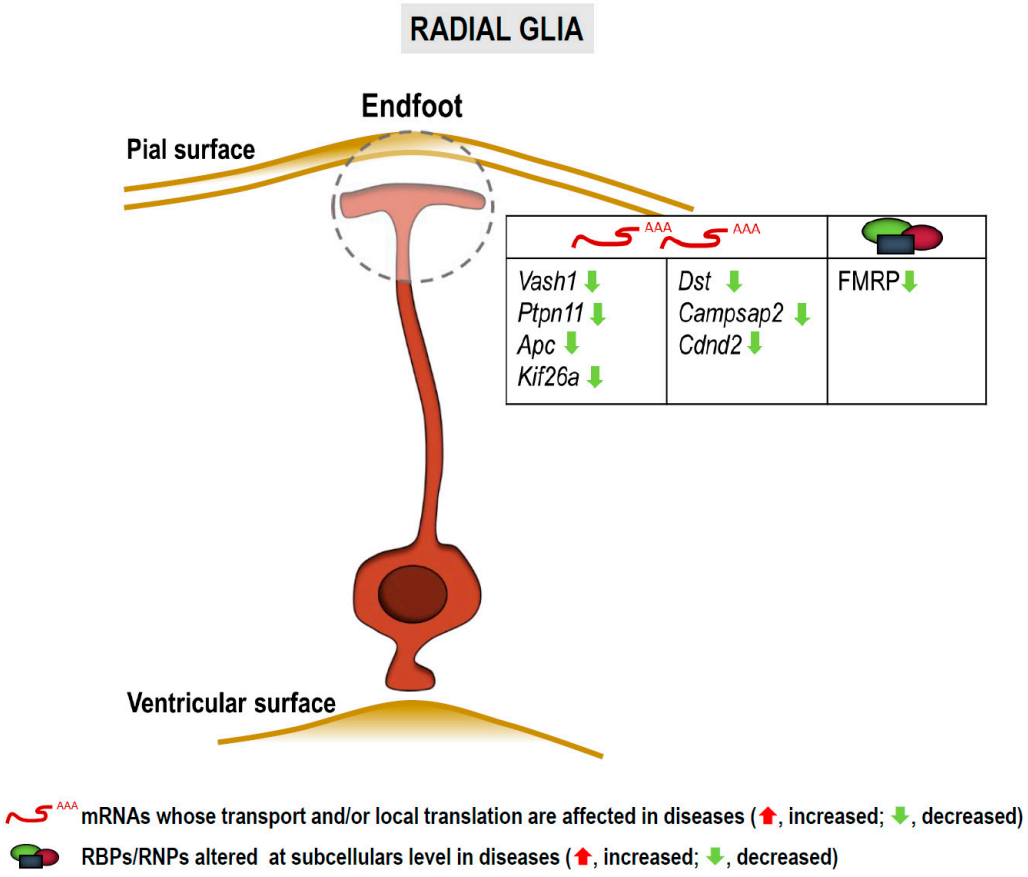

Figure 5. Transcripts and RBPs localized to subcellular compartments in radial glia potentially involved in neurological and neurodegenerative diseases. Arrows indicate altered levels (green, decrease) of mRNAs and/or proteins.

Hence, the basal process would work as a communication road between the basal and the apical sides of the cell [156,157]. Some mRNAs are locally translated into protein in RGC endfeet as reviewed by Pilaz and Silver in 2017 [158]. Among these transcripts those encoding nuclear proteins such as cyclin D2 (*Ccnd2*) have been found, suggesting that proteins translated locally in endfeet could elicit their function in the nucleus as a means of communication between the pial and the ventricular surfaces of the neuroepithelium [91,156]. Indeed, a similar mechanism involving transcription factors has been reported in neurons in both physiological and pathological contexts [14,52–54]. Transcripts for cytoskeleton components and signaling molecules are also present in endfeet [156].

The only characterized RBP able to transport mRNAs to RGC endfeet is FMRP [156]. Given that loss of FMRP is associated to FXS among other diseases, we will discuss below the possibility that dysregulation of endfeet FMRP targets participates in NS dysfunction.

3.3.1. In Fragile X Syndrome, Autism Spectrum Disorders and Intellectual Disabilities

Transcriptome analyses performed so far in RGC endfeet have focused on targets of the RBP FMRP [156]. Pilaz and colleagues performed RIP-Seq and identified 115 potential FMRP targets. Interestingly, 31% of the identified transcripts are involved in neurological diseases, more than 20 of them being encoded by ASD-related genes. Moreover, some pulled-down transcripts are associated with intellectual disabilities. From all identified FMRP-bound mRNAs, six were further validated by in situ hybridization: *Vash1*, *Ptpn11*, *Apc*, *Kif26a*, *Dst* and *Campsap2*. Importantly *Kif26a* mRNA localization to endfeet and transport are impaired in *FMR1* knockout animals. Taken together, these results (summarized in Figure 5) suggest that mRNA localization to and localized translation within endfeet are affected in FXS, other ASDs and likely in intellectual disabilities.

3.3.2. In Other Neurological Disorders

As stated before, *Ccnd2* is locally translated in RGC endfeet and is also an FMRP target [91,156]. Additionally, mutations in the *CCND2* gene have been linked to megalencephaly-polymicrogyria-polydactyly-hydrocephalus syndrome (MPPHS), a rare neurodevelopmental disorder that leads to severe brain malformations [159]. It would be interesting to address whether megalencepahly syndromes are accompanied by dysregulation of local CCND2 production in RGC endfeet during cortical development.

To sum up, although local protein synthesis in RGCs has been by far less studied than it has in other neural cells, the limited existing evidence on this phenomenon (Figure 5 and Table 2) reveal the intriguing possibility that local translation in processes of neural progenitors has important implications in brain development. More interestingly, dysregulation of mRNA localization and localized translation in these cell types could contribute to neurodevelopmental disorders.

4. Concluding Remarks

The information gathered herein (summarized in Table 2) regarding localized translation in glial processes indicate that despite this phenomenon not being extensively studied, there is already a decent amount of evidence suggesting that dysregulation of mRNA localization and local translation in glia might significantly contribute to NS dysfunction. It is worth mentioning that the fact that microglia have not been mentioned in this review article relates to the lack of evidence that local protein synthesis occurs in this cell type until fairly recently [160]. Although it is still too early to venture that RNA localization and/or local translation in microglia play significant roles in CNS disease progression, it is foreseen that this cell type will definitely emerge into the picture of localized translation soon and will deserve future mention. This possibility, together with the evidences reviewed in this article, open new and exciting avenues for the search for novel (and localized) therapeutic targets for neurological and neurodegenerative diseases involving RNA localization and localized translation in glia.

Table 2. List of RNAs and RBPs whose localization and /or local translation is proven or suggested to be linked to neurological and/or neurodegenerative diseases. AD, Alzheimer's disease; ALS, Amyotrophic lateral sclerosis; ASD, Autism spectrum disorder; DS, Down syndrome; FTD, Frontotemporal dementia; FXS, Fragile X syndrome; HD, Huntington's disease; MS, Multiple sclerosis; SMA; Spinal muscular atrophy. Others include stroke, dementia, intellectual disabilities and neurodevelopmental disorders. N, neurons; A, astrocytes; R, radial glia; O, oligodendrites. N^1 refers to significantly changed transcripts in Aβ-treated axons vs. controls that have not been further referred to in the literature and are thus not included in Figure 2. MS^2 includes MS and demyelination.

List of mRNAs/microRNAs Localized to Subcellular Compartments in Neurons and Glia and Implicated in Diseases			
Transcript	**Disease**	**Cell Type**	**References**
Actb	SMA, HTT	N	[13,73,75]
Aldoc	AD	N^1, A	[14,111,130]
Anxa2	SMA	N	[11]
Apc	FXS	R	[158]
ApoE	AD	N	[6,14]
App	AD	N	[6,14]
Aqp4	AD, MS, other	N^1, A	[14,131,145,150]
Arc	FXS	N	[79,80]
Atf4	AD	N	[14]
Bdnf	HTT, DS, other	N	[59,86]

Table 2. *Cont.*

List of mRNAs/microRNAs Localized to Subcellular Compartments in Neurons and Glia and Implicated in Diseases			
Transcript	**Disease**	**Cell Type**	**References**
Bin1	AD	N	[6,14]
Camk2a	FXS	N	[79,80]
Campsap2	FXS	R	[156]
Ccdn2	FXS, other	R	[156,159]
Celf1	AD	N	[6,14]
Clu	AD	N, A	[6,14,111,130]
Cnp	GGT	O	[117]
Cox4i2	SMA	N	[11]
Dlg4	FXS	N	[79,80]
Dscam	DS	N	[59,87]
Dst	FXS	R	[156]
Eef2	AD	N[1], A	[14,111,130]
Fads1	AD	N[1], A	[14,111,130]
Fermt2	AD	N	[6,14]
Fmrp (*Fmr1*)	FXS	N	[79,80]
Fth1	other	A	[141]
Ftl1	other	A	[141]
Gap43	SMA	N	[13]
Gfap	AD	N[1], A	[6,14,111,130,131,139]
Gja1	AD, MS	N[1], A	[14,131,145]
Glt1	ALS, FXS	A	[124,143,144]
Gpm6b	AD	N[1], A	[14,131]
Kpnb	TNI	N	[56]
Kcnj10	HTT	A	[142]
Ki26a	FXS	R	[156]
Lrp1	AD	N[1], A	[14,111,130]
Mag	GGT	O	[117]
Mal	GGT	O	[117]
Mapb1	ALS, FXS	N	[8,79,80]
Mapt	AD, GGT	N, O	[16,17,117]
Mbp	ALS, MS[2], AD, GGT, FXS	O	[107,110,111,113,117,122,123]
miR-183	SMA	N	[12]
Mlc1	AD	N[1], A	[14,131]
Mobp	GGT	O	[117]
Mog	GGT	O	[117]
mTor	TNI, SMA, ASD, DS	N	[12,25,84–86]
Nrn1	SMA	N	[13]
Picalm	AD	N	[6,14]

Table 2. *Cont.*

List of mRNAs/microRNAs Localized to Subcellular Compartments in Neurons and Glia and Implicated in Diseases			
Transcript	**Disease**	**Cell Type**	**References**
Plp1	GGT	O	[117]
Pparg	TNI	N	[55]
Ptk2	AD	N	[6,14]
Ptpn11	FXS	R	[156]
Sorl1	AD	N	[6,14]
Stat3	TNI	N	[54]
Timp3	AD	N[1], A	[14,111,130]
Vash1	FXS	R	[156]
Vim	AD	N, A	[14,15,111,130]
Ago2	HD	N	[73–75]
FMRP	FXS	N, O, A, R	[79,80,122,133,143,144,156]
FUS	FTD	N	[8,9,59]
hnRNP A/B	AD, ALS	N, O	[67,68,105–107,161]
HTT	HD	N	[73–75]
QKI	MS, ALS, AD	O, A	[110,111,136,140,162]
RBPMS	TNI	N	[57]
SMN	SMA	N	[13]
TDP-43	ALS, FTD	N, A	[8,9,59,124]

Author Contributions: J.B. conceived the work. M.B.-U., A.G.-B., M.G. and A.d.l.C. drafted the manuscript. M.B.-U., A.G.-B. and J.B. composed figures and tables. M.B.-U., A.G.-B., M.G., A.d.l.C., E.V., E.A. and J.B. performed literature searching and edited the manuscript. All authors have read and agreed to the published version of the manuscript.

Funding: This paper was partially funded by grants awarded to J.B. (MICINN grants SAF2016-76347-R, RYC-2016-19837 and PID2019-110721RB-I00; The Alzheimer's Association grant AARG-19-618303) and E.A. (MICINN grant PID2019-108465RB-I00; Basque Government grant PIBA-2020-1-0012). M.B.-U. is a UPV/EHU fellow; A.G.-B. is a FPU (FPU17/04891) fellow; M.G. and A.d.l.C. are GV fellows.

Institutional Review Board Statement: Not applicable.

Informed Consent Statement: Not applicable.

Data Availability Statement: Not applicable.

Conflicts of Interest: The authors declare no conflict of interest.

References

1. Alberts, B.; Lewis, J.; Raff, M.; Roberts, K.; Walter, P. *Molecular Biology of the Cell*, 4th ed.; Garland Science: New York, NY, USA, 2002.
2. Martin, K.C.; Ephrussi, A. mRNA localization: Gene expression in the spatial dimension. *Cell* **2009**, *136*, 719–730. [CrossRef]
3. Lin, J.Q.; van Tartwijk, F.W.; Holt, C.E. Axonal mRNA translation in neurological disorders. *RNA Biol.* **2020**, 1–26. [CrossRef]
4. Holt, C.E.; Martin, K.C.; Schuman, E.M. Local translation in neurons: Visualization and function. *Nat. Struct. Mol. Biol.* **2019**, *26*, 557–566. [CrossRef]
5. Jung, H.; Yoon, B.C.; Holt, C.E. Axonal mRNA localization and local protein synthesis in nervous system assembly, maintenance and repair. *Nat. Rev. Neurosci.* **2012**, *13*, 308–324. [CrossRef]
6. Baleriola, J.; Hengst, U. Targeting axonal protein synthesis in neuroregeneration and degeneration. *Neurotherapeutics* **2015**, *12*, 57–65. [CrossRef]

7. Zheng, J.Q.; Kelly, T.K.; Chang, B.; Ryazantsev, S.; Rajasekaran, A.K.; Martin, K.C.; Twiss, J.L. A functional role for intra-axonal protein synthesis during axonal regeneration from adult sensory neurons. *J. Neurosci. Off. J. Soc. Neurosci.* **2001**, *21*, 9291–9303. [CrossRef]
8. Coyne, A.N.; Siddegowda, B.B.; Estes, P.S.; Johannesmeyer, J.; Kovalik, T.; Daniel, S.G.; Pearson, A.; Bowser, R.; Zarnescu, D.C. Futsch/MAP1B mRNA is a translational target of TDP-43 and is neuroprotective in a Drosophila model of amyotrophic lateral sclerosis. *J. Neurosci.* **2014**, *34*, 15962–15974. [CrossRef]
9. Lopez-Erauskin, J.; Tadokoro, T.; Baughn, M.W.; Myers, B.; McAlonis-Downes, M.; Chillon-Marinas, C.; Asiaban, J.N.; Artates, J.; Bui, A.T.; Vetto, A.P.; et al. ALS/FTD-Linked Mutation in FUS Suppresses Intra-axonal Protein Synthesis and Drives Disease Without Nuclear Loss-of-Function of FUS. *Neuron* **2018**, *100*, 816–830.e7. [CrossRef]
10. Alami, N.H.; Smith, R.B.; Carrasco, M.A.; Williams, L.A.; Winborn, C.S.; Han, S.S.W.; Kiskinis, E.; Winborn, B.; Freibaum, B.D.; Kanagaraj, A.; et al. Axonal transport of TDP-43 mRNA granules is impaired by ALS-causing mutations. *Neuron* **2014**, *81*, 536–543. [CrossRef]
11. Rage, F.; Boulisfane, N.; Rihan, K.; Neel, H.; Gostan, T.; Bertrand, E.; Bordonne, R.; Soret, J. Genome-wide identification of mRNAs associated with the protein SMN whose depletion decreases their axonal localization. *RNA* **2013**, *19*, 1755–1766. [CrossRef] [PubMed]
12. Kye, M.J.; Niederst, E.D.; Wertz, M.H.; Goncalves Ido, C.; Akten, B.; Dover, K.Z.; Peters, M.; Riessland, M.; Neveu, P.; Wirth, B.; et al. SMN regulates axonal local translation via miR-183/mTOR pathway. *Hum. Mol. Genet.* **2014**, *23*, 6318–6331. [CrossRef]
13. Khalil, B.; Morderer, D.; Price, P.L.; Liu, F.; Rossoll, W. mRNP assembly, axonal transport, and local translation in neurodegenerative diseases. *Brain Res.* **2018**, *1693*, 75–91. [CrossRef]
14. Baleriola, J.; Walker, C.A.; Jean, Y.Y.; Crary, J.F.; Troy, C.M.; Nagy, P.L.; Hengst, U. Axonally synthesized ATF4 transmits a neurodegenerative signal across brain regions. *Cell* **2014**, *158*, 1159–1172. [CrossRef]
15. Walker, C.A.; Randolph, L.K.; Matute, C.; Alberdi, E.; Baleriola, J.; Hengst, U. Abeta1-42 triggers the generation of a retrograde signaling complex from sentinel mRNAs in axons. *EMBO Rep.* **2018**, *19*. [CrossRef]
16. Kobayashi, S.; Tanaka, T.; Soeda, Y.; Almeida, O.F.X.; Takashima, A. Local Somatodendritic Translation and Hyperphosphorylation of Tau Protein Triggered by AMPA and NMDA Receptor Stimulation. *EBioMedicine* **2017**, *20*, 120–126. [CrossRef]
17. Li, C.; Gotz, J. Somatodendritic accumulation of Tau in Alzheimer's disease is promoted by Fyn-mediated local protein translation. *EMBO J.* **2017**, *36*, 3120–3138. [CrossRef] [PubMed]
18. Dieterich, D.C.; Link, A.J.; Graumann, J.; Tirrell, D.A.; Schuman, E.M. Selective identification of newly synthesized proteins in mammalian cells using bioorthogonal noncanonical amino acid tagging (BONCAT). *Proc. Natl. Acad. Sci. USA* **2006**, *103*, 9482–9487. [CrossRef]
19. Dieterich, D.C.; Hodas, J.J.; Gouzer, G.; Shadrin, I.Y.; Ngo, J.T.; Triller, A.; Tirrell, D.A.; Schuman, E.M. In situ visualization and dynamics of newly synthesized proteins in rat hippocampal neurons. *Nat. Neurosci.* **2010**, *13*, 897–905. [CrossRef] [PubMed]
20. Ong, S.E.; Blagoev, B.; Kratchmarova, I.; Kristensen, D.B.; Steen, H.; Pandey, A.; Mann, M. Stable isotope labeling by amino acids in cell culture, SILAC, as a simple and accurate approach to expression proteomics. *Mol. Cell Proteom.* **2002**, *1*, 376–386. [CrossRef]
21. Cagnetta, R.; Frese, C.K.; Shigeoka, T.; Krijgsveld, J.; Holt, C.E. Rapid Cue-Specific Remodeling of the Nascent Axonal Proteome. *Neuron* **2018**, *99*, 29–46.e4. [CrossRef]
22. Schmidt, E.K.; Clavarino, G.; Ceppi, M.; Pierre, P. SUnSET, a nonradioactive method to monitor protein synthesis. *Nat. Methods* **2009**, *6*, 275–277. [CrossRef]
23. Gamarra, M.; Blanco-Urrejola, M.; Batista, A.F.R.; Imaz, J.; Baleriola, J. Object-Based Analyses in FIJI/ImageJ to Measure Local RNA Translation Sites in Neurites in Response to Abeta1-42 Oligomers. *Front. Neurosci.* **2020**, *14*, 547. [CrossRef]
24. Hafner, A.S.; Donlin-Asp, P.G.; Leitch, B.; Herzog, E.; Schuman, E.M. Local protein synthesis is a ubiquitous feature of neuronal pre- and postsynaptic compartments. *Science* **2019**, *364*. [CrossRef] [PubMed]
25. Terenzio, M.; Koley, S.; Samra, N.; Rishal, I.; Zhao, Q.; Sahoo, P.K.; Urisman, A.; Marvaldi, L.; Oses-Prieto, J.A.; Forester, C.; et al. Locally translated mTOR controls axonal local translation in nerve injury. *Science* **2018**, *359*, 1416–1421. [CrossRef] [PubMed]
26. Aviner, R.; Geiger, T.; Elroy-Stein, O. Novel proteomic approach (PUNCH-P) reveals cell cycle-specific fluctuations in mRNA translation. *Genes Dev.* **2013**, *27*, 1834–1844. [CrossRef]
27. Shigeoka, T.; Jung, H.; Jung, J.; Turner-Bridger, B.; Ohk, J.; Lin, J.Q.; Amieux, P.S.; Holt, C.E. Dynamic Axonal Translation in Developing and Mature Visual Circuits. *Cell* **2016**, *166*, 181–192. [CrossRef]
28. Zappulo, A.; van den Bruck, D.; Ciolli Mattioli, C.; Franke, V.; Imami, K.; McShane, E.; Moreno-Estelles, M.; Calviello, L.; Filipchyk, A.; Peguero-Sanchez, E.; et al. RNA localization is a key determinant of neurite-enriched proteome. *Nat. Commun.* **2017**, *8*, 583. [CrossRef]
29. Bannister, N.J.; Larkman, A.U. Dendritic morphology of CA1 pyramidal neurones from the rat hippocampus: II. Spine distributions. *J. Comp. Neurol.* **1995**, *360*, 161–171. [CrossRef]
30. Rangaraju, V.; Tom Dieck, S.; Schuman, E.M. Local translation in neuronal compartments: How local is local? *EMBO Rep.* **2017**, *18*, 693–711. [CrossRef]
31. Yoon, B.C.; Jung, H.; Dwivedy, A.; O'Hare, C.M.; Zivraj, K.H.; Holt, C.E. Local translation of extranuclear lamin B promotes axon maintenance. *Cell* **2012**, *148*, 752–764. [CrossRef]
32. Garner, C.C.; Tucker, R.P.; Matus, A. Selective localization of messenger RNA for cytoskeletal protein MAP2 in dendrites. *Nature* **1988**, *336*, 674–677. [CrossRef]

33. Burgin, K.E.; Waxham, M.N.; Rickling, S.; Westgate, S.A.; Mobley, W.C.; Kelly, P.T. In situ hybridization histochemistry of Ca2+/calmodulin-dependent protein kinase in developing rat brain. *J. Neurosci. Off. J. Soc. Neurosci.* **1990**, *10*, 1788–1798. [CrossRef]
34. Landry, C.F.; Watson, J.B.; Kashima, T.; Campagnoni, A.T. Cellular influences on RNA sorting in neurons and glia: An in situ hybridization histochemical study. *Brain Res. Mol. Brain Res.* **1994**, *27*, 1–11. [CrossRef]
35. Furuichi, T.; Simon-Chazottes, D.; Fujino, I.; Yamada, N.; Hasegawa, M.; Miyawaki, A.; Yoshikawa, S.; Guenet, J.L.; Mikoshiba, K. Widespread expression of inositol 1,4,5-trisphosphate receptor type 1 gene (Insp3r1) in the mouse central nervous system. *Recept. Channels.* **1993**, *1*, 11–24.
36. Miyashiro, K.; Dichter, M.; Eberwine, J. On the nature and differential distribution of mRNAs in hippocampal neurites: Implications for neuronal functioning. *Proc. Natl. Acad. Sci. USA* **1994**, *91*, 10800–10804. [CrossRef]
37. Racca, C.; Gardiol, A.; Triller, A. Dendritic and postsynaptic localizations of glycine receptor alpha subunit mRNAs. *J. Neurosci. Off. J. Soc. Neurosci.* **1997**, *17*, 1691–1700. [CrossRef]
38. Link, W.; Konietzko, U.; Kauselmann, G.; Krug, M.; Schwanke, B.; Frey, U.; Kuhl, D. Somatodendritic expression of an immediate early gene is regulated by synaptic activity. *Proc. Natl. Acad. Sci. USA* **1995**, *92*, 5734–5738. [CrossRef]
39. Lyford, G.L.; Yamagata, K.; Kaufmann, W.E.; Barnes, C.A.; Sanders, L.K.; Copeland, N.G.; Gilbert, D.J.; Jenkins, N.A.; Lanahan, A.A.; Worley, P.F. Arc, a growth factor and activity-regulated gene, encodes a novel cytoskeleton-associated protein that is enriched in neuronal dendrites. *Neuron* **1995**, *14*, 433–445. [CrossRef]
40. Tiruchinapalli, D.M.; Oleynikov, Y.; Kelic, S.; Shenoy, S.M.; Hartley, A.; Stanton, P.K.; Singer, R.H.; Bassell, G.J. Activity-dependent trafficking and dynamic localization of zipcode binding protein 1 and beta-actin mRNA in dendrites and spines of hippocampal neurons. *J. Neurosci. Off. J. Soc. Neurosci.* **2003**, *23*, 3251–3261. [CrossRef]
41. Tongiorgi, E.; Righi, M.; Cattaneo, A. Activity-dependent dendritic targeting of BDNF and TrkB mRNAs in hippocampal neurons. *J. Neurosci. Off. J. Soc. Neurosci.* **1997**, *17*, 9492–9505. [CrossRef]
42. Kang, H.; Schuman, E.M. A requirement for local protein synthesis in neurotrophin-induced hippocampal synaptic plasticity. *Science* **1996**, *273*, 1402–1406. [CrossRef]
43. Yoon, Y.J.; Wu, B.; Buxbaum, A.R.; Das, S.; Tsai, A.; English, B.P.; Grimm, J.B.; Lavis, L.D.; Singer, R.H. Glutamate-induced RNA localization and translation in neurons. *Proc. Natl. Acad. Sci. USA* **2016**, *113*, E6877–E6886. [CrossRef]
44. Bassell, G.J.; Zhang, H.; Byrd, A.L.; Femino, A.M.; Singer, R.H.; Taneja, K.L.; Lifshitz, L.M.; Herman, I.M.; Kosik, K.S. Sorting of beta-actin mRNA and protein to neurites and growth cones in culture. *J. Neurosci.* **1998**, *18*, 251–265. [CrossRef]
45. Leung, K.M.; van Horck, F.P.; Lin, A.C.; Allison, R.; Standart, N.; Holt, C.E. Asymmetrical beta-actin mRNA translation in growth cones mediates attractive turning to netrin-1. *Nat. Neurosci.* **2006**, *9*, 1247–1256. [CrossRef]
46. Wong, H.H.; Lin, J.Q.; Strohl, F.; Roque, C.G.; Cioni, J.M.; Cagnetta, R.; Turner-Bridger, B.; Laine, R.F.; Harris, W.A.; Kaminski, C.F.; et al. RNA Docking and Local Translation Regulate Site-Specific Axon Remodeling In Vivo. *Neuron* **2017**, *95*, 852–868.e8. [CrossRef]
47. Wu, K.Y.; Hengst, U.; Cox, L.J.; Macosko, E.Z.; Jeromin, A.; Urquhart, E.R.; Jaffrey, S.R. Local translation of RhoA regulates growth cone collapse. *Nature* **2005**, *436*, 1020–1024. [CrossRef]
48. Hengst, U.; Deglincerti, A.; Kim, H.J.; Jeon, N.L.; Jaffrey, S.R. Axonal elongation triggered by stimulus-induced local translation of a polarity complex protein. *Nat. Cell Biol.* **2009**, *11*, 1024–1030. [CrossRef]
49. Gracias, N.G.; Shirkey-Son, N.J.; Hengst, U. Local translation of TC10 is required for membrane expansion during axon outgrowth. *Nat. Commun.* **2014**, *5*, 3506. [CrossRef]
50. Taylor, A.M.; Wu, J.; Tai, H.C.; Schuman, E.M. Axonal translation of beta-catenin regulates synaptic vesicle dynamics. *J. Neurosci.* **2013**, *33*, 5584–5589. [CrossRef]
51. Batista, A.F.R.; Martinez, J.C.; Hengst, U. Intra-axonal Synthesis of SNAP25 Is Required for the Formation of Presynaptic Terminals. *Cell Rep.* **2017**, *20*, 3085–3098. [CrossRef]
52. Cox, L.J.; Hengst, U.; Gurskaya, N.G.; Lukyanov, K.A.; Jaffrey, S.R. Intra-axonal translation and retrograde trafficking of CREB promotes neuronal survival. *Nat. Cell Biol.* **2008**, *10*, 149–159. [CrossRef]
53. Ji, S.J.; Jaffrey, S.R. Intra-axonal translation of SMAD1/5/8 mediates retrograde regulation of trigeminal ganglia subtype specification. *Neuron* **2012**, *74*, 95–107. [CrossRef]
54. Ben-Yaakov, K.; Dagan, S.Y.; Segal-Ruder, Y.; Shalem, O.; Vuppalanchi, D.; Willis, D.E.; Yudin, D.; Rishal, I.; Rother, F.; Bader, M.; et al. Axonal transcription factors signal retrogradely in lesioned peripheral nerve. *EMBO J.* **2012**, *31*, 1350–1363. [CrossRef]
55. Lezana, J.P.; Dagan, S.Y.; Robinson, A.; Goldstein, R.S.; Fainzilber, M.; Bronfman, F.C.; Bronfman, M. Axonal PPARgamma promotes neuronal regeneration after injury. *Dev. Neurobiol.* **2016**, *76*, 688–701. [CrossRef]
56. Hanz, S.; Perlson, E.; Willis, D.; Zheng, J.Q.; Massarwa, R.; Huerta, J.J.; Koltzenburg, M.; Kohler, M.; van-Minnen, J.; Twiss, J.L.; et al. Axoplasmic importins enable retrograde injury signaling in lesioned nerve. *Neuron* **2003**, *40*, 1095–1104. [CrossRef]
57. Pereiro, X.; Ruzafa, N.; Urcola, J.H.; Sharma, S.C.; Vecino, E. Differential Distribution of RBPMS in Pig, Rat, and Human Retina after Damage. *Int. J. Mol. Sci.* **2020**, *21*, 9330. [CrossRef]
58. Scotter, E.L.; Chen, H.J.; Shaw, C.E. TDP-43 Proteinopathy and ALS: Insights into Disease Mechanisms and Therapeutic Targets. *Neurotherapeutics* **2015**, *12*, 352–363. [CrossRef]
59. Swanger, S.A.; Bassell, G.J. Dendritic protein synthesis in the normal and diseased brain. *Neuroscience* **2013**, *232*, 106–127. [CrossRef]

60. Rehorst, W.A.; Thelen, M.P.; Nolte, H.; Turk, C.; Cirak, S.; Peterson, J.M.; Wong, G.W.; Wirth, B.; Kruger, M.; Winter, D.; et al. Muscle regulates mTOR dependent axonal local translation in motor neurons via CTRP3 secretion: Implications for a neuromuscular disorder, spinal muscular atrophy. *Acta Neuropathol. Commun.* **2019**, *7*, 154. [CrossRef]
61. Pearson, R.C.; Esiri, M.M.; Hiorns, R.W.; Wilcock, G.K.; Powell, T.P. Anatomical correlates of the distribution of the pathological changes in the neocortex in Alzheimer disease. *Proc. Natl. Acad. Sci. USA* **1985**, *82*, 4531–4534. [CrossRef]
62. Busche, M.A.; Hyman, B.T. Synergy between amyloid-beta and tau in Alzheimer's disease. *Nat. Neurosci.* **2020**, *23*, 1183–1193. [CrossRef]
63. Rabbito, A.; Dulewicz, M.; Kulczynska-Przybik, A.; Mroczko, B. Biochemical Markers in Alzheimer's Disease. *Int. J. Mol. Sci.* **2020**, *21*, 1989. [CrossRef]
64. Tiwari, S.; Atluri, V.; Kaushik, A.; Yndart, A.; Nair, M. Alzheimer's disease: Pathogenesis, diagnostics, and therapeutics. *Int. J. Nanomed.* **2019**, *14*, 5541–5554. [CrossRef] [PubMed]
65. Aronov, S.; Aranda, G.; Behar, L.; Ginzburg, I. Axonal tau mRNA localization coincides with tau protein in living neuronal cells and depends on axonal targeting signal. *J. Neurosci.* **2001**, *21*, 6577–6587. [CrossRef]
66. Aronov, S.; Aranda, G.; Behar, L.; Ginzburg, I. Visualization of translated tau protein in the axons of neuronal P19 cells and characterization of tau RNP granules. *J. Cell Sci.* **2002**, *115*, 3817–3827. [CrossRef]
67. Hoek, K.S.; Kidd, G.J.; Carson, J.H.; Smith, R. hnRNP A2 selectively binds the cytoplasmic transport sequence of myelin basic protein mRNA. *Biochemistry* **1998**, *37*, 7021–7029. [CrossRef]
68. Munro, T.P.; Magee, R.J.; Kidd, G.J.; Carson, J.H.; Barbarese, E.; Smith, L.M.; Smith, R. Mutational analysis of a heterogeneous nuclear ribonucleoprotein A2 response element for RNA trafficking. *J. Biol. Chem.* **1999**, *274*, 34389–34395. [CrossRef] [PubMed]
69. Goedert, M.; Ghetti, B.; Spillantini, M.G. Frontotemporal dementia: Implications for understanding Alzheimer disease. *Cold Spring Harb. Perspect. Med.* **2012**, *2*, a006254. [CrossRef]
70. Walker, F.O. Huntington's disease. *Lancet* **2007**, *369*, 218–228. [CrossRef]
71. Block-Galarza, J.; Chase, K.O.; Sapp, E.; Vaughn, K.T.; Vallee, R.B.; DiFiglia, M.; Aronin, N. Fast transport and retrograde movement of huntingtin and HAP 1 in axons. *Neuroreport* **1997**, *8*, 2247–2251. [CrossRef] [PubMed]
72. Brunholz, S.; Sisodia, S.; Lorenzo, A.; Deyts, C.; Kins, S.; Morfini, G. Axonal transport of APP and the spatial regulation of APP cleavage and function in neuronal cells. *Exp. Brain Res.* **2012**, *217*, 353–364. [CrossRef] [PubMed]
73. Savas, J.N.; Ma, B.; Deinhardt, K.; Culver, B.P.; Restituito, S.; Wu, L.; Belasco, J.G.; Chao, M.V.; Tanese, N. A role for huntington disease protein in dendritic RNA granules. *J. Biol. Chem.* **2010**, *285*, 13142–13153. [CrossRef] [PubMed]
74. Ma, B.; Culver, B.P.; Baj, G.; Tongiorgi, E.; Chao, M.V.; Tanese, N. Localization of BDNF mRNA with the Huntington's disease protein in rat brain. *Mol. Neurodegener.* **2010**, *5*, 22. [CrossRef]
75. Ma, B.; Savas, J.N.; Yu, M.S.; Culver, B.P.; Chao, M.V.; Tanese, N. Huntingtin mediates dendritic transport of beta-actin mRNA in rat neurons. *Sci. Rep.* **2011**, *1*, 140. [CrossRef]
76. Hernandez, I.H.; Cabrera, J.R.; Santos-Galindo, M.; Sanchez-Martin, M.; Dominguez, V.; Garcia-Escudero, R.; Perez-Alvarez, M.J.; Pintado, B.; Lucas, J.J. Pathogenic SREK1 decrease in Huntington's disease lowers TAF1 mimicking X-linked dystonia parkinsonism. *Brain* **2020**, *143*, 2207–2219. [CrossRef]
77. Creus-Muncunill, J.; Badillos-Rodriguez, R.; Garcia-Forn, M.; Masana, M.; Garcia-Diaz Barriga, G.; Guisado-Corcoll, A.; Alberch, J.; Malagelada, C.; Delgado-Garcia, J.M.; Gruart, A.; et al. Increased translation as a novel pathogenic mechanism in Huntington's disease. *Brain* **2019**, *142*, 3158–3175. [CrossRef]
78. Salcedo-Arellano, M.J.; Cabal-Herrera, A.M.; Punatar, R.H.; Clark, C.J.; Romney, C.A.; Hagerman, R.J. Overlapping Molecular Pathways Leading to Autism Spectrum Disorders, Fragile X Syndrome, and Targeted Treatments. *Neurotherapeutics* **2020**, *19*. [CrossRef]
79. Banerjee, A.; Ifrim, M.F.; Valdez, A.N.; Raj, N.; Bassell, G.J. Aberrant RNA translation in fragile X syndrome: From FMRP mechanisms to emerging therapeutic strategies. *Brain Res.* **2018**, *1693*, 24–36. [CrossRef]
80. Antar, L.N.; Afroz, R.; Dictenberg, J.B.; Carroll, R.C.; Bassell, G.J. Metabotropic glutamate receptor activation regulates fragile x mental retardation protein and FMR1 mRNA localization differentially in dendrites and at synapses. *J. Neurosci.* **2004**, *24*, 2648–2655. [CrossRef]
81. Christie, S.B.; Akins, M.R.; Schwob, J.E.; Fallon, J.R. The FXG: A presynaptic fragile X granule expressed in a subset of developing brain circuits. *J. Neurosci.* **2009**, *29*, 1514–1524. [CrossRef]
82. Akins, M.R.; Berk-Rauch, H.E.; Fallon, J.R. Presynaptic translation: Stepping out of the postsynaptic shadow. *Front. Neural Circuits* **2009**, *3*, 17. [CrossRef]
83. Akins, M.R.; Berk-Rauch, H.E.; Kwan, K.Y.; Mitchell, M.E.; Shepard, K.A.; Korsak, L.I.; Stackpole, E.E.; Warner-Schmidt, J.L.; Sestan, N.; Cameron, H.A.; et al. Axonal ribosomes and mRNAs associate with fragile X granules in adult rodent and human brains. *Hum. Mol. Genet.* **2017**, *26*, 192–209. [CrossRef] [PubMed]
84. Wang, L.W.; Berry-Kravis, E.; Hagerman, R.J. Fragile X: Leading the way for targeted treatments in autism. *Neurotherapeutics* **2010**, *7*, 264–274. [CrossRef]
85. Hagerman, R.; Hoem, G.; Hagerman, P. Fragile X and autism: Intertwined at the molecular level leading to targeted treatments. *Mol. Autism* **2010**, *1*, 12. [CrossRef]

86. Troca-Marin, J.A.; Alves-Sampaio, A.; Montesinos, M.L. An increase in basal BDNF provokes hyperactivation of the Akt-mammalian target of rapamycin pathway and deregulation of local dendritic translation in a mouse model of Down's syndrome. *J. Neurosci.* **2011**, *31*, 9445–9455. [CrossRef]
87. Alves-Sampaio, A.; Troca-Marin, J.A.; Montesinos, M.L. NMDA-mediated regulation of DSCAM dendritic local translation is lost in a mouse model of Down's syndrome. *J. Neurosci.* **2010**, *30*, 13537–13548. [CrossRef] [PubMed]
88. Darnell, J.C.; Richter, J.D. Cytoplasmic RNA-binding proteins and the control of complex brain function. *Cold Spring Harb. Perspect. Biol.* **2012**, *4*, a012344. [CrossRef]
89. Colman, D.R.; Kreibich, G.; Frey, A.B.; Sabatini, D.D. Synthesis and incorporation of myelin polypeptides into CNS myelin. *J. Cell Biol.* **1982**, *95*, 598–608. [CrossRef]
90. Berger, U.V.; DeSilva, T.M.; Chen, W.; Rosenberg, P.A. Cellular and subcellular mRNA localization of glutamate transporter isoforms GLT1a and GLT1b in rat brain by in situ hybridization. *J. Comp. Neurol.* **2005**, *492*, 78–89. [CrossRef]
91. Tsunekawa, Y.; Britto, J.M.; Takahashi, M.; Polleux, F.; Tan, S.S.; Osumi, N. Cyclin D2 in the basal process of neural progenitors is linked to non-equivalent cell fates. *EMBO J.* **2012**, *31*, 1879–1892. [CrossRef]
92. Pfeiffer, S.E.; Warrington, A.E.; Bansal, R. The oligodendrocyte and its many cellular processes. *Trends Cell Biol.* **1993**, *3*, 191–197. [CrossRef]
93. Yeung, M.S.; Zdunek, S.; Bergmann, O.; Bernard, S.; Salehpour, M.; Alkass, K.; Perl, S.; Tisdale, J.; Possnert, G.; Brundin, L.; et al. Dynamics of oligodendrocyte generation and myelination in the human brain. *Cell* **2014**, *159*, 766–774. [CrossRef]
94. Ghandour, M.S.; Skoff, R.P. Double-labeling in situ hybridization analysis of mRNAs for carbonic anhydrase II and myelin basic protein: Expression in developing cultured glial cells. *Glia* **1991**, *4*, 1–10. [CrossRef]
95. LoPresti, P.; Szuchet, S.; Papasozomenos, S.C.; Zinkowski, R.P.; Binder, L.I. Functional implications for the microtubule-associated protein tau: Localization in oligodendrocytes. *Proc. Natl. Acad. Sci. USA* **1995**, *92*, 10369–10373. [CrossRef]
96. Holz, A.; Schaeren-Wiemers, N.; Schaefer, C.; Pott, U.; Colello, R.J.; Schwab, M.E. Molecular and developmental characterization of novel cDNAs of the myelin-associated/oligodendrocytic basic protein. *J. Neurosci.* **1996**, *16*, 467–477. [CrossRef]
97. Garcia-Ladona, F.J.; Huss, Y.; Frey, P.; Ghandour, M.S. Oligodendrocytes express different isoforms of beta-amyloid precursor protein in chemically defined cell culture conditions: In situ hybridization and immunocytochemical detection. *J. Neurosci. Res.* **1997**, *50*, 50–61. [CrossRef]
98. Thakurela, S.; Garding, A.; Jung, R.B.; Muller, C.; Goebbels, S.; White, R.; Werner, H.B.; Tiwari, V.K. The transcriptome of mouse central nervous system myelin. *Sci. Rep.* **2016**, *6*, 25828. [CrossRef]
99. White, R.; Gonsior, C.; Kramer-Albers, E.M.; Stohr, N.; Huttelmaier, S.; Trotter, J. Activation of oligodendroglial Fyn kinase enhances translation of mRNAs transported in hnRNP A2-dependent RNA granules. *J. Cell Biol.* **2008**, *181*, 579–586. [CrossRef]
100. Laursen, L.S.; Chan, C.W.; Ffrench-Constant, C. Translation of myelin basic protein mRNA in oligodendrocytes is regulated by integrin activation and hnRNP-K. *J. Cell Biol.* **2011**, *192*, 797–811. [CrossRef]
101. Torvund-Jensen, J.; Steengaard, J.; Reimer, L.; Fihl, L.B.; Laursen, L.S. Transport and translation of MBP mRNA is regulated differently by distinct hnRNP proteins. *J. Cell Sci.* **2014**, *127*, 1550–1564. [CrossRef]
102. Herbert, A.L.; Fu, M.M.; Drerup, C.M.; Gray, R.S.; Harty, B.L.; Ackerman, S.D.; O'Reilly-Pol, T.; Johnson, S.L.; Nechiporuk, A.V.; Barres, B.A.; et al. Dynein/dynactin is necessary for anterograde transport of Mbp mRNA in oligodendrocytes and for myelination in vivo. *Proc. Natl. Acad. Sci. USA* **2017**, *114*, E9153–E9162. [CrossRef] [PubMed]
103. Lorente Pons, A.; Higginbottom, A.; Cooper-Knock, J.; Alrafiah, A.; Alofi, E.; Kirby, J.; Shaw, P.J.; Wood, J.D.; Highley, J.R. Oligodendrocyte pathology exceeds axonal pathology in white matter in human amyotrophic lateral sclerosis. *J. Pathol.* **2020**, *251*, 262–271. [CrossRef]
104. Kang, S.H.; Li, Y.; Fukaya, M.; Lorenzini, I.; Cleveland, D.W.; Ostrow, L.W.; Rothstein, J.D.; Bergles, D.E. Degeneration and impaired regeneration of gray matter oligodendrocytes in amyotrophic lateral sclerosis. *Nat. Neurosci.* **2013**, *16*, 571–579. [CrossRef]
105. Highley, J.R.; Kirby, J.; Jansweijer, J.A.; Webb, P.S.; Hewamadduma, C.A.; Heath, P.R.; Higginbottom, A.; Raman, R.; Ferraiuolo, L.; Cooper-Knock, J.; et al. Loss of nuclear TDP-43 in amyotrophic lateral sclerosis (ALS) causes altered expression of splicing machinery and widespread dysregulation of RNA splicing in motor neurones. *Neuropathol. Appl. Neurobiol.* **2014**, *40*, 670–685. [CrossRef]
106. Kim, H.J.; Kim, N.C.; Wang, Y.D.; Scarborough, E.A.; Moore, J.; Diaz, Z.; MacLea, K.S.; Freibaum, B.; Li, S.; Molliex, A.; et al. Mutations in prion-like domains in hnRNPA2B1 and hnRNPA1 cause multisystem proteinopathy and ALS. *Nature* **2013**, *495*, 467–473. [CrossRef]
107. Wang, J.; Ho, W.Y.; Lim, K.; Feng, J.; Tucker-Kellogg, G.; Nave, K.A.; Ling, S.C. Cell-autonomous requirement of TDP-43, an ALS/FTD signature protein, for oligodendrocyte survival and myelination. *Proc. Natl. Acad. Sci. USA* **2018**, *115*, E10941–E10950. [CrossRef]
108. Balendra, R.; Isaacs, A.M. C9orf72-mediated ALS and FTD: Multiple pathways to disease. *Nat. Rev. Neurol.* **2018**, *14*, 544–558. [CrossRef]
109. Li, Z.; Zhang, Y.; Li, D.; Feng, Y. Destabilization and mislocalization of myelin basic protein mRNAs in quaking dysmyelination lacking the QKI RNA-binding proteins. *J. Neurosci. Off. J. Soc. Neurosci.* **2000**, *20*, 4944–4953. [CrossRef]
110. Larocque, D.; Pilotte, J.; Chen, T.; Cloutier, F.; Massie, B.; Pedraza, L.; Couture, R.; Lasko, P.; Almazan, G.; Richard, S. Nuclear retention of MBP mRNAs in the quaking viable mice. *Neuron* **2002**, *36*, 815–829. [CrossRef]

111. Sakers, K.; Lake, A.M.; Khazanchi, R.; Ouwenga, R.; Vasek, M.J.; Dani, A.; Dougherty, J.D. Astrocytes locally translate transcripts in their peripheral processes. *Proc. Natl. Acad. Sci. USA* **2017**, *114*, E3830–E3838. [CrossRef]
112. Nasrabady, S.E.; Rizvi, B.; Goldman, J.E.; Brickman, A.M. White matter changes in Alzheimer's disease: A focus on myelin and oligodendrocytes. *Acta Neuropathol. Commun.* **2018**, *6*, 22. [CrossRef] [PubMed]
113. Quintela-Lopez, T.; Ortiz-Sanz, C.; Serrano-Regal, M.P.; Gaminde-Blasco, A.; Valero, J.; Baleriola, J.; Sanchez-Gomez, M.V.; Matute, C.; Alberdi, E. Abeta oligomers promote oligodendrocyte differentiation and maturation via integrin beta1 and Fyn kinase signaling. *Cell Death Dis.* **2019**, *10*, 445. [CrossRef] [PubMed]
114. Wu, Y.; Ma, Y.; Liu, Z.; Geng, Q.; Chen, Z.; Zhang, Y. Alterations of myelin morphology and oligodendrocyte development in early stage of Alzheimer's disease mouse model. *Neurosci. Lett.* **2017**, *642*, 102–106. [CrossRef] [PubMed]
115. Ferreira, S.; Pitman, K.A.; Wang, S.; Summers, B.S.; Bye, N.; Young, K.M.; Cullen, C.L. Amyloidosis is associated with thicker myelin and increased oligodendrogenesis in the adult mouse brain. *J. Neurosci. Res.* **2020**, *98*, 1905–1932. [CrossRef]
116. Ahmed, Z.; Bigio, E.H.; Budka, H.; Dickson, D.W.; Ferrer, I.; Ghetti, B.; Giaccone, G.; Hatanpaa, K.J.; Holton, J.L.; Josephs, K.A.; et al. Globular glial tauopathies (GGT): Consensus recommendations. *Acta Neuropathol.* **2013**, *126*, 537–544. [CrossRef]
117. Ferrer, I.; Andres-Benito, P.; Zelaya, M.V.; Aguirre, M.E.E.; Carmona, M.; Ausin, K.; Lachen-Montes, M.; Fernandez-Irigoyen, J.; Santamaria, E.; Del Rio, J.A. Familial globular glial tauopathy linked to MAPT mutations: Molecular neuropathology and seeding capacity of a prototypical mixed neuronal and glial tauopathy. *Acta Neuropathol.* **2020**, *139*, 735–771. [CrossRef]
118. Seiberlich, V.; Bauer, N.G.; Schwarz, L.; Ffrench-Constant, C.; Goldbaum, O.; Richter-Landsberg, C. Downregulation of the microtubule associated protein tau impairs process outgrowth and myelin basic protein mRNA transport in oligodendrocytes. *Glia* **2015**, *63*, 1621–1635. [CrossRef]
119. Pasciuto, E.; Bagni, C. SnapShot: FMRP mRNA targets and diseases. *Cell* **2014**, *158*, 1446–1446.e1. [CrossRef] [PubMed]
120. Giampetruzzi, A.; Carson, J.H.; Barbarese, E. FMRP and myelin protein expression in oligodendrocytes. *Mol. Cell Neurosci.* **2013**, *56*, 333–341. [CrossRef]
121. Wang, H.; Ku, L.; Osterhout, D.J.; Li, W.; Ahmadian, A.; Liang, Z.; Feng, Y. Developmentally-programmed FMRP expression in oligodendrocytes: A potential role of FMRP in regulating translation in oligodendroglia progenitors. *Hum. Mol. Genet.* **2004**, *13*, 79–89. [CrossRef]
122. Pacey, L.K.; Xuan, I.C.; Guan, S.; Sussman, D.; Henkelman, R.M.; Chen, Y.; Thomsen, C.; Hampson, D.R. Delayed myelination in a mouse model of fragile X syndrome. *Hum. Mol. Genet.* **2013**, *22*, 3920–3930. [CrossRef]
123. Doll, C.A.; Yergert, K.M.; Appel, B.H. The RNA binding protein fragile X mental retardation protein promotes myelin sheath growth. *Glia* **2020**, *68*, 495–508. [CrossRef]
124. Blackburn, D.; Sargsyan, S.; Monk, P.N.; Shaw, P.J. Astrocyte function and role in motor neuron disease: A future therapeutic target? *Glia* **2009**, *57*, 1251–1264. [CrossRef] [PubMed]
125. Alvarez, J.I.; Katayama, T.; Prat, A. Glial influence on the blood brain barrier. *Glia* **2013**, *61*, 1939–1958. [CrossRef] [PubMed]
126. Zhou, B.; Zuo, Y.X.; Jiang, R.T. Astrocyte morphology: Diversity, plasticity, and role in neurological diseases. *CNS Neurosci.* **2019**, *25*, 665–673. [CrossRef] [PubMed]
127. Thomsen, R.; Pallesen, J.; Daugaard, T.F.; Borglum, A.D.; Nielsen, A.L. Genome wide assessment of mRNA in astrocyte protrusions by direct RNA sequencing reveals mRNA localization for the intermediate filament protein nestin. *Glia* **2013**, *61*, 1922–1937. [CrossRef] [PubMed]
128. Thomsen, R.; Daugaard, T.F.; Holm, I.E.; Nielsen, A.L. Alternative mRNA splicing from the glial fibrillary acidic protein (GFAP) gene generates isoforms with distinct subcellular mRNA localization patterns in astrocytes. *PLoS ONE* **2013**, *8*, e72110. [CrossRef]
129. Ogata, K.; Kosaka, T. Structural and quantitative analysis of astrocytes in the mouse hippocampus. *Neuroscience* **2002**, *113*, 221–233. [CrossRef]
130. Mazare, N.; Oudart, M.; Moulard, J.; Cheung, G.; Tortuyaux, R.; Mailly, P.; Mazaud, D.; Bemelmans, A.P.; Boulay, A.C.; Blugeon, C.; et al. Local Translation in Perisynaptic Astrocytic Processes Is Specific and Changes after Fear Conditioning. *Cell Rep.* **2020**, *32*, 108076. [CrossRef]
131. Boulay, A.C.; Saubamea, B.; Adam, N.; Chasseigneaux, S.; Mazare, N.; Gilbert, A.; Bahin, M.; Bastianelli, L.; Blugeon, C.; Perrin, S.; et al. Translation in astrocyte distal processes sets molecular heterogeneity at the gliovascular interface. *Cell Discov.* **2017**, *3*, 17005. [CrossRef]
132. Iadecola, C. The Neurovascular Unit Coming of Age: A Journey through Neurovascular Coupling in Health and Disease. *Neuron* **2017**, *96*, 17–42. [CrossRef] [PubMed]
133. Dossi, E.; Vasile, F.; Rouach, N. Human astrocytes in the diseased brain. *Brain Res. Bull.* **2018**, *136*, 139–156. [CrossRef]
134. Tong, J.; Huang, C.; Bi, F.; Wu, Q.; Huang, B.; Liu, X.; Li, F.; Zhou, H.; Xia, X.G. Expression of ALS-linked TDP-43 mutant in astrocytes causes non-cell-autonomous motor neuron death in rats. *EMBO J.* **2013**, *32*, 1917–1926. [CrossRef]
135. Rothstein, J.D.; Van Kammen, M.; Levey, A.I.; Martin, L.J.; Kuncl, R.W. Selective loss of glial glutamate transporter GLT-1 in amyotrophic lateral sclerosis. *Ann. Neurol.* **1995**, *38*, 73–84. [CrossRef]
136. Barton, S.K.; Gregory, J.M.; Chandran, S.; Turner, B.J. Could an Impairment in Local Translation of mRNAs in Glia be Contributing to Pathogenesis in ALS? *Front. Mol. Neurosci.* **2019**, *12*, 124. [CrossRef]
137. Liedtke, W.; Edelmann, W.; Bieri, P.L.; Chiu, F.C.; Cowan, N.J.; Kucherlapati, R.; Raine, C.S. GFAP is necessary for the integrity of CNS white matter architecture and long-term maintenance of myelination. *Neuron* **1996**, *17*, 607–615. [CrossRef]

138. Kamphuis, W.; Middeldorp, J.; Kooijman, L.; Sluijs, J.A.; Kooi, E.J.; Moeton, M.; Freriks, M.; Mizee, M.R.; Hol, E.M. Glial fibrillary acidic protein isoform expression in plaque related astrogliosis in Alzheimer's disease. *Neurobiol. Aging* **2014**, *35*, 492–510. [CrossRef]
139. Oudart, M.; Tortuyaux, R.; Mailly, P.; Mazare, N.; Boulay, A.C.; Cohen-Salmon, M. AstroDot—A new method for studying the spatial distribution of mRNA in astrocytes. *J. Cell Sci.* **2020**, *133*. [CrossRef]
140. Farnsworth, B.; Peuckert, C.; Zimmermann, B.; Jazin, E.; Kettunen, P.; Emilsson, L.S. Gene Expression of Quaking in Sporadic Alzheimer's Disease Patients is Both Upregulated and Related to Expression Levels of Genes Involved in Amyloid Plaque and Neurofibrillary Tangle Formation. *J. Alzheimers Dis.* **2016**, *53*, 209–219. [CrossRef]
141. Vidal, R.; Ghetti, B.; Takao, M.; Brefel-Courbon, C.; Uro-Coste, E.; Glazier, B.S.; Siani, V.; Benson, M.D.; Calvas, P.; Miravalle, L.; et al. Intracellular ferritin accumulation in neural and extraneural tissue characterizes a neurodegenerative disease associated with a mutation in the ferritin light polypeptide gene. *J. Neuropathol. Exp. Neurol.* **2004**, *63*, 363–380. [CrossRef]
142. Tong, X.; Ao, Y.; Faas, G.C.; Nwaobi, S.E.; Xu, J.; Haustein, M.D.; Anderson, M.A.; Mody, I.; Olsen, M.L.; Sofroniew, M.V.; et al. Astrocyte Kir4.1 ion channel deficits contribute to neuronal dysfunction in Huntington's disease model mice. *Nat. Neurosci.* **2014**, *17*, 694–703. [CrossRef]
143. Higashimori, H.; Morel, L.; Huth, J.; Lindemann, L.; Dulla, C.; Taylor, A.; Freeman, M.; Yang, Y. Astroglial FMRP-dependent translational down-regulation of mGluR5 underlies glutamate transporter GLT1 dysregulation in the fragile X mouse. *Hum. Mol. Genet.* **2013**, *22*, 2041–2054. [CrossRef] [PubMed]
144. Higashimori, H.; Schin, C.S.; Chiang, M.S.; Morel, L.; Shoneye, T.A.; Nelson, D.L.; Yang, Y. Selective Deletion of Astroglial FMRP Dysregulates Glutamate Transporter GLT1 and Contributes to Fragile X Syndrome Phenotypes In Vivo. *J. Neurosci.* **2016**, *36*, 7079–7094. [CrossRef] [PubMed]
145. Cohen-Salmon, M.; Slaoui, L.; Mazare, N.; Gilbert, A.; Oudart, M.; Alvear-Perez, R.; Elorza-Vidal, X.; Chever, O.; Boulay, A.C. Astrocytes in the regulation of cerebrovascular functions. *Glia* **2020**, *69*, 817–841. [CrossRef] [PubMed]
146. Tang, G.; Yang, G.Y. Aquaporin-4: A Potential Therapeutic Target for Cerebral Edema. *Int J. Mol. Sci.* **2016**, *17*, 1413. [CrossRef]
147. Zheng, L.; Cheng, W.; Wang, X.; Yang, Z.; Zhou, X.; Pan, C. Overexpression of MicroRNA-145 Ameliorates Astrocyte Injury by Targeting Aquaporin 4 in Cerebral Ischemic Stroke. *Biomed. Res. Int.* **2017**, *2017*, 9530951. [CrossRef] [PubMed]
148. Chen, B.; Yang, L.; Chen, J.; Chen, Y.; Zhang, L.; Wang, L.; Li, X.; Li, Y.; Yu, H. Inhibition of Connexin43 hemichannels with Gap19 protects cerebral ischemia/reperfusion injury via the JAK2/STAT3 pathway in mice. *Brain Res. Bull.* **2019**, *146*, 124–135. [CrossRef]
149. Eilam, R.; Segal, M.; Malach, R.; Sela, M.; Arnon, R.; Aharoni, R. Astrocyte disruption of neurovascular communication is linked to cortical damage in an animal model of multiple sclerosis. *Glia* **2018**, *66*, 1098–1117. [CrossRef] [PubMed]
150. Alvestad, S.; Hammer, J.; Hoddevik, E.H.; Skare, O.; Sonnewald, U.; Amiry-Moghaddam, M.; Ottersen, O.P. Mislocalization of AQP4 precedes chronic seizures in the kainate model of temporal lobe epilepsy. *Epilepsy Res.* **2013**, *105*, 30–41. [CrossRef] [PubMed]
151. Gotz, M.; Barde, Y.A. Radial glial cells defined and major intermediates between embryonic stem cells and CNS neurons. *Neuron* **2005**, *46*, 369–372. [CrossRef]
152. Yao, B.; Christian, K.M.; He, C.; Jin, P.; Ming, G.L.; Song, H. Epigenetic mechanisms in neurogenesis. *Nat. Rev. Neurosci.* **2016**, *17*, 537–549. [CrossRef]
153. Martinez-Cerdeno, V.; Noctor, S.C. Neural Progenitor Cell Terminology. *Front. Neuroanat.* **2018**, *12*, 104. [CrossRef]
154. Komada, M.; Saitsu, H.; Kinboshi, M.; Miura, T.; Shiota, K.; Ishibashi, M. Hedgehog signaling is involved in development of the neocortex. *Development* **2008**, *135*, 2717–2727. [CrossRef]
155. Lee, H.; Song, M.R. The structural role of radial glial endfeet in confining spinal motor neuron somata is controlled by the Reelin and Notch pathways. *Exp. Neurol.* **2013**, *249*, 83–94. [CrossRef] [PubMed]
156. Pilaz, L.J.; Lennox, A.L.; Rouanet, J.P.; Silver, D.L. Dynamic mRNA Transport and Local Translation in Radial Glial Progenitors of the Developing Brain. *Curr. Biol.* **2016**, *26*, 3383–3392. [CrossRef] [PubMed]
157. Tsunekawa, Y.; Kikkawa, T.; Osumi, N. Asymmetric inheritance of Cyclin D2 maintains proliferative neural stem/progenitor cells: A critical event in brain development and evolution. *Dev. Growth Differ.* **2014**, *56*, 349–357. [CrossRef] [PubMed]
158. Pilaz, L.J.; Silver, D.L. Moving messages in the developing brain-emerging roles for mRNA transport and local translation in neural stem cells. *FEBS Lett.* **2017**, *591*, 1526–1539. [CrossRef]
159. Mirzaa, G.; Parry, D.A.; Fry, A.E.; Giamanco, K.A.; Schwartzentruber, J.; Vanstone, M.; Logan, C.V.; Roberts, N.; Johnson, C.A.; Singh, S.; et al. De novo CCND2 mutations leading to stabilization of cyclin D2 cause megalencephaly-polymicrogyria-polydactyly-hydrocephalus syndrome. *Nat. Genet.* **2014**, *46*, 510–515. [CrossRef] [PubMed]
160. Vasek, M.J.; Deajon-Jackson, J.D.; Liu, Y.; Crosby, H.W.; Yi, J.; Dougherty, J.D. Microglia perform local protein synthesis at perisynaptic and phagocytic structures. *bioRxiv* **2021**. [CrossRef]
161. Berson, A.; Barbash, S.; Shaltiel, G.; Goll, Y.; Hanin, G.; Greenberg, D.S.; Ketzef, M.; Becker, A.J.; Friedman, A.; Soreq, H. Cholinergic-associated loss of hnRNP-A/B in Alzheimer's disease impairs cortical splicing and cognitive function in mice. *EMBO Mol. Med.* **2012**, *4*, 730–742. [CrossRef] [PubMed]
162. Lavon, I.; Leykin, I.; Charbit, H.; Binyamin, O.; Brill, L.; Ovadia, H.; Vaknin-Dembinsky, A. QKI-V5 is downregulated in CNS inflammatory demyelinating diseases. *Mult. Scler. Relat. Disord.* **2019**, *39*, 101881. [CrossRef]

frontiers in Neuroscience

ORIGINAL RESEARCH
published: 03 June 2020
doi: 10.3389/fnins.2020.00547

Object-Based Analyses in FIJI/ImageJ to Measure Local RNA Translation Sites in Neurites in Response to Aβ1-42 Oligomers

*María Gamarra[1,2], Maite Blanco-Urrejola[1,2,3], Andreia F. R. Batista[1,4,5], Josune Imaz[2] and Jimena Baleriola[1,3,6]**

[1] Achucarro Basque Center for Neuroscience, Leioa, Spain, [2] Department of Neurosciences, Faculty of Medicine and Nursing, University of the Basque Country, Bilbao, Spain, [3] Department of Cell Biology and Histology, Faculty of Medicine and Nursing, University of the Basque Country, Leioa, Spain, [4] Life and Health Sciences Research Institute, School of Medicine, University of Minho, Braga, Portugal, [5] ICVS/3B's, PT Associate Laboratory, Universidade do Minho, Guimarães, Portugal, [6] IKERBASQUE Basque Foundation for Science, Bilbao, Spain

Subcellular protein delivery is especially important in signal transduction and cell behavior, and is typically achieved by localization signals within the protein. However, protein delivery can also rely on localization of mRNAs that are translated at target sites. Although once considered heretical, RNA localization has proven to be highly conserved in eukaryotes. RNA localization and localized translation are especially relevant in polarized cells like neurons where neurites extend dozens to hundreds of centimeters away from the soma. Local translation confers dendrites and axons the capacity to respond to their environment in an acute manner without fully relying on somatic signals. The relevance of local protein synthesis in neuron development, maintenance and disease has not been fully acknowledged until recent years, partly due to the limited amount of locally produced proteins. For instance, in hippocampal neurons levels of newly synthesized somatic proteins can be more than 20–30 times greater than translation levels of neuritic proteins. Thus local translation events can be easily overlooked under the microscope. Here we describe an object-based analysis used to visualize and quantify local RNA translation sites in neurites. Newly synthesized proteins are tagged with puromycin and endogenous RNAs labeled with SYTO. After imaging, signals corresponding to neuritic RNAs and proteins are filtered with a Laplacian operator to enhance the edges. Resulting pixels are converted into objects and selected by automatic masking followed by signal smoothing. Objects corresponding to RNA or protein and colocalized objects (RNA and protein) are quantified along individual neurites. Colocalization between RNA and protein in neurites correspond to newly synthesized proteins arising from localized RNAs and represent localized translation sites. To test the validity of our analyses we have compared control neurons to $A\beta_{1-42}$-treated neurons. Aβ is involved in the pathology of Alzheimer's disease and was previously reported to induce local translation in axons and dendrites which in

OPEN ACCESS

Edited by:
João O. Malva, University of Coimbra, Portugal

Reviewed by:
Luisa Cortes, University of Coimbra, Portugal
Ramiro Almeida, University of Aveiro, Portugal

***Correspondence:**
Jimena Baleriola
jimena.baleriola@achucarro.org

Specialty section:
This article was submitted to Brain Imaging Methods, a section of the journal Frontiers in Neuroscience

Received: *19 December 2019*
Accepted: *04 May 2020*
Published: *03 June 2020*

Citation:
Gamarra M, Blanco-Urrejola M, Batista AFR, Imaz J and Baleriola J (2020) Object-Based Analyses in FIJI/ImageJ to Measure Local RNA Translation Sites in Neurites in Response to Aβ1-42 Oligomers. Front. Neurosci. 14:547. doi: 10.3389/fnins.2020.00547

turn contributes to the disease. We have observed that Aβ increases the synthesis of neuritic proteins as well as the fraction of translating RNAs in distal sites of the neurite, suggesting an induction of local protein synthesis. Our results thus confirm previous reports and validate our quantification method.

Keywords: local protein synthesis, RNA localization, neurites, fluorescence microscopy, FIJI/ImageJ analyses, colocalization analyses

INTRODUCTION

Among all cell types, neurons are the most morphologically complex. The nucleus is contained in a cell body or soma, from where several neurites emerge. Neuronal dendrites measure around ten millimeters and axons can reach one meter of length in vertebrates (Bannister and Larkman, 1995b). This extremely polarized morphology reflects the also polarized function of neurons. Whereas dendrites receive signals, the cell body processes them and axons are responsible for transmitting information to adjacent neurons. To maintain a proper function, each neuronal compartment needs to react temporally and spatially in an acute manner in order to rapidly adapt to changes in the environment. These implies that compartmentalized signaling events are required and therefore neuronal proteins must be asymmetrically distributed.

The origin of neuritic proteins (both dendritic and axonal) has been discussed for years. It was classically thought that proteins that support dendritic and axonal functions are synthesized in the soma and then transported to the target compartment at peripheral sites of the neuron. However, in the 19th century, the possibility of neurites, especially axons, producing their own proteins locally was already hypothesized (review in Bolton, 1901). This unconventional view of protein distribution to different neuronal compartments has been finally accepted by the scientific community. In order to synthesize proteins locally, messenger RNAs (mRNAs) and components of translational machinery must be transported to neurites. mRNAs are localized to dendrites and axons as part of ribonucleoprotein (RNPs) complexes in a translationally repressed state. Exogenous stimulus sensed by neurites influence the local translation machinery and mRNAs are released from RNPs complexes. Once associated to localized ribosomes, mRNAs are translated and proteins are synthesized independently from the soma and thus the endoplasmic reticulum (ER) (Jung et al., 2012).

The requirement of local intra-dendritic translation for nervous system plasticity has been extensively studied. Local translation in axons is involved in growth cone behavior, axonal pathfinding and maintenance, as well as in retrograde signaling (reviewed in Jung et al., 2014; Holt et al., 2019). More recently, it has been reported that adult axons are also able to respond to pathological insults by changing their local translatome. In particular, after a nerve injury, mRNAs are locally translated and newly synthesized proteins contribute to axonal regeneration (Terenzio et al., 2018). Similarly, in the central nervous system (CNS) intra-axonal protein synthesis induced by $A\beta_{1-42}$ oligomers, whose accumulation is central to Alzheimer's disease (AD), contributes to neurodegeneration (Baleriola et al., 2014; Walker et al., 2018). Interestingly some authors have linked intra-dendritic translation and Tau mislocalization and hyperphosphorylation (Kobayashi et al., 2017; Li and Gotz, 2017). Thus, dysregulation of local protein synthesis might play a more relevant role in nervous system dysfunction than previously acknowledged.

AD is characterized by synaptic dysfunction during early stages (Palop and Mucke, 2010). Understanding dynamic early changes in the local proteome is in our view crucial to understand basic pathological mechanisms underlying AD and likely other neurological diseases. An accurate quantification of local translation foci, which is the aim of this study, might therefore give important clues to the extent to which changes in the local translatome contribute to the disease. Currently the most frequently used techniques to detect local translation in neurons are FUNCAT (FlUorescent Non–Canonical Amino acid Tagging) and SUnSET (SUrface SEnsing of Translation). The first utilizes modified amino acids, such azidohomoalanine, that get incorporated into the nascent polypeptide chain. The non-canonical amino acids are then tagged with a fluorophore in a cycloaddition reaction (Dieterich et al., 2010). SUnSET is based in the use of the antibiotic puromycin, which mimics an aminoacyl-transfer RNA (tRNA). Puromycin binds to the acceptor site of the ribosome during translation elongation leading to translation termination. The truncated puromycilated polypeptide can be detected by immunofluorescence using an anti-puromycin antibody (Schmidt et al., 2009). The fluorescence signal measured by both approaches is used as a readout of protein synthesis. Nevertheless, the low amount of locally produced proteins entails a limitation in the study of this phenomenon. For instance, our own results indicate that levels of newly synthesized neuritic proteins can be 20 to 30 times lower than somatic protein levels in unstimulated conditions. Thus, local translation sites in neurites can be easily overlooked when analyzing *de novo* synthesis by fluorescence microscopy. To overcome this situation, we have developed a simple method that helps visualize and quantify puromycin-positive sites in neurites by filtering and binarizing imaged cells using FIJI/ImageJ. Moreover, we have used a combination of RNA and protein staining techniques followed by object-based colocalization to detect sites of local RNA translation in neurons.

MATERIALS AND METHODS

Animals

All animal protocols followed the European directive 2010/63/EU and were approved by the UPV/EHU ethics committee.

Sprague-Dawley rats were bred in local facilities and embryonic brains were obtained from CO_2 euthanized pregnant rats.

Neuronal Cultures

Hippocampal neurons were prepared from embryonic day 18 rat embryos (E18) as described (Banker and Goslin, 1998). Briefly, hippocampi were dissected from embryonic brains and dissociated in TrypLE Express (Gibco, Thermo Fisher Scientific, Waltham MA, United States) for 10 min at 37°C. Cells were washed twice with Hank's balanced salt solution (HBSS, Gibco) and resuspended in plating medium containing 10% fetal bovine serum, 2 mM L-glutamine and 50 $U.ml^{-1}$ penicillin-streptomycin in Neurobasal (all from Gibco). Cells were homogenized with a pasteur pipette and centrifuged for 5 min at 800 rpm. Cells were resuspended in plating medium. Hippocampal neurons were cultured on poly-D-lysine-coated coverslips in 24-well plates at low density (35.000 cells/cm^2), similar to previous reports in which newly synthesized proteins along individual neurites were visualized (Dieterich et al., 2010; Graber et al., 2013; Hafner et al., 2019). Cultures were maintained at 37°C in a 5% CO_2 humidified incubator. After 1 day *in vitro* (1 DIV) the medium was replaced with growth medium (1× B27, 2 mM glutamine, and 50 $U.ml^{-1}$ penicillin-streptomycin in Neurobasal). To avoid the growth of glia, half of the medium was replaced with fresh medium containing 20 μM of 5-fluorodeoxyuridine and uridine (Sigma Aldrich, Merck, Darmstadt, Germany) every 3 days. Treatments were performed at 9–10 DIV.

Oligomeric Aβ Preparation and Treatments

Soluble oligomeric amyloid-β ($A\beta_{1-42}$) was prepared as previously described (Quintela-Lopez et al., 2019). Synthetic $A\beta_{1-42}$ (Bachem, Bubendorf, Switzerland) was dissolved in hexafluoroisopropanol (HFIP, Sigma Aldrich) to 1 mM, aliquoted and dried. For oligomer formation, the peptides were resuspended in dry dimethylsulfoxide (DMSO; 5 mM, Sigma Aldrich) and Hams F-12 (PromoCell Labclinics, Barcelona, Spain) was added to adjust the final concentration to 100 μM. Peptides were incubated overnight at 4°C. Oligomerized Aβ was added to neurons at 9 DIV at a 3 μM concentration and incubated for 24 h. DMSO was used as vehicle control.

Puromycylation Assay

Puromicyn is a tRNA analog, which is incorporated into the nascent polypeptide chain in a ribosome-catalyzed reaction. This technique allows the *in situ* detection of protein synthesis with an anti-puromicyn antibody. At 10 DIV, DMSO- and Aβ-treated neurons were exposed to 2 μM puromycin (Sigma Aldrich) for 5–30 min as indicated. Control conditions with no puromicyn received only fresh growth medium (vehicle). To verify that puromycin labels newly synthesized proteins, 40 μM of the translation inhibitor anisomycin (Sigma Aldrich) was co-incubated with puromycin. Cells were washed with cold PBS with 3 $\mu g.ml^{-1}$ digitonin (Sigma Aldrich) and fixed in 4% paraformaldehyde (PFA), 4% sucrose in PBS.

Immunocytochemistry

Neurons were fixed for 20 min at room temperature in 4% PFA, 4% sucrose in PBS. Cells were washed three times with PBS, permeabilized and blocked for 30 min in 3% BSA, 100 mM glycine and 0.25% Triton X-100. Next, samples were incubated overnight at 4°C with primary antibodies including mouse anti-puromycin (1:500, MABE343, Merck Millipore), rabbit and chicken anti-βIII tubulin (1:500, ab18207 and ab107216, respectively, Abcam, Cambridge, United Kingdom), rabbit anti-Tau (1:1000, ab32057, Abcam) and rabbit anti-calreticulin (1:500, ab92516, Abcam). After three PBS washes, cells were incubated for 1 hr at room temperature with fluorophore-conjugated secondary antibodies: anti-mouse Alexa Fluor 594 (1:200, A-11005, Invitrogen, Thermo Fisher Scientific), anti-rabbit Alexa Fluor 488 (1:200, A-21206, Invitrogen), anti-chicken DyLight 350 (1:200, SA5-10069, Invitrogen), anti-rabbit Alexa Fluor 647 (1:200, A-31573, Invitrogen) and anti-rabbit DyLight 405 (1:200, 611-146-002, Rockland Immunochemicals, Pottstown, PA, United States). Samples were washed three times with PBS and mounted with ProLong Gold antifade reagent (P-36930, Invitrogen). Whenever stated, a no-primary-antibody negative control was used.

To label endogenous RNAs neurons were washed once with cold PBS with 3 $\mu g.ml^{-1}$ digitonin (Sigma Aldrich), once with 50% methanol in PBS and fixed in cold 100% methanol for 5 min. Samples were rehydrated by washing them in 50% methanol in PBS once and in PBS three times. Following the standard immunocytochemistry procedure, cells were incubated for 20 min at room temperature with SYTO RNASelect green fluorescent dye in PBS (500 nM, S-32703, Invitrogen). Samples were washed with PBS and mounted with ProLong Gold antifade reagent. Some fixed neurons were incubated with 50 μg/ml DNAse or RNAse (Sigma) for 10 min at room temperature to assess the selectivity of the SYTO labeling.

Image Acquisition and Processing

Images were acquired using an objective EC Plan-Neofluar 40×/1,30 Oil DIC M27 on an Axio-Observer Z1 microscope equipped with AxioCam MRm Rev. 3 (Zeiss, Oberkochen, Germany) and Hamamatsu EM-CCD ImagEM (Hamamatsu Photonics, Hamamatsu, Japan) digital cameras. Settings for image acquisition where determined in a random field of a DMSO-treated sample ensuring pixel intensities were within the linear range and avoiding pixel saturation. Images were acquired with ZEN 2 (blue edition) version 2.0.0.0. software (Zeiss). Settings were kept identical for all sampled cells in any given experiment. Whenever possible, five random fields per coverslip and two coverslips per experimental condition were imaged. Most images were acquired with AxioCam, however if cells were imaged in the far red spectrum, the Hamamatsu camera was used.

For figure preparation, the staining of interest (puromycin, calreticulin, SYTO) was converted from grayscale to RGB or to a colorimetric scale (heatmaps) in non-binarized images. Binarized images used for assisted quantification of translation sites were obtained as will be specified below. In all cases

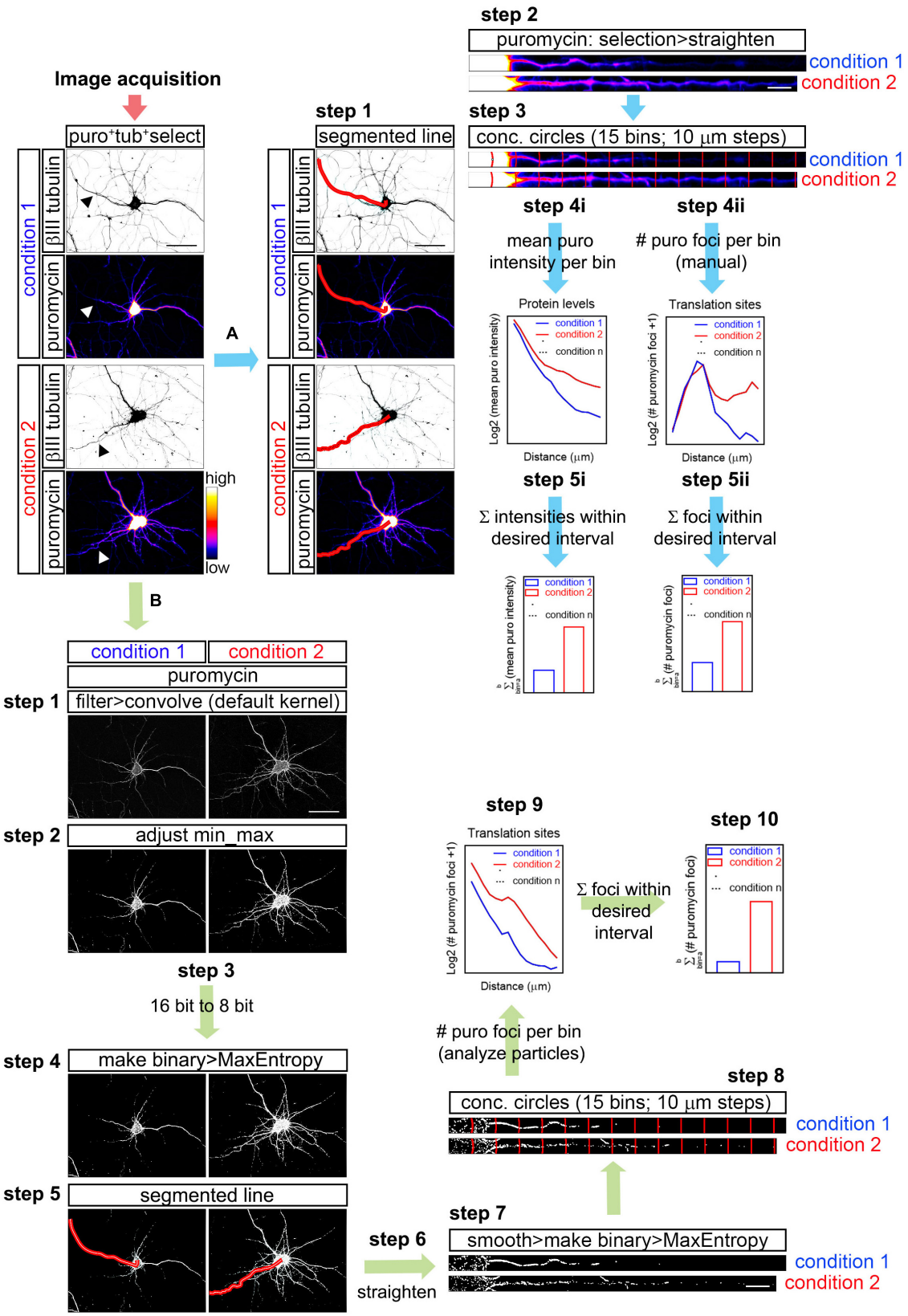

FIGURE 1 | Continued

FIGURE 1 | Workflow for puromycin quantification in unprocessed and processed images. **(A)** Workflow A shows puromycin intensity analyses (**path i**) and visual inspection of puromycin translation sites in raw images (**path ii**). After image acquisition, the longest puromycin- and βIII-positive neurite (arrowheads in the first panel) was selected with a segmented line, straighten and divided into 10 μm bins with the concentric_circles plugin (**steps 2** and **3**). Mean puromycin intensity per bin, corresponding to protein levels, was measured and represented as the Log2 (mean puro intensity) vs. distance (**step 4i**). The total fluorescent intensity of the puromycin within the desired interval (soma, neurites, etc. . .) disregarding the bin position is shown as Σ (mean puro intensity; **step 5i**). For visual inspection of puromycin foci, path ii was followed. Number of puromycin foci per bin, corresponding to translation sites, was quantified (Log2 (# puromycin foci + 1) vs. distance; **step 4ii**). The total number of puromycin foci within the desired interval (soma, meurites, etc. . .) disregarding the bin position is plotted as Σ (# puromycin foci; **step 5ii**). **(B)** The assisted analyses of puromycin-positive foci in binarized images were performed following the workflow B. Once the images were acquired, puromycin staining was filtered with the convolver applying the default normalized kernel and minimum and maximum intensities were adjusted (**steps 1** and **2**). 16-bit images were coverted to 8-bit (**step 3**) and binarized with the MaxEntropy mask (**step 4**). Neurites were selected with a segmented line (**step 5**), straighten, smoothen and binarized with the MaxEntropy mask (**steps 6** and **7**). Discrete puromycin puncta were measured (analyze particles) in neurons in 15 bins covering a distance of 150 μm from the cell nucleus or from the edge of the soma using the concentric_circles plugin (**step 8**). Graphs show the translation sites represented as Log2 (# puromycin foci + 1) vs. distance (**step 9**). Discrete puromycin foci within desired interval (soma, neurites, etc. . .) disregarding the bin position are represented as Σ (# puromycin foci; **step 10**). Scale bars, 50 μm in whole-cell micrographs and 10 μm in straighten neurites.

background, contrast and sharpness were adjusted and set the same in control and experimental conditions. Markers used as counterstain for neurite selection were adjusted for an optimal visualization in figures.

Puromycin and SYTO Intensity Analysis in Non-binarized Images

To quantify the puromycin fluorescent intensity as a measure of protein production (**Figure 1**; workflow A), the longest puromycin- and βIII tubulin-positive neurite or puromycin- and Tau-positive neurite from randomly selected cells was straightened with the Segmented Line tool in FIJI/ImageJ:

FIJI/ImageJ > File > Open (do not autoscale) > Segmented Line (**Figure 1**; workflow A; step 1) > Selection > Straighten (**Figure 1**; workflow A; step 2).

Images obtained from AxioCam measure 1038 × 1040 pixels, whereas those obtained from the Hamamatsu camera measure 512 × 512 pixels. Thus, straighten lines were 40 pixel-wide in images taken with the first camera and 20 pixel-wide in images taken with the latter. Since experiments were always compared using a randomized block design (see "Statistical Analyses"), direct comparison between neurites imaged with different cameras is never performed.

Concentric circles at 10 μm intervals emerging from the center of the cell nucleus or from the edge of the soma were generated with an in-house designed FIJI/ImageJ macro (concentric_circles, **Figure 1**; workflow A; step 3) (Quintela-Lopez et al., 2019). 15 bins were generated covering a length of 150 μm of the straighten neurites. Fluorescence intensity was measured in each bin. Background pixel intensity was measured outside the area covered by the neurite and substracted (**Figure 1**; workflow A; step 4i). To calculate the total fluorescent intensity in the soma, in neurites or in other desired interval disregarding the bin position, values retrieved from each bin of interest were summed up (**Figure 1**; workflow A; step 5i).

The same method was used to measure RNA levels in neurites stained with SYTO.

Note that workflow A (**Figure 1**) exemplifies the procedure in neurites doubly labeled for βII tubulin and puromycin, however it also applies to neurites stained for Tau and puromycin, for SYTO and Tau, for calreticulin and puromycin, etc. . .

Visual Inspection of Puromycin-Positive Translation Foci in Non-binarized Images (Manual Analyses)

As described above, the longest puromycin- and βIII-positive neurite, or puromycin- and Tau-positive neurite, etc. . . from randomly selected cells was straightened and divided into 15 10 μm-wide bins with the concentric_circles plugin (**Figure 1**; workflow A; step 3). Discrete puromycin puncta were visually scored in each bin covering a distance of 150 μm from the center of the cell nucleus or from the edge of the soma (**Figure 1**; workflow A; step 4ii). To calculate the total translation foci in the soma or in neurites or in any other desired interval disregarding the bin position, values retrieved from each bin of interest were summed up (**Figure 1**; workflow A; step 5ii). The bin ranging from 0 to 10 μm (first bin within the soma) was discarded as no discrete puncta could be visualized (N/A in **Figures 3D,E**).

Assisted Analyses of Puromycin- and SYTO-Positive Foci in Binarized Images

The assisted analysis of translation sites was performed using the following step-by-step protocol (**Figure 1**; workflow B):

FIJI/ImageJ > File > Open (do not autoscale). Go to the staining of interest (e.g., puromycin) > Process > Filter > Convolve (if a stack is opened, do not process all the images in the stack). The default normalized kernel is sufficient to enhance structures in the periphery of the neurons smaller than 5 × 5 pixels and it is thus suitable to highlight puromycin-positive translation sites distal to the center of the cell nucleus (**Figure 1**; workflow B; step 1).

Following image convolution:

Image > Adjust > Brightness/Contrast (equal min/max adjustment in all samples within the same experiment; **Figure 1**; workflow B; step 2) > Image > Type > 8-bit (**Figure 1**; workflow B; step 3) > Process > Binary > Make Binary (Method, MaxEntropy; Background, Default; Black background. Only convert current image; **Figure 1**; workflow B; step 4).

Once the image is binarized select the longest positive neurite:

Segmented Line (**Figure 1**; workflow B; step 5) > Edit > Selection > Straighten (line width: 20 pixels for Hamamatsu images; 40 pixels for AxioCam images; Process Entire Stack unclicked; **Figure 1**; workflow B; step

6) > Process > Smooth > Process > Binary > Make binary (Method, MaxEntropy; **Figure 1**; workflow B; step 7).

Straighten neurites are finally divided in 15 concentric circles at 10 μm intervals emerging from the center of the cell nucleus or from the edge of the soma with the concentric_circles plugin (**Figure 1**; workflow B; step 8). The number of objects (translation sites. . .) are scored in each interval (bin) with the Analyze Particles function (default settings; **Figure 1**; workflow B; step 9). To calculate the total translation sites in the soma or in neurites or in any other desired interval disregarding the bin position, values retrieved from each bin of interest were summed up (**Figure 1**; workflow B; step 10).

Although this procedure is described for the puromycin staining as an example, the same steps were followed to binarize and quantify SYTO-positive discrete puncta (RNA) in Tau-positive neurites. When binarization of puromycin and SYTO labeling was performed for the same neurite, colocalization between RNA and protein was performed as follows:

Process > Image Calculator > Image 1 (e.g., puromycin) AND Image 2 (e.g., SYTO; click create new window).

The resulting image is smoothen and binarized with the Mask Entropy mask. The image is finally divided in 15 concentric circles at 10 μm intervals emerging from the edge of the soma with the concentric_circles plugin. The number of objects (considered actively translating RNAs) are scored in each interval (bin) with the Analyze Particles function (default settings).

Intensity Profiles

We used intensity profiles to exemplify fluorescent signal distributions in neurites Briefly, neurites were selected with the Segmented Line tool (line width: 20 pixels for Hamamatsu images; 40 pixels for AxioCam images) and analyzed with Plot Profile.

Statistical Analyses

The sample size is specified in the figure legends. Statistical analyses were performed with Prism 7 (GraphPad Software, San Diego, CA, United States) following a randomized block design where samples from the same experiment were matched to eliminate inter-experimental variability. When comparing the means of two groups taking one variable into account, two-tailed *t*-tests were performed. When comparing the means of two groups taking two variables into account, two-way ANOVA was used. If more than two groups and more than one variable were analyzed, we performed two-way ANOVA followed by Tukey's multiple comparison test or Holm-Sidak's *post hoc* test depending on the samples requirements.

For correlation analyses we performed a normality test on the data to determine if they followed a Gaussian distribution, which most of them didn't. Thus, we chose to perform Spearman non-parametric correlation test to retrieve the correlation coefficients. In the correlation graphs, linear regression of the data was performed to evaluate the differences between slopes (ANCOVA).

Note that in some cases, Y axes are represented as Log2 of the actual measured raw values to better visualize the results. In other experiments where some values equaled zero, one unit was added to all values in order to apply a Log2 function. Regardless of the transformation, all statistical analyses were performed on raw data and not on transformed data.

RESULTS

Detection of Newly Synthesized Neuritic Proteins by Puromycilation

Based on previously published data (Baleriola et al., 2014), rat hippocampal neurons grown for 9 days *in vitro* (DIV) were treated with vehicle (DMSO) or 3 μM $A\beta_{1-42}$ oligomers for 24 h by bath application. As a first step to quantify RNA translation sites in neurites we first detected *de novo* production of neuritic proteins by puromycilation/SUnSET (Schmidt et al., 2009; **Figure 2A**). The antibiotic puromycin is an aminoacyl-tRNA analog that incorporates into the polypeptide chains during translation elongation, leading to translation termination (Yarmolinsky and Haba, 1959). The development of specific antibodies has allowed the immunodetection of puromycilated polypeptides as a measure of protein synthesis. Control and Aβ-treated cells were fed with 2 μM puromycin for 30 min prior to fixation. Following fixation with a PFA/sucrose mix, cells were stained for puromycin and counterstained with an anti-βIII tubulin antibody to visualize the neuronal cytoskeleton (**Figure 2A**). As a negative control, immunostaining was performed on neurons that had not been treated with puromycin (-puro, **Figure 2A**). Fluorescence intensity for the raw puromycin signal, represented in a colorimetric scale (**Figure 2A**), was measured along the longest puromycin- and βIII-positive neurite in randomly selected cells (1–6, **Figure 2A**). Fluorescence levels in puromycin-labeled neurites (3 and 4, **Figures 2A–C**) were well above the levels measured in negative controls (1 and 2, **Figures 2A–C**). Additionally, puromycin hotspots were readily visible in distal sites of the neurites, especially in Aβ-treated cells (4, intensity profile and heatmap in **Figure 2B**). Finally, regardless of the effect of $A\beta_{1-42}$, puromycin intensity was significantly reduced in neurites when cells were co-incubated with the translation inhibitor anisomycin (+ anis + puro, **Figure 2A**; 5 and 6, **Figures 2A–C**). Altogether these results indicate that in our system puromycin labeling can be used to detect *de novo* synthesis of neuritic proteins as previously reported in similar experimental setups (Walker et al., 2018; Rangaraju et al., 2019).

$A\beta_{1-42}$ Oligomers Increases New Synthesis of Neuritic Proteins Detected Beyond the Canonical Endoplasmic Reticulum

Then we asked whether the puromycin signal likely arose from the endoplasmic reticulum (ER). Soma-centric views consider that most protein synthesis in eukaryotic cells occurs in the ER (specifically in the rough ER). In neurons, however, the positioning of the rough ER (RER) with respect to distal sites of neurites does not explain how in some experimental

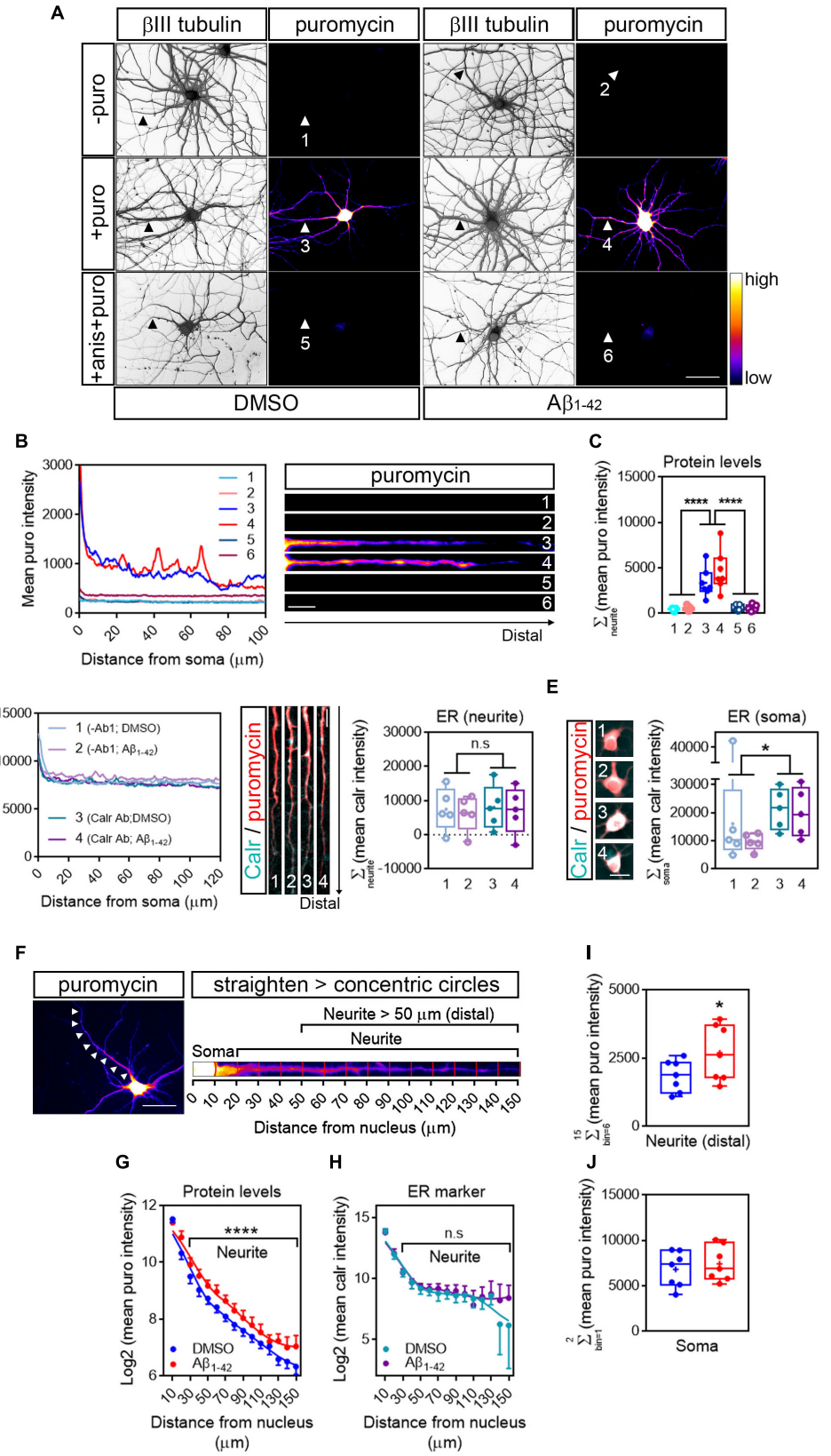

FIGURE 2 | Continued

FIGURE 2 | Detection of newly synthesized proteins by puromycilation. **(A)** Rat hippocampal neurons were grown for 9 DIV and were treated with DMSO (left panels) or $A\beta_{1-42}$ oligomers (right panels) for 24 h. Before fixing, cells were incubated with vehicle (-puro; neurites 1 and 2), with puromycin (+ puro; neurites 3 and 4) or with puromycin and anisomycin (+ anis + puro; neurites 5 and 6) for 30 mins. Cells were immunostained with an anti-βIII tubulin antibody to visualize the neuronal cytoskeleton (gray) and with an anti-puromycin antibody to analyze newly synthesized proteins (heatmaps). Scale bar, 50 μm. **(B)** Intensity profiles were measured in the longest puromycin- and βIII tubulin-positive neurite from randomly selected cells as exemplified. 1 and 2: no puromycin incubation in DMSO- and Aβ-treated neurons, respectively. 3 and 4: 30 min puromycin incubation in DMSO- and Aβ-treated cells, respectively. 5 and 6: co-incubation with anisomycin and puromycin for 30 mins in DMSO- and Aβ-treated cells, respectively. Scale bar, 10 μm in heatmaps. **(C)** Box and whisker graph representing protein levels as the total fluorescent intensity of the puromycin staining along 130 μm of βIII tubulin-positive neurites. 1 and 2: no puromycin incubation in DMSO- and Aβ-treated neurons, respectively. 3 and 4: 30 min puromycin incubation in DMSO- and Aβ-treated cells, respectively. 5 and 6: co-incubation with anisomycin and puromycin for 30 mins in DMSO- and Aβ-treated cells, respectively. Data represent the average value of 5–10 sampled cells per condition shown as individual data points, and the mean and median of 7 independent experiments ($n = 7$). $^{****}p < 0.0001$; two-way ANOVA followed by Tukey's multiple comparison test. **(D)** The "canonical" endoplasmic reticulum (ER) was defined by Calreticulin staining (Carl Ab in intensity profiles). To determine the background signal, some cells were stained only with the secondary antibody (no-primary antibody control; -Ab1 in intensity profiles). Images exemplify neurites processed for calreticulin staining (cyan) to measure the area covered by the ER and counterstained with an anti-puromycin antibody (red). Box and whisker graph representing the total fluorescent intensity of the calreticulin staining along 130 μm of calreticulin- and puromycin-positive neurites. 1 and 2: no-primary antibody control (-Ab1) in DMSO- and Aβ-treated neurons, respectively. 3 and 4: calreticulin antibody incubation (Calr Ab) in DMSO- and Aβ-treated neurons, respectively. Data represent the average value of 5–10 sampled cells per condition shown as individual data points, and the mean and median of 5 independent experiments ($n = 5$). n.s, no significant; two-way ANOVA followed by Holm-Sidak's *post hoc* test. Scale bar, 10 μm. **(E)** Calreticulin immunostaining signal (cyan) in somata from DMSO- and Aβ-treated cells and counterstained with an anti-puromycin antibody (red). Scale bar, 10 μm in images. Box and whisker graph representing the total fluorescent intensity of the calreticulin staining along the first 20 μm of calreticulin- and puromycin-positive somata. 1 and 2: no-primary antibody control (-Ab1) in DMSO- and Aβ-treated neurons, respectively. 3 and 4: calreticulin antibody incubation (Calr Ab) in DMSO- and Aβ-treated neurons, respectively. Data represent the average value of 5–10 sampled cells per condition shown as individual data points, and the mean and median of 5 independent experiments ($n = 5$). $^{*}p < 0.05$; two-way ANOVA followed by Holm-Sidak's *post hoc* test. Scale bar, 20 μm. **(F)** Cells were processed for puromycin staining to measure protein synthesis (heatmap) and counterstained with an anti-βIII tubulin antibody to visualize the neuronal cytoskeleton (not shown). The longest positive neurite (arrowheads in left micrograph) was selected with a segmented line, straighten and divided into 10 μm bins with the concentric_circles plugin (straighten neurite right) following workflow Ai in **Figure 1**. Scale bar, 50 μm. **(G)** Puromycin intensity was measured in DMSO- and Aβ-treated neurons in 15 bins covering a distance of 150 μm from the cell nucleus (as also shown in the straighten micrograph exemplified in **(F)**. The graph shows the average intensity of puromycin per condition represented as Log2 (mean puro intensity) vs. distance ± SEM measured in 7 independent experiments ($n = 7$). $^{****}p < 0.0001$; two-way ANOVA. **(H)** Calreticulin intensity was measured in DMSO- and Aβ-treated neurons in 15 bins covering a distance of 150 μm from the cell nucleus. The graph shows the average intensity of calreticulin per condition represented as Log2 (mean calr intensity) vs. distance ± SEM measured in 5 independent experiments ($n = 5$). n.s, no significant; two-way ANOVA. **(I)** Box and whisker graphs representing the total fluorescent intensity of the puromycin staining in βIII tubulin- and puromycin-positive neurites within the range of 50–150 μm from the nucleus [Neurite (distal)] as also exemplified in **(F)**. Data represent the average value of 5–10 sampled cells per condition shown as individual data points, and the mean and median of 7 independent experiments ($n = 7$). $^{*}p < 0.05$; two-tailed *t*-test. **(J)** Box and whisker graphs representing the total fluorescent intensity of the puromycin staining in βIII tubulin- and puromycin-positive somata within the range of 0–20 μm from the nucleus (Soma) as also exemplified in **(F)**. Data represent the average value of 5–10 sampled cells per condition shown as individual data points, and the mean and median of 7 independent experiments ($n = 7$).

setups that allow to study the local response of dendrites and axons (reviewed in Holt et al., 2019) newly synthesized proteins are detected peripherally, unless they are produced locally beyond the "canonical" ER. The RER is enriched in proteins involved in the folding of nascent polypeptides, being the Calnexin/Calreticulin system one the best known protein complexes (Rutkevich and Williams, 2011). After culturing hippocampal neurons for 9 days and following 24-h treatments with DMSO or $A\beta_{1-42}$, neurons were labeled with puromycin. Cells were then processed for Calreticulin (Calr) and puromycin immunostaining. As a negative control, some neurons were subjected to the immunocytochemistry procedure but were not incubated with anti-Calr antibody (no-primary antibody control). To determine the presence of Calreticulin in neurites we compared the fluorescent signal of cells incubated with anti-Carl antibody with those incubated with no primary antibody (**Figure 2D**). Results showed that both DMSO- and Aβ-treated neurites were devoid of Calreticulin, and thus of "canonical" ER (**Figure 2D**, right graph). Conversely, Calreticulin could be detected above background levels in neuronal somata of cells treated with DMSO or $A\beta_{1-42}$ oligomers (**Figure 2E**).

We then asked whether Aβ oligomers induced changes in the distribution pattern of newly synthesized proteins along neurites, beyond the canonical ER domain. The longest puromycin-positive neurite (**Figure 2F**; left micrograph) of randomly selected cells was straighten and divided into 10 μm bins following the workflow Ai (**Figure 1**). Puromycin intensity was measured in 15 bins covering a length of 150 μm from the center of the cell nucleus using the concentric_circles plugin in FIJI/ImageJ (**Figure 2F**; right micrograph). A significantly distinct distribution in the levels of newly produced proteins was observed in Aβ-treated neurites compared to controls (positions beyond 20 μm, **Figure 2G**). In line with the absence of a canonical ER in neurites, no differences were detected in the Calreticulin staining pattern between DMSO- and Aβ-treated neurites (**Figure 2H**). Finally, we focused on neuritic positions distal to the ER to increase the chances that newly synthesized proteins measured in neurites did not rely on the ER-dependent translation machinery. We summed up puromycin intensity signals in bins corresponding to the 50 to 150 μm range measured from the center of the nucleus (distal neurite; **Figure 2I**). $A\beta_{1-42}$ significantly increased the levels of newly synthesized proteins in this interval. More importantly the effect of Aβ was restricted to neurites and did not affect the neuronal soma (**Figure 2J**) in accordance with previously published data (Walker et al., 2018).

It is noteworthy pointing out that in our experimental system the effect of Aβ oligomers was not evident with puromycin pulses shorter than 30 min (e.g., 10 min. Data not shown).

Image Processing Unravels a Previously Unreported Effect of $A\beta_{1-42}$ Oligomers on Translation Foci in Neurites

Measuring puromycin intensity can give an idea of the amount of protein being produced distal from the ER within neurites and/or diffused from the actual translation site, but it does not report on the number and position of the translation sites themselves. In the case of Aβ treated cells, increased puromycin intensity might be a result of the emergence of new translation sites, a consequence of an increased rate of protein production in preexisting sites or both. To determine whether Aβ oligomers modify the amount of translation sites in neurites we quantified the number of puromycin discrete puncta. Discrete puncta in distal neuritic sites likely reflect foci of localized translation (Graber et al., 2013; Rangaraju et al., 2019). Such foci can be easily overlooked since their intensity can be ∼20 to 30 times less than somatic puromycin fluorescent levels (as implicitly shown in **Figure 2**). We have developed a strategy to enhance puromycin hotspots in neurites based solely on image processing and the assisted quantification of the resulting objects (**Figure 1**; workflow B).

The number of discrete puromycin foci was quantified along the longest puromycin- and βIII tubulin-positive neurite of randomly sampled cells (**Figure 3A**). Image acquisition was identical in control and Aβ-treated neurons. We selected neurites from raw and binarized images in order to compare quantifications performed by visual inspection of the puromycin staining (manual; **Figures 1**, **3**, workflow A) and by analyzing particles (assisted; **Figures 1**, **3**, workflow B), respectively. On the one hand DMSO- and Aβ-treated neurites were selected from raw images (represented as heatmaps; 1 and 2 in **Figure 3A**) with a segmented line 20 or 40 pixels wide and straighten (1 and 2; **Figure 3B**). On the other hand, images were filtered with the convolver in FIJI/ImageJ applying the default normalized kernel. The default kernel was sufficient to enhance structures in the periphery of the neurons and thus was suitable to highlight puromycin-positive translation foci distal to the center of the cell nucleus. Published data have reported spot quantification procedures without applying convolution filters. However, in our case image filtering prior to binarization enhanced the detection of discrete foci compared to unfiltered images, especially in Aβ-treated neurons (condition 2 in **Supplementary Figure S1**).

Following image convolution, minimum and maximum intensities (B&C menu in FIJI/ImageJ) were then manually adjusted in order to eliminate pixels outside the stained cells (background) and enhance the intensity of those inside. 16-bit images were coverted to 8-bit and binarization was performed using the MaxEntropy mask. As in the case of the raw images, DMSO- and Aβ-treated neurites were selected with a 20- or 40-pixel wide segmented line and straighten. Finally, straighten neurites were smoothen and binarized again using the MaxEntropy mask (1 and 2; **Figure 3C**). As exemplified by the number of peaks in the intensity profiles image conversion increased the number of detected sites (foci in 3B and C) and slightly enhanced the effect of Aβ oligomers, which increased from 2.7- to 3.3-fold. We then analyzed the distribution pattern of translation foci along neurites. Neurites were divided into 10 μm bins and positive puromycin puncta within each bin were visually scored prior to image conversion (1 and 2 in **Figure 3D**; wA) or were counted with the particle analyzer in binarized images (1 and 2 in **Figure 3D**; wB). In all cases 15 bins were quantified per cell, covering a distance of 150 μm from the cell nucleus. Both quantification methods revealed a significantly distinct distribution of translation sites in neurites in Aβ-treated cells compared to controls (**Figure 3E**). However, an average of almost 10-fold increase in the number of total foci in neurites was observed when using the assisted quantification method compared to visual inspection (**Figures 3E,F**).

The default matrix in FIJI's convolver is a Laplacian operator-based edge detector that allows to find discontinuities in the puromycin labeling that could result from a punctate staining arising from discrete positive foci. Laplacian operators are very accurate in finding edges in an image but also very sensitive to background noise. Thus, we quantified the amount of foci also in neurons that had not been fed with puromycin. Negative controls showed significantly less amount of foci in neurites regardless of whether quantification was performed manually in non-binarized images (**Figure 3F**; left graph) or with the particle analyzer in filtered and binarized images (**Figure 3F**; right graph). In conclusion the 5 × 5 Laplacian operator used in our approach can be successfully applied to highlight positive translation foci in distal neuritic sites.

When comparing the scores performed at each distance by manual inspection in raw images and with the assisted method in binarized images we observed a significant positive correlation between both procedures that ranged from moderate to high in DMSO- and Aβ-treated cells, respectively (**Figure 3G**). To determine which method was closer to the unbiased measurement of protein production represented by puromycin intensity (**Figure 2**), we then compared data obtained from binarized images and from raw images with the intensity values. In both cases we found a significant high positive correlation (**Figure 3H**). However, when fitting the translation sites at each distance to a regression line, a significant increase in the slope was observed when data were obtained from binarized images, suggesting increased similarities between the number of discrete puromycin foci and puromycin intensity values when using the assisted quantification method.

Finally, we focused on distal sites of the neurites (> 50 μm from the nucleus) disregarding the bin position and were unable to detect any significant change between DMSO- or Aβ-treated cells when translation foci were quantified in raw images by visual inspection (manual, **Figure 3I**; wA). Conversely, we did observe a significant effect of Aβ oligomers when quantification was performed with the particle analyzer in binarized images (assisted, **Figure 3I**; wB). In no case did we detect any changes induced by Aβ in the soma (**Figure 3I**). Altogether, results so far indicate that binarizing images from puromycin-positive cells allows the assisted quantification of neuritic translation sites yielding results that resemble those obtained from an unbiased measurement of raw puromycin intensity. Additionally, assisted quantification in binarized

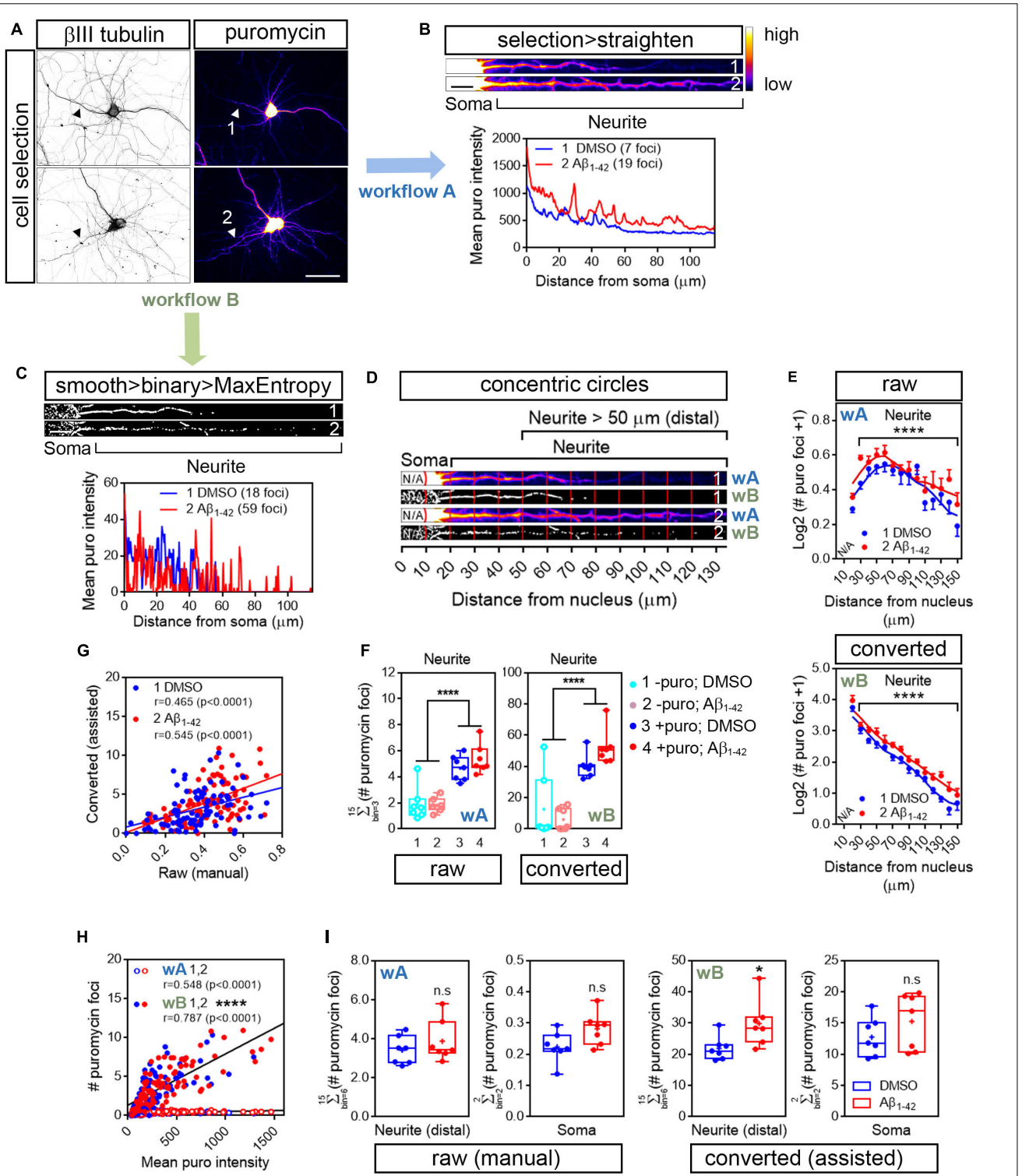

FIGURE 3 | Image processing reveals an effect of Aβ1-42 oligomers on neuritic translation sites. **(A)** Rat hippocampal neurons were grown for 9 DIV and were treated with DMSO or $A\beta_{1-42}$ oligomers for 24 h. Cells were incubated with puromycin for 30 mins and processed for βIII tubulin (gray) and puromycin immunostaining (heatmaps). Scale bar, 50 μm. **(B)** Following workflow A, the longest puromycin- and βIII-positive neurite in raw images was selected with a segmented line and straighten. Puromycin-positive discrete puncta were analyzed by visual inspection as exemplified in the intensity profiles obtained from straighten neurites (heatmaps). 1 and 2: 30 min puromycin incubation in DMSO- and Aβ-treated cells, respectively. Scale bar, 10 μm. **(C)** Following workflow B, selected neurites were straighten, smoothen and binarized with the MaxEntropy mask (smooth > binary > MaxEntropy). Puromycin-positive discrete puncta were analyzed

(Continued)

FIGURE 3 | with the particle analyzer as exemplified in the intensity profiles from straighten neurites. 1 and 2: 30 min puromycin incubation in DMSO- and Aβ-treated cells, respectively. Scale bar, 10 μm. **(D)** Discrete puromycin puncta were measured in DMSO- and Aβ-treated neurons in 15 bins covering a distance of 150 μm from the cell nucleus using the concentric_circles plugin. Measurements were performed by visual inspection in raw images (workflow Aii, wA) and with the particle analyzer in binarized images (workflow B, wB). 1: DMSO-; 2: Aβ-treated neurites. N/A, not applicable. **(E)** Graphs show the average puromycin foci per condition represented as Log2 (# puro foci + 1) vs. distance ± SEM measured in raw (wA) and binarized images (wB) from 7 independent experiments ($n = 7$). ****$p < 0.0001$; two-way ANOVA. N/A, not applicable. **(F)** Box and whisker graph representing translation sites as the total number of puromycin foci along 130 μm of βIII tubulin-positive neurites following visual inspection of raw images (raw; workflow A, wA) or assisted quantification in binarized images (converted; workflow B, wB). 1 and 2: no puromycin incubation in DMSO- and Aβ-treated neurons, respectively. 3 and 4: 30 min puromycin incubation in DMSO- and Aβ-treated cells, respectively. Data represent the average value of 5–10 sampled cells per condition shown as individual data points, and the mean and median of 7 independent experiments ($n = 7$). ****$p < 0.0001$; two-way ANOVA followed by Holm-Sidak's *post hoc* test. **(G)** Spearman correlation between quantifications in raw and in binarized images. Graphs represent each scored value per distance using both methods in DMSO- (1, blue) and Aβ-treated neurons (2, red) cultured in 7 independent experiments ($n = 7$). $p < 0.05$ indicate a significant correlation. **(H)** Spearman correlation between non-assisted (wA; 1, DMSO-; 2, Aβ-treated cells) or assisted quantification (wB; 1, DMSO-; 2, Aβ-treated neurons) of translation sites (# puromycin foci) and protein production (mean puro intensity). Graphs represent each scored value per distance from 7 independent experiments ($n = 7$). $p < 0.05$ indicate a significant correlation. ****$p < 0.0001$; significant differences between slopes. **(I)** Box and whisker graphs representing the total puromycin foci in βIII tubulin- and puromycin-positive neurites within the range of 50 to 150 μm [Neurite (distal)] and in the soma (soma; 10–20 μm) following visual inspection of raw images (raw (manual); workflow A, wA) or assisted quantification in binarized images (converted (assisted); workflow B, wB). Data represent the average value of 5–10 sampled cells per condition shown as individual data points, and the mean and median of 7 independent experiments ($n = 7$). *$p < 0.05$; n.s, no significant; two-tailed *t*-test.

images enhances the effect of $A\beta_{1-42}$ oligomers on discrete puromycin puncta in distal neurites.

Image Processing Reveals an Increase in Translation Foci in Axons in Response to $A\beta_{1-42}$ Oligomers

The first evidence of Aβ oligomers regulating local translation in neurons was reported in axons (Baleriola et al., 2014). Thus, we next tried our assisted quantification method in neurites positive for the axonal protein Tau. Additionally, after treatment with DMSO or Aβ oligomers for 24 h, we fed the cells with puromycin for 5, 10, or 30 min. Shorter puromycin pulses were tested to decrease the chances of protein diffusion from the actual translation site. We additionally sought to test whether the rate of puromycin incorporation in axons, unlike in all βIII tubulin-positive neurites, allowed us to detect increased translation in response to Aβ oligomers with pulses as short as 5 min. 5- and 10-min puromycin treatments have been successfully used to detect localized translation in neurites in other experimental setups (Graber et al., 2013; Walker et al., 2018; Rangaraju et al., 2019).

We first analyzed the distribution pattern of puromycin intensity along Tau-positive neurites. The longest puromycin-, Tau-positive neurite was selected from randomly sampled cells imaged with identical settings. Neurites from raw images (exemplified as heatmaps in **Figure 4A**) were straighten and divided into 10 μm bins. Puromycin intensity was measured in 15 bins covering a distance of 150 μm from the edge of the soma (**Figure 4B**). No changes in newly synthesized proteins were observed between control and Aβ-treated cells when neurons were exposed to puromycin for 5 or 10 min. However, a significantly distinct pattern in protein production induced by Aβ oligomers was detected in Tau-positive neurites following a 30-min treatment with puromycin (**Figure 4B**). Focusing on distal sites of the neurite (beyond 30 μm from the soma in these sets of experiments) we observed a significant accumulation of newly synthesized proteins after 30 min of puromycin treatment compared to shorter exposures in both DMSO- and Aβ-treated cells. A significant increase in puromycin intensity in Aβ-treated neurites compared to controls was also detected with the longest puromycin exposure (**Figure 4C**). These results, similar to the ones obtained in βIII tubulin-positive neurites, confirm that $A\beta_{1-42}$ oligomers induce *de novo* synthesis of axonal proteins as previously reported (Baleriola et al., 2014; Walker et al., 2018). We then quantified the number of discrete puromycin foci in binarized images. Images were convolved with the default normalized kernel in FIJI/ImageJ and processed like βIII tubulin neurites as described before (**Figure 4D**). Translation foci were scored with the particle analyzer in 15 bins covering a distance of 150 μm from the edge of the cell body. Again, a distinct pattern of translation was observed between DMSO- and Aβ-treated neurites only when cells were fed with puromycin for 30 min (**Figure 4E**). Similarly, despite detecting a significant accumulation of discrete puromycin foci in both control and Aβ-treated cells after 30 min of puromycin exposure compared to shorter pulses, these were significantly higher when Aβ oligomers were added to the cultures (**Figure 4F**).

To determine if our assisted scoring method correlated better than manual quantification with the unbiased measurements of fluorescence intensity also in Tau-positive neurites, two independent observers quantified the number of puromycin-positive puncta along neurites by visual inspection of raw images (**Figures 4G–J**). Both observers reported a significantly distinct distribution of discrete foci in DMSO- and Aβ-treated samples when scores were performed in 10 μm bins (**Figures 4G,I**). However, when focusing on distal sites of the neurites (> 30 μm from the soma) disregarding the bin position, none of them detected changes between controls and Aβ treatments (**Figures 4H,J**), in line with previous results (**Figure 3I**). Data retrieved from observer 1 revealed a low yet significant correlation between scores obtained in binarized images and those obtained in raw images in both control and Aβ-treated neurons, whereas the correlation between both scoring methods was only significant upon Aβ treatment based on results from observer 2 (**Figure 4K**). We then compared data obtained from binarized images and the averaged data retrieved from observers 1 and 2 with the intensity values. We found no significant correlation between the fluorescent intensity at each

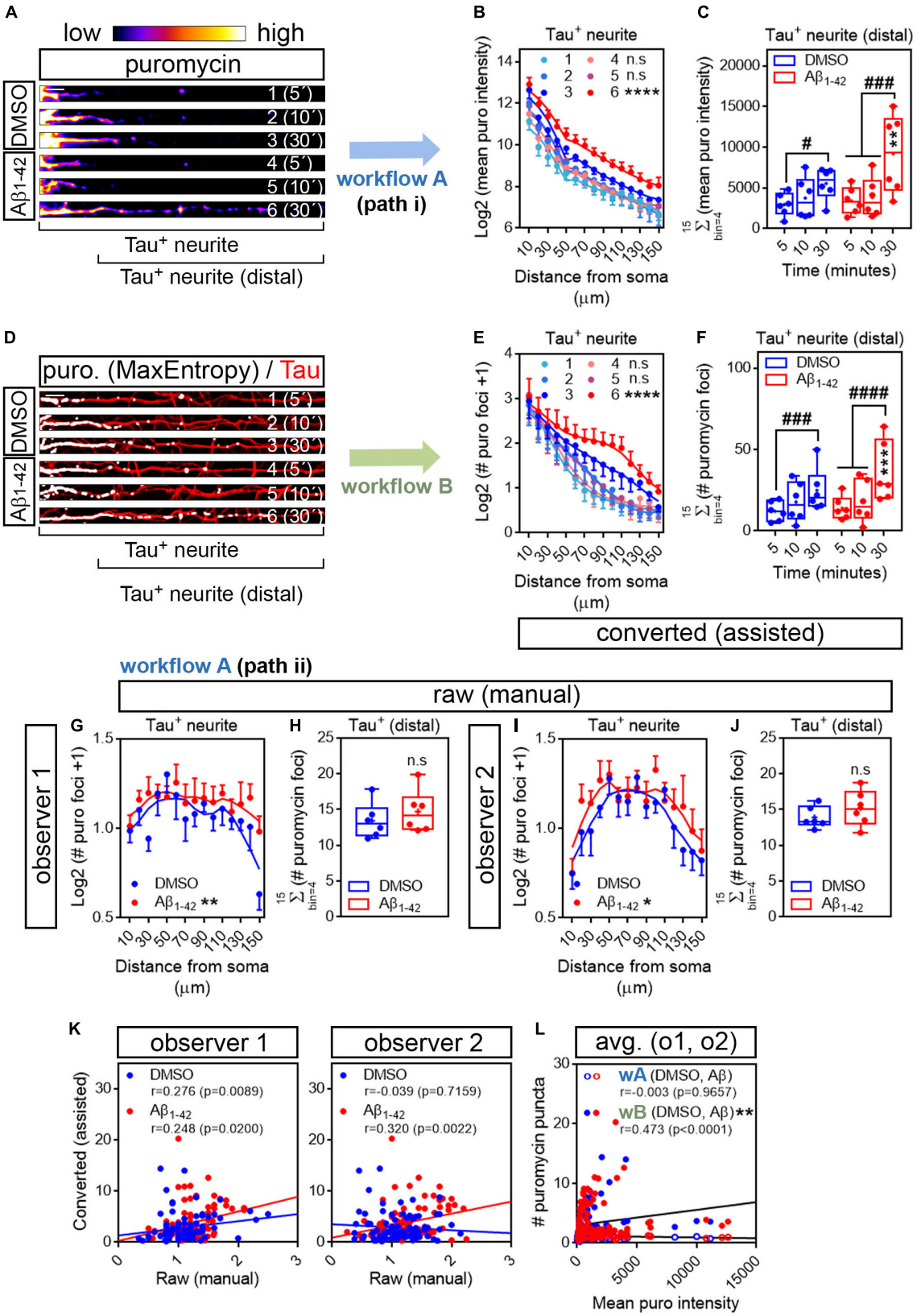

FIGURE 4 | Continued

FIGURE 4 | $A\beta_{1-42}$ oligomers increase translation sites in Tau-positive neurites. **(A)** Rat hippocampal neurons were grown for 9 DIV and treated with DMSO or with $A\beta_{1-42}$ oligomers for 24 h. Cells were fed with puromycin for 5, 10 or 30 mins, fixed and immunostained with an anti-puromycin antibody to measure protein synthesis (heatmaps) and counterstained with an anti-Tau antibody (not shown). The longest Tau-and puromycin-positive neurite was selected with a segmented line and straighten. 1, 2, and 3, DMSO-treated cells exposed to puromycin for 5, 10, and 30 mins, respectively; 4, 5 and 6, Aβ-treated cells exposed to puromycin for 5, 10, and 30 mins, respectively. Scale bar, 10 μm. **(B)** Puromycin intensity was measured in DMSO- and Aβ-treated neurons in 15 bins covering a distance of 150 μm from the edge of the soma (Tau^+ neurite) following workflow Ai in raw images. The graph shows the average intensity of puromycin per condition represented as Log2 (mean puro intensity) vs. distance ± SEM measured in 6 independent experiments ($n = 6$). 1, 2, and 3, DMSO-treated cells exposed to puromycin for 5, 10, and 30 mins respectively; 4, 5, and 6, Aβ-treated cells exposed to puromycin for 5, 10, and 30 mins, respectively. $^{****}p < 0.0001$, DMSO vs. Aβ, 30 mins puromycin; two-way ANOVA followed by Tukey's multiple comparison test. **(C)** Box and whisker graphs representing the total fluorescent intensity of the puromycin staining in Tau-positive neurites within the range of 30 to 150 μm [Tau^+ neurite (distal) as exemplified in **(A)**]. Data represent the average value of 10–20 sampled cells per condition shown as individual data points, and the mean and median of 6 independent experiments ($n = 6$). $^{\#}p < 0.05$ 5 vs. 30 mins puromycin in DMSO-treated cells; $^{\#\#\#}p < 0.001$ 5 vs. 30 mins and 10 vs. 30 mins in Aβ-treated neurons; $^{**}p < 0.01$ DMSO vs. Aβ, 30 mins puromycin; two-way ANOVA followed by Tukey's multiple comparison test. **(D)** The longest puromycin- and Tau-positive neurite was selected with a segmented line and straighten, smoothen and binarized with the MaxEntropy mask (MaxEntropy). Counterstain with the anti-Tau antibody is shown (red). 1, 2, and 3, DMSO-treated cells exposed to puromycin for 5, 10, and 30 mins, respectively; 4, 5 and 6, Aβ-treated cells exposed to puromycin for 5, 10, and 30 mins, respectively. Scale bar, 10 μm. **(E)** Puromycin-positive discrete foci were scored with the particle analyzer in 15 bins covering a distance of 150 μm from the edge of the soma (Tau^+ neurite) as explained in workflow B. The graph shows the average translation events per condition represented as Log2 (# puromycin foci + 1) vs. distance ± SEM measured in 6 independent experiments ($n = 6$). 1, 2, and 3, DMSO-treated cells exposed to puromycin for 5, 10, and 30 mins, respectively; 4, 5 and 6, Aβ-treated cells exposed to puromycin for 5, 10, and 30 mins, respectively. $^{****}p < 0.0001$ DMSO vs. Aβ, 30 mins puromycin; two-way ANOVA followed by Tukey's multiple comparison test. **(F)** Box and whisker graphs representing the total number of translation events scored in Tau-positive neurites within the range of 30 to 150 μm (Tau^+ neurite (distal) as exemplified in **(D)**). Data represent the average value of 10–20 sampled cells per condition shown as individual data points, and the mean and median of 6 independent experiments ($n = 6$). $^{\#\#\#}p < 0.001$ 5 vs. 30 mins puromycin in DMSO-treated cells; $^{\#\#\#\#}p < 0.0001$ 5 vs. 30 mins and 10 vs. 30 mins in Aβ-treated neurons; $^{***}p < 0.001$ DMSO vs. Aβ, 30 mins puromycin; two-way ANOVA followed by Tukey's multiple comparison test. **(G)** Discrete puromycin puncta scored by observer 1 in DMSO- and Aβ-treated neurons in 15 bins covering a distance of 150 μm from the edge of the soma (Tau^+ neurite) and in **(H)** distal sites of Tau-positive neurites disregarding the bin position [Tau^+ (distal)]. **(I)** Discrete puromycin puncta scored by observer 2 in DMSO- and Aβ-treated neurons in 15 bins covering a distance of 150 μm from the edge of the soma (Tau^+ neurite) and in **(J)** distal sites of Tau-positive neurites disregarding the bin position [Tau^+ (distal)]. All measurements were performed by visual inspection in raw images according to workflow Aii. Graphs in **(G)** and **(I)** show the average number of translation events per condition represented as Log2 (# puro foci + 1) vs. distance ± SEM measured following a 30-min puromycin pulse in 6 independent experiments ($n = 6$). $^{*}p < 0.05$; $^{**}p < 0.01$; two-way ANOVA followed by Tukey's multiple comparison test. Box and whisker graphs in **(H,J)** show the total number of translation events scored in Tau-positive neurites within the range of 30 to 150 μm [Tau^+ (distal)]. Data represent the average value of 10–20 sampled cells per condition shown as individual data points, and the mean and median of 6 independent experiments ($n = 6$). n.s, no significant; two-tailed *t*-tests. **(K)** Spearman correlation between quantifications in raw (manual) and in binarized (assisted) images. Graphs show values scored in raw (manual) images by observer 1 and observer 2 in DMSO- (blue) and Aβ-treated neurons (red) cultured in 6 independent experiments ($n = 6$). $p < 0.05$ indicate a significant correlation. **(L)** Spearman correlation between non-assisted [wA (DMSO, Aβ)] or assisted quantification [wB (DMSO, Aβ)] of translation sites (# puromycin foci) and protein production (mean puro intensity). Graphs represent the non-assisted counts per distance as the average score obtained by observers 1 and 2. Data correspond to 6 independent experiments ($n = 6$). $p < 0.05$ indicate a significant correlation. $^{**}p < 0.01$; significant differences between slopes.

neuritic position and the number puromycin foci scored by visual inspection (wA, **Figure 4L**). Conversely, a significant moderate positive correlation was observed between parameters when translation sites were counted in binarized images with the particle analyzer (wB, **Figure 4L**). Furthermore, when fitting the translation sites at each distance to a regression line, a significant increase in the slope was observed when data were obtained from binarized images, suggesting increased similarities between the number of puromycin foci and the puromycin intensity when using the assisted quantification method (**Figure 4L**). These results not only confirm that scoring puromycin-positive sites in neurites in binarized images by assisted means show a better fit with the unbiased measurement of raw puromycin intensity, but also reveal an effect of Aβ oligomers on discrete translation sites in neurites that was previously unreported.

Object-Based Colocalization Analyses Confirm That Peripheral Translation Sites in Axons Arise From Localized RNAs

As mentioned previously, discrete puromycin-positive puncta in distal neurites likely reflect sites of local translation. Nevertheless, we sought to determine if in our system what we had reported as neuritic translation sites did in fact colocalize with neuritic RNAs. Samples processed for puromycin detection in Tau-positive neurites were incubated for 20 min with 500 nM SYTO RNASelect, a fluorescent dye that selectively binds RNA (Savas et al., 2010). To verify that SYTO could be successfully used in our system to label neuritic RNA we compared the fluorescent intensity of the dye within Tau-positive neurites to background fluorescent levels in cells that had not been incubated with SYTO. Additionally, some fixed cells were digested with 50 μg/ml DNAse or RNAse prior to labeling. Neurites from SYTO-positive cells showed significantly higher levels of fluorescence than those not incubated with the dye (Compare dashed line with -SYTO in graph and neurites 1 and 2 in **Figure 5A**). More importantly, levels of SYTO were similar in positive neurites incubated in the presence or absence of DNAse (Compare dashed line with + SYTO + DNAse in graph and neurites 2 and 3 in **Figure 5A**), whereas incubation with RNAse moderately yet significantly reduced the fluorescence intensity (Compare dashed line with + SYTO + RNAse in graph and neurites 2 and 4 in **Figure 5A**). These results indicate that indeed neuritic RNAs can be labeled with SYTO RNASelect dye.

We then analyzed the distribution of RNA granules, measured as SYTO-stained foci, along Tau-positive neurites. For this purpose, raw images stained for SYTO were processed following the exact same protocol as for puromycin labeling (**Figure 1**;

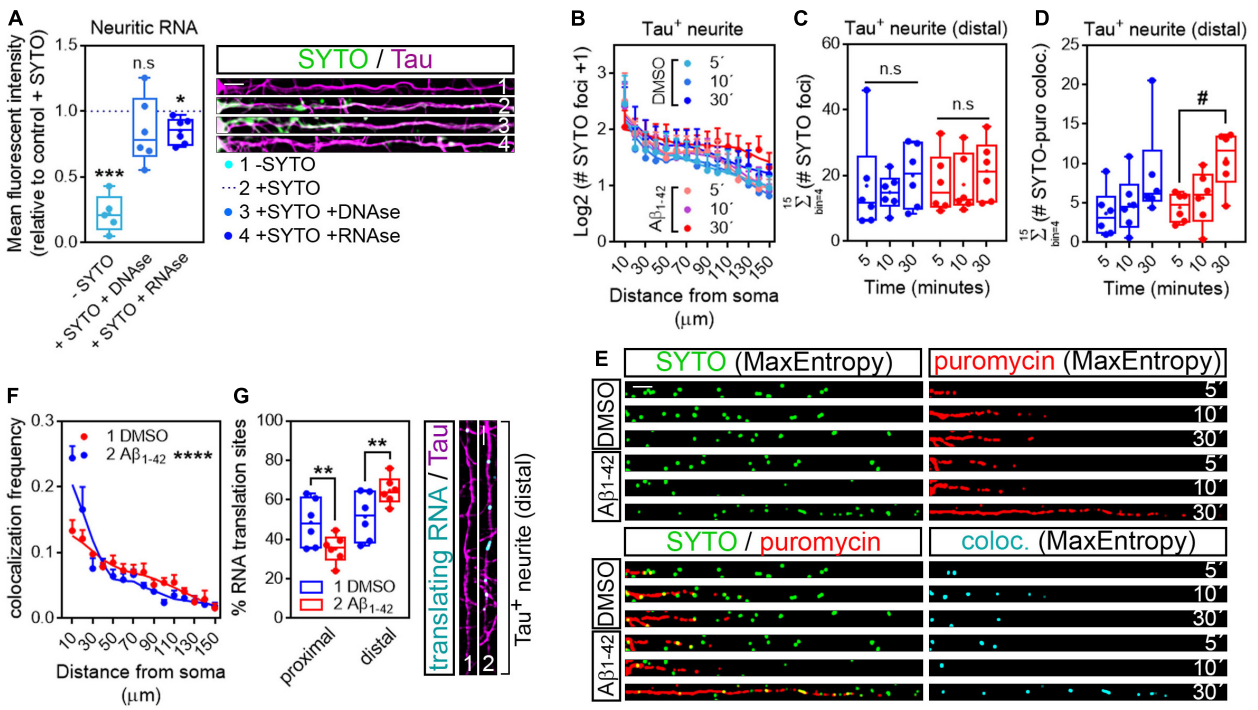

FIGURE 5 | Puromycin-positive foci in axons are a result of local protein synthesis. **(A)** Cells grown for 9 DIV and treated with DMSO for 24 h. Cells immunostained with an anti-Tau antibody (magenta) were incubated with SYTO RNASelect green fluorescent dye to label endogenous RNA (green). Total green fluorescence intensity was measured in neurites covering a distance of 150 μm from the edge of the soma (2, + SYTO). As negative control, green fluorescence was measured in cells that had not been incubated with SYTO (1, -SYTO). To determine if SYTO selectively labeled RNA, some fixed cells were digested with DNAse (3, + SYTO + DNAse) or with RNAse (4, + SYTO + RNAse). Box and whisker graphs represent the average relative fluorescence intensity of 10 neurites per condition, shown as individual data points, and the mean and median of 5 (n = 5, -SYTO negative samples compared to their corresponding + SYTO controls) or 6 (n = 6, + SYTO + DNAse and + SYTO + RNAse compared to their corresponding + SYTO controls) independent experiments. ***$p < 0.001$; *$p < 0.05$; n.s, not significant; two-tailed t-tests. Scale bar, 10 μm. **(B)** SYTO-positive staining (as represented in green in **(E)**) from randomly selected cells was filtered with the convolver, brightness and contrast were adjusted. Images were converted to 8-bit and binarized with the MaxEntropy mask. The longest Tau-positive neurite was selected with a segmented line and straighten, smoothen and binarized with the MaxEntropy mask (MaxEntropy). SYTO-positive discrete puncta were scored with the particle analyzer in 15 bins covering a distance of 150 μm from the edge of the soma. The graph shows the average number on puncta represented as Log2 (SYTO foci + 1) vs. distance ± SEM measured in 6 independent experiments (n = 6). No statistical differences were detected between DMSO- and Aβ-treated cells incubated with puromycin for 5, 10, or 30 mins. **(C)** Box and whisker graphs show the total number of RNA granules in distal sites of Tau-positive neurites [Σ (# SYTO foci)] from DMSO- and Aβ-treated cells incubated with puromycin for 5, 10, or 30 mins. Data represent the average value of 10 sampled cells per condition plotted as individual data points, and the mean and median of 6 independent experiments (n = 6). n.s, no significant; two-way ANOVA followed by Tukey's multiple comparison test. **(D)** Parallel to processing SYTO-labeled images, puromycin staining was filtered with the convolver, brightness and contrast were adjusted. Images were converted to 8-bit and binarized with the MaxEntropy mask. Same Tau-positive neurites selected for SYTO quantification (green channel) were selected in the red channel (puromycin staining in **(E)**), straighten, smoothen and binarized with the MaxEntropy mask. Co-localized objects were obtained with the AND function in the image calculator (cyan in **(E)**) and scored in distal sites of Tau-positive neurites with the particle analyzer. Box and whisker graphs show the total RNA-protein colocalized puncta in DMSO- and Aβ-treated cells incubated with puromycin for 5, 10, or 30 mins [Σ (# SYTO-puro coloc.)]. Data represent the average value of 10 sampled neurites per condition plotted as individual data points, and the mean and median of 6 independent experiments (n = 6). #$p < 0.05$ 5 vs. 30 min puromycin in Aβ-treated cells; two-way ANOVA followed by Tukey's multiple comparison test. **(E)** Micrographs from straighten, binarized neurites stained with SYTO RNASelect green fluorescent dye to label RNA (green), with an anti-puromycin antibody to label protein (red) and the resulting images when merging both channels (green, red, and yellow) and when combining both with the AND function in the image calculator (cyan). Cells treated with puromycin for 5, 10, or 30 mins are shown. Scale bar, 10 μm. **(F)** The graph represents the frequency distribution of SYTO- and puromycin-positive objects (colocalization frequency) in DMSO- and Aβ-treated neurites following 30-min puromycin exposure. Colocalized objects were measured with the particle analyzer in 15 bins covering a distance of 150 μm from the edge of the cell body. ****$p < 0.0001$ (interaction); two-way ANOVA. **(G)** Box and whisker graph representing the proportion of colocalized objects (% RNA translation sites) in proximal (0–30 μm) and distal (last 120 μm) sites of Tau-positive neurites. Data represent the average value of 10 sampled cells per condition shown as individual data points, and the mean and median of 6 independent experiments (n = 6). **$p < 0.01$; two-tailed t-test. Micrographs show colocalized objects (translating RNAs, cyan) detected within the last 120 μm (distal) of Tau positive neurites (magenta). Scale bar, 10 μm.

workflow B): images were convolved with the default normalized kernel in FIJI/ImageJ, minimum and maximum intensity values were adjusted, 16-bit images were converted to 8-bit and binarized using the MaxEntropy mask. Neurites were then selected with a segmented line, straighten, smoothen and binarized again with the MaxEntropy function (green, **Figure 5E**). The number of RNA granules was scored in 15 bins covering a distance of 150 μm from the edge of the soma and no significant differences were observed between experimental conditions, regardless of whether neurons were fed

with puromycin for 5, 10, or 30 min (**Figure 5B**). Similarly, no significant changes were detected in distal sites (> 30 μm from the soma in these sets of experiments) between DMSO- and Aβ-treated neurites (**Figure 5C**). Thus, Aβ treatment does not affect RNA recruitment to neurites. In these experiments, green and red channels corresponding to RNA (SYTO, **Figure 5E**) and protein (puromycin, **Figure 5E**) were binarized in parallel and colocalization between objects in both channels was calculated using the AND function in the FIJI/ImageJ image calculator. The resulting puncta (cyan, **Figure 5E**) were scored in 10 μm bins covering a distance of 150 μm from the edge of the cell body. No significant differences between DMSO- and Aβ-treated cells were observed in the distribution of colocalized puncta along neurites (data not shown). Given the high variability, especially in control cells, we did not detect differences between DMSO and Aβ treatments when focusing on distal sites of Tau-positive neurites either. However, we did observe an accumulation of co-localized foci in Aβ-treated cells that was not detected in controls when neurons were exposed to puromycin for 30 min compared to the 5-min treatment (**Figure 5D**). We therefore focused on the 30-min puromycin treatment and analyzed the frequency distribution of translating RNAs, measured as the proportion of colocalized puncta. Interestingly, from all translating RNAs detected, half of them were found within the first 30 μm proximal to the soma in control cells, whereas this proportion was significantly reduced in Aβ-treated cells and consequently the percentage of peripheral translating RNAs increased (**Figures 5F,G**). Altogether these results show that Aβ oligomers increase the sites of localized translation in distal Tau-positive neurites in line with previously published reports (Baleriola et al., 2014; Li and Gotz, 2017; Walker et al., 2018). Thus, the combination of RNA and protein staining techniques followed by image processing and binarization, and object-based colocalization can be successfully used to detect sites of local RNA translation in neurons which might be important to unravel the extent of local changes in early stages of AD and other neurological diseases.

DISCUSSION

Highly polarized cells like neurons heavily rely on the asymmetric distribution of their proteome for their functionality. It was classically thought that proteins that support dendritic and axonal functions are synthesized in the soma and then transported to their target destination at peripheral sites of the neuron. This soma-centric view of protein synthesis has slowly changed over the last two decades and it is now accepted that neurites contain mRNAs and components of the translation machinery and are thus able to produce proteins locally. Local protein synthesis enables neurites (both dendrites and axons) to change their proteome in an acute manner in order to adapt to fast environmental changes. Since the first studies that unambiguously demonstrated the existence of local translation in neurons (Koenig, 1967; Giuditta et al., 1968; Steward and Levy, 1982; Torre and Steward, 1992; Feig and Lipton, 1993) most work in the field has focused on understanding the role of locally produced proteins in brain physiology. For example, a subset of mRNAs translated in dendrites, which include CamK2a, Calmodulin or Bassoon, is involved in synaptic plasticity (reviewed in Holt et al., 2019). Intra-axonal synthesis of β-actin (Leung et al., 2006), RhoA (Wu et al., 2005), or Par3 (Hengst et al., 2009) is important in growth cone behavior and axon elongation during nervous system development. Proteins involved in mitochondrial function such as LaminB2 (Yoon et al., 2012) or COXIV (Aschrafi et al., 2010) are locally synthesized in axons and contribute to their maintenance in post-developmental stages. However much less is known on the role of local protein synthesis in nervous system pathologies, especially those of the CNS.

Alzheimer's disease (AD), like other neurodegenerative diseases, is characterized by synaptic dysfunction during early stages (Palop and Mucke, 2010). Understanding dynamic early changes in the local proteome (axonal, dendritic or synaptic) is in our view crucial to understand basic pathological mechanisms underlying AD and likely other neurological diseases. Recent work has shown that regulation of intra-axonal protein synthesis induced by $A\beta_{1-42}$ oligomers, whose accumulation is central to AD, contributes to neurodegeneration (Baleriola et al., 2014). These findings support a model in which retrograde transport of locally produced proteins leads to pathological, transcriptional changes in the neuronal soma. More recently, a link between intra-dendritic translation, and Tau mislocalization and hyperphosphorylation has been found (Kobayashi et al., 2017; Li and Gotz, 2017). Thus, dysregulation of the local translatome in neurons might play a more relevant role in AD than previously acknowledged. It is therefore important to know the extent and location of newly synthesized proteins in order to understand early changes in the AD brain.

Despite local translation is finally being accepted by the scientific community, the accurate measurement of this phenomenon is still challenging partly due to the limited amount of proteins that are locally produced, especially in adult axons (Rangaraju et al., 2017). There are other experimental challenges that will be not be discussed herein since the technicalities are beyond the scope of this manuscript. Our own results show that new-synthesized neuritic proteins measured at distal positions (100–150 μm from the cell nucleus) can be ∼20 to 30 times less abundant than those measured in the soma in a 30-min time frame (**Figure 2**). Thus, local translation events can be easily overlooked when visualizing *in situ* protein production under the microscope. FUNCAT (Dieterich et al., 2010), and SUnSET (Schmidt et al., 2009) are commonly used techniques in the field of local translation. Both are based on the labeling of newly synthesized proteins, with non-canonical amino acids in the case of FUNCAT or a tRNA analog in the case of SUnSET. In both cases the non-canonical molecules can be fluorescently tagged. Yet when these methods have proven very helpful to analyze the amount of newly synthesized dendritic (Dieterich et al., 2010) and axonal (Wong et al., 2017; Walker et al., 2018) proteins measured as fluorescent intensity in labeled cells, discrete foci of newly produced proteins can come unnoticed unless enhanced.

Some variations of the aforementioned techniques such as Puro-PLA or FUNCAT-PLA have been used to accurately

measure discrete translation sites of specific proteins along neurites (Tom Dieck et al., 2015). Both proximity ligation assays (PLA) are based on the spatial coincidence of two antibodies, one that recognizes the recently synthesized polypeptide chain (anti-puromycin in the case of Puro-PLA; anti-biotin for FUNCAT-PLA) and another one that recognizes a specific protein of interest. However, neither PLA approach is useful to analyze all translation foci. Other modifications of SUnSET have been recently used to evaluate overall discrete intra-neuritic and intra-dendritic translation events. For example, co-incubation of neurons with both puromycin and the translation inhibitor emetine prior to fixation prevents the puromycylated polypeptide chain release from the ribosomes. This approach is known as ribopuromycilation (RPM) and it allows the visualization of active polyribosomes in the neuronal soma and along neurites (Graber et al., 2013). Additionally, in puromycin-labeled fixed cells, proximity ligation assay (Puro-PLA) employing a single antibody against puromycin has been used to accurately identify discrete local translation sites in dendrites (Rangaraju et al., 2019). Here we describe a strategy to enhance puromycin hotspots in neurites following SUnSET, based solely on image processing and the assisted quantification of the resulting objects. Our technique does not require the incubation of the cells with any translation inhibitor besides puromycin, and it avoids the processing of the samples for proximity ligation assay, which can be pricy and time consuming.

We first performed edge detection to find discontinuities in our puromycin labeling that could result from a punctate staining arising from discrete positive foci. Instead of using the Find Edges command in FIJI/ImageJ which applies a Sobel edge detector, we used the default 5×5 kernel in the convolver which is a Laplacian edge detector instead. Laplacian operators are very accurate in finding edges in an image but also very sensitive to background noise (Bannister and Larkman, 1995a). We therefore adjusted the minimum and maximum intensities of our micrographs after applying the filter in order to eliminate highlighted pixels outside the area established by the neuronal/axonal markers βIII tubulin and Tau (**Figure 1**; workflow B). We additionally compared the processing workflow between puromycin-positive and puromycin-negative cells and determined that despite possible noise enhancement, positive puncta could be significantly detected over background (**Figure 3F**, right graph). Image processing with the Laplacian operator highlighted events in the periphery of neurons that could be selected and binarized with the MaxEntropy mask (**Figures 1B**, **3C**, **4D**, **5E** and **Supplementary Figure S1B**). Binarization in unprocessed images failed to detect discrete puncta in neurites to the same extent as when images were processed (**Supplementary Figure S1**).

To determine if our processing method worked in highlighting local events, we evaluated the effect of $A\beta_{1-42}$ oligomers on hippocampal neurites. Aβ oligomers are known to increase puromycin intensity when applied locally to axons, which reflects changes in local protein synthesis (Walker et al., 2018). In our case, we observed similar results in neurites following bath application of hippocampal neurons with Aβ (**Figure 2**): the effect elicited by Aβ was visible beyond the canonical ER domain and did not affect the cell body (**Figures 2C,G–J**). These results are compatible with changes in local translation but they do not address whether actual local sites of protein synthesis are affected by Aβ oligomers. Discrete puncta in distal neuritic sites likely reflect foci of localized translation (Graber et al., 2013; Rangaraju et al., 2019). We quantified discrete puromycin-positive foci in distal neuritic sites in response to $A\beta_{1-42}$ with the particle analyzer after image processing with the convolver (assisted quantification). We observed (1) an enhancement of discrete puromycin staining in both DMSO- and Aβ-treated neurites compared to visual inspection of raw puromycin staining (**Figures 3B,C**), (2) an enhancement of the effect of Aβ on newly synthesized neuritic proteins compared to controls (**Figures 3B,C,I**), and (3) a better correlation between the unbiased measurement of puromycin intensity and the number of discrete puromycin-positive sites in processed images (**Figure 3H**). Altogether these results indicate that binarizing images from puromycin-positive cells after applying a Laplacian edge detector allows the assisted quantification of neuritic translation sites yielding results that resemble those obtained from an unbiased measurement of raw puromycin intensity (**Figure 3H**). Additionally, our results unravel a previously unreported effect of Aβ oligomers on discrete translation events in neurites (**Figures 3E,I**).

Our first approach was performed in βIII tubulin-positive neurites which correspond to both dendrites and axons. We sought to increase the changes of detecting discrete translation sites since dendrites have been historically reported to have a higher translation capacity than axons (Rangaraju et al., 2017) but because changes in local neuronal translation upon Aβ treatment were first described in axons (Baleriola et al., 2014), we applied the same processing workflow to neurites stained with the axonal marker Tau. Results were very similar to those obtained for βIII tubulin-positive neurites when cells were fed with puromycin for 30 min (**Figure 4**). Shorter exposures to puromycin were also performed in order to minimize the possible detection of newly synthesized proteins diffused from the soma. Puromycin pulses as short as 10–15 min have been successfully used to detect changes in intra-axonal protein synthesis upon acute exposure of axons to Aβ oligomers (Walker et al., 2018). However, we did not observe changes between DMSO- and Aβ-treated cells possibly due to the slow pace of the translation machinery after a 24-h treatment.

In light of our results we addressed whether distal puromycin-positive events in neurites arose from localized RNAs to determine if we were actually measuring local protein synthesis. We applied the processing protocol followed for puromycin staining to SYTO-positive neurites. SYTO RNASelect green fluorescent dye selectively binds neuritic RNA (**Figure 5A**). We observed that Aβ oligomers did not change the distribution of RNA granules along neurites (**Figures 5B,E**) nor their amount in distal sites (**Figure 5C**). These results are compatible with other experiments performed in our laboratory aimed

at labeling neuritic RNAs with alternative techniques (data not shown). Taking advantage of the fact that SYTO-labeled cells were also labeled with puromycin, after binarizing the images corresponding to both stains we applied the AND function in the image calculator which essentially retrieves the colocalization between objects. In our system colocalized objects (cyan, **Figure 5E**) represent sites of actively translating RNAs. We particularly focused on colocalized objects resulting from 30-min puromycin pulses, which were higher than for shorter puromycin exposures (**Figure 5D**). Interestingly, $A\beta_{1-42}$ increased the proportion of RNA translation in distal sites of Tau-positive neurites, beyond the ER domain. Thus, the combination of RNA and protein staining techniques followed by image processing and binarization, and object-based colocalization can be successfully used to detect sites of local RNA translation in neurons.

Other edge detectors, Laplacian operators distinct to 5×5 matrices or other background subtraction methods can be used depending on the sample requirements and the researcher's criteria. However, the image processing approach described herein has proven very useful to detect discrete events with low pixel intensity, which is the expected characteristic of neuritic local translation sites.

Altogether, this study provides a simple method of quantifying local RNA translation foci using object-recognition and object-based colocalization analyses which allows a better understanding the effect of $A\beta_{1-42}$ in neurites.

DATA AVAILABILITY STATEMENT

The datasets generated for this study are available on request to the corresponding author.

ETHICS STATEMENT

The animal study was reviewed and approved by Ethics Committee for Animal Care and Use in Research (CEEA) of the University of the Basque Country (UPV/EHU).

AUTHOR CONTRIBUTIONS

JB conceived the project and designed the experiments. MG, MB-U, AB, JI, and JB performed experiments. MG, MB-U, and JB performed data analysis and wrote the manuscript.

FUNDING

JB was supported by two grants from the Spanish Ministry of Science, Innovation and Universities (RYC-2016-19837 start-up funds and SAF2016-76347-R) and start-up funds from the Basque Foundation for Science (IKERBASQUE). MG is a predoctoral fellow funded by the Basque Government. MB-U is a predoctoral fellow funded by the University of the Basque Country (UPV/EHU). AB received funding from the Portuguese Foundation for Science and Technology (FCT) in the context of the FCT funded University of Minho M.D./Ph.D. Program (SFRH/BD/52322/2013).

ACKNOWLEDGMENTS

We thank member of the Neurobiology Lab (Achucarro Basque Center for Neuroscience) for sharing the Aβ peptides with us.

SUPPLEMENTARY MATERIAL

The Supplementary Material for this article can be found online at: https://www.frontiersin.org/articles/10.3389/fnins.2020.00547/full#supplementary-material

FIGURE S1 | Workflows for image processing with or without applying the default convolution kernel (Laplacian filter). Images show the same cells used as examples for the workflow in **Figure 1**. **(B)** Represents the same step by step processing method described **Figure 1B**. **(B^{I})** Corresponds to the same workflow as in **Figure 1B** excluding **step 1** which corresponds to the application of the Laplacian filter to enhance the edges. Both workflows converge in graphs comparing both methods (green line, filter application; red line, no filter) in two experimental conditions (condition 1, blue; condition 2, red). Graphs represent Log2(#puromycin foci +1) vs. distance. Scale bars, 50 μm in whole-cell micrographs and 10 μm in straighten neurites.

REFERENCES

Aschrafi, A., Natera-Naranjo, O., Gioio, A. E., and Kaplan, B. B. (2010). Regulation of axonal trafficking of cytochrome c oxidase IV mRNA. *Mol. Cell Neurosci.* 43, 422–430. doi: 10.1016/j.mcn.2010.01.009

Baleriola, J., Walker, C. A., Jean, Y. Y., Crary, J. F., Troy, C. M., Nagy, P. L., et al. (2014). Axonally synthesized ATF4 transmits a neurodegenerative signal across brain regions. *Cell* 158, 1159–1172. doi: 10.1016/j.cell.2014.07.001

Banker, G., and Goslin, K. (1998). *Culturing Nerve Cells*, 2nd Edn. Cambridge: MIT Press.

Bannister, N. J., and Larkman, A. U. (1995a). Dendritic morphology of CA1 pyramidal neurones from the rat hippocampus: I. Branching patterns. *J. Comp. Neurol.* 360, 150–160. doi: 10.1002/cne.903600111

Bannister, N. J., and Larkman, A. U. (1995b). Dendritic morphology of CA1 pyramidal neurones from the rat hippocampus: II. Spine distributions. *J. Comp. Neurol.* 360, 161–171. doi: 10.1002/cne.903600112

Bolton, J. S. (1901). The nervous system and its constituent neurones, designed for the use of practitioners of medicine and of students of medicine and psychology. *Edinb. Med. J.* 10:4.

Dieterich, D. C., Hodas, J. J., Gouzer, G., Shadrin, I. Y., Ngo, J. T., Triller, A., et al. (2010). In situ visualization and dynamics of newly synthesized proteins in rat hippocampal neurons. *Nat. Neurosci.* 13, 897–905. doi: 10.1038/nn.2580

Feig, S., and Lipton, P. (1993). Pairing the cholinergic agonist carbachol with patterned Schaffer collateral stimulation initiates protein synthesis in hippocampal CA1 pyramidal cell dendrites via a muscarinic, NMDA-dependent mechanism. *J. Neurosci.* 13, 1010–1021. doi: 10.1523/JNEUROSCI.13-03-01010.1993

Giuditta, A., Dettbarn, W. D., and Brzin, M. (1968). Protein synthesis in the isolated giant axon of the squid. *Proc. Natl. Acad. Sci. U.S.A.* 59, 1284–1287. doi: 10.1073/pnas.59.4.1284

Graber, T. E., Hebert-Seropian, S., Khoutorsky, A., David, A., Yewdell, J. W., Lacaille, J. C., et al. (2013). Reactivation of stalled polyribosomes in synaptic

plasticity. *Proc. Natl. Acad. Sci. U.S.A.* 110, 16205–16210. doi: 10.1073/pnas.1307747110

Hafner, A. S., Donlin-Asp, P. G., Leitch, B., Herzog, E., and Schuman, E. M. (2019). Local protein synthesis is a ubiquitous feature of neuronal pre- and postsynaptic compartments. *Science* 364:6441. doi: 10.1126/science.aau3644

Hengst, U., Deglincerti, A., Kim, H. J., Jeon, N. L., and Jaffrey, S. R. (2009). Axonal elongation triggered by stimulus-induced local translation of a polarity complex protein. *Nat. Cell Biol.* 11, 1024–1030. doi: 10.1038/ncb1916

Holt, C. E., Martin, K. C., and Schuman, E. M. (2019). Local translation in neurons: visualization and function. *Nat. Struct. Mol. Biol.* 26, 557–566. doi: 10.1038/s41594-019-0263-5

Jung, H., Gkogkas, C. G., Sonenberg, N., and Holt, C. E. (2014). Remote control of gene function by local translation. *Cell* 157, 26–40. doi: 10.1016/j.cell.2014.03.005

Jung, H., Yoon, B. C., and Holt, C. E. (2012). Axonal mRNA localization and local protein synthesis in nervous system assembly, maintenance and repair. *Nat. Rev. Neurosci.* 13, 308–324. doi: 10.1038/nrn3210

Kobayashi, S., Tanaka, T., Soeda, Y., Almeida, O. F. X., and Takashima, A. (2017). Local somatodendritic translation and hyperphosphorylation of tau protein triggered by AMPA and NMDA receptor stimulation. *EBioMedicine* 20, 120–126. doi: 10.1016/j.ebiom.2017.05.012

Koenig, E. (1967). Synthetic mechanisms in the axon. IV. In vitro incorporation of [3H]precursors into axonal protein and RNA. *J. Neurochem.* 14, 437–446. doi: 10.1111/j.1471-4159.1967.tb09542.x

Leung, K. M., van Horck, F. P., Lin, A. C., Allison, R., Standart, N., and Holt, C. E. (2006). Asymmetrical beta-actin mRNA translation in growth cones mediates attractive turning to netrin-1. *Nat. Neurosci.* 9, 1247–1256. doi: 10.1038/nn1775

Li, C., and Gotz, J. (2017). Somatodendritic accumulation of Tau in Alzheimer's disease is promoted by Fyn-mediated local protein translation. *EMBO J.* 36, 3120–3138. doi: 10.15252/embj.201797724

Palop, J. J., and Mucke, L. (2010). Amyloid-beta-induced neuronal dysfunction in Alzheimer's disease: from synapses toward neural networks. *Nat. Neurosci.* 13, 812–818. doi: 10.1038/nn.2583

Quintela-Lopez, T., Ortiz-Sanz, C., Serrano-Regal, M. P., Gaminde-Blasco, A., Valero, J., Baleriola, J., et al. (2019). Abeta oligomers promote oligodendrocyte differentiation and maturation via integrin beta1 and Fyn kinase signaling. *Cell Death Dis.* 10:445. doi: 10.1038/s41419-019-1636-8

Rangaraju, V., Lauterbach, M., and Schuman, E. M. (2019). Spatially stable mitochondrial compartments fuel local translation during plasticity. *Cell* 7:e15. doi: 10.1016/j.cell.2018.12.013

Rangaraju, V., Tom Dieck, S., and Schuman, E. M. (2017). Local translation in neuronal compartments: how local is local? *EMBO Rep.* 18, 693–711. doi: 10.15252/embr.201744045

Rutkevich, L. A., and Williams, D. B. (2011). Participation of lectin chaperones and thiol oxidoreductases in protein folding within the endoplasmic reticulum. *Curr. Opin. Cell Biol.* 23, 157–166. doi: 10.1016/j.ceb.2010.10.011

Savas, J. N., Ma, B., Deinhardt, K., Culver, B. P., Restituito, S., Wu, L., et al. (2010). A role for huntington disease protein in dendritic RNA granules. *J. Biol. Chem.* 285, 13142–13153. doi: 10.1074/jbc.M110.114561

Schmidt, E. K., Clavarino, G., Ceppi, M., and Pierre, P. (2009). SUnSET, a nonradioactive method to monitor protein synthesis. *Nat. Methods* 6, 275–277. doi: 10.1038/nmeth.1314

Steward, O., and Levy, W. B. (1982). Preferential localization of polyribosomes under the base of dendritic spines in granule cells of the dentate gyrus. *J. Neurosci.* 2, 284–291. doi: 10.1523/JNEUROSCI.02-03-00284.1982

Terenzio, M., Koley, S., Samra, N., Rishal, I., Zhao, Q., Sahoo, P. K., et al. (2018). Locally translated mTOR controls axonal local translation in nerve injury. *Science* 359, 1416–1421. doi: 10.1126/science.aan1053

Tom Dieck, S., Kochen, L., Hanus, C., Heumuller, M., Bartnik, I., Nassim-Assir, B., et al. (2015). Direct visualization of newly synthesized target proteins in situ. *Nat. Methods* 12, 411–414. doi: 10.1038/nmeth.3319

Torre, E. R., and Steward, O. (1992). Demonstration of local protein synthesis within dendrites using a new cell culture system that permits the isolation of living axons and dendrites from their cell bodies. *J. Neurosci.* 12, 762–772. doi: 10.1523/JNEUROSCI.12-03-00762.1992

Walker, C. A., Randolph, L. K., Matute, C., Alberdi, E., Baleriola, J., and Hengst, U. (2018). Abeta1-42 triggers the generation of a retrograde signaling complex from sentinel mRNAs in axons. *EMBO Rep.* 19:e45435. doi: 10.15252/embr.201745435

Wong, H. H., Lin, J. Q., Strohl, F., Roque, C. G., Cioni, J. M., Cagnetta, R., et al. (2017). RNA docking and local translation regulate site-specific axon remodeling in vivo. *Neuron* 85:e858. doi: 10.1016/j.neuron.2017.07.016

Wu, K. Y., Hengst, U., Cox, L. J., Macosko, E. Z., Jeromin, A., Urquhart, E. R., et al. (2005). Local translation of RhoA regulates growth cone collapse. *Nature* 436, 1020–1024. doi: 10.1038/nature03885

Yarmolinsky, M. B., and Haba, G. L. (1959). Inhibition by puromycin of amino acid incorporation into protein. *Proc. Natl. Acad. Sci. U.S.A.* 45, 1721–1729. doi: 10.1073/pnas.45.12.1721

Yoon, B. C., Jung, H., Dwivedy, A., O'Hare, C. M., Zivraj, K. H., and Holt, C. E. (2012). Local translation of extranuclear lamin B promotes axon maintenance. *Cell* 148, 752–764. doi: 10.1016/j.cell.2011.11.064

Conflict of Interest: The authors declare that the research was conducted in the absence of any commercial or financial relationships that could be construed as a potential conflict of interest.

frontiers in Integrative Neuroscience

REVIEW
published: 29 June 2021
doi: 10.3389/fnint.2021.689208

Local Translation in Nervous System Pathologies

María Gamarra[1,2†], Aida de la Cruz[1,2†], Maite Blanco-Urrejola[1,2,3] and Jimena Baleriola[1,3,4]*

[1] Laboratory of Local Translation in Neurons and Glia, Achucarro Basque Center for Neuroscience, Leioa, Spain, [2] Departamento de Neurociencias, Universidad del País Vasco (UPV/EHU), Leioa, Spain, [3] Departamento de Biología Celular e Histología, Universidad del País Vasco (UPV/EHU), Leioa, Spain, [4] Ikerbasque, Basque Foundation for Science, Bilbao, Spain

Dendrites and axons can extend dozens to hundreds of centimeters away from the cell body so that a single neuron can sense and respond to thousands of stimuli. Thus, for an accurate function of dendrites and axons the neuronal proteome needs to be asymmetrically distributed within neurons. Protein asymmetry can be achieved by the transport of the protein itself or the transport of the mRNA that is then translated at target sites in neuronal processes. The latter transport mechanism implies local translation of localized mRNAs. The role of local translation in nervous system (NS) development and maintenance is well established, but recently there is growing evidence that this mechanism and its deregulation are also relevant in NS pathologies, including neurodegenerative diseases. For instance, upon pathological signals disease-related proteins can be locally synthesized in dendrites and axons. Locally synthesized proteins can exert their effects at or close to the site of translation, or they can be delivered to distal compartments like the nucleus and induce transcriptional responses that lead to neurodegeneration, nerve regeneration and other cell-wide responses. Relevant key players in the process of local protein synthesis are RNA binding proteins (RBPs), responsible for mRNA transport to neurites. Several neurological and neurodegenerative disorders, including amyotrophic lateral sclerosis or spinal motor atrophy, are characterized by mutations in genes encoding for RBPs and consequently mRNA localization and local translation are impaired. In other diseases changes in the local mRNA repertoire and altered local protein synthesis have been reported. In this review, we will discuss how deregulation of localized translation at different levels can contribute to the development and progression of nervous system pathologies.

Keywords: local translation, RNA localization, RNA binding proteins, mRNA transport, nervous system pathologies

OPEN ACCESS

Edited by:
Paul Donlin-Asp, Max Planck Institute for Brain Research, Germany

Reviewed by:
Angel Nunez, Autonomous University of Madrid, Spain
Adrian Rodriguez-Contreras, The City College of New York (CUNY), United States

***Correspondence:**
Jimena Baleriola
jimena.baleriola@achucarro.org

† These authors have contributed equally to this work and share first authorship

Received: *31 March 2021*
Accepted: *03 June 2021*
Published: *29 June 2021*

Citation:
Gamarra M, de la Cruz A, Blanco-Urrejola M and Baleriola J (2021) Local Translation in Nervous System Pathologies. Front. Integr. Neurosci. 15:689208. doi: 10.3389/fnint.2021.689208

INTRODUCTION

Neurons are morphologically the most complex cells in the nervous system (NS). They consist of a soma, from which several processes emerge. The characteristic asymmetric morphology of neurons allows them to create stable neural circuits. Through their dendrites and axons, neuronal processes are capable of receiving and integrating incoming signals from presynaptic terminals and

transmitting them through signaling pathways to give response to diverse stimuli. The structural and functional asymmetry of neurons requires the asymmetrical distribution of the neuronal proteome, which is achieved by the transport of mature proteins or the transport of transcripts to target compartments in neuronal processes. In this article, we focus on the latter mechanism by which localized messenger RNAs (mRNAs) are transformed into proteins through a process known as local translation or local protein synthesis (Rangaraju et al., 2017; Holt et al., 2019) (**Figure 1A**).

LOCAL TRANSLATION FOR NEURONAL HOMEOSTASIS

Protein synthesis is an essential mechanism to ensure proper cell homeostasis. Thereby, RNA translation and protein transport to subneuronal domains have been the focus of particular concern for many researchers. Although for years it was thought that protein synthesis takes place only in the soma, it is now accepted that the transport of proteins from the soma to target subcellular regions is not the only way to supply proteins to distal neuronal processes (Alberts et al., 2002). mRNAs can also be transported to subcellular domains for their subsequent translation into proteins. This phenomenon is known as local protein synthesis (Holt et al., 2019). Taking into consideration that in some vertebrates dendrites can extend up to a dozen millimeters from the soma and that axons can measure more than one meter (Bannister and Larkman, 1995) it is not surprising that local protein synthesis serves as a means for neuronal processes to rapidly react to diverse environmental stimuli. This translation mechanism was first described in 1960 when local synthesis of acetylcholinesterase in axons was detected using isotopically labeled amino acids (Koenig and Koelle, 1960). Subsequently, some other studies were carried out in different species: local protein synthesis was also observed in isolated axons of the giant squid (Giuditta et al., 1968) and nerve fibers in goldfish (Edstrom and Sjostrand, 1969). Ever since, local protein synthesis has been studied in cells of the NS with a particular emphasis on neurons. To date, it is known that local translation is involved in axonal maintenance, guidance and arborization, and it promotes synapse formation and synaptic plasticity (Zhang and Poo, 2002; Martin, 2004; Yoon et al., 2012; Leal et al., 2014). Given that neuronal processes might as well receive environmental stimuli with potential detrimental effects, local protein synthesis also becomes relevant upon neuronal damage and in response to stress as previously reviewed (Baleriola and Hengst, 2015; Lin et al., 2020).

Although the local synthesis of acetylcholinesterase in axons was discovered by Koenig and Koelle (1960) it took two decades to detect the presence of ribosomes in neuronal peripheral processes: in 1982 polyribosomes (or polysomes) were detected for the first time in dendritic spines of neurons located in the dentate gyrus (Steward and Levy, 1982; Steward and Fass, 1983) and later, in 1986 polysomes were detected in axons (Steward and Ribak, 1986). The discovery of dendritic polysomes encouraged researchers to focus on mRNA localization and localized translation in dendrites, and soon various dendritic transcripts were identified, such as microtubule-associated protein 2 (*Map2a*) (Garner and Matus, 1988), calcium/calmodulin- dependent protein kinase 2 alpha (*Camk2α*) (Burgin et al., 1990) or activity-regulated cytoskeleton-associated protein (*Arc*) (Steward et al., 1998), among others. *Actb* was the first transcript identified in vertebrate axons (Bassell et al., 1998) and its translation in *Xenopus* embryos is involved in growth cone behavior during development. Other cytoskeleton- and membrane-associated proteins have more recently been identified as locally produced in rodent axons (e.g., RhoA, Par3, and SNAP25. . .) (Wu et al., 2005; Hengst et al., 2009; Batista et al., 2017). Transcripts encoding proteins associated with cytoskeleton and membrane dynamics are not the only locally translated in neuronal processes. Local production of proteins involved in mitochondrial function and even transcription factors have been detected in both dendrites and axons as recently reviewed by Blanco-Urrejola and colleagues (Blanco-Urrejola et al., 2021). In essence, local translation is a crucial mechanism that contributes to many neuronal functions and although this phenomenon has been mainly studied in physiological conditions it is now accepted that its deregulation is involved in various neurological diseases (Khalil et al., 2018), which we will review in this article. However, before we delve into local translation in NS pathologies, we will briefly describe the process that transcripts follow since leaving the nucleus until they get translated in target subcellular compartments.

LOCAL TRANSLATION: FROM mRNA TRANSPORT TO PROTEIN SYNTHESIS

The canonical view of protein synthesis is that mRNA translation occurs in the soma either by ribosomes associated to the rough endoplasmic reticulum (RER) (**Figure 1B**^{i}) or by free ribosomes present in the cytosol (**Figure 1B**^{ii}). The newly synthesized proteins are then processed and once mature they are transported through microtubules by dyneins and kinesins to different subneuronal domains (**Figure 1C**^{i}), where they carry out their function (**Figure 1D**^{i}). Conversely, local protein synthesis requires transcripts to leave the nucleus and bind ribonucleoprotein (RNP) granules (**Figure 1B**^{iii}). RNP granules are then transported to target compartments (**Figures 1C**^{ii,iii}) and once there, mRNAs are translated into protein (**Figure 1D**^{ii}).

mRNA Transport to Neuronal Peripheral Processes

When mRNAs exit the nucleus, RNA binding proteins (RBPs) recognize specific localization elements typically found in the 3′-Untranslated Regions (3′-UTR) of the transcripts known as zip codes (Perry and Fainzilber, 2011; Szostak and Gebauer, 2013; Berkovits and Mayr, 2015). Interestingly, evidence suggest that long 3′-UTRs provide a longer life span to RNAs favoring their long distance transport and hence their localization to peripheral neuronal processes (Tushev et al., 2018). Besides binding the transcripts, RBPs associate with translation regulators including ribosomal proteins and other

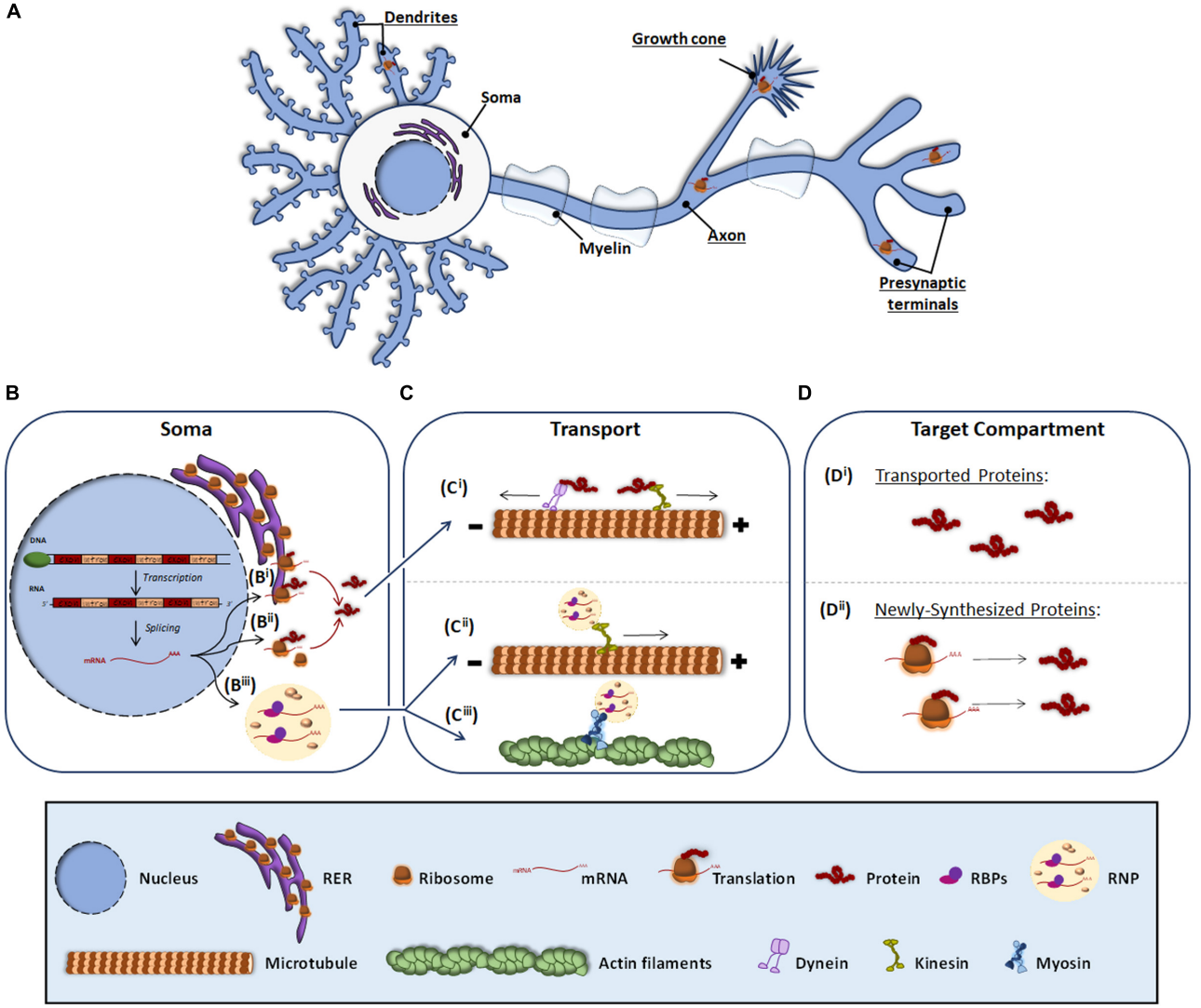

FIGURE 1 | Protein and RNA transport to peripheral subneuronal compartments. Roughly it is underlined the neuronal compartments where local protein synthesis occurs **(A)**. In the soma, expressly in the nucleus, DNA is transcribed to RNA and after splicing, the resulting mRNA **(B)** can be either processed by the classical somatic translation or the local protein synthesis. For the classical one, the mRNA is translated by ribosomes associated to RER **(B^{i})** and free cytosolic ribosomes **(B^{ii})**. Synthetized proteins are transported **(C)** through dyneins or kinesis associated to microtubules **(C^{i})** to target compartments where elicit their function **(D^{i})**. For local translation, mRNA is associated to RBPs and assembled as RNP granules **(B^{iii})**, which can be transported through kinesis **(C^{ii})** or by myosins linked to actin filaments **(C^{iii})**. At the target compartments **(D)**, transported mRNAs are locally translated, and the newly synthesized proteins **(D^{ii})** elicit their function.

components of the translation machinery, ribosomal RNAs, and non-coding RNAs (Kim et al., 2005; Skup, 2008), and assemble into membraneless RNPs (Formicola et al., 2019; Pushpalatha and Besse, 2019; **Figure 1B**^{iii}). RNPs bind to motor proteins directly or indirectly via adapters and the transport of the transcripts to distal compartments is initiated. Depending on the target compartment, transport occurs via microtubules bound to kinesins (in the case of axons and dendrites) (Dixit et al., 2008; Guillaud et al., 2020; **Figure 1C**^{ii}) or through actin microfilaments associated to myosin (in axonal growth cone, presynaptic terminals and dendritic spines) (Hirokawa et al., 2010; Shirao and Gonzalez-Billault, 2013; Craig, 2018; **Figure 1C**^{iii}). During transport, RNP granules participate in the repression of translation but they are also involved in the local translation of proteins when remodeling of the RNP granules occurs driven by external signals. Interestingly, recent evidence indicates that RNP granules bind to membranous organelles located in axons such as endosomes and mitochondria, which serve as platforms to aid with local protein synthesis (Baumann et al., 2014; Cioni et al., 2019).

Local Protein Synthesis in Subcellular Compartments

As in the soma, the ribosomes are the molecular machines responsible for protein synthesis in subcellular domains. For

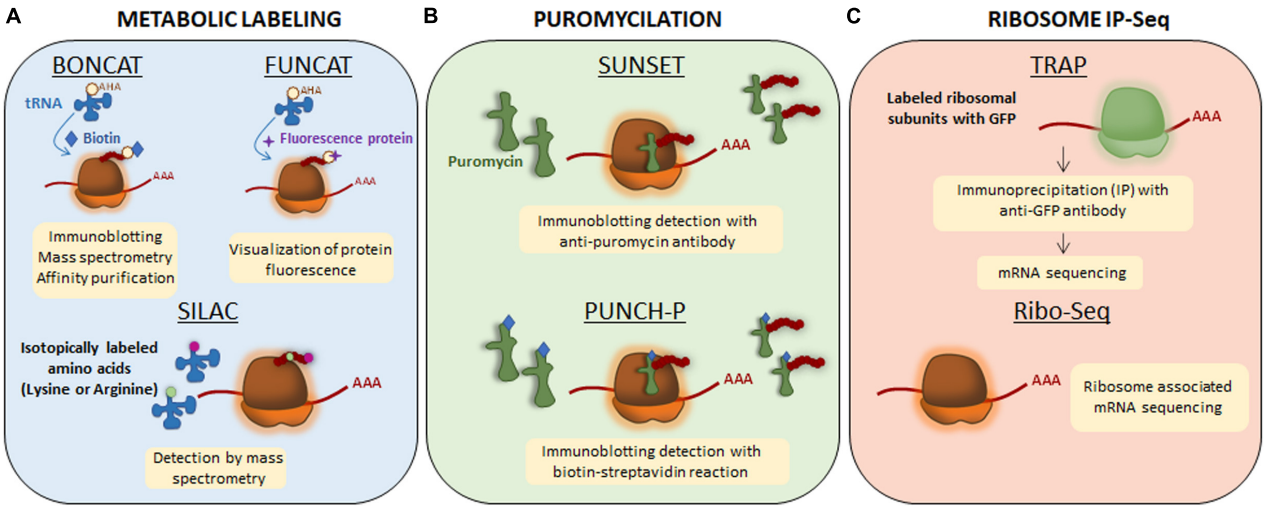

FIGURE 2 | Techniques to detect newly synthesized proteins. **(A)** Metabolic labeling. Bioorthogonal non-canonical amino acid tagging (BONCAT) and fluorescent non-canonical amino acid techniques (FUNCAT) are based on non-canonical methionine derivates (an azide or an alkaline) and therefore, they are able to get incorporated to the nascent protein as methionine through endogenous methyionil-transfer RNA (tRNA) synthetase. The newly synthesized proteins will be labeled with azide or alkyne groups. For their detection, exogenous reactive groups are then incorporated to azide or alkyne groups: biotin in BONCAT and a fluorescence protein in FUNCAT. For stable isotope labeling using amino acids in cell culture (SILAC), lysine and arginine are isotopically labeled with ^{12}C (light amino acids) and ^{13}C (heavy amino acids). The incorporation of labeled amino acids allows them to enter into newly synthesized proteins and be detected by mass spectrometry. **(B)** Puromycilation. Puromycin is an antibiotic that structurally mimics tRNAs so it can get incorporated into the nascent polypeptide chain and elongation is stopped. Puromycilated-proteins can be detected by immunochemistry directly using an anti-puromycin antibody for surface sensing of translation technique (SUNSET) or indirectly when puromycin is bound to biotin for puromycin-associated nascent chain proteomics (PUNCH-P). **(C)** Ribosome immunoprecipitation-sequencing (IP-Seq). Translating ribosome affinity purification (TRAP) method consists on labeling ribosomal subunits with Green Fluorescence Protein (GFP) followed by immunoprecipitation approach. Transcripts bound to ribosomes containing GFP will be isolated and sequenced by RNA-sequencing. Ribo-Seq technique is based on sequencing all mRNA transcripts which are associated to ribosomes.

many years it was assumed that ribosomes were translationally active when associated forming polysomes, as these structures where the first detected in dendrites and axons (Steward and Levy, 1982; Steward and Fass, 1983; Steward and Ribak, 1986). However, a recent study has published the existence of both polysomes and monosomes in synaptosomes. This same study suggests that while in the soma the vast majority of transcripts associate to polyribosomes, most synaptic mRNAs bind to and are translated by monosomes compared to a few synaptic transcripts that preferentially bind polysomes (Biever et al., 2020).

Local translation, like any other cellular process, requires energy. Recently, Rangaraju et al. (2019) described that mitochondrial compartments present in dendrites contribute to synaptic plasticity by supplying the energy required to synthesize proteins in spines. However, some subneuronal domains (e.g., the presynaptic terminals) do not contain mitochondria and the energy demands are met by local ATP produced by synaptic cycles in response to neuronal activity (Rangaraju et al., 2014). Independently on how subcellular compartments provide the necessary energy for protein synthesis, transcripts are considered locally translated if they meet the following requirements: (1) coding transcripts to be translated need to colocalize with ribosomes and other components of the translation machinery in a given subcellular domain, (2) newly synthesized proteins need to be detected at subcellular levels by techniques such as protein metabolic labeling (**Figure 2A**), puromycilation of nascent peptides (**Figure 2B**) or ribosome immunoprecipitation followed by sequencing (**Figure 2C**), and (3) levels of newly synthesized proteins need to drop when blocking protein synthesis (e.g., with pharmacological inhibitors such as anisomycin or emetine) (Holt et al., 2019).

LOCAL TRANSLATION IN NERVOUS SYSTEM PATHOLOGIES

Since the study of the first proteins synthesized in different subneuronal domains, most research has focused on discovering new localized transcripts in neurons. However, there was no evidence linking local synthesis deregulation with neuronal pathologies until 2001 when Zheng and colleagues described that intra-axonal RNA translation was activated in response to nerve injury (Zheng et al., 2001). From then on, there is growing evidence on the translation of localized transcripts upon nerve injury and on the role of locally produced proteins in the response of neurons to damage. For instance, the axonal synthesis of the transcription factors STAT3 and PPARγ after sciatic nerve crush is followed by their retrograde transport toward the neuronal cell body. Once there, both STAT3 and PPARγ trigger transcriptional programs contributing to nerve regeneration (Ben-Yaakov et al., 2012). Interestingly, at least one component of the importin α/β complex required for retrograde transport is also synthesized in injured axons (Hanz et al., 2003). These data point at the implication of local

translation in neuronal survival following nerve lesions in the peripheral nervous system. In addition, a deregulation of local protein synthesis upon damage was also recently suggested in the central nervous system. In retinal ganglion cells, the RBP RBPMS is expressed exclusively in the soma but upon hypoxia and axotomy, RBPMS is redistributed to dendrites and axons, respectively (Pereiro et al., 2020). Authors have also identified alterations of various RBPs in different neurological diseases, including amyotrophic lateral sclerosis, frontotemporal dementia or spinal muscular atrophy. Likewise, in other disorders such as Alzheimer's disease, deregulation of translation of certain mRNAs in neuronal processes seems to contribute to the pathology. We will now summarize the current knowledge on how deregulation of local protein synthesis at different levels can contribute to the development and progression of NS pathologies (**Table 1**).

Amyotrophic Lateral Sclerosis (ALS) and Frontotemporal Dementia (FTD)

Amyotrophic lateral sclerosis is the most common motor neuron disease with an adult onset and it is characterized by the degeneration of upper and lower motor neurons. Most of ALS patients –around 90%– suffer the sporadic form of the disease whereas the remaining 10% of the cases correspond to familial ALS with a genetic inheritance (Scotter et al., 2015). Different genes have been associated to ALS pathology including those encoding for Cu-Zn superoxide dismutase 1 (SOD1), Tar DNA binding-protein 43 (TDP-43), fused in sarcoma/translocated in liposarcoma (FUS), or chromosome 9 open reading frame 72 (C9orf72). Interestingly, some of the ALS-linked genes have also been related to FTD. FTD is a group of disorders whose main feature is the loss of neurons in frontal and temporal brain lobes leading to cognitive impairment. Similarly to ALS, FTD is mainly a sporadic disorder although 40% of cases have family history with a 10% of autosomal dominant inheritance (Bott et al., 2014). In this section we will review the ALS/FTD-associated genes involved in mRNA localization and translation within neurites.

Tar DNA binding-protein-43 is an RBP involved in mRNA splicing, transport and translation in neuronal processes. The presence of TDP-43 aggregates in the cell cytoplasm in ALS and FTD patients has been reported. TDP-43 associates to specific mRNAs in RNP granules and transports them to the target neuronal compartment where mRNAs can be translated by the localized translation machinery (Alami et al., 2014). In 2014, *futsch* mRNA was identified as a TDP-43 target in a *Drosophila* ALS model. *Futsch* is known to be involved in the development and maintenance of synaptic contacts at the neuromuscular junctions (NMJ). Mutant TDP-43 alters *futsch* localization: mRNA levels are significantly reduced at the NMJ while higher levels are detected in neuronal somata. In addition to mislocalization, TDP-43 also regulates *futsch* translation by shifting mRNA from actively translating polysomes to non-translating ribonuclear protein particles. Similarly, the mammalian homolog of Futsch, MAP1B accumulates in motor neuron cell bodies in the spinal cord from ALS patients (Coyne et al., 2014). As both Futsch and MAP1B are part of the microtubule cytoskeleton, defects in their local translation due to mutant TDP-43 could lead to cytoskeletal defects, contributing to ALS development (as summarized in **Figure 3A**).

Another important RBP linked to ALS and FTD is FUS, which, as TDP-43, plays a role in RNA metabolism (splicing, trafficking and translation). FUS also appears in cytoplasmic inclusions in diseases. However, it was reported that FUS deposits are post-translationally modified by arginine unmethylation only in postmortem tissue from FTD patients but not in ALS ones. Indeed, FUS hypomethylation triggers its aggregation and consequently alters RNP granules and local protein synthesis in neurites (Qamar et al., 2018). On the other hand, wild type FUS is present in somata and along neuronal processes as well, including dendrites, spines and the NMJ. Specifically, FUS has been detected at translation sites in axons. ALS-linked mutations in FUS lead to its accumulation in neurites of hippocampal and sciatic nerve neurons. Moreover, mutant FUS leads to stress-mediated inhibition of intra-axonal protein synthesis and therefore to synaptic dysfunction (Lopez-Erauskin et al., 2018; **Figure 3A**). In fact, a previous study had already reported the incorporation of cytoplasmic mutant FUS into stress granules (Bosco et al., 2010). Some FUS target mRNAs are abnormally expressed when FUS is mutated. For instance, *Fos-B* is upregulated in axons in FUS-mutant motor neurons causing an increase in axonal branching. The axonal morphology can be rescued by the suppression of exacerbated *Fos-B* expression by locally applying siRNAs to axons. Interestingly, an abnormal Fos-B upregulation in ventral horn neurons in ALS autopsy samples has also been reported (Akiyama et al., 2019).

In addition to the contribution to intra-axonal translation, both FUS and TDP-43 are also localized to dendrites and dendritic spines (Swanger and Bassell, 2013). Furthermore, TDP-43 does not only regulate mRNA translation but is also involved in dendritic mRNA trafficking (Chu et al., 2019).

Notably, an interaction between FUS and TDP-43 was identified in 2010. It is of interest to highlight that this FUS/TDP-43 association is enhanced by ALS-linked mutant variants in TDP-43 (Ling et al., 2010). Therefore, this report reveals the possible convergence of pathogenic mechanisms from both FUS and TDP-43 in ALS. Similarly, other interactions between proteins associated to NS disorders have been identified. TDP-43 seems to interact to disrupted in schizophrenia 1 (DISC1) in brains of both FTD mouse model and patients. The TDP-43/DISC1 complex negatively regulates dendritic local translation in response to neuronal activity. This association might explain some psychiatric behaviors observed in FTD patients since DISC1 is a relevant player in the pathology of psychiatric disorders (Endo et al., 2018). In the case of FUS, it interacts with the survival motor neuron protein (SMN), the main responsible for the development of spinal muscular atrophy (SMA). The relationship between both disease-linked proteins will be discussed in the next paragraph corresponding to SMA.

The GGGGCC repeat expansion in the *C9orf72* gene is associated to a significant percentage of familial ALS cases. Although C9orf72 function remains unclear, authors have demonstrated that the repeat expansion can form G-quadruplexes, which are known to participate in splicing,

TABLE 1 | Summary of altered proteins and mRNAs involved in local translation in different nervous system pathologies.

Disease	Protein/mRNA	Altered mechanism on local translation	Model system	References
ALS/FTD	TDP-43	Abnormal trafficking of *futsch*/*Map1b* mRNAs to neurites leading to cytoskeleton defects	*Drosophila* model of ALS *in vivo*, ALS vs. control postmortem brain tissue	Coyne et al., 2014
	FUS	Stress-mediated inhibition of intra-axonal translation	HEK-293 cell line and zebrafish embryo spinal cords; mutant FUS mice and mouse hippocampal neuron culture	Bosco et al., 2010; Lopez-Erauskin et al., 2018
	C9orf72	mRNP granules mislocalization to neuritic compartments affecting to branching	Rat spinal cord neuron culture, *Drosophila* model *in vivo*	Burguete et al., 2015
SMA	SMN	*Actb*, *Nrn1*, *Gap43*, *Anxa2* mislocalization altering neurite growth, presynaptic function, and cytoskeleton Repression of axonal mTOR through miR-183	NSC-34 cell line; mouse motor neuron culture Rat hippocampal, cortical, and motor neuron culture	Rage et al., 2013; Fallini et al., 2014, 2016; Kye et al., 2014; Rihan et al., 2017
AD	*Mapt*	*Mapt* mislocalization to dendrites and hyperphosphorylation	Mouse hippocampal neuron culture, WT vs. Tau KO mice; hippocampal neuron culture from WT and Fyn KO mice, HEK-293 cell line, WT, APP23 and FynCA Tg mouse models *in vivo*	Kobayashi et al., 2017; Li and Gotz, 2017
	Atf4	*Atf4* recruitment to axons induced by Aβ oligomers, leading to neuronal death	Rat hippocampal neuron culture, mouse model *in vivo*, AD and control postmortem human brain tissue	Baleriola et al., 2014; Walker et al., 2018
PD	UPR genes	UPR altered. A compartment-dependent UPR involving local translation?	α-synuclein Tg mice	Hetz and Saxena, 2017
	LRRK2	Deregulation of global eIF4E/4E-BP. Defects in axonal 4E-BP dependent translation? Axonal microRNAs deregulation?	HEK-293 and SH-SY5Y cell lines; rat superior cervical ganglia neuron culture; rat cortical neuron culture, WTvs. LRRK2 KO mice	Imai et al., 2008; Kumar et al., 2010; Natera-Naranjo et al., 2010; Herzig et al., 2011; Trancikova et al., 2012
	PINK1/PARK2	Pumilio and Glorund/hnRNP-F displacement: altered translation in the mitochondrion surface (within axons?) due to *PINK1*/*PARK2* mutations.	*Drosophila* PINK1 model and HEK 293T cell line	Mouton-Liger et al., 2017; Martinez et al., 2019
HD	HTT	Impaired dendritic levels of *Actb* mRNA, Ago2 protein and P-bodies Altered axonal BDNF delivery leading to neurotoxicity	Homozygous *Htt* mutant cell lines (109Q/109Q); HeLa S3 cells Flagged-Htt590; rat cortical neuron culture and brain sections	Gauthier et al., 2004; Savas et al., 2008; Ma et al., 2010, 2011; Savas et al., 2010
ASD and FXS	FMRP	Deregulation of local mRNAs linked to abnormal spine morphology and plasticity Upregulation of dendritic *Dlg4* translation through inhibition of miR-125a with spine morphology defects Dendritic mTOR upregulation	Rat hippocampal neuron culture; cortical neuron culture from *Fmr1* KO mice; *in vivo* Fmr1 KO mouse model; Organotypic hippocampal slice cultures from *Fmr1* KO mice	Antar et al., 2004; Muddashetty et al., 2011; Pyronneau et al., 2017; Banerjee et al., 2018; Feuge et al., 2019
DS	*Dscam*	Upregulation of dendritic mRNA and protein levels with defects in dendrite branching	Mouse hippocampal neuron culture from Ts1Cje mice, DS mouse model	Alves-Sampaio et al., 2010
	Bdnf	Upregulation within dendrites leading to an aberrant activation of dendritic translation	*In vitro* hippocampal dendrites from Ts1Cje mice	Troca-Marin et al., 2011; Swanger and Bassell, 2013
Other	*Bdnf* (depression and bipolar disorder)	Dendritic *Bdnf* localization to dendrites disrupted	Ts1 Cje mouse hippocampal neuron culture	Swanger and Bassell, 2013
	Pumilio-2 (epilepsy)	Erroneous mRNAs localization to axons Upregulation of overall translation in axons with branching defects	*In vivo* 5 month Pum2 gene-trap mice; Pum2 knockdown in primary dorsal root ganglion rat neuron culture and mouse model *in vivo*	Follwaczny et al., 2017; Martinez et al., 2019

ALS, amyotrophic lateral sclerosis; FTD, frontotemporal dementia; SMA, spinal muscular atrophy; AD, Alzheimer's disease; PD, Parkinson's disease; HD, Huntington's disease; ASD, autism spectrum disorders; FXS, fragile-X syndrome; DS: down syndrome.

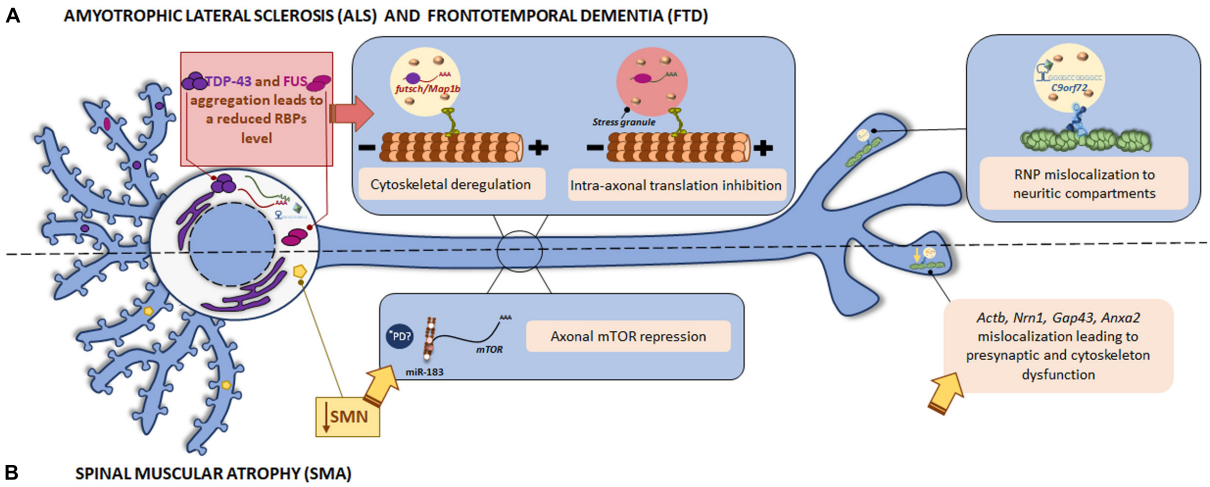

FIGURE 3 | Local translation defects in ALS/FTD and SMN. **(A)** Among ALS/FTD-linked proteins, TDP-43, FUS, and C9orf72 are found. The RBPs TDP-43 and FUS play a role in RNA metabolism. The aggregates usually found in ALS and FTD patients impair TDP-43 and FUS function leading to altered mRNA localization and the consequent cytoskeletal deregulation and stress-mediated intra-axonal translation inhibition, respectively. The GGGCC repeat expansion in the *C9orf72* mRNA triggers its assembly in RNP granules, which are erroneously localized to neuritic compartments and affect to nerve branching. **(B)** Loss of SMN is the main cause of SMA. SMN is involved in the localization of mRNAs to the axonal compartment. SMN defects lead to *Actb*, *Nrn1*, *Gap43,* and *Anxa2* mislocalization with important impact in neurite growth, presynaptic function, and cytoskeleton plasticity. SMN also controls the regulator of local translation mTOR through miR-183. *PD miRNAs are also involved in the translation repression induced by mutant LRRK2 in PD. Due to local miRNAs have been identified as contributors to other pathologies, a similar local mechanism could participate in the pathogenesis of PD.

mRNA trafficking and translation regulation (Fratta et al., 2012). In addition, GGGGCC repeat RNAs are assembled into mRNA transport granules and wrongly localized to neuritic compartments. The consequent mislocalization of mRNA granules alters nerve branching (**Figure 3A**). These observations suggest a novel mechanism underlying neuronal defects in disease-associated expanded repeats like ALS (Burguete et al., 2015).

As mentioned above, late endosomes act as platforms for local protein synthesis in axons and dendrites. Moreover, other organelles, including mitochondria or lysosomes, can be "vehicles" for RNP granule transport and localization. ANXA11 is an RNA granule-associated protein that acts as an adaptor between lysosomes and RNP granules. ALS-associated mutations in ANXA11 prevents RNP granule association to lysosomes and impaired RNP transport which results in altered RNA localization to axons what might contribute to axonal degeneration in ALS (Liao et al., 2019).

Together, these findings underline the relevance of a correct localization of mRNAs for neuronal physiology: while mutant forms of the RBPs TDP-43 and FUS alter localization of certain mRNAs within neurites and lead to the consequent impairment on cytoskeleton and synapses, the defective localization of mRNA granules in neurites caused by the GGGGCC repeat expansion in *C9orf72* results in altered branching (**Figure 3A** and **Table 1**).

Spinal Muscular Atrophy (SMA)

Spinal muscular atrophy is another example of a motor neuron disease in which both RBP deregulation and mRNA mislocalization have been reported. SMA is an autosomal disorder characterized by the progressive loss of spinal motor neurons and skeletal muscle atrophy. Mutations in the *SMN1* gene leading to reduced SMN levels haven been identified as the cause of SMA pathology. SMN is a ubiquitously expressed RBP whose main function is the assembly of small nuclear RNPs for mRNA splicing. However, neuronal SMN is also involved in the assembly of RNP complexes required for mRNA transport to axons and for local translation. Fallini and colleagues described that the association of SMN to messenger RBPs (mRBPs) such as HuD and IMP1 is involved in the localization of poly(A) mRNAs to the axonal compartment (Fallini et al., 2011, 2014). Defects in axonal SMN thus lead to mRNA mislocalization. Among mislocalized mRNAs, some relevant for neurite growth and presynaptic function can be found, including *Actb*, *Nrn1*, and *Gap43*, to mention but a few. For instance, *Gap43* is reduced in growth cones of SMA motor neurons at mRNA and protein levels. Interestingly, HuD and IMP1, both of them altered by defects in SMN, control the transport of *Gap43* mRNA. Conversely, the overexpression of these mRBPs is sufficient to restore axon growth (Fallini et al., 2016). Likewise, 50% of SMN reduction impairs the localization of other mRNAs such as *Anxa2* (encoding Annexin A2) and *Cox4i2* (Rage et al., 2013). Annexin A2 is involved in actin cytoskeleton plasticity. The observed defects in cytoskeleton organization in SMN deficiency models could be explained at least in part by the mislocalization of *Anxa2* and its consequent impaired axonal translation (Rihan et al., 2017). Altogether, these data suggest that deregulation of mRNA localization to axonal compartments and local protein synthesis are key players in the development of SMA pathology.

Survival motor neuron protein also controls local translation through microRNA (miR) expression. In SMN-deficient neurons, miR-183 is increased in neurites. miR-183 targets axonal mTOR, a master regulator of local protein synthesis, leading to reduction of its own translation. Therefore, overall mTOR-dependent local translation is decreased in SMN-deficient axons (Kye et al., 2014).

We have mentioned in previous paragraphs the existent interaction between proteins associated to different neurodegenerative diseases. A 2013 study identified FUS, one of the ALS/FTD-linked RBPs, as an interactor of SMN. The association between both RBPs appears to be influenced by FUS mutations and leads to a redistribution of SMN toward FUS deposits with the consequent impairment in axonal localization of SMN (Groen et al., 2013). Moreover, there is evidence of the association of SMN and FMRP (fragile X mental retardation protein, involved in Fragile X syndrome) in neuronal mRNP granules (Piazzon et al., 2008).

To summarize, SMN contributes to local protein synthesis regulation through its interaction with RBPs and the control of miRNAs. Therefore, mutations in this protein result in mRNA mislocalization and repression of axonal translation (**Table 1**). The data reviewed so far overall suggest that dysfunction of RBPs and the consequent mRNA mislocalization alter localized translation and underly the pathophysiological features of motor neuron diseases as depicted in **Figure 3B**.

Alzheimer's Disease (AD)

Alzheimer's disease is the most common cause of dementia among the elderly. It is an incurable neurodegenerative disease characterized by the gradual loss of cognitive and functional abilities. Pathological cellular dysfunction in AD begins many years before the onset of the symptoms. Two hallmarks have been identified in postmortem brains as main contributors to AD pathology: the neurofibrillary tangles, composed of hyperphosphorylated microtubule associated protein Tau (MAPT or Tau) and the extracellular β-amyloid (Aβ) plaques (Tiwari et al., 2019; Busche and Hyman, 2020). Although the mechanisms leading to the development and spread of the disease through the brain are not fully understood, it is known that synapse loss is one of the first pathological signs of AD (Selkoe, 2002). Alterations in the axonal and dendritic proteomes could underlie synaptic dysfunction and thereby the study of local protein synthesis in this context might provide clearer knowledge on the development of the disease.

Tau is mainly localized to axons though is also present in the somatodendritic compartment at very low levels in healthy neurons (Tashiro et al., 1997). Axonal Tau is partially the product of locally translated *Mapt* mRNA (Aronov et al., 2001; Gauthier-Kemper et al., 2018). Nevertheless, *Mapt* gets aberrantly localized to dendrites in tauopathies such as AD. For instance, Aβ peptides induce *Mapt* mRNA localization to dendrites and its localized translation. Intriguingly, the mislocalization and dendritic synthesis of Tau enhances its hyperphosphorylation (Kobayashi et al., 2017; Li and Gotz, 2017), indicating that Tau synthesis in the inappropriate subneuronal compartment contributes to neurodegenerative diseases such as AD.

Aβ peptides are the result of incorrect proteolytic cleavage of amyloid precursor protein (APP) and are prone to aggregate, which results in the formation of senile plaques (Rabbito et al., 2020). We have stated that Aβ triggers Tau synthesis in dendrites but it also induces local protein synthesis in axons (Baleriola et al., 2014; Gamarra et al., 2020). The mRNA encoding the transcription factor ATF4 (previously known as CREB2) is among the proteins whose local translation is induced by Aβ peptides. Interestingly, axonally synthesized ATF4 is retrogradely transported to the nucleus where it alters transcription leading to neuronal death both *in vitro* and *in vivo* (Baleriola et al., 2014; **Figure 4A**). Additionally, *Atf4* recruitment to Aβ-exposed axons is itself triggered by local translation of sentinel mRNAs such as the intermediate filament protein vimentin (*Vim*) (Walker et al., 2018). These studies suggest a common axon-to-soma communication mechanism in injured nerves and in response to amyloid based on axonally synthesized transcription factors although the outcome of the transcriptional response differs: a regenerative response of injured nerves vs. neuronal death following the local exposure to Aβ oligomers.

Atf4 is not the only mRNA found in Aβ-treated axons. Interestingly, transcripts from 9 of the 20 susceptibility genes associated to late onset AD are axonally localized following exposure to Aβ oligomers: *App, Clu, ApoE, Sorl1, Bin1, Picalm, Ptk2, Celf1*, and *Fermt2* (Blanco-Urrejola et al., 2021).

Local translation has also been described in other neural cells like oligodendrocytes. For example, the heterogeneous nuclear RNP A2 (hnRNP A2) is part of the transport granules responsible for mRNA localization to peripheral processes in oligodendrocytes (Hoek et al., 1998; Munro et al., 1999). Intriguingly, loss of hnRNP A/B in entorhinal cortices from AD brains has been reported. Experiments performed in neurons indicate that defects in hnRNP A/B lead to dendritic loss *in vitro* and memory and electrocorticographic alterations *in vivo* (Berson et al., 2012). Based on the role of hnRNP A2 in oligodendrocytes a possible involvement of hnRNP A/B in neuronal mRNA metabolism cannot be discarded. Further investigation should be carried out in order to fully understand the role of hnRNPs in RNA localization and protein synthesis in neuronal processes in disease.

Regarding interaction between proteins associated to different NS pathologies, in 50% of FTD cases an accumulation of Tau fibrils has been observed (Goedert et al., 2012). Interestingly, reduced levels of the ALS/FTD-linked TDP-43 are detected in the AD brain. Indeed, TDP-43 promotes *Mapt* mRNA instability through its 3′-UTR, suggesting that altered TDP-43 might contribute to Tau aggregation (Gu et al., 2017). Taking into account that axonal localization signals are usually located at the 3′-UTR, we can speculate that deregulation of TDP-43 also affects Tau localization and therefore might also contribute to Tau pathology in FTD.

Results reviewed in these paragraphs strongly point toward the importance of mRNA localization and localized translation and/or deregulation of both phenomena in the development of AD and related disorders. One of the main hallmark of AD, Aβ aggregates, lead to deregulation of local protein synthesis in both dendrites and axons. These events contribute to Tau

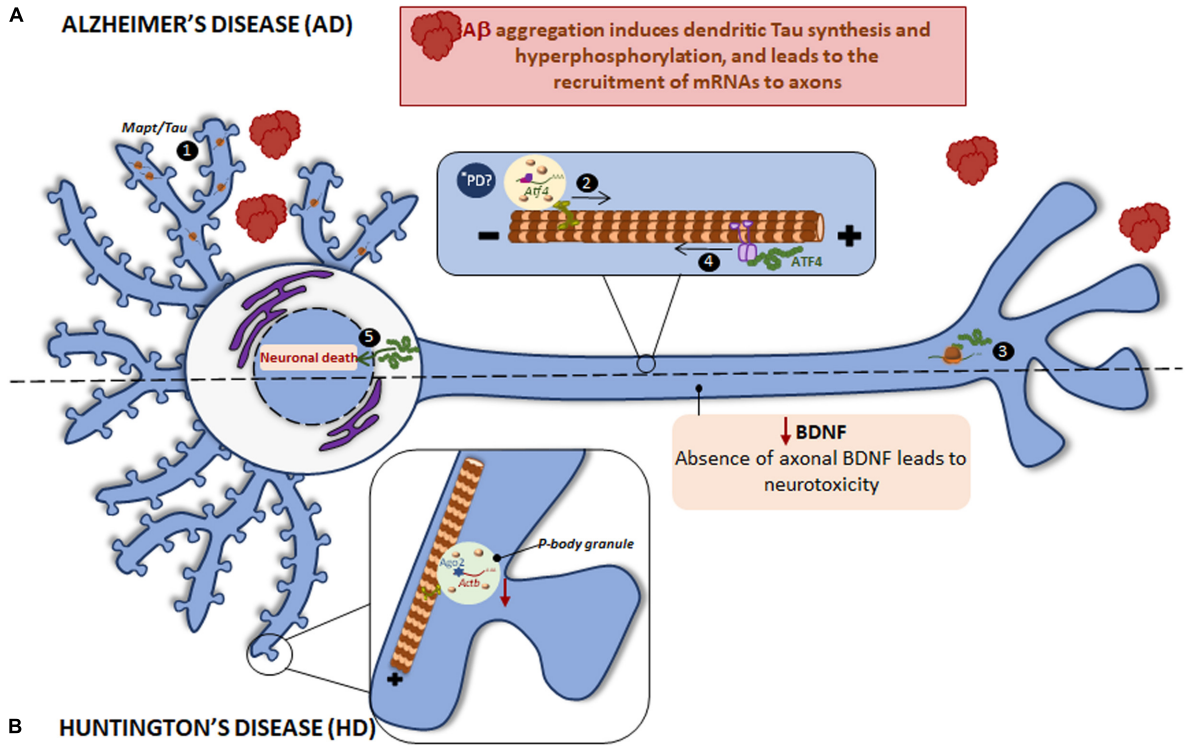

FIGURE 4 | Local translation defects in AD and HD. **(A)** The two main hallmarks in AD brains are the accumulation of intracellular hyperphosphorylated Tau and extracellular Aβ plaques. Aβ induces the incorrect localization of *Mapt* mRNA to dendrites with the consequent, local synthesis of Tau and its hyperphosphorylation (1). Aβ also induces the recruitment of certain mRNAs to axons, among them *Atf4* is found (2). Once ATF4 is axonally synthesized (3), it is retrogradely transported to cell body (4) where enhances death transcriptional programs (5). *PD ATF4 is also a component of UPR. The UPR is altered in PD and therefore the local ATF4 could be involved in PD progression. **(B)** HD is caused by a mutant CAG expansion in *HTT* gene. HTT KO leads to reduced levels of *Actb* mRNA, Ago2 protein, and p-bodies in dendrites. Mutant HTT impairs BDNF transport to axons resulting in neurotoxicity and probably affects to local protein synthesis since BDNF regulate this process in subneuronal compartments.

hyperphosphorylation and neuronal death respectively (**Table 1**). Thus, restoring levels of localized mRNAs and/or their localized translation could alleviate cell dysfunction linked to AD.

Huntington's Disease (HD)

Huntingtin (HTT) is a protein expressed at high levels in several brain regions like the hippocampus, the cortex, the cerebellum and the striatum. CAG repeat expansions in the *HTT* gene result in a repeated polyQ tract in the N-terminal region of the HTT protein, causing HD. HD is an autosomal dominant neurodegenerative disease characterized by uncontrolled movements, and behavior and cognitive impairments (Landles and Bates, 2004; Li and Li, 2004). HTT, as well as APP, is transported along axons and has been implicated in dendritic RNA delivery (Ma et al., 2010; Savas et al., 2010). Importantly, HTT inactivation leads to impaired localization of RNAs and membranous organelles (Gauthier et al., 2004), indicating that HTT plays an important role in RNA transport.

Similar to other previously mentioned neurodegenerative disorders, RBPs colocalize with the main driver of HD: HTT interacts with Ago2 and Staufen in processing bodies (P bodies) which contain translationally repressed mRNAs (Savas et al., 2008), and in dendritic RNA granules involved in transport and local translation (Savas et al., 2010). Additionally, HTT was reported to bind to the 3′-UTR of dendritically targeted mRNAs including *Ip3r1*, *Actb*, and *Bdnf*. Moreover, HTT knockout (KO) reduces levels of dendritic *Actb* mRNA, Ago2 protein, and P bodies (Ma et al., 2010, 2011; Savas et al., 2010). HTT is also required for BDNF vesicular transport along microtubules toward the axons. Mutant HTT impairs BDNF transport leading to neurotoxicity (Gauthier et al., 2004) (as summarized in **Figure 4B**). Noteworthy, BDNF is known to regulate local translation (Swanger and Bassell, 2013) and thus local protein synthesis in HD might be impaired via defective axonal BDNF delivery.

Huntingtin is thus yet another example of a main contributor to NS pathology involved in mRNA trafficking to neuronal processes by its interaction with RBPs or by its direct binding to mRNA 3′-UTRs (**Table 1**).

Parkinson's Disease (PD)

Parkinson's disease is a chronic neurodegenerative disorder in which dopaminergic neurons of the *substantia nigra* progressively die and there is an accumulation of Lewy bodies composed of abnormal intracellular aggregates of alpha synuclein protein (αSyn) and ubiquitin (Goedert et al., 2013). The

pathogenic process in PD involves regions of the central and peripheral NS with bradykinesia, rigidity and other motor symptoms being the main clinical manifestations (Halliday and McCann, 2010). As in AD, pathological signs at cellular levels appear before clinical symptoms and lead to the loss of 60-70% of neurons in the *substantia nigra pars compacta* (Radhakrishnan and Goyal, 2018).

Impairment of local protein synthesis in PD has not been fully demonstrated. However, a recent review by Lin and colleagues commented on this possibility. Given their complex morphology, neurons cope with stress in a compartmentalized manner (Lin et al., 2020). In PD, as in AD, prion disease and other disorders in which protein aggregation occurs, stress responses in neurons are evident before the pathological hallmarks of the disease are apparent. Oxidative stress and ER stress induce mechanisms able to cope with basal levels of neuronal damage. However, when a certain threshold is reached, those same mechanisms might backfire and contribute to neurodegeneration. Interestingly, the dual role and compartmentalized nature of stress mechanisms was implicitly reported in a mouse model of acute amyloid pathology where locally translated ATF4 mediates neurodegeneration while global increases of this same transcription factor allows neurons to adapt to Aβ-induced stress (Baleriola et al., 2014). ATF4 is an important component of the unfolded protein response (UPR). The UPR involves a global shutdown of protein synthesis via eIf2α while promoting translation of mRNAs encoding stress-related proteins. ATF4 is classically synthesized upon accumulation of unfolded and misfolded proteins and the consequent UPR activation due to ER stress. However, in Aβ-treated axons, ATF4 translation (likely via eIf2α) but no other canonical signs of the UPR, such as protein synthesis shutdown, are apparent. A partial, non-canonical activation of the UPR has also been observed in developing axons when challenged with Sema3a (Cagnetta et al., 2019). The UPR is known to be altered in AD, PD with Lewy bodies, prion disease, HD and even ALS (Hetz and Saxena, 2017). It would be interesting to address if in neurodegenerative diseases other than AD, such as PD, a compartment-dependent UPR involving local translation contributes to disease progression (**Figure 4A**).

On the other hand, several studies implicate translation in PD pathogenesis. Proteins encoded by PD-associated genes have recently been shown to interact with components of the translation initiation complex. For instance, Leucine-rich repeat kinase 2 (LRRK2) whose mutations are involved in autosomal dominant Parkinson's disease, phosphorylates 4E-BP, releasing the repression from the initiation factors eIF4E/eIF4G. Mutant forms of LRRK2 in *Drosophila* stimulate eIF4E inducing aberrantly high protein synthesis accompanied by loss of dopaminergic neurons (Imai et al., 2008). LRRK2 is also known to regulate eIF4E/4E-BP in mammals but results seem to be conflicting. Whereas *in vitro* experiments indicate increased 4E-BP phosphorylation induced by LRRK2 (Kumar et al., 2010), Trancikova and colleagues did not observe any effect on 4E-BP with *in vivo* gain- or loss-of-function approaches (Trancikova et al., 2012). Others, however, have observed increased phospho-4E-BP levels in LRRK2 KO and LRRK2 kinase dead but not in knock-in transgenic mice (Herzig et al., 2011). The so far inconclusive results on the effect of LRRK2 on the eIF4E/4E-BP axis might be due to the analyses being performed in whole cells and tissues. It would be interesting to determine whether in PD, as in Aβ pathology, 4E-BP dependent translation is enhanced in axons (Baleriola et al., 2014).

Work from Gehrke and colleagues suggested that translation repression induced by pathogenic LRRK2 is elicited through repression of miRNAs. Interestingly, miRNAs can be found in axons (Natera-Naranjo et al., 2010) and as mentioned before miR-183 regulates axonally synthesized mTOR which in turn modulates local protein synthesis in SMA (Kye et al., 2014). It would be worth determining if a similar local mechanism is involved in the pathogenesis of PD (see *PD in **Figure 3B**).

Mutations in Pten-induced kinase 1 (PINK1/PARK6) or Parkin (PARK2), which are involved in early-onset autosomal recessive PD alter mitochondrial function. PINK1 and PARK2 promote mitochondrial localization and translation of specific mRNAs at the mitochondrial outer membrane (Gehrke et al., 2015). Translation activation via PINK1 and PARK2 implies the displacement of the repressive RBPs Pumilio and Glorund/hnRNP-F (Mouton-Liger et al., 2017). Both proteins influence mitochondrial function and play an important role in translation. Whether both RBPs play a role in localized translation in PD remains unknown. Interestingly, however, Pumilio 2 is known to regulate the local transcriptome of developing axons (Martinez et al., 2019) (*PD in **Figure 5C**).

Although there are so far no concluding remarks on how local translation could contribute to PD pathogenesis, the fact that global protein synthesis is likely aberrantly high and that there are similarities with AD and HD strongly point to the possibility that RNA localization and localized translation in neurons are compromised in this disease and might even contribute to its progression.

Autism Spectrum Disorders (ASD) and Fragile X Syndrome (FXS)

Autism spectrum disorders is a term referred to heterogeneous behavioral disorders with a combination of difficulties in different areas including intellectual, communication or social interaction. The most common monogenic cause of ASD is FXS, a neurodevelopmental disorder which causes intellectual disability attributed to FMRP protein deficiency as a result of a mutation in the *FMR1* gene (Salcedo-Arellano et al., 2020). One of the main cell-pathological features of FXS is the high levels of dendritic spines with an abnormal morphology linked to delayed maturation (Banerjee et al., 2018).

Fragile X mental retardation protein is a well-known RBP whose implication in dendritic local translation has been widely studied. FMRP is involved in several steps of local protein synthesis: from mRNA trafficking to peripheral processes to ribosome stalling or microRNA regulation. In relation to mRNA transport, Feuge et al. (2019) described that FMRP binds to *Cof1* mRNA and regulates its localization to and translation within dendrites. *Cof1* encodes cofilin 1, an actin-binding protein involved in dendritic spine structure and plasticity, and it was

recently associated with the FXS pathology (Pyronneau et al., 2017). In *Fmr1* KO mice, defects on local *Cof1* mRNA were observed with the consequent plasticity impairment (Feuge et al., 2019). Additionally, FMRP target mRNAs encoding synaptic proteins have also been reported, including *Arc*, *Camk2a*, *Dlg4*, or *Map1b*. Interestingly, *Frm1* mRNA itself is localized to dendrites (Antar et al., 2004; Banerjee et al., 2018). Hence, the loss of FMRP leads to mislocalization and altered local translation of FMRP binding mRNAs, and FMRP deficiency is likely linked to defects in spine morphology and in neuronal plasticity observed in FXS.

Besides interacting with target mRNAs, FMRP can also bind reversibly to ribosomes and paralyzes the elongation phase of translation (Feng et al., 1997; Darnell et al., 2011; Chen et al., 2014). Furthermore, deregulated miRNAs were observed in postmortem brain tissue from ASD patients (Abu-Elneel et al., 2008). Interestingly, PSD-95 (encoded by *Dlg4*) local synthesis in dendritic compartments is mediated by the also dendritically localized miR-125a in FXS. FMRP is required for miR-125a activity through the RNA-induced silencing complex (RISC). Indeed, in *Fmr1* KO neurons *Dlg4* translation is increased while miR-125a levels are reduced in *Fmr1* KO synaptoneurosomes, affecting spine morphology and branching (Muddashetty et al., 2011).

Fragile X mental retardation protein binds ALS/FTD-linked TDP-43 to regulate the transport of mRNP granules in mouse dendrites. The association between FMRP and TDP-43 RBPs in mRNPs trafficking again opens new venues to shed light on common pathophysiological mechanisms of mRNA localization and localized translation underlying neurodevelopmental and neurodegenerative diseases (Chu et al., 2019).

Despite most evidence links FMRP to local translation in dendrites, FMRP-containing RNP granules have been detected in developing and mature axons as well (Christie et al., 2009; Akins et al., 2012, 2017). Additionally, axonal *Map1b* and *Calm1* mRNAs have been identified as miR-181d targets. FMRP appears to associate with miR-181d and its target mRNAs in dorsal root ganglion neurons (DRGs) upon nerve growth factor (NGF) stimulation and regulates axon outgrowth. FMRP deficiency *in vitro* and in a FXS mouse model leads to the mislocalization of miR-181d, *Map1b* and *Calm1* (Wang et al., 2015). Further research is required on this regard to clarify the involvement of FMRP in intra-axonal protein synthesis and the more than likely contribution thereof to FXS pathology.

Finally, FMRP is able to regulate mTOR activity in dendrites. mTOR is not only considered a regulator of axonal translation but it is also involved in intra-dendritic protein synthesis. In *Fmr1* KO mice and in studies of FXS patients, an upregulation of mTOR was detected. In addition, mTOR is also altered in other FMRP-deficiency diseases, such as tuberous sclerosis, Rett syndrome, and Down syndrome (Hagerman et al., 2010; Wang et al., 2010; Troca-Marin et al., 2011).

From all the documented evidence gathered in this section it seems clear that FXS is one of the best examples of the extent to which deregulation of local mRNA translation contributes to disease progression. The abnormal morphology of dendritic spines typically observed in FXS could be explained by the wide involvement of FMRP in dendritic local protein synthesis. As summarized in **Table 1**, FMRP defects entail deregulation of dendritically localized mRNAs and miRNAs, which results in spine morphology and plasticity impairment. Furthermore, dendritic mTOR is also controlled by FMRP. All this knowledge will allow a better understanding of ASD and will hopefully help develop new therapeutic strategies (**Figure 5A**).

Down Syndrome (DS)

Down syndrome is the most common genetic cause of intellectual disability triggered by trisomy of human chromosome 21. Neurological symptoms are accompanied by abnormal physical growth. In some DS cases congenital heart defects are apparent. Duodenal stenosis or leukemia are also more frequent in DS patients than in the general population (Antonarakis et al., 2004). Although the specific mechanisms leading to neurological signs remain poorly understood, it is known that DS is characterized by defects in dendrite morphology and synaptic plasticity similarly to other developmental diseases like FXS (Alves-Sampaio et al., 2010). The mRNA encoding the DS cell adhesion molecule (DSCAM) is present in dendrites and DSCAM has been suggested to play a role in synaptic plasticity. Therefore, altered *Dscam* mRNA localization and defects in DSCAM local synthesis might contribute to DS-related pathogenic features in neurons. In fact, *Dscam* mRNA levels as well as its localized translation are increased within dendrites of hippocampal neurons leading to a negative effect on dendrite branching in a DS mouse model (Alves-Sampaio et al., 2010). Additionally, the same DS model presents increased dendritic levels of BDNF, which is a local protein synthesis modulator (Swanger and Bassell, 2013). Consequently, the rate of local translation in dendrites is aberrantly increased (Troca-Marin et al., 2011; **Figure 5B**).

Other Neurological Disorders

Interestingly, a point mutation in the human *BDNF* gene is associated with depression and bipolar disorder. The presence of the human *BDNF* mutation in a mouse model disrupts the localization of *Bdnf* mRNA to dendrites (Swanger and Bassell, 2013). These data suggest that altered *Bdnf* localization and the consequent defects in its translation might contribute to psychiatric disorders (**Figure 5B**), although this contribution should be explored further.

Finally, epilepsy is also associated with deficiencies in RBPs. For instance, in 2017 Pumilio-2 was described as an RBP involved in epileptogenesis (Follwaczny et al., 2017). A recent study has described Pumilio-2 as a regulator of the axonal transcriptome in developing axons, whose mechanism of action is the exclusion of RNAs from the axonal compartment by retaining them in the cell body. Importantly, Pumilio-2 knockdown not only leads to the erroneous axonal mRNAs localization and increased overall translation levels in axons, but also to branching defects (Martinez et al., 2019) as summarized in **Figure 5C**.

To sum up, increasing evidence suggest that mRNA localization and local protein synthesis might be a key contributor to NS pathological conditions, not only in neurodegenerative diseases but also in other neurological disorders as discussed in these paragraphs.

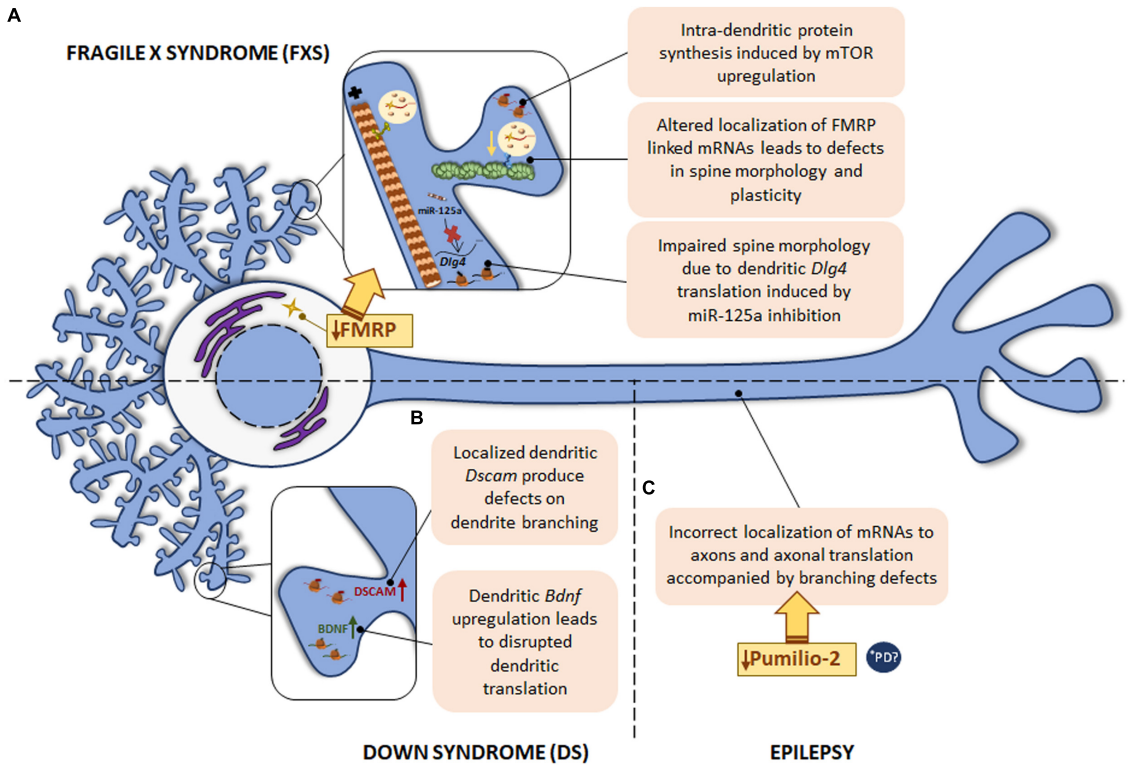

FIGURE 5 | Local translation defects in FXS, DS and epilepsy. **(A)** The most common monogenic cause of ASD is FXS, caused by a mutation in *FMR1* gene with the consequent FMRP protein deficiency. FMRP regulates RNA metabolism at different levels and therefore, intra-dendritic translation is altered at several points: mTOR-mediated local protein synthesis is upregulated; deregulation of local mRNAs-linked to FMRP leads to abnormal spine morphology and plasticity; deregulation of miR-125a induces *Dlg4* mRNA dendritic translation with spine morphology defects. **(B)** DS, caused by trisomy of chromosome 21, is characterized by defects in dendrite morphology, which can be due to the increased levels of *Dscam* and *Bdnf* mRNAs in dendrites. The localization of *Bdnf* to dendrites is also disrupted in psychiatric disorders. **(C)** In epilepsy, deficiency in the RBP Pumilio-2 results in incorrect localization of mRNAs to axons and increased overall intra-axonal translation with the consequent branching defects. *PD PINK1 and PARK2, involved in PD pathogenesis, regulate translation of mitochondrial proteins by displacement of Pumilio-2 and other RBPs. Due to the local role of Pumilio-2 in translation in developing axons, localized translation in PD could also be altered.

CONCLUDING REMARKS

The data reviewed in this article bring to light the increasing body of evidence on the relevance of mRNA localization and local protein synthesis not only in brain development and physiology but also in NS pathologies including neurodegenerative diseases (**Table 1**). We cannot, however, overlook the limitations in studying local protein synthesis. While we can separate different subneuronal compartments *in vitro* using diverse specialized culture systems (microfluidic chambers, modified Boyden chambers. . .), this task cannot be performed *in vivo*. In whole animals, neuronal processes are intermingled and cannot be found in isolation. Even when synaptosomes can be isolated from entire tissues, thorough controls have to be performed in order to ensure that RNAs and proteins of interest are indeed localized to neuronal peripheral domains and/or are a result of local protein synthesis. Additionally, often times the amount of material obtained from synaptosomes or brain regions enriched in neurites (e.g., the neuropil) is limiting. Identification of specific transcripts and proteins along neuronal processes is possible also by *in situ* hybridization and immunohistochemical approaches, which can also be performed in human brain tissue and thereby, this kind of samples contribute to clarify the findings in culture and animal brains, supporting the significance of localized mRNAs and the translation machinery in several pathophysiological contexts. However, postmortem tissue does not allow mechanistic assessment and cell-compartment isolation from brain neurons is not possible at clinical stages. Human studies are thus one of the main challenges in the field of local protein synthesis.

On the other hand, localized translation research in the context of pathologies provides new exciting venues for the development of novel therapeutic targets for nervous system pathologies although localized strategies should be explored more in detail. For instance, current technologies do not allow the knockdown of specific axonal mRNAs without altering the somatic counterparts. Every effort should be done to develop new approaches on this matter. Nevertheless, it is worth noting that local protein synthesis in neurons does not seem to rely only on the neurons but that glial cells might contribute to this phenomenon. Interestingly, in the peripheral nervous system, Schwann cells transfer ribosomes to injured sciatic nerves

(Court et al., 2008) whereas in the spinal cord, a transference of ribosome-like particles at the axonal-myelin sheath interface has suggested (Li et al., 2005). These data point at the possibility of a novel therapeutic strategy based on modulating glia-neuron transference instead of interfering directly with translation at subneuronal compartments. In either case, further research is still required.

AUTHOR CONTRIBUTIONS

JB conceived the work. MG, AC, and MB-U drafted the manuscript. MG, AC, and JB composed figures and tables. MG, AC, MB-U, and JB performed literature searching and edited the manuscript. All authors contributed to the article and approved the submitted version.

FUNDING

This work was partially funded by grants awarded to JB (MICINN grants SAF2016-76347-R, RYC-2016-19837, and PID2019-110721RB-I00; The Alzheimer's Association grants AARG-19-618303 and AARG-19-618303-RAPID). MG and AC are GV fellows; MB-U is a UPV/EHU fellow.

REFERENCES

Abu-Elneel, K., Liu, T., Gazzaniga, F. S., Nishimura, Y., Wall, D. P., Geschwind, D. H., et al. (2008). Heterogeneous dysregulation of microRNAs across the autism spectrum. *Neurogenetics* 9, 153–161. doi: 10.1007/s10048-008-0133-5

Akins, M. R., Berk-Rauch, H. E., Kwan, K. Y., Mitchell, M. E., Shepard, K. A., Korsak, L. I., et al. (2017). Axonal ribosomes and mRNAs associate with fragile X granules in adult rodent and human brains. *Hum Mol Genet* 26, 192–209. doi: 10.1093/hmg/ddw381

Akins, M. R., Leblanc, H. F., Stackpole, E. E., Chyung, E., and Fallon, J. R. (2012). Systematic mapping of fragile X granules in the mouse brain reveals a potential role for presynaptic FMRP in sensorimotor functions. *J Comp Neurol* 520, 3687–3706. doi: 10.1002/cne.23123

Akiyama, T., Suzuki, N., Ishikawa, M., Fujimori, K., Sone, T., Kawada, J., et al. (2019). Aberrant axon branching via Fos-B dysregulation in FUS-ALS motor neurons. *EBioMedicine* 45, 362–378. doi: 10.1016/j.ebiom.2019.06.013

Alami, N. H., Smith, R. B., Carrasco, M. A., Williams, L. A., Winborn, C. S., Han, S. S. W., et al. (2014). Axonal transport of TDP-43 mRNA granules is impaired by ALS-causing mutations. *Neuron* 81, 536–543. doi: 10.1016/j.neuron.2013.12.018

Alberts, B., Johnson, A., Lewis, J., Raff, M., Roberts, K., and Walter, P. (2002). *Molecular Biology of the Cell*, 4th Edn. New York, NY: Garland Science.

Alves-Sampaio, A., Troca-Marin, J. A., and Montesinos, M. L. (2010). NMDA-mediated regulation of DSCAM dendritic local translation is lost in a mouse model of Down's syndrome. *J Neurosci* 30, 13537–13548. doi: 10.1523/JNEUROSCI.3457-10.2010

Antar, L. N., Afroz, R., Dictenberg, J. B., Carroll, R. C., and Bassell, G. J. (2004). Metabotropic glutamate receptor activation regulates fragile x mental retardation protein and FMR1 mRNA localization differentially in dendrites and at synapses. *J Neurosci* 24, 2648–2655. doi: 10.1523/JNEUROSCI.0099-04.2004

Antonarakis, S. E., Lyle, R., Dermitzakis, E. T., Reymond, A., and Deutsch, S. (2004). Chromosome 21 and down syndrome: from genomics to pathophysiology. *Nat Rev Genet* 5, 725–738. doi: 10.1038/nrg1448

Aronov, S., Aranda, G., Behar, L., and Ginzburg, I. (2001). Axonal tau mRNA localization coincides with tau protein in living neuronal cells and depends on axonal targeting signal. *J Neurosci* 21, 6577–6587.

Baleriola, J., and Hengst, U. (2015). Targeting axonal protein synthesis in neuroregeneration and degeneration. *Neurotherapeutics* 12, 57–65. doi: 10.1007/s13311-014-0308-8

Baleriola, J., Walker, C. A., Jean, Y. Y., Crary, J. F., Troy, C. M., Nagy, P. L., et al. (2014). Axonally synthesized ATF4 transmits a neurodegenerative signal across brain regions. *Cell* 158, 1159–1172. doi: 10.1016/j.cell.2014.07.001

Banerjee, A., Ifrim, M. F., Valdez, A. N., Raj, N., and Bassell, G. J. (2018). Aberrant RNA translation in fragile X syndrome: From FMRP mechanisms to emerging therapeutic strategies. *Brain Res* 1693(Pt A), 24–36. doi: 10.1016/j.brainres.2018.04.008

Bannister, N. J., and Larkman, A. U. (1995). Dendritic morphology of CA1 pyramidal neurones from the rat hippocampus: II. Spine distributions. *J Comp Neurol* 360, 161–171. doi: 10.1002/cne.903600112

Bassell, G. J., Zhang, H., Byrd, A. L., Femino, A. M., Singer, R. H., Taneja, K. L., et al. (1998). Sorting of beta-actin mRNA and protein to neurites and growth cones in culture. *J Neurosci* 18, 251–265.

Batista, A. F. R., Martinez, J. C., and Hengst, U. (2017). Intra-axonal Synthesis of SNAP25 Is Required for the Formation of Presynaptic Terminals. *Cell Rep* 20, 3085–3098. doi: 10.1016/j.celrep.2017.08.097

Baumann, S., Konig, J., Koepke, J., and Feldbrugge, M. (2014). Endosomal transport of septin mRNA and protein indicates local translation on endosomes and is required for correct septin filamentation. *EMBO Rep* 15, 94–102. doi: 10.1002/embr.201338037

Ben-Yaakov, K., Dagan, S. Y., Segal-Ruder, Y., Shalem, O., Vuppalanchi, D., Willis, D. E., et al. (2012). Axonal transcription factors signal retrogradely in lesioned peripheral nerve. *EMBO J* 31, 1350–1363. doi: 10.1038/emboj.2011.494

Berkovits, B. D., and Mayr, C. (2015). Alternative 3′ UTRs act as scaffolds to regulate membrane protein localization. *Nature* 522, 363–367. doi: 10.1038/nature14321

Berson, A., Barbash, S., Shaltiel, G., Goll, Y., Hanin, G., Greenberg, D. S., et al. (2012). Cholinergic-associated loss of hnRNP-A/B in Alzheimer's disease impairs cortical splicing and cognitive function in mice. *EMBO Mol Med* 4, 730–742. doi: 10.1002/emmm.201100995

Biever, A., Glock, C., Tushev, G., Ciirdaeva, E., Dalmay, T., Langer, J. D., et al. (2020). Monosomes actively translate synaptic mRNAs in neuronal processes. *Science* 367, eaay4991. doi: 10.1126/science.aay4991

Blanco-Urrejola, M., Gaminde-Blasco, A., Gamarra, M., de la Cruz, A., Vecino, E., Alberdi, E., et al. (2021). RNA Localization and Local Translation in Glia in Neurological and Neurodegenerative Diseases: Lessons from Neurons. *Cells* 10, 632.

Bosco, D. A., Lemay, N., Ko, H. K., Zhou, H., Burke, C., Kwiatkowski, T. J. Jr., et al. (2010). Mutant FUS proteins that cause amyotrophic lateral sclerosis incorporate into stress granules. *Hum Mol Genet* 19, 4160–4175. doi: 10.1093/hmg/ddq335

Bott, N. T., Radke, A., Stephens, M. L., and Kramer, J. H. (2014). Frontotemporal dementia: diagnosis, deficits and management. *Neurodegener Dis Manag* 4, 439–454. doi: 10.2217/nmt.14.34

Burgin, K. E., Waxham, M. N., Rickling, S., Westgate, S. A., Mobley, W. C., and Kelly, P. T. (1990). In situ hybridization histochemistry of Ca2+/calmodulin-dependent protein kinase in developing rat brain. *J Neurosci* 10, 1788–1798.

Burguete, A. S., Almeida, S., Gao, F. B., Kalb, R., Akins, M. R., and Bonini, N. M. (2015). GGGGCC microsatellite RNA is neuritically localized, induces branching defects, and perturbs transport granule function. *Elife* 4, e08881. doi: 10.7554/eLife.08881

Busche, M. A., and Hyman, B. T. (2020). Synergy between amyloid-beta and tau in Alzheimer's disease. *Nat Neurosci* 23, 1183–1193. doi: 10.1038/s41593-020-0687-6

Cagnetta, R., Wong, H. H., Frese, C. K., Mallucci, G. R., Krijgsveld, J., and Holt, C. E. (2019). Noncanonical Modulation of the eIF2 Pathway Controls an Increase in Local Translation during Neural Wiring. *Mol Cell* 73, 474.e–489.e. doi: 10.1016/j.molcel.2018.11.013

Chen, E., Sharma, M. R., Shi, X., Agrawal, R. K., and Joseph, S. (2014). Fragile X mental retardation protein regulates translation by binding directly to the ribosome. *Mol Cell* 54, 407–417. doi: 10.1016/j.molcel.2014.03.023

Christie, S. B., Akins, M. R., Schwob, J. E., and Fallon, J. R. (2009). The FXG: a presynaptic fragile X granule expressed in a subset of developing brain circuits. *J Neurosci* 29, 1514–1524. doi: 10.1523/JNEUROSCI.3937-08.2009

Chu, J. F., Majumder, P., Chatterjee, B., Huang, S. L., and Shen, C. J. (2019). TDP-43 Regulates Coupled Dendritic mRNA Transport-Translation Processes in Co-operation with FMRP and Staufen1. *Cell Rep* 29, 3118.e–3133.e. doi: 10.1016/j.celrep.2019.10.061

Cioni, J. M., Lin, J. Q., Holtermann, A. V., Koppers, M., Jakobs, M. A. H., Azizi, A., et al. (2019). Late Endosomes Act as mRNA Translation Platforms and Sustain Mitochondria in Axons. *Cell* 176, 56.e–72.e. doi: 10.1016/j.cell.2018.11.030

Court, F. A., Hendriks, W. T., MacGillavry, H. D., Alvarez, J., and van Minnen, J. (2008). Schwann cell to axon transfer of ribosomes: toward a novel understanding of the role of glia in the nervous system. *J Neurosci* 28, 11024–11029. doi: 10.1523/JNEUROSCI.2429-08.2008

Coyne, A. N., Siddegowda, B. B., Estes, P. S., Johannesmeyer, J., Kovalik, T., Daniel, S. G., et al. (2014). Futsch/MAP1B mRNA is a translational target of TDP-43 and is neuroprotective in a Drosophila model of amyotrophic lateral sclerosis. *J Neurosci* 34, 15962–15974. doi: 10.1523/JNEUROSCI.2526-14.2014

Craig, E. M. (2018). Model for Coordination of Microtubule and Actin Dynamics in Growth Cone Turning. *Front Cell Neurosci* 12:394. doi: 10.3389/fncel.2018.00394

Darnell, J. C., Van Driesche, S. J., Zhang, C., Hung, K. Y., Mele, A., Fraser, C. E., et al. (2011). FMRP stalls ribosomal translocation on mRNAs linked to synaptic function and autism. *Cell* 146, 247–261. doi: 10.1016/j.cell.2011.06.013

Dixit, R., Ross, J. L., Goldman, Y. E., and Holzbaur, E. L. (2008). Differential regulation of dynein and kinesin motor proteins by tau. *Science* 319, 1086–1089. doi: 10.1126/science.1152993

Edstrom, A., and Sjostrand, J. (1969). Protein synthesis in the isolated Mauthner nerve fibre of goldfish. *J Neurochem* 16, 67–81. doi: 10.1111/j.1471-4159.1969.tb10344.x

Endo, R., Takashima, N., Nekooki-Machida, Y., Komi, Y., Hui, K. K., Takao, M., et al. (2018). TAR DNA-Binding Protein 43 and Disrupted in Schizophrenia 1 Coaggregation Disrupts Dendritic Local Translation and Mental Function in Frontotemporal Lobar Degeneration. *Biol Psychiatry* 84, 509–521. doi: 10.1016/j.biopsych.2018.03.008

Fallini, C., Donlin-Asp, P. G., Rouanet, J. P., Bassell, G. J., and Rossoll, W. (2016). Deficiency of the Survival of Motor Neuron Protein Impairs mRNA Localization and Local Translation in the Growth Cone of Motor Neurons. *J Neurosci* 36, 3811–3820. doi: 10.1523/JNEUROSCI.2396-15.2016

Fallini, C., Rouanet, J. P., Donlin-Asp, P. G., Guo, P., Zhang, H., Singer, R. H., et al. (2014). Dynamics of survival of motor neuron (SMN) protein interaction with the mRNA-binding protein IMP1 facilitates its trafficking into motor neuron axons. *Dev Neurobiol* 74, 319–332. doi: 10.1002/dneu.22111

Fallini, C., Zhang, H., Su, Y., Silani, V., Singer, R. H., Rossoll, W., et al. (2011). The survival of motor neuron (SMN) protein interacts with the mRNA-binding protein HuD and regulates localization of poly(A) mRNA in primary motor neuron axons. *J Neurosci* 31, 3914–3925. doi: 10.1523/JNEUROSCI.3631-10.2011

Feng, Y., Absher, D., Eberhart, D. E., Brown, V., Malter, H. E., and Warren, S. T. (1997). FMRP associates with polyribosomes as an mRNP, and the I304N mutation of severe fragile X syndrome abolishes this association. *Mol Cell* 1, 109–118. doi: 10.1016/s1097-2765(00)80012-x

Feuge, J., Scharkowski, F., Michaelsen-Preusse, K., and Korte, M. (2019). FMRP Modulates Activity-Dependent Spine Plasticity by Binding Cofilin1 mRNA and Regulating Localization and Local Translation. *Cereb Cortex* 29, 5204–5216. doi: 10.1093/cercor/bhz059

Follwaczny, P., Schieweck, R., Riedemann, T., Demleitner, A., Straub, T., Klemm, A. H., et al. (2017). Pumilio2-deficient mice show a predisposition for epilepsy. *Dis Model Mech* 10, 1333–1342. doi: 10.1242/dmm.029678

Formicola, N., Vijayakumar, J., and Besse, F. (2019). Neuronal ribonucleoprotein granules: Dynamic sensors of localized signals. *Traffic* 20, 639–649. doi: 10.1111/tra.12672

Fratta, P., Mizielinska, S., Nicoll, A. J., Zloh, M., Fisher, E. M., Parkinson, G., et al. (2012). C9orf72 hexanucleotide repeat associated with amyotrophic lateral sclerosis and frontotemporal dementia forms RNA G-quadruplexes. *Sci Rep* 2, 1016. doi: 10.1038/srep01016

Gamarra, M., Blanco-Urrejola, M., Batista, A. F. R., Imaz, J., and Baleriola, J. (2020). Object-Based Analyses in FIJI/ImageJ to Measure Local RNA Translation Sites in Neurites in Response to Abeta1-42 Oligomers. *Front Neurosci* 14:547. doi: 10.3389/fnins.2020.00547

Garner, C. C., and Matus, A. (1988). Different forms of microtubule-associated protein 2 are encoded by separate mRNA transcripts. *J Cell Biol* 106, 779–783. doi: 10.1083/jcb.106.3.779

Gauthier, L. R., Charrin, B. C., Borrell-Pages, M., Dompierre, J. P., Rangone, H., Cordelieres, F. P., et al. (2004). Huntingtin controls neurotrophic support and survival of neurons by enhancing BDNF vesicular transport along microtubules. *Cell* 118, 127–138. doi: 10.1016/j.cell.2004.06.018

Gauthier-Kemper, A., Suarez Alonso, M., Sundermann, F., Niewidok, B., Fernandez, M. P., Bakota, L., et al. (2018). Annexins A2 and A6 interact with the extreme N terminus of tau and thereby contribute to tau's axonal localization. *J Biol Chem* 293, 8065–8076. doi: 10.1074/jbc.RA117.000490

Gehrke, S., Wu, Z., Klinkenberg, M., Sun, Y., Auburger, G., Guo, S., et al. (2015). PINK1 and Parkin control localized translation of respiratory chain component mRNAs on mitochondria outer membrane. *Cell Metab* 21, 95–108. doi: 10.1016/j.cmet.2014.12.007

Giuditta, A., Dettbarn, W. D., and Brzin, M. (1968). Protein synthesis in the isolated giant axon of the squid. *Proc Natl Acad Sci U S A* 59, 1284–1287. doi: 10.1073/pnas.59.4.1284

Goedert, M., Ghetti, B., and Spillantini, M. G. (2012). Frontotemporal dementia: implications for understanding Alzheimer disease. *Cold Spring Harb Perspect Med* 2, a006254. doi: 10.1101/cshperspect.a006254

Goedert, M., Spillantini, M. G., Del Tredici, K., and Braak, H. (2013). 100 years of Lewy pathology. *Nat Rev Neurol* 9, 13–24. doi: 10.1038/nrneurol.2012.242

Groen, E. J., Fumoto, K., Blokhuis, A. M., Engelen-Lee, J., Zhou, Y., van den Heuvel, D. M., et al. (2013). ALS-associated mutations in FUS disrupt the axonal distribution and function of SMN. *Hum Mol Genet* 22, 3690–3704. doi: 10.1093/hmg/ddt222

Gu, J., Wu, F., Xu, W., Shi, J., Hu, W., Jin, N., et al. (2017). TDP-43 suppresses tau expression via promoting its mRNA instability. *Nucleic Acids Res* 45, 6177–6193. doi: 10.1093/nar/gkx175

Guillaud, L., El-Agamy, S. E., Otsuki, M., and Terenzio, M. (2020). Anterograde Axonal Transport in Neuronal Homeostasis and Disease. *Front Mol Neurosci* 13:556175. doi: 10.3389/fnmol.2020.556175

Hagerman, R., Hoem, G., and Hagerman, P. (2010). Fragile X and autism: Intertwined at the molecular level leading to targeted treatments. *Mol Autism* 1, 12. doi: 10.1186/2040-2392-1-12

Halliday, G. M., and McCann, H. (2010). The progression of pathology in Parkinson's disease. *Ann N Y Acad Sci* 1184, 188–195. doi: 10.1111/j.1749-6632.2009.05118.x

Hanz, S., Perlson, E., Willis, D., Zheng, J. Q., Massarwa, R., Huerta, J. J., et al. (2003). Axoplasmic importins enable retrograde injury signaling in lesioned nerve. *Neuron* 40, 1095–1104. doi: 10.1016/s0896-6273(03)00770-0

Hengst, U., Deglincerti, A., Kim, H. J., Jeon, N. L., and Jaffrey, S. R. (2009). Axonal elongation triggered by stimulus-induced local translation of a polarity complex protein. *Nat Cell Biol* 11, 1024–1030. doi: 10.1038/ncb1916

Herzig, M. C., Kolly, C., Persohn, E., Theil, D., Schweizer, T., Hafner, T., et al. (2011). LRRK2 protein levels are determined by kinase function and are crucial for kidney and lung homeostasis in mice. *Hum Mol Genet* 20, 4209–4223. doi: 10.1093/hmg/ddr348

Hetz, C., and Saxena, S. (2017). ER stress and the unfolded protein response in neurodegeneration. *Nat Rev Neurol* 13, 477–491. doi: 10.1038/nrneurol.2017.99

Hirokawa, N., Niwa, S., and Tanaka, Y. (2010). Molecular motors in neurons: transport mechanisms and roles in brain function, development, and disease. *Neuron* 68, 610–638. doi: 10.1016/j.neuron.2010.09.039

Hoek, K. S., Kidd, G. J., Carson, J. H., and Smith, R. (1998). hnRNP A2 selectively binds the cytoplasmic transport sequence of myelin basic protein mRNA. *Biochemistry* 37, 7021–7029. doi: 10.1021/bi9800247

Holt, C. E., Martin, K. C., and Schuman, E. M. (2019). Local translation in neurons: visualization and function. *Nat Struct Mol Biol* 26, 557–566. doi: 10.1038/s41594-019-0263-5

Imai, Y., Gehrke, S., Wang, H. Q., Takahashi, R., Hasegawa, K., Oota, E., et al. (2008). Phosphorylation of 4E-BP by LRRK2 affects the maintenance of dopaminergic neurons in Drosophila. *EMBO J* 27, 2432–2443. doi: 10.1038/emboj.2008.163

Khalil, B., Morderer, D., Price, P. L., Liu, F., and Rossoll, W. (2018). mRNP assembly, axonal transport, and local translation in neurodegenerative diseases. *Brain Res* 1693(Pt A), 75–91. doi: 10.1016/j.brainres.2018.02.018

Kim, H. K., Kim, Y. B., Kim, E. G., and Schuman, E. (2005). Measurement of dendritic mRNA transport using ribosomal markers. *Biochem Biophys Res Commun* 328, 895–900. doi: 10.1016/j.bbrc.2005.01.041

Kobayashi, S., Tanaka, T., Soeda, Y., Almeida, O. F. X., and Takashima, A. (2017). Local Somatodendritic Translation and Hyperphosphorylation of Tau Protein Triggered by AMPA and NMDA Receptor Stimulation. *EBioMedicine* 20, 120–126. doi: 10.1016/j.ebiom.2017.05.012

Koenig, E., and Koelle, G. B. (1960). Acetylcholinesterase regeneration in peripheral nerve after irreversible inactivation. *Science* 132, 1249–1250. doi: 10.1126/science.132.3435.1249

Kumar, A., Greggio, E., Beilina, A., Kaganovich, A., Chan, D., Taymans, J. M., et al. (2010). The Parkinson's disease associated LRRK2 exhibits weaker in vitro phosphorylation of 4E-BP compared to autophosphorylation. *PLoS One* 5:e8730. doi: 10.1371/journal.pone.0008730

Kye, M. J., Niederst, E. D., Wertz, M. H., Goncalves Ido, C., Akten, B., Dover, K. Z., et al. (2014). SMN regulates axonal local translation via miR-183/mTOR pathway. *Hum Mol Genet* 23, 6318–6331. doi: 10.1093/hmg/ddu350

Landles, C., and Bates, G. P. (2004). Huntingtin and the molecular pathogenesis of Huntington's disease. Fourth in molecular medicine review series. *EMBO Rep* 5, 958–963. doi: 10.1038/sj.embor.7400250

Leal, G., Comprido, D., and Duarte, C. B. (2014). BDNF-induced local protein synthesis and synaptic plasticity. *Neuropharmacology* 76(Pt C), 639–656. doi: 10.1016/j.neuropharm.2013.04.005

Li, C., and Gotz, J. (2017). Somatodendritic accumulation of Tau in Alzheimer's disease is promoted by Fyn-mediated local protein translation. *EMBO J* 36, 3120–3138. doi: 10.15252/embj.201797724

Li, S. H., and Li, X. J. (2004). Huntingtin and its role in neuronal degeneration. *Neuroscientist* 10, 467–475. doi: 10.1177/1073858404266777

Li, Y. C., Li, Y. N., Cheng, C. X., Sakamoto, H., Kawate, T., Shimada, O., et al. (2005). Subsurface cisterna-lined axonal invaginations and double-walled vesicles at the axonal-myelin sheath interface. *Neurosci Res* 53, 298–303. doi: 10.1016/j.neures.2005.07.006

Liao, Y. C., Fernandopulle, M. S., Wang, G., Choi, H., Hao, L., Drerup, C. M., et al. (2019). RNA Granules Hitchhike on Lysosomes for Long-Distance Transport, Using Annexin A11 as a Molecular Tether. *Cell* 179, 147.e–164.e. doi: 10.1016/j.cell.2019.08.050

Lin, J. Q., van Tartwijk, F. W., and Holt, C. E. (2020). Axonal mRNA translation in neurological disorders. *RNA Biol* 1–26. doi: 10.1080/15476286.2020.1822638

Ling, S. C., Albuquerque, C. P., Han, J. S., Lagier-Tourenne, C., Tokunaga, S., Zhou, H., et al. (2010). ALS-associated mutations in TDP-43 increase its stability and promote TDP-43 complexes with FUS/TLS. *Proc Natl Acad Sci U S A* 107, 13318–13323. doi: 10.1073/pnas.1008227107

Lopez-Erauskin, J., Tadokoro, T., Baughn, M. W., Myers, B., McAlonis-Downes, M., Chillon-Marinas, C., et al. (2018). ALS/FTD-Linked Mutation in FUS Suppresses Intra-axonal Protein Synthesis and Drives Disease Without Nuclear Loss-of-Function of FUS. *Neuron* 100, 816.e–830.e. doi: 10.1016/j.neuron.2018.09.044

Ma, B., Culver, B. P., Baj, G., Tongiorgi, E., Chao, M. V., and Tanese, N. (2010). Localization of BDNF mRNA with the Huntington's disease protein in rat brain. *Mol Neurodegener* 5, 22. doi: 10.1186/1750-1326-5-22

Ma, B., Savas, J. N., Yu, M. S., Culver, B. P., Chao, M. V., and Tanese, N. (2011). Huntingtin mediates dendritic transport of beta-actin mRNA in rat neurons. *Sci Rep* 1, 140. doi: 10.1038/srep00140

Martin, K. C. (2004). Local protein synthesis during axon guidance and synaptic plasticity. *Curr Opin Neurobiol* 14, 305–310. doi: 10.1016/j.conb.2004.05.009

Martinez, J. C., Randolph, L. K., Iascone, D. M., Pernice, H. F., Polleux, F., and Hengst, U. (2019). Pum2 Shapes the Transcriptome in Developing Axons through Retention of Target mRNAs in the Cell Body. *Neuron* 104, 931.e–946.e. doi: 10.1016/j.neuron.2019.08.035

Mouton-Liger, F., Jacoupy, M., Corvol, J. C., and Corti, O. (2017). PINK1/Parkin-Dependent Mitochondrial Surveillance: From Pleiotropy to Parkinson's Disease. *Front Mol Neurosci* 10:120. doi: 10.3389/fnmol.2017.00120

Muddashetty, R. S., Nalavadi, V. C., Gross, C., Yao, X., Xing, L., Laur, O., et al. (2011). Reversible inhibition of PSD-95 mRNA translation by miR-125a, FMRP phosphorylation, and mGluR signaling. *Mol Cell* 42, 673–688. doi: 10.1016/j.molcel.2011.05.006

Munro, T. P., Magee, R. J., Kidd, G. J., Carson, J. H., Barbarese, E., Smith, L. M., et al. (1999). Mutational analysis of a heterogeneous nuclear ribonucleoprotein A2 response element for RNA trafficking. *J Biol Chem* 274, 34389–34395. doi: 10.1074/jbc.274.48.34389

Natera-Naranjo, O., Aschrafi, A., Gioio, A. E., and Kaplan, B. B. (2010). Identification and quantitative analyses of microRNAs located in the distal axons of sympathetic neurons. *RNA* 16, 1516–1529. doi: 10.1261/rna.1833310

Pereiro, X., Ruzafa, N., Urcola, J. H., Sharma, S. C., and Vecino, E. (2020). Differential Distribution of RBPMS in Pig, Rat, and Human Retina after Damage. *Int J Mol Sci* 21, 9330. doi: 10.3390/ijms21239330

Perry, R. B., and Fainzilber, M. (2011). When zip codes are in short supply. *EMBO J* 30, 4520–4522. doi: 10.1038/emboj.2011.389

Piazzon, N., Rage, F., Schlotter, F., Moine, H., Branlant, C., and Massenet, S. (2008). In vitro and in cellulo evidences for association of the survival of motor neuron complex with the fragile X mental retardation protein. *J Biol Chem* 283, 5598–5610. doi: 10.1074/jbc.M707304200

Pushpalatha, K. V., and Besse, F. (2019). Local Translation in Axons: When Membraneless RNP Granules Meet Membrane-Bound Organelles. *Front Mol Biosci* 6:129. doi: 10.3389/fmolb.2019.00129

Pyronneau, A., He, Q., Hwang, J. Y., Porch, M., Contractor, A., and Zukin, R. S. (2017). Aberrant Rac1-cofilin signaling mediates defects in dendritic spines, synaptic function, and sensory perception in fragile X syndrome. *Sci Signal* 10, eaan0852. doi: 10.1126/scisignal.aan0852

Qamar, S., Wang, G., Randle, S. J., Ruggeri, F. S., Varela, J. A., Lin, J. Q., et al. (2018). FUS Phase Separation Is Modulated by a Molecular Chaperone and Methylation of Arginine Cation-pi Interactions. *Cell* 173, 720.e–734.e. doi: 10.1016/j.cell.2018.03.056

Rabbito, A., Dulewicz, M., Kulczynska-Przybik, A., and Mroczko, B. (2020). Biochemical Markers in Alzheimer's Disease. *Int J Mol Sci* 21, 1989. doi: 10.3390/ijms21061989

Radhakrishnan, D. M., and Goyal, V. (2018). Parkinson's disease: A review. *Neurol India* 66(Suppl.), S26–S35. doi: 10.4103/0028-3886.226451

Rage, F., Boulisfane, N., Rihan, K., Neel, H., Gostan, T., Bertrand, E., et al. (2013). Genome-wide identification of mRNAs associated with the protein SMN whose depletion decreases their axonal localization. *RNA* 19, 1755–1766. doi: 10.1261/rna.040204.113

Rangaraju, V., Calloway, N., and Ryan, T. A. (2014). Activity-driven local ATP synthesis is required for synaptic function. *Cell* 156, 825–835. doi: 10.1016/j.cell.2013.12.042

Rangaraju, V., Lauterbach, M., and Schuman, E. M. (2019). Spatially Stable Mitochondrial Compartments Fuel Local Translation during Plasticity. *Cell* 176, 73.e–84.e. doi: 10.1016/j.cell.2018.12.013

Rangaraju, V., Tom Dieck, S., and Schuman, E. M. (2017). Local translation in neuronal compartments: how local is local? *EMBO Rep* 18, 693–711. doi: 10.15252/embr.201744045

Rihan, K., Antoine, E., Maurin, T., Bardoni, B., Bordonne, R., Soret, J., et al. (2017). A new cis-acting motif is required for the axonal SMN-dependent Anxa2 mRNA localization. *RNA* 23, 899–909. doi: 10.1261/rna.056788.116

Salcedo-Arellano, M. J., Cabal-Herrera, A. M., Punatar, R. H., Clark, C. J., Romney, C. A., and Hagerman, R. J. (2020). Overlapping Molecular Pathways Leading to Autism Spectrum Disorders, Fragile X Syndrome, and Targeted Treatments. *Neurotherapeutics* 18, 265–283. doi: 10.1007/s13311-020-00968-6

Savas, J. N., Ma, B., Deinhardt, K., Culver, B. P., Restituito, S., Wu, L., et al. (2010). A role for huntington disease protein in dendritic RNA granules. *J Biol Chem* 285, 13142–13153. doi: 10.1074/jbc.M110.114561

Savas, J. N., Makusky, A., Ottosen, S., Baillat, D., Then, F., Krainc, D., et al. (2008). Huntington's disease protein contributes to RNA-mediated gene silencing through association with Argonaute and P bodies. *Proc Natl Acad Sci U S A* 105, 10820–10825. doi: 10.1073/pnas.0800658105

Scotter, E. L., Chen, H. J., and Shaw, C. E. (2015). TDP-43 Proteinopathy and ALS: Insights into Disease Mechanisms and Therapeutic Targets. *Neurotherapeutics* 12, 352–363. doi: 10.1007/s13311-015-0338-x

Selkoe, D. J. (2002). Alzheimer's disease is a synaptic failure. *Science* 298, 789–791. doi: 10.1126/science.1074069

Shirao, T., and Gonzalez-Billault, C. (2013). Actin filaments and microtubules in dendritic spines. *J Neurochem* 126, 155–164. doi: 10.1111/jnc.12313

Skup, M. (2008). Dendrites as separate compartment - local protein synthesis. *Acta Neurobiol Exp (Wars)* 68, 305–321.

Steward, O., and Fass, B. (1983). Polyribosomes associated with dendritic spines in the denervated dentate gyrus: evidence for local regulation of protein synthesis during reinnervation. *Prog Brain Res* 58, 131–136. doi: 10.1016/S0079-6123(08)60013-8

Steward, O., and Levy, W. B. (1982). Preferential localization of polyribosomes under the base of dendritic spines in granule cells of the dentate gyrus. *J Neurosci* 2, 284–291.

Steward, O., and Ribak, C. E. (1986). Polyribosomes associated with synaptic specializations on axon initial segments: localization of protein-synthetic machinery at inhibitory synapses. *J Neurosci* 6, 3079–3085.

Steward, O., Wallace, C. S., Lyford, G. L., and Worley, P. F. (1998). Synaptic activation causes the mRNA for the IEG Arc to localize selectively near activated postsynaptic sites on dendrites. *Neuron* 21, 741–751. doi: 10.1016/s0896-6273(00)80591-7

Swanger, S. A., and Bassell, G. J. (2013). Dendritic protein synthesis in the normal and diseased brain. *Neuroscience* 232, 106–127. doi: 10.1016/j.neuroscience.2012.12.003

Szostak, E., and Gebauer, F. (2013). Translational control by 3′-UTR-binding proteins. *Brief Funct Genomics* 12, 58–65. doi: 10.1093/bfgp/els056

Tashiro, K., Hasegawa, M., Ihara, Y., and Iwatsubo, T. (1997). Somatodendritic localization of phosphorylated tau in neonatal and adult rat cerebral cortex. *Neuroreport* 8, 2797–2801. doi: 10.1097/00001756-199708180-00029

Tiwari, S., Atluri, V., Kaushik, A., Yndart, A., and Nair, M. (2019). Alzheimer's disease: pathogenesis, diagnostics, and therapeutics. *Int J Nanomedicine* 14, 5541–5554. doi: 10.2147/IJN.S200490

Trancikova, A., Mamais, A., Webber, P. J., Stafa, K., Tsika, E., Glauser, L., et al. (2012). Phosphorylation of 4E-BP1 in the mammalian brain is not altered by LRRK2 expression or pathogenic mutations. *PLoS One* 7:e47784. doi: 10.1371/journal.pone.0047784

Troca-Marin, J. A., Alves-Sampaio, A., and Montesinos, M. L. (2011). An increase in basal BDNF provokes hyperactivation of the Akt-mammalian target of rapamycin pathway and deregulation of local dendritic translation in a mouse model of Down's syndrome. *J Neurosci* 31, 9445–9455. doi: 10.1523/JNEUROSCI.0011-11.2011

Tushev, G., Glock, C., Heumuller, M., Biever, A., Jovanovic, M., and Schuman, E. M. (2018). Alternative 3′ UTRs Modify the Localization, Regulatory Potential, Stability, and Plasticity of mRNAs in Neuronal Compartments. *Neuron* 98, 495.e–511.e. doi: 10.1016/j.neuron.2018.03.030

Walker, C. A., Randolph, L. K., Matute, C., Alberdi, E., Baleriola, J., and Hengst, U. (2018). Abeta1-42 triggers the generation of a retrograde signaling complex from sentinel mRNAs in axons. *EMBO Rep* 19, e45435. doi: 10.15252/embr.201745435

Wang, B., Pan, L., Wei, M., Wang, Q., Liu, W. W., Wang, N., et al. (2015). FMRP-Mediated Axonal Delivery of miR-181d Regulates Axon Elongation by Locally Targeting Map1b and Calm1. *Cell Rep* 13, 2794–2807. doi: 10.1016/j.celrep.2015.11.057

Wang, L. W., Berry-Kravis, E., and Hagerman, R. J. (2010). Fragile X: leading the way for targeted treatments in autism. *Neurotherapeutics* 7, 264–274. doi: 10.1016/j.nurt.2010.05.005

Wu, K. Y., Hengst, U., Cox, L. J., Macosko, E. Z., Jeromin, A., Urquhart, E. R., et al. (2005). Local translation of RhoA regulates growth cone collapse. *Nature* 436, 1020–1024. doi: 10.1038/nature03885

Yoon, B. C., Jung, H., Dwivedy, A., O'Hare, C. M., Zivraj, K. H., and Holt, C. E. (2012). Local translation of extranuclear lamin B promotes axon maintenance. *Cell* 148, 752–764. doi: 10.1016/j.cell.2011.11.064

Zhang, X., and Poo, M. M. (2002). Localized synaptic potentiation by BDNF requires local protein synthesis in the developing axon. *Neuron* 36, 675–688. doi: 10.1016/s0896-6273(02)01023-1

Zheng, J. Q., Kelly, T. K., Chang, B., Ryazantsev, S., Rajasekaran, A. K., Martin, K. C., et al. (2001). A functional role for intra-axonal protein synthesis during axonal regeneration from adult sensory neurons. *J Neurosci* 21, 9291–9303.

Conflict of Interest: The authors declare that the research was conducted in the absence of any commercial or financial relationships that could be construed as a potential conflict of interest.